

FEEDBACK REGULATION OF WNT SIGNALING BY NAKED CUTICLE (NKD)
DURING *DROSOPHILA* EMBRYOGENESIS

APPROVED BY SUPERVISORY COMMITTEE

Mentor: Keith A. Wharton, Jr., M.D., Ph.D.

Committee Chairman: Jin Jiang, Ph.D.

Committee Member: Zhijian Chen, Ph.D.

Committee Member: Michael G. Roth, Ph.D.

TO DAMORE, BENBEN, JEFFREY, AND SHUYI

FEEDBACK REGULATION OF WNT SIGNALING BY NAKED CUTICLE (NKD)
DURING *DROSOPHILA* EMBRYOGENESIS

by

CHIH-CHIANG CHAN

DISSERTATION / THESIS

Presented to the Faculty of the Graduate School of Biomedical Sciences

The University of Texas Southwestern Medical Center at Dallas

In Partial Fulfillment of the Requirements

For the Degree of

DOCTOR OF PHILOSOPHY

The University of Texas Southwestern Medical Center at Dallas

Dallas, Texas

May, 2008

Copyright

by

CHIH-CHIANG CHAN, 2008

All Rights Reserved

ACKNOWLEDGEMENTS

I thank my mentor Keith for his encouragement, skillful guidance, and formidable patience. I thank my thesis committee, Dr. Chen, Dr. Jiang, and Dr. Roth, for insightful advice. I thank my lab mates and collaborators who have made significant contributions to this work. I am particularly grateful to Raphael Rousset, PhD (U. Nice, France), who contributed primary data to Chapter 3, as indicated therein. Carl Parker, PhD, kindly provided anti-Importin- α 3 antibody for Importin- α 3 experiments.

From the Wharton lab, I am thankful for Sharon Waldrop, who contributed primary data for the early work of Chapter 2, as indicated therein. I would like to especially recognize Tolga Cagatay, PhD for intelligent discourse on everything from molecules to music. I thank Shu Zhang for everyday help in the lab. I thank Manami Amanai for her enduring friendship.

FEEDBACK REGULATION OF WNT SIGNALING BY NAKED CUTICLE (NKD)
DURING *DROSOPHILA* EMBRYOGENESIS

Chih-Chiang Chan

The University of Texas Southwestern Medical Center at Dallas, 2008

Keith A. Wharton, Jr., M.D., Ph.D.

Wnt/ β -catenin signals are essential for many developmental and physiological processes in animals. Deregulation of the Wnt signaling pathway in mammals can cause diseases such as birth defects, cancer, osteoporosis, and diabetes. In *Drosophila*, the *naked cuticle* (*nkd*) gene antagonizes the Wnt/ β -catenin signaling in every segment of the embryo. Nkd is a modular, evolutionarily conserved protein that uses an EF-hand motif and adjacent sequences to target the cytoplasmic Wnt signal transducer Disheveled (Dsh). The mechanism by which Nkd antagonizes Wnt signaling in *Drosophila* embryos is not well understood. The abundance and bulk distribution of Dsh is not altered in *nkd*

mutants as compared to wild type embryos, and overexpression of Nkd transgenes in *nkd* mutants did not alter Dsh distribution or abundance by confocal microscopy. Nkd transgenes lacking Dsh-binding regions were mostly able to rescue *nkd* mutants, suggesting that the Dsh-binding regions of Nkd contribute little to Nkd activity, at least when the transgenes were overexpressed. In this thesis, I have investigated non-Dsh binding regions that are critical for Nkd function. Our lab's findings indicate that a conserved 30 amino acid motif is essential for Nkd nuclear localization and function. Substitution of the 30aa motif with a heterologous nuclear localization sequence (NLS) rescued some *nkd* mutants to adulthood. In support of Nkd's role in the nucleus, Nkd binds to Importin- α 3, an adaptor for the canonical nuclear import apparatus. I identified that Nkd associates with Importin- α 3 via a motif ("D6") that is conserved between *D. melanogaster* and *D. pseudoobscura*. Nkd ^{Δ D6}, lacking the Importin- α 3-binding motif, was defective in nuclear localization and in rescuing *nkd* mutants. RNAi knockdown of *importin- α 3* prevented the nuclear localization of Nkd. The findings that Nkd possesses two NLSs, each of which is required for function, and that Nkd associates with a component of the nuclear import apparatus, suggest that Nkd antagonizes the Wnt/ β -catenin signaling in the nucleus.

Furthermore, I also addressed the function of the N-terminus of *Drosophila* Nkd. Unlike mammalian Nkd homologs that have N-terminal myristoylation consensus sequences responsible for membrane association, the N-terminus of *Drosophila* Nkd, also conserved in mosquito Nkd, lack such a sequence. Nonetheless, Nkd's N-terminus was required for function and membrane association. Substitution of the N-terminus with

heterologous myristoylation sequences did not restore *nkd* function, indicating that the mechanism by which *Drosophila* Nkd associates with the membrane is different than mammalian Nkds. Therefore, Nkd appears to function in the membrane, in the cytoplasm to target Dsh, and in the nucleus to antagonize Wg signaling.

TABLE OF CONTENTS

COMMITTEE SIGNATURES	i
DEDICATION	ii
TITLE PAGE	iii
ACKNOWLEDGEMENT	v
ABSTRACT	vi
TABLE OF CONTENTS	ix
PRIOR PUBLICATIONS	xiv
LIST OF FIGURES	xv
LIST OF TABLES	xvii
CHAPTER I: INTRODUCTION	1
1.1 Overview of segmentation in <i>Drosophila</i> and vertebrates	1
1.1.1 The <i>Drosophila</i> paradigm: the hierarchical regulation of gap, pair-rule and segment polarity genes	3
1.1.2 Vertebrate somitogenesis: the vertebrate segmentation clock	5
1.2 Overview of pattern formation during <i>Drosophila</i> embryogenesis	7
1.2.1 Establishment of parasegments	7
1.3 Introduction to segment polarity genes	8
1.3.1 Discovery of segment polarity genes	8
1.3.2 The phenotypes of mutations in segment polarity genes	9
1.3.3 Classification of segment polarity genes based on molecular structures ...	11
1.4 Wnt signaling during segmentation process in <i>Drosophila</i>	12

1.4.1 Mutual reinforcement of Wg and Hh signaling in adjacent groups of cells defines the boundary of a parasegment.....	12
1.4.2 The Wingless gradient becomes asymmetrical due to signal-regulated Wg uptake/degradation.....	13
1.5 Overview of Wnt signaling pathways	14
1.5.1 The impact of Wnt signaling in development and disease.....	14
1.5.2 The molecular function of Wingless signaling components	14
1.5.3 The regulation of Wingless synthesis during embryo segmentation	15
1.5.4 The regulation of Wingless distribution during embryo segmentation.....	17
1.6 <i>nkd</i> is an inducible antagonist of the Wnt signaling pathway	19
1.6.1 Review of the <i>nkd</i> gene: the discovery and its role in segmentation	19
1.6.2 Nkd is conserved in evolution and each conserved motif performs unique functions.....	20
1.6.3 Nkd functions in a feedback loop to limit Wingless signaling cell-autonomously.....	22
1.6.4 Nkd targets the intracellular signal transducer Dishevelled.....	23
1.7 Summary of my recent findings	24
1.7.1 Nkd possesses two nuclear localization sequences (NLSs), both of which are required for function	25
1.7.2 Nkd engages the nuclear import adaptor Importin- α 3 to antagonize Wingless signaling.....	26
1.7.3 Nkd functions cell autonomously and in a myristyl-independent fashion to antagonize Wingless signaling in the embryo.....	26

CHAPTER II: An unconventional nuclear localization motif is crucial for function of the <i>Drosophila</i> Wnt/Wingless antagonist Naked cuticle	28
2.1 Introduction	29
2.2 Materials and methods.....	35
2.3 Results	41
2.4 Discussion	61
CHAPTER III: Cell-autonomous, myristyl-independent activity of the <i>Drosophila</i> Wnt/Wingless antagonist Naked cuticle	68
3.1 Introduction	69
3.2 Materials and methods.....	76
3.3 Results	80
3.4 Discussion	97
CHAPTER IV: <i>Drosophila</i> Naked cuticle engages the nuclear import adaptor Importin- α 3 to antagonize Wnt/ β -catenin signaling	104
4.1 Introduction	105
4.2 Materials and methods.....	108
4.3 Results	114
4.4 Discussion	132
CHAPTER V: Experiments in progress to investigate Nkd function	140
5.1 <i>nkd</i> loss-of-function by RNAi causes post-embryonic phenotypes.....	140
5.1.1 <i>nkd</i> knockdown mimics Wg gain-of-function phenotype.....	140
5.1.2 Experiments to verify specificity of <i>nkd</i> knockdown effect	142
5.1.3 Experiments to discover the function of <i>nkd</i> in post-embryonic stages...	143

5.2 α -Actinin negatively regulates Nkd activity	145
5.2.1 Introduction to α -Actinin	145
5.2.2 Nkd uses a conserved 30aa motif, previously reported to be critical for function, to interact with α -Actinin.....	148
5.2.3 The mechanism by which α -Actinin regulates Nkd activity	149
CHAPTER VI: DISCUSSION AND CONCLUSIONS	153
6.1 The domain functions of Nkd protein	153
6.1.1 N-terminus confers membrane association and is required for function .	153
6.1.2 The Dsh-interacting domain (“R1S” region) is required for cytoplasmic localization of Nkd, and is required for the full activity of Nkd.....	154
6.1.3 The 30 aa motif, most critical for function, is a NLS	155
6.1.4 The D6 region, interacting with importin- α 3, is a second NLS	156
6.2 Working models of Nkd function.....	158
6.2.1 Model 1: Separate pools of Nkd proteins antagonize Wingless signaling in different compartments: membrane, cytoplasm, and nucleus.....	158
6.2.2 Model 2: Nkd circulates intracellularly among membrane, cytoplasm and nucleus. The cycling is required for Nkd to inhibit Wingless signaling.....	159
6.2.3 Experimental strategies to discern the above two models	160
6.3 Future directions in unveiling the molecular mechanisms of Nkd function.....	161
6.3.1 Focus on the nucleus: by what mechanism does Nkd antagonize Wingless signaling in the nucleus?	161
6.3.2 To identify additional Nkd-interacting proteins.....	163

6.3.3 Does Nkd associate with chromatin in Wg-signaling-dependent target genes?.....	164
BIBLIOGRAPHY	166
VITAE	180

PRIOR PUBLICATIONS

Chih-Chiang Chan, Shu Zhang, Raphael Rousset, and Keith A. Wharton, Jr., *Drosophila Naked cuticle (Nkd) engages the nuclear import adaptor Importin- α 3 to antagonize Wnt/ β -catenin signaling*. Developmental Biology (2008), in press.

Chih-Chiang Chan, Shu Zhang, Tolga Cagatay, and Keith A. Wharton, Jr., *Cell-autonomous, myristyl-independent activity of the Drosophila Wnt/Wingless antagonist Naked cuticle (Nkd)*. Developmental Biology, 311: 538-553 (2007)

Sharon Waldrop, Chih-Chiang Chan, Tolga Cagatay, Shu Zhang, Raphael Rousset, Judy Mack, Wenlin Zeng, Matt Fish, Mei Zhang, Manami Amanai, and Keith A. Wharton, Jr., *An unconventional nuclear localization motif is crucial for function of the Drosophila Wnt/Wingless antagonist Naked cuticle*. Genetics 174: 331-348 (2006)

Abstract. “Importin- α 3-dependent engagement of the nuclear transport apparatus is required for Naked cuticle function during *Drosophila* segmentation” Chih-Chiang Chan, Raphael Rousset, and Keith A. Wharton, Jr. June 2007, The Wnt Meeting.
Winner of the Travel Award

Abstract. “Interaction between the nuclear import adapter importin- α 3 and the Wnt antagonist Naked cuticle” Chih-Chiang Chan, Raphael Rousset, and Keith A. Wharton, Jr. March 2007, 48th Annual *Drosophila* Research Conference “Pattern formation II: Platform presentation”.

LIST OF FIGURES

FIGURE 1.1	3
FIGURE 1.2	5
FIGURE 1.3	8
FIGURE 1.4	10
FIGURE 1.5	13
FIGURE 1.6	16
FIGURE 1.7	22
FIGURE 2.1	34
FIGURE 2.2	42
FIGURE 2.3	45
FIGURE 2.4	48
FIGURE 2.5	49
FIGURE 2.6	51
FIGURE 2.7	52
FIGURE 2.8	54
FIGURE 2.9	55
FIGURE 2.10	57
FIGURE 2.11	58
FIGURE 2.12	59
FIGURE 2.13	61
FIGURE 3.1	75
FIGURE 3.2	83

FIGURE 3.3	86
FIGURE 3.4	89
FIGURE 3.5	92
FIGURE 3.6	94
FIGURE 3.7	96
FIGURE 3.8	102
FIGURE 4.1	117
FIGURE 4.2	121
FIGURE 4.3	123
FIGURE 4.4	126
FIGURE 4.5	129
FIGURE 4.6	130
FIGURE 4.7	131
FIGURE 5.1	142
FIGURE 5.2	142
FIGURE 5.3	146
FIGURE 5.4	149
FIGURE 5.5	150

LIST OF TABLES

TABLE 1.1	11
-----------------	----

CHAPTER ONE

INTRODUCTION

1.1 Overview of segmentation in *Drosophila* and vertebrates

Many animals on the earth, including annelids, arthropods, and chordates, have a segmented body plan. The “protostomes” - an animal taxon that includes Arthropods and Annelids - and “deuterostomes” - an animal taxon that includes vertebrates - diverged at least 500 million years ago (Fig 1.1) (Davis and Patel, 1999). It is unclear whether segmentation in the aforementioned 3 animal phyla was independently derived or there was a common segmented ancestor (Davis and Patel, 1999; Peel et al., 2005; Damen, 2007). Much about what we know about the mechanisms of segmentation were discovered in the model organism *Drosophila melanogaster*. The systematic genetic screens performed by Nusslein-Volhard and Wieschaus uncovered mutations in 139 zygotic genes that are required for normal cuticle patterning (Nusslein-Volhard and Wieschaus, 1980; Jurgens et al., 1984; Wieschaus et al., 1984), setting the stage for researchers to discover the underlying mechanisms that regulate segmentation (See section 1.3 for more discussion). Because of the availability of sophisticated genetic and molecular biological tools, much progress have been made toward our understanding of the regulation of segmentation in *Drosophila*, although recent reports suggest that the paradigm of segmentation established in *Drosophila* may not even apply to all Arthropods {reviewed in (Peel et al., 2005; Damen, 2007)}.

Segmentation of the *Drosophila* embryo is initiated by a hierarchical cascade of expression of maternal, gap, pair-rule and segment polarity genes that subdivide the anteroposterior axis (as will be discussed in detail in section 1.1.1) (Sanson, 2001). Many genes that regulate segmentation have mammalian homologs, which when misregulated can cause diseases such as cancer. Many segment polarity genes, such as *armadillo* (*arm*), *pangolin* (*dTCF*), and *wingless* (*wg*), are components of the Wg signal transduction pathway, which plays an important role in *Drosophila* segmentation (as will be discussed in sections 1.2 and 1.3). In mammals, deregulation of the Wnt pathway can cause birth defects and diseases such as cancer, diabetes and osteoporosis {reviewed in (Clevers, 2006; Krishnan et al., 2006; Smith, 2007)}. Therefore, elucidating the mechanisms by which *Drosophila* segmentation is regulated might not only provide further insight into developmental biology, but also help gain insight into possible cures for human disease.

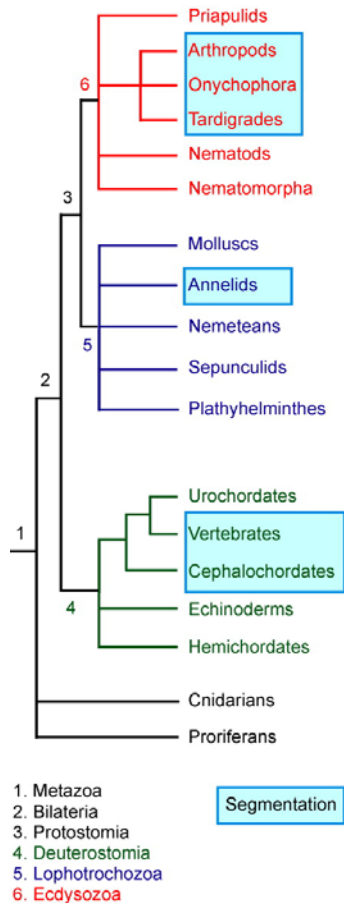


Figure 1.1. (from Damen 2007) Relationships of animal phyla. The diplobasts (animals with two germ layers) are in black, deuterostomes (“second mouth”; the first opening (the blastopore) becomes the anus) in green, lophotrochozoans (“crest-bearing animals”) in blue, and ecdysozoans (animals that undergo “ecdysis” – able to shed their exoskeleton) in red. Segmented phyla are in blue boxes. Note that not all phyla are included, but the omission does not affect the subdivision of the bilaterians into deuterostomes, lophotrochozoans, and ecdysozoans.

1.1.1 The *Drosophila* paradigm: the hierarchical regulation of gap, pair-rule and segment polarity genes

The interplay of maternal, gap, pair-rule and segment polarity gene expression from 5:20-7:20 hr AEL (After Egg Laying) (until mid-stage 11) establishes the repetitive segmental pattern of the embryo body plan (Fig. 1.2) (Hooper and Scott, 1992; Sanson 2001). After fertilization, the protein products of the spatially localized maternal genes, such as *bicoid*, *nanos*, and *caudal*, diffuse from the anterior or posterior poles of the embryo. These maternal factors regulate the spatial patterns of transcription of the gap genes, such as

hunchback and *knirps* {Reviewed in (Hoch and Jackle, 1993; Kornberg and Tabata, 1993)}. Gap genes are the earliest genes to be expressed from the zygotic genome, starting at stage 3 (1:05-1:20 h AEL). There are at least 11 gap genes, all of which encode transcription factors (Hulskamp and Tautz, 1991). Gap genes are expressed in discrete domains along the anterior posterior axis of the fly embryo by stage 4 (1:20-2:10 h AEL), thereby subdividing the embryo into broad domains. The gap genes regulate each other's expression domain as well as activate a set of 8 pair-rule genes such as *even-skipped* (*eve*), *hairy*, and *fushi-tarazu* (*ftz*) starting at stage 5 (2:10-2:50 h AEL (Campos-Ortega and Hartenstein, 1985). Pair-rule genes are expressed in 7 stripes of cells corresponding to every other presumptive segment. Almost all of the pair-rule genes encode for transcription factors (Pankratz and Jackle, 1993), except for *Tenascin major* which encodes a predicted transmembrane protein (Ben-Zur et al., 2000; Dgany and Wides, 2002). Pair-rule genes regulate the expression of genes in the next level of the hierarchy, the segment polarity genes such as *wg*, *hedgehog* (*hh*), and *engrailed* (*en*). Many of the segment-polarity genes are expressed in 14 segmentally repeated stripes, and they encode for a variety of protein products, such as secreted signaling molecules, receptors, kinases, etc. Segment-polarity genes regulate interactions between cells. One result of this hierarchy is the maintenance of the repeated expression patterns of segment polarity genes in every segment. Functional data to support the role of segment polarity genes in defining segments exists only from insects (DiNardo et al., 1988; Oppenheimer et al., 1999); however, similar expression patterns of segment polarity genes found in arthropods other than insects, such as spiders and millipedes, indicate that their functions are conserved (Damen, 2002; Hughes and Kaufman, 2002). The expression patterns of

pair-rule genes are more divergent in various arthropods, suggesting that the regulation of genes that control pair-rule gene expression has diverged in various arthropods (Maderspacher et al., 1998; Dearden and Akam, 2001; Damen, 2002). It has been proposed that Notch signaling, or a combination of Notch signaling and gap genes, controlled pair-rule and downstream genes to regulate segmentation in the common ancestor of arthropods. Through evolution, the influence of Notch signaling on pair-rule genes has been reduced, and gap genes gained more control of pair rule genes in more recent species, such as *Drosophila* (Damen, 2007).

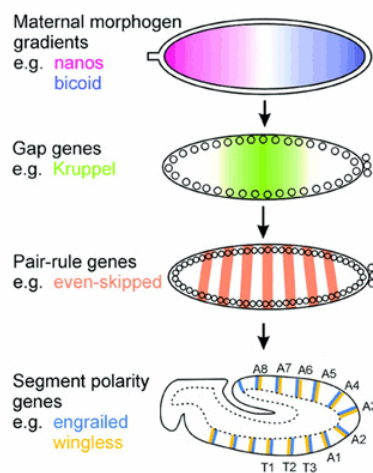


Fig. 1.2 (Modified from Sanson, 2001). Patterning along the anteroposterior axis of the *Drosophila* embryo. A cascade of maternal and zygotic genes is activated in the syncytial embryo to subdivide the ectoderm into smaller domains. The embryo cellularizes after activation of the pair-rule genes. The segment polarity genes are activated by the pair-rule genes. Segment polarity genes control the differentiation of each segment of the future larva.

1.1.2 Vertebrate somitogenesis: the vertebrate segmentation clock

That vertebrates are segmented is evidenced by the structure of our own backbones. In vertebrate segmentation, the somites - masses of mesodermal cells - are patterned during embryogenesis and give rise to skeletal muscles and vertebrae (Pourquie 1999, 2001). Somites form sequentially by budding off from the anterior end of the presomitic

mesoderm (PSM), while the PSM grows posteriorly (Saga and Tanaka, 2001). Somite patterning requires oscillatory gene expression driven by a “segmentation clock” that is controlled by Notch, FGF, and Wnt signaling (Bessho et al., 2001; Dubrulle et al., 2001; Aulehla et al., 2003). Activation of the Notch pathway results in activation of downstream targets such as the *Hes* genes, *Lunatic Fringe*, *Axin2* and *Nkd1* (Forsberg et al., 1998; Jouve et al., 2000; Audehla et al., 2003; Ishikawa et al., 2004). Notch signaling has been proposed to generate oscillations by negative feedback regulation of its downstream targets, *Lunatic Fringe* (Forsberg et al., 1998; Aulehla and Johnson, 1999) and *HES* genes (Jouve et al., 2000; Palmeirim et al., 1997). The FGF pathway can influence Notch signaling because ERK - a downstream target of FGF signaling – regulates cleavage of the Notch receptor (Kim et al., 2006). Wnt signaling can influence Notch signaling because the Wnt signal transducer Dishevelled can physically interact with Notch and block Notch signaling (Axelrod et al., 1996; Romain et al., 2001). And Notch signaling can influence Wnt signaling because *Nkd1* is a target of Notch signaling (Ishikawa et al., 2004). These and other links between these pathways results in oscillations of the gene expression in the PSM. A “clock and wavefront” model has been proposed to explain how segmentation is regulated by the interaction between a clock and a wavefront of cell maturity (Cooke and Zeeman, 1976). During somitogenesis, the clock is the oscillatory gene expression pattern, which determines the time of segmentation. The wavefront that determines the somite size depends on a gradient of FGF signaling pathway (Dubrulle et al., 2001; Sawada et al., 2001). The segmentation clock thus converts rhythmic gene expressions into spatial patterns.

1.2 Overview of pattern formation during *Drosophila* embryogenesis

1.2.1 Establishment of parasegments

The establishment of “parasegments” - organizing centers for later, definitive segmentation - is a crucial process during early embryogenesis in *Drosophila*. The genetic cascade described in section 1.1.1 subdivides the fly embryo into 14 repeating stripes, prefiguring the future segments of the embryo. The anterior and posterior boundaries of each parasegment are defined by stripes of cells expressing *wg* and *en*, respectively (Martinez-Arias and Lawrence, 1985) (Fig. 1.3). At stage 9-10, *en* and *wg* are required for each other’s expression: *wg* transcription disappears in *en* mutant embryos, while *en* transcription disappears in *wg* mutant embryos. *en*-expressing cells secrete Hh, which in turn maintains *wg*-expression in the anterior neighboring cell (DiNardo et al., 1988; Martinez-Arias et al., 1988; van den Heuvel et al., 1989; Hidalgo and Ingham, 1990; Gonzales et al., 1991). Each domain between the parasegment boundaries develops independently. At stage 12 the segmental boundaries are formed at the posterior edge of the *en* stripes (DiNardo et al., 1985; Weir and Kornberg, 1985). However the earliest repetitive units of patterning are the parasegments, although they are out of phase with the morphologically visible segments of the larva.

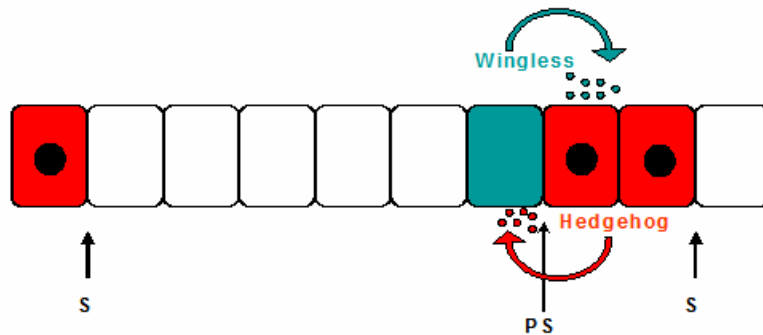


Fig 1.3. Schematic presentation of Wg-Hh mutual reinforcement to establish the parasegmental boundary. Depicted above is a schematic segment of the ventral epidermis of wild type stage 9-10 embryo, with anterior to the left. The parasegmental (PS) boundary corresponds to the interface between *wg* (blue) and *en* (black dot) / *hh* (red) transcriptional domains, whereas the segment (S) boundary forms posterior to *en/hh* domain. Blue square is Wg-expressing cell; Red squares are Eh/Hh-expressing cells. The interval between two S boundaries defines a segment.

1.3 Introduction to segment polarity genes

The segment polarity genes specify anteroposterior polarity within individual embryonic segments. Mutations of these genes showed disruption in patterning in each segment (Nusslein-Volhard and Wieschaus, 1980).

1.3.1 Discovery of segment polarity genes

The systemic screen for cuticle patterning mutations revealed 15 genes that were required for segmentation (Nusslein-Volhard and Wieschaus, 1980). However, the screens performed by Nusslein-Volhard and Wieschaus did not aim to discover maternally loaded components that function in during segmentation. By using X-ray irradiation to construct

germline clones, the segmentation phenotypes associated with the complete loss of some maternal genes were revealed. These maternal genes include *arm*, *dsh*, *porcupine* (*porc*), and *shaggy* (*sgg*) (Perrimon et al., 1989). These maternal and zygotic segmentation genes together organize the segmentally repeating pattern of the embryo. Some examples of the segment polarity genes include *naked cuticle* (*nkd*), *disheveled* (*dsh*), *hh*, and *patched* (*ptc*), all of which have been shown to be involved in either Wg or Hh signaling pathways through epistatic analysis (Noordermeer et al, 1994; Peifer et al., 1994; Siegfried et al., 1994; Hahn, 1999; Ingham and McMahon, 2001).

1.3.2 The phenotypes of mutations in segment polarity genes

The ventral cuticle of a wild type embryo is decorated with repeated denticle belts in the anterior part of each segment and naked areas in the posterior part. Mutations in segment polarity genes typically result in deleted regions of either denticle belts or naked areas in every segment. The deleted regions are often replaced with mirror-image duplication of the remaining area (Nusslein-Volhard and Wieschaus, 1980). Segment polarity genes have been placed into three categories based on their recessive embryonic-lethal mutant phenotypes (Fig 1.4) (Hooper and Scott, 1992):

Class I mutants have their posterior region (naked areas) replaced by a mirror-image duplication of the anterior region (i.e. denticles). The resultant phenotype is a cuticle consisting of all denticles. These genes are positive regulators of either the Wg or Hh signaling pathway. This is the largest group and includes *arrow* (*arr*), *arm*, *cubitus interruptus* *Dominant* (*ciD*), *dsh*, *en*, *fused* (*fu*), *gooseberry* (*gsb*), *hh*, *porc*, *smoothened*

(*smo*), and *wg* (Nusslein-Volhard et al, 1980, 1984; Kornberg, 1981; Orenic et al, 1987; Perrimon and Mahowald 1987; Perrimon et al., 1989).

Class II mutants have their anterior denticles deleted and replaced by posterior naked areas. Therefore the phenotype is a partial to complete naked cuticle. Examples are *apc2* (McCartney et al., 1999), *D-axin* (Willert et al., 1999), *chibby* (Takemaru et al., 2003), *nkd* (Jurgens et al., 1984) and *sgg* (Perrimon and Smouse, 1989), all of which are negative regulators of Wg pathway.

Class III mutants have their central region of each segment deleted and replaced by a mirror-image duplication of the segment border; hence they have mirror symmetric denticle belt duplications separated by naked areas. This class includes *ptc* and *costal-2* (*cos-2*), two negative regulators of the Hh signaling pathway (Nusslein-Volhard and Wieschaus, 1980; Grau and Simpson 1987; Hooper and Scott, 1989).

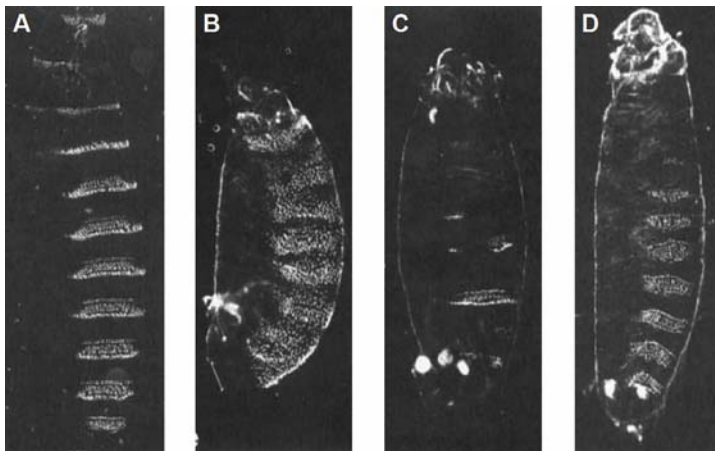


Fig. 1.4. Phenotypic classes of segment polarity genes. Dark field photographs of ventral cuticle patterns of wild type (A) and mutant larvae (B, C, D). The wild type larva is characterized by alternate denticle belts and naked areas. In type I larvae mutants the smooth posterior cuticle is replaced by denticle belt with reversed polarity. Examples are *arm*, *dsh*, *hh*, *porc*, and *wg*. In type II larvae mutants the denticle belts are deleted and

replaced by smooth posterior regions. Examples are *nkd* and *zw3*. Class III larvae mutants have mirror symmetric denticle belts separated by smooth posterior cuticle. *ptc* is one example. These photographs are taken from Ingham and Nakano, 1989.

1.3.3 Classification of segment polarity genes based on molecular structures

The segment polarity genes encode a diverse group of proteins, most of which have vertebrate homologues (Table 1.1). The molecular structures of segment polarity genes and their known homologs are summarized in Table 1.1.

Table 1.1 Segment Polarity Genes

Gene	Maternal / Zygotic	Protein product	Embryonic phenotype	Mammalian homolog
<i>armadillo</i>	Maternal	plakoglobin homolog	denticles replace naked cuticles	β -Catenin
<i>axin</i>	Maternal	intracellular scaffold	naked cuticle replaces denticles	Axin1, Axin2
<i>chibby</i>	?	?	naked cuticle replaces denticles	Chibby
<i>ciD</i>	Zygotic	transcription factor	denticles replace naked cuticles	Gli1, Gli2, Gli3, Gli4
<i>costal-2</i>	Maternal	intracellular scaffold	ectopic segment replaces central region	KIF4, KIF27
<i>dishevelled</i>	Maternal	intracellular scaffold	denticles replace naked cuticles	Dvl1, Dvl2, Dvl3
<i>engrailed</i>	Zygotic	homeodomain protein	denticles replace naked cuticles	En-1, En-2
<i>fused</i>	Maternal	serine/threonine kinase	similar to <i>arm</i> phenotype, but weaker	Stk36
<i>gooseberry</i>	Zygotic	homeodomain protein	similar to <i>arm</i> phenotype, but weaker	Pax3
<i>hedgehog</i>	Zygotic	secreted protein	denticles replace naked cuticles	Shh, Dhh, Ihh
<i>legless</i>	Maternal	?	denticles replace naked cuticles	BCL9, BCL9L
<i>naked cuticle</i>	Zygotic	intracellular scaffold	naked cuticle replaces denticles	Nkd1, Nkd2
<i>pangolin</i>	Maternal	transcription factor	denticles replace naked cuticles	LEF1
<i>patched</i>	Zygotic	transmembrane protein	ectopic segment and parasegment borders replaces central region	Ptch1, Ptch2
<i>pigopus</i>	Maternal	transcription factor	denticles replace naked cuticles	Pigo1, Pygo2
<i>porcupine</i>	Maternal	lipid modification enzyme	denticles replace naked cuticles	Porcn
<i>RacGAP50C</i>	?	Rho GTPase	naked cuticle replaces denticles	mgcRacGAP
<i>shaggy</i>	Maternal	serine/threonine kinase	naked cuticle replaces denticles	GSK-3 β
<i>smoothened</i>	Zygotic	transmembrane protein	denticles replace naked cuticles	Smo
<i>wingless</i>	Zygotic	extracellular matrix-associated protein	denticles replace naked cuticles	19 Wnts (Wnt1-11)

1.4 Wnt signaling during segmentation process in *Drosophila*

1.4.1 Mutual reinforcement of *Wg* and *Hh* signaling in adjacent groups of cells defines the boundary of a parasegment

The parasegmental boundary forms between *Wg*- and *En/Hh*-expressing cells, with boundary formation being disrupted when either *Wg* or *Hh* is mutant (Baker, 1988; Mohler, 1988). *Wg* and *Hh* act in a mutually reinforcing, positive feedback loop (Fig. 1.3): *Wingless* is expressed in a one cell wide stripe anterior to cells expressing *En* which coexpress the secreted signaling protein *Hh*. *Wg* is secreted and signals to adjacent posterior cells. Through the *Wg* signaling cascade, *en* and *hh* expression is maintained in *Wg* signal-receiving cells in stages 9-10 (3:40-5:20 h AEL). *hh* encodes a secreted molecule that can then maintain *wg* transcription in adjacent anterior cells. This mutual reinforcement ensures the maintenance of the parasegmental subdivisions along the anteroposterior axis. During stage 11 (5:20-7:20 h AEL), the expression of *wg* and *en* become independent of each other, and later *Wg* signaling defines specific cell fates. In the ventral epidermis, cells of each segment secrete either denticles or smooth cuticle. *Wg* signaling instructs anterior *En*-expressing cells differentiate the smooth (naked) cell fate (Dougan and DiNardo, 1992). Also at stage 11, the transmembrane Notch-pathway ligand *Serrate* (*Ser*) is expressed in the middle of the parasegment (Fleming et al., 1990). *Ser* activates the production of *Rhomboid* (*Rho*) - an activator of *Epidermal Growth Factor* (*EGF*) signaling (Gritzan et al., 1999; Sanson et al., 1999) - in the cells anterior to *Ser*-producing cells. *rho*-expression is activated by both *Ser* and *Hh* signaling, and resultant *EGF* signaling will instruct cells to adopt denticle cell fate via expression of the

Shavenbaby (Svb) transcription factor (O’Keefe et al., 1997; Szuts et al., 1997). At stages 11-12, cells anterior to Wg-expressing cells adopt naked cuticle fates by Wg suppressing Rho expression and EGF signaling (Fig 1.5). Nonetheless, low levels of EGF signaling are required to protect smooth cuticle cells from apoptosis, and thus EGF signaling is required for the survival of the naked and denticle-bearing cells (Urban et al., 2004).

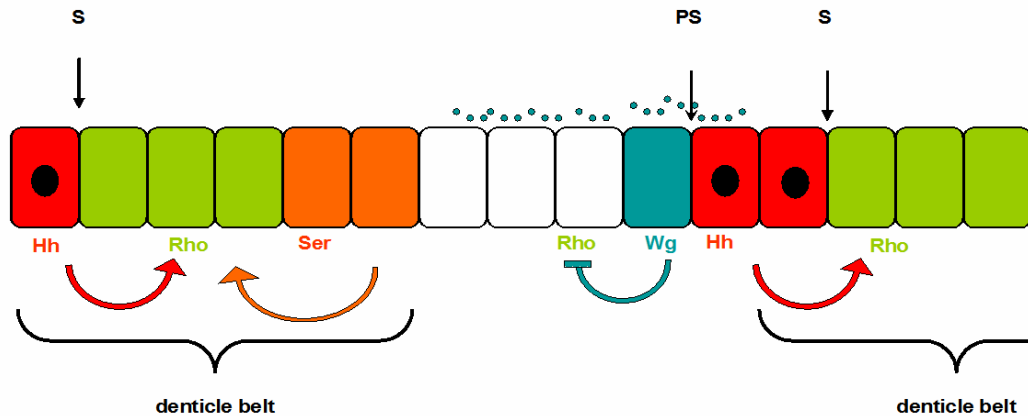


Fig. 1.5 A schematic segment of the ventral epidermis of wild type stage 12 embryo, with anterior to the left. The parasegmental (PS) boundary corresponds to the interface between *wg* (blue) and *en* (black dot) / *hh* (red) transcriptional domains, whereas the segment (S) boundary forms posterior to *en/hh* domain. Blue square is Wg-producing row of cells; Red squares are *Eh/Hh*-producing cells. Orange squares are *Ser*-producing cells. Green squares are *Rho*-producing cells. At the end of embryogenesis a denticle belt is seen in each segment, created by the second *Hh*-producing row of cells (row 1 denticle), *Rho*-producing cells (row 2-4 denticles), and *Ser*-producing cells (row 5-6 denticles).

1.4.2 The Wingless gradient becomes asymmetrical due to signal-regulated *Wg* uptake/degradation

Wg protein is symmetrically distributed during early embryonic development at stage 9; but, by later stage 11, the gradient of *Wg* distribution and activity is asymmetric.

Proposed explanations for the distribution preference include 1) restriction of the movement of Wg into the posterior region; and 2) selective degradation of Wg protein into the posterior region. By examining of the distribution dynamics of an epitope-tagged Wg protein, Wg was found at higher levels in the endolysosomal compartment in the posterior signal-receiving cells than in anterior cells (Dubois et al., 2001). This evidence favored the latter preferential degradation model. In the posterior En expressing cells Hh signaling is active and is required to prevent Wg degradation (Sanson et al., 1999). Posterior Wg degradation was reduced when the EGF pathway was blocked, suggesting that high levels of EGF signaling in the regions posterior to *en* stripes cause preferential Wg degradation in posterior signal-receiving cells at stages 11-12 (Dubois et al., 2001).

1.5 Overview of Wnt signaling pathways

1.5.1 The impact of Wnt signaling in development and disease

During animal development, Wnt ligands regulate several key processes, such as cell proliferation, cell migration and cell differentiation (Cadigan and Nusse, 1997; Wodarz and Nusse, 1998; Moon et al., 2002). In mammals, over-activation of the Wnt signaling pathway has been implicated in many diseases including cancer (Bienz and Clevers, 2000; Logan and Nusse, 2004). Wnt signals also govern stem cell renewal in several organs, such as hair and intestine (Kleber and Sommer, 2004; Polakis, 2007). Deregulation of Wnt signaling also causes osteoporosis, diabetes, and aging (Gong et al., 2001; Grant et al., 2006; Liu et al., 2007).

1.5.2 The molecular function of Wingless signaling components

Studies in numerous animals have led to a “standard model” for canonical Wnt signaling. When the Wnt receptor Frizzled (Wodarz and Nusse, 1998) and coreceptor LRP (Pinson et al., 2000; Tamai et al., 2000; Wehrli et al., 2000) are not bound by ligand, phosphorylation of β -catenin by a “destruction complex” (Kimelman and Xu, 2006) - consisting of the scaffold proteins Axin (Ikeda et al., 1998; Itoh et al., 1998) and Apc (Ahmed et al., 2002; Akong et al., 2002) as well as the serine/threonine kinases CK1 (Liu et al., 2002) and GSK3 (Behrens et al., 1998; Itoh et al., 1998) - is recognized by the F-box/WD repeat protein β -TrCP (Jiang and Struhl, 1998), a component of an E3 ligase complex which can promote the proteasome-dependent degradation of phosphorylated β -catenin (Bienz and Clevers, 2000; Polakis, 2000). In the nucleus, the binding of co-repressors including Groucho (Cavallo et al., 1998) to the transcription factor TCF (Bienz and Clevers, 2003; Cong et al., 2003; Tolwinski and Wieschaus, 2004) suppresses the transcription of Wnt-target genes (Fig. 1.6).

Once bound by Wnt, the Frizzled/LRP coreceptor complex activates the “canonical” signaling pathway. Frizzled interacts with Dsh (Wong et al., 2003), a cytoplasmic scaffolding signal transducer, and Axin is recruited to bind signal-induced phospho-LRP (Mao et al., 2001; Tolwinski et al., 2003), hence disrupting the destruction complex. Stabilized β -catenin then translocates into the nucleus and binds TCF to promote the transcription of Wnt target genes (Willert, 2006) (Fig. 1.6). *nkd* is one of the target genes of the Wg signal, and the Nkd protein antagonizes Wnt signaling, thereby constituting a negative feedback loop (Zeng et al., 2000).

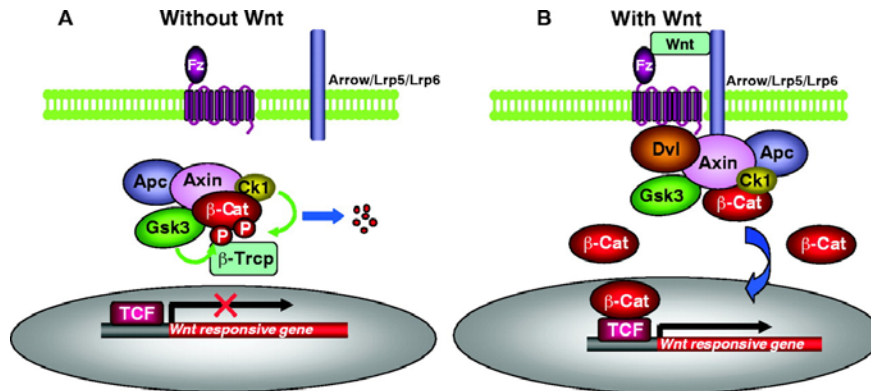


Fig 1. 6. A simplified view of Wnt/β-catenin signaling. (A) Without Wnt, the scaffolding protein Axin assembles a protein complex that contains Apc, Gsk3, Ck1. In this complex, β-catenin is sequentially phosphorylated by Ck1 and Gsk3. Phosphorylated β-catenin is recognized by β-Trcp. Poly-ubiquitinated β-catenin is degraded by the proteasome. (B) In the presence of Wnt, β-catenin phosphorylation and degradation is inhibited. Accumulated β-catenin forms a nuclear complex with the TCF transcription factor, and together they activate Wnt-responsive genes. This figure is from He et al., 2004.

1.5.3 The regulation of Wingless synthesis during embryo segmentation

Wnt signaling is tightly regulated at multiple steps ranging from ligand production, ligand delivery, and control of signaling activity at the receiving end. Recent discoveries have revealed insight into the maturation steps of Wnt protein, including post-translational modification, sorting, and secretion (Mann and Beachy, 2004; Miura and Treisman, 2006). In Wnt-expressing cells, multiple steps of quality control are necessary to make an optimal, mature Wnt protein that is functional upon secretion. Porcupine, a membrane-bound *O*-acyltransferase that resides in endoplasmic reticulum (ER), stimulates *N*-glycosylation of Wg by anchoring it at the ER membrane (Tanaka et al., 2002). Porcupine is also required for Wg palmitoylation, which increases Wg hydrophobicity and promotes membrane association (Zhai et al, 2004). Wnt3A is

palmitoylated at Cysteine⁷⁷ near the N-terminus, which may be required for proper intracellular routing, and which is required for function (Willert et al., 2003; Zhai et al., 2004).

Besides the default ER-Golgi-secretion route, some papers have suggested an alternative route of Wnt secretion. Because of lipid modification, the hydrophobic property of Wnt gives it a strong affinity for membranes. Therefore, free diffusion of Wnt seems unlikely over long distances. A fraction of Wnt that is dedicated to long-range signaling might be sorted to the endosome to be associated with lipoprotein particles (Panakova et al., 2005). Endosomal budding and formation of recycling vesicles might subsequently release the Wnt-lipoprotein-particle complex outside of the producing cells through exocytosis, thus allowing long range signaling along the developing field (Vincent and Dubois, 2002).

The membrane-bound protein Wntless is required for the secretion of Wnt from the signal-producing cells (Bartscherer et al., 2006). The retromer complex, a multiprotein complex that regulates intracellular protein sorting, is also responsible for the production of a functional Wnt (Coudreuse et al., 2006). Recent studies suggest that retromer and Wntless function cooperatively. The cycling of Wntless is retromer-dependent, and is promoted by Wnt secretion (Belenkaya et al., 2008; Franch-Marro et al., 2008; Port et al., 2008; Yang et al., 2008). In the absence of retromer, Wntless is degraded in lysosomes and Wnt secretion is impaired (Eaton 2008).

1.5.4 The regulation of Wingless distribution during embryo segmentation

The mechanism of Wnt protein distribution and/or transport is a subject of intense investigation, because it interests both researchers in the Wnt signaling field as well as those who study “morphogens” - molecules such as Decapentaplegic (Dpp), Hh, and Wg that spread from a localized site and form a concentration gradient across the developing region. Currently, three models have been proposed for Wg transport from site of synthesis to its delivery and interpretation in signal-receiving cells: cellular projection, diffusion, and transcytosis. The cellular projection model proposes that cell-cell contact through thin, actin-based cellular projections termed “cytonemes” can mediate morphogen transport (Ramirez-Weber and Kornberg, 1999). It has been shown that cytonemes play a role in Dpp signaling in the wing imaginal discs (Hsiung et al, 2005). However, currently there is no data regarding the functional significance of cell projections in Wingless transport.

The diffusion model suggests that secreted Wnt diffuses through the extracellular space to the target cells independent of intracellular trafficking (Strigini and Cohen, 2000). Even though this model seems intuitive, the fact that extracellular Wingless protein is found tightly associated with cell membranes and the extracellular matrix (Nusse et al, 1997) seems to argue that free diffusion is not sufficient to account for Wnt distribution and activity. A “facilitated diffusion” model has been proposed, in which Wg movement is facilitated or restricted by extracellular matrix components (Lin and Perrimon, 1999; Tsuda et al., 1999). For example, Dally - a glycosylphosphatidylinositol (GPI)-linked proteoglycan – preferentially localizes Wg on the basal surface of wing disc epithelium

where Dally is attached. The interaction between Wnt proteins and extracellular proteins or matrix components may promote low-level Wnt activity distant from Wnt source, but reduces signaling near the Wnt-producing site (Kirkpatrick et al., 2004; Kreuger et al., 2004). Extracellular proteins or matrix components may also help transport Wg through vesicles called argosomes, which are generated from membranes of signal-producing cells, and which can travel to distant regions of the wing disc (Greco et al., 2001).

Transcytosis refers to the vesicular transport of proteins from one side of cell to the other (Tuma and Hubbard, 2003). In the transcytosis model, the morphogen is passed from cell to cell through consecutive rounds of internalization, recycling to the cell surface, and release into the extracellular space for uptake by the neighboring cell.

Most of the data that support the transcytosis model derives from studies of the *Drosophila* embryo (Bejsovec and Wieschaus, 1995; Dierick and Bejsovec, 1998; Moline et al., 1999); whereas evidence for the “facilitated diffusion” model is gathered from the wing imaginal discs (Lin and Perrimon, 1999; Tsuda et al., 1999). It is still debatable which model of Wnt transport is correct. It is possible that in different contexts, such as in the fly wing disc vs. the embryo that one model of Wg transport is more likely to account for the action of Wg at a distance than the other model. Therefore, to distinguish under physiological conditions which model is more dominant in each context will help us understand the regulation of Wnt signaling.

1.6 *nkd* is an inducible antagonist of the Wnt signaling pathway

*1.6.1 Review of the *nkd* gene: the discovery and its role in segmentation*

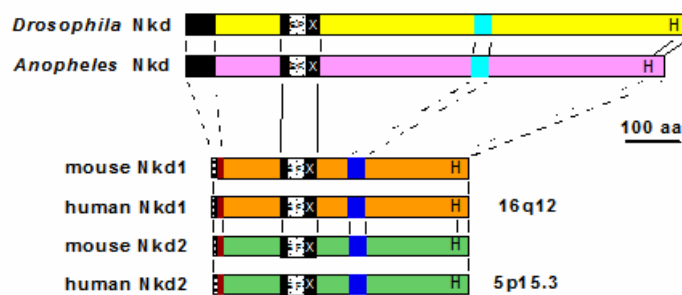
The *nkd* mutant was discovered in the Nusslein-Volhard and Wieschaus screens, and was classified as a segment-polarity gene (Jurgens et al., 1984). *nkd* loss of function results in segment polarity defects and embryonic death. In stage 9, *nkd* mutants have expanded *en* stripes probably due to mutant cells being hypersensitive to Wg (Martinez-Arias et al., 1988; Bejsovec and Wieschaus, 1993). Later in stage 11, an ectopic *wg* stripe posterior to the *en* stripe is formed in most segments, directing nearby cells to adopt the naked cuticle fate (Martinez-Arias et al., 1988). The *nkd* phenotype resembles that caused by widespread activation of Wingless cascade, which is similar to the phenotype caused by mutation in other negative regulators of the Wingless signaling pathway such as *apc2* or *zw3* (Siegfried et al., 1992; McCartney et al., 1999). *nkd* encodes an antagonist that functions in a negative feedback loop for signal transduction by Wg (Zeng et al., 2000). Misexpression of Nkd phenocopied adult phenotypes due to reduced function of *wg*, in support of Nkd's role as an inhibitor of Wnt signaling (Zeng et al., 2000). Injection of fly *nkd* RNA into frog embryos disrupted anteroposterior axis specification, and blocked XWnt8-dependent induction of the second axis, two events that depend on the canonical Wnt cascade (Zeng et al., 2000). This cross-species antagonism suggests that the inhibitory action of Nkd on Wnt signaling is evolutionarily conserved. Both *Drosophila nkd* and mammalian *nkd1* mRNAs are up-regulated by Wnt signaling, suggesting that the inhibition of Wnt signaling by Nkd in a negative feedback fashion is also conserved in mammals (Wharton et al., 2001; Yan et al., 2001).

1.6.2 Nkd is conserved in evolution and each conserved motif performs unique functions

The Nkd protein family is conserved through evolution (Fig 1.7). *Drosophila* has a single *nkd* gene, whereas known mammals have two homologs (Wharton et al., 2001). Sequence comparisons between mosquito and fly Nkd revealed four major blocks of similarity: the N-terminus, the EFX motif, a 30-aa motif, and a C-terminus histidine-rich region (Waldrop et al., 2006). Through our structure-function study described in Chapters 2-4, each domain's function has been investigated. Furthermore, within the genus *Drosophila*, *D. melanogaster* and *D. pseudoobscura* diverged at least 25 million years ago; hence the protein sequences shared between the two species must be important for protein function. A putative *nkd* cDNA sequence was assembled from *D. pseudoobscura* genome (Richards et al., 2005). Under the selection pressure, there are nine blocks of similarity in Nkd protein sequences (Chan et al., 2008). We recently discovered that conserved region number six ("D6" motif) is sufficient and required for binding to the nuclear import adaptor Importin- α 3 and is also required for Nkd function, as described in Chapter Four.

Like the fly and mosquito Nkds, mammalian Nkd1 and Nkd2 proteins also share four major blocks of sequence similarity. The N-terminus of Nkd2 was required for membrane association when overexpressed in cultured mammalian cells (Li et al., 2004). The EFX domain interacts with the bPDZ domain of Dsh and its mammalian homologs Dvl1, 2, and 3 (Rousset et al., 2001; Wharton et al., 2001). The fly and mammalian 30-aa motifs do not possess sequence similarity, but each is predicted to be an amphipathic α -helix (Waldrop et al., 2006).

Although both *Drosophila* and mammalian Nkds have a histidine-rich region in the C-terminal region, deletion of this region in *Drosophila* Nkd did not affect *nkd* rescue. Therefore in *Drosophila* the C-terminal motif seems dispensable for Nkd function. Truncation of the C-terminus increased Nkd protein accumulation, suggesting that degradation signals might reside in this region (Waldrop et al., 2006). Consistent with this observation, human Nkd1 mutant proteins truncated C-terminal of the 30 aa motif found in cancer samples accumulated to high levels in mammalian cell culture (Tolga Cagatay and Keith Wharton, unpublished data).



By Keith Wharton

Fig. 1.7. Schematic alignment of the Nkd protein family in the fruit fly *Drosophila*, the mosquito *Anopheles*, the mouse, and the human. The EFX domain and the histidine-rich C-terminal are conserved in all species compared. Blue boxes indicate 30-aa motif.

1.6.3 Nkd functions in a feedback loop to limit Wingless signaling cell-autonomously

Antagonists that restrain Wg signaling might limit the duration or range of the signal, or shut down the signal in the receiving end. Consequently, antagonists can function cell autonomously or non-autonomously. Nkd functions in a cell autonomous fashion in the

eye imaginal disc and in the embryo (Rousset et al., 2001; Chan et al., 2007). Nkd overexpression suppressed the effects of Wg or Dsh overexpression (Rousset et al., 2001). However, Nkd failed to suppress constitutively activated Armadillo; consistent with Nkd acting at the level of or upstream of Dsh but not downstream of Armadillo (Rousset et al., 2001). Moreover, Nkd uses its EFX domain and adjacent region to interact with the basic PDZ domain of the signal transducer Dsh (Rousset et al., 2002), in support of Nkd antagonizing Wnt signaling in a feedback fashion by targeting Dsh.

1.6.4 Nkd targets the intracellular signal transducer Dishevelled

Several lines of evidence suggest that the Nkd/Dsh interaction is critical for Nkd to antagonize Wnt signaling: 1) Nkd and Dsh interact in yeast two-hybrid, GST pulldown, and co-immunoprecipitation assays (Rousset et al., 2001, 2002); 2) fly or vertebrate EFX domains bind to both fly and vertebrate Dsh/Dvl proteins, indicating that Nkd/Dsh interaction is ancient in evolution (Wharton et al., 2001); 3) Nkd and Dsh colocalize in several *Drosophila* tissues, although in the embryo the colocalization is only observed for a subset of each protein in a punctate fashion (Waldrop et al., 2006); 4) Nkd misexpression specifically phenocopied loss of *dsh* activity in PCP (Planar Cell Polarity) signaling - a non-canonical Wnt signaling pathway that functions in a β -catenin independent fashion to regulate the polarity of hairs, bristles, and ommatidia in *Drosophila* {reviewed in (Peifer and Polakis, 2000; Veeman et al., 2003)} - possibly by sequestering Dsh from its normal sites of action (Rousset et al., 2001).

However, our studies have suggested that Nkd/Dsh association is not sufficient for Nkd function (Rousset et al., 2001; Waldrop et al., 2006). Moreover, recent findings in our lab have revealed that Nkd requires nuclear localization in order to function (see chapters 2 and 4). Whether Nkd and Dsh interact in the nucleus remains to be elucidated. Two nuclear localization sequences (NLSs) in fly Nkd have been identified (Waldrop et al., 2006; Chan et al., 2008); whereas *Xenopus* Dsh also possesses a NLS (Itoh et al., 2005), which is conserved in fly when both sequences are aligned and examined (Tolga Cagatay and Keith Wharton, unpublished data). *nkd* transgenes that are capable of rescuing *nkd* mutants did not cause obvious changes in intracellular localization of Dsh in the embryo, and no abnormalities in Dsh abundance or distribution were observed in *nkd* mutants (Waldrop et al., 2006). Because only a small fraction of Nkd appears to colocalize with Dsh, it is possible that the non-Dsh-interacting fraction of Nkd inhibits Wg signaling by mechanisms other than targeting Dsh in the cytoplasm. The fact that Nkd possesses 2 NLSs, both of which are required for function, suggests that Nkd plays a role in the nucleus. Therefore, it is critical to investigate whether the nuclear function of Nkd is Dsh-dependent or -independent.

1.7 Summary of my recent findings

I have been interested in understanding the regulation of Wnt signaling during pattern formation, and in particular the role of Nkd family of proteins in this process. My studies have focused mainly on the identification of proteins that regulate Nkd function. Through yeast two-hybrid screens, several Nkd-interacting proteins were identified.

Further experiments are ongoing to validate interactions between Nkd and retrieved interacting proteins, as well as to investigate how these novel proteins regulate Nkd function.

1.7.1 Nkd possesses two nuclear localization sequences (NLSs), both of which are required for function

Nkd was first thought to function in the cytoplasm based on its localization in embryos as measured by DAB immunohistochemistry (Zeng et al., 2000). However, by using confocal microscopy, we showed that a fraction of Nkd is in the nucleus. Furthermore, a structure-function study revealed two regions critical for Nkd function that also promoted nuclear localization of Nkd. In chapter 2 and 4, the major findings are that Nkd has 2 NLSs, the “30-aa” and the “D6” motifs, with the latter being a stronger NLS that interacts with nuclear import adaptor Importin- α 3 (Waldrop et al., 2006; Chan et al., 2008).

Deletion of either motif resulted in compromised *nkd* rescue activity, with deletion of the former motif compromising the ability of the mutant Nkd protein to reduce Arm levels and limit the expansion of En stripes, whereas deletion of the latter motif only affected En stripes (Waldrop et al., 2006; Chan et al., 2008). Unlike the prevailing view that Nkd antagonizes Wnt signaling by targeting Dsh in the cytoplasm, our findings indicate that Nkd plays a novel role in the nucleus to antagonize Wnt signaling. However, the mechanism by which Nkd functions in the nucleus, as well as whether Nkd/Dsh interaction occurs in the nucleus, remains to be elucidated.

1.7.2 Nkd engages the nuclear import adaptor Importin- α 3 to antagonize Wingless signaling

The canonical nuclear transport apparatus includes nuclear import adaptors of the Importin- α family, which link NLS-containing cargoes to importin- β for translocation into the nucleus. In chapter 4, I report that Nkd interacts with Importin- α 3, one of three Importin- α s in *Drosophila*. Importin- α 3 is required for the nuclear localization and function of Nkd. Knockdown of Importin- α 3 precluded Nkd from nuclear entry in salivary gland cells. These findings further support the hypothesis that Nkd inhibits Wnt signaling by functioning in the nucleus.

1.7.3 Nkd functions cell autonomously and in a myristyl-independent fashion to antagonize Wingless signaling in the embryo

Wg signaling is required for suppression of interommatidial bristle formation in the eye margin (Cadigan et al., 2002). Mutant clones of one *nkd* hypomorphic allele *nkd*^{7E89} mimicked the bristle suppression phenotype, suggesting that *nkd* regulates Wg signaling in the developing eye (Rousset et al., 2001). It has also been shown that Nkd functions cell-autonomously when misexpressed in eye imaginal discs (Rousset et al., 2001). However, whether Nkd functions cell-autonomously in the embryo had not been demonstrated. It was previously shown that in *nkd* mutant embryo, when a mutant dynamin protein (*shibire*) was overexpressed to block endocytosis in *en* domain, the En stripes were narrowed (Moline et al., 1999). This finding suggested that Nkd is required for Wg transport in cells posterior to Wg-producing cells; i.e. Nkd might function in cell

non-autonomous fashion. In chapter 3, our experiments suggest that Nkd functions in a cell autonomous manner in the embryo.

Mammalian Nkd1 and Nkd2 possess a myristoylation consensus sequence at their N-terminus for post-translational lipid modification (Wharton et al., 2001). This sequence is crucial for Nkd2 membrane association and Nkd2 function in promoting apical secretion of TGF α (Li et al., 2004). Similarly, in *Drosophila*, the N-terminus of Nkd, conserved between *Drosophila* and mosquito Nkd, is required for membrane attachment and function (Chan et al., 2007). This finding and the results from chapters 2-3 suggest that Nkd acts at multiple subcellular locations in signal-receiving cells to attenuate the response to Wnt signaling.

PREFACE TO CHAPTER TWO

CHAPTER TWO describes a mechanistic view of Nkd function in antagonizing Wnt signaling. It is adapted from “Waldrop *et al.*, 2006 S. Waldrop, C.C. Chan, T. Cagatay, S. Zhang, R. Rousset, J. Mack, W. Zeng, M. Fish, M. Zhang, M. Amanai and K.A. Wharton Jr., *An unconventional nuclear localization motif is crucial for function of the Drosophila Wnt/wingless antagonist Naked cuticle*, *Genetics* 174 (2006), pp. 331–348.”

FOR THIS WORK, I HAVE CONTRIBUTED IN SEVERAL WAYS. I EXAMINED THE INTERACTION BETWEEN DSH AND NKD MUTANT PROTEINS IN Y2H ASSAY, AND SHOWED THAT THE NKD^{RIS} REGION IS REQUIRED FOR NKD/DSH INTERACTION. I ALSO SHOWED THAT THE 30AA MOTIF DOES NOT INTERACT WITH DSH IN Y2H. I ALSO GENERATED *UAS-NKD* ^{Δ 30AANLS/GFPC} TRANSGENIC FLY AND PUT IT INTO *NKD* MUTANT BACKGROUND FOR SUBSEQUENT STAINING AND CUTICLE PREP. IN ADDITION, I ALSO HELPED IN SEQUENCING *NKD* MUTANT ALLELES. SHARON WALDROP AND KEITH WHARTON DID ALL THE RESCUE ASSAYS AND EMBRYO STAINING. KEITH WHARTON DID ALL THE CONFOCAL IMAGING. TOLGA CAGATAY SHOWED THAT NKD AND DSH ARE NOT CLEAVED IN THE EMBRYOS BY WESTERN BLOT.

CHAPTER TWO

AN UNCONVENTIONAL NUCLEAR LOCALIZATION MOTIF IS CRUCIAL FOR FUNCTION OF THE *DROSOPHILA* WNT/WINGLESS ANTAGONIST NAKED CUTICLE

2.1 Introduction

Pattern formation in multicellular animals is governed by the intensity, duration, and combination of signals received by each developing cell. Wnts are a family of highly potent and potentially oncogenic protein signals that specify cell fate and behavior throughout the animal kingdom, and, in the vertebrate, renew stem cells (Logan and Nusse 2004; Reya and Clevers 2005). Abnormal Wnt signaling perturbs development and can cause human diseases (Moon et al. 2004). Feedback regulation—the signal-dependent induction of genes that control signal flux—is a prominent mechanism by which responses to Wnt and other signals are kept within a physiological range, thereby ensuring accurate patterning in the face of environmental perturbation or altered gene dosage (Freeman 2000).

Many Wnts manifest activity via accumulation of β -catenin, a bifunctional, intracellular adaptor protein that regulates cell adhesion at the plasma membrane and transmits Wnt signals into the nucleus (Bienz 2005; Harris and Peifer 2005). Indeed, in a variety of contexts and animals, loss or gain of β -catenin activity mimics absent or maximal Wnt signaling, respectively (*e.g.*, Pai et al. 1997; Gat et al. 1998; Huelsken et al. 2001; Zechner et al. 2003). In the canonical "Wnt/ β -catenin" pathway (recently reviewed by

Cadigan and Liu 2006; Willert and Jones 2006), Wnt engages Fz/LRP receptors to activate Dishevelled (Dsh), which inactivates a β -catenin "destruction complex" composed of the tumor suppressors Axin/Apc and kinases CK1/GSK3 β , leading to intracellular β -catenin accumulation and activation of Wnt target genes via binding to Lef/TCF and other transcriptional regulatory proteins (see <http://www.stanford.edu/~rnusse/wntwindow.html>). Dsh also relays a parallel, LRP-dependent signal that culminates in Axin/LRP association and Axin degradation (Cliffe et al. 2003; Tolwinski et al. 2003; Davidson et al. 2005; Zeng et al. 2005). Fz and Dsh, but not LRP or downstream proteins that regulate β -catenin turnover, participate in noncanonical pathways, the best understood of which executes planar cell polarity (PCP) (Veeman et al. 2003).

Although often dubbed a "scaffolding protein" by virtue of its ability to bind a multitude of proteins, Dsh has been likened to a network hub or node because it links distinct signaling inputs to pathway-specific effectors. However, Dsh's dynamic localization to several subcellular compartments, its tendency to aggregate, and its apparent lack of catalytic activity have rendered accurate comprehension of its molecular and cell biological mechanisms an unexpectedly daunting prospect (Torres and Nelson 2000; Capelluto et al. 2002; Schwarz-Romond et al. 2005; Smalley et al. 2005; reviewed by Boutros and Mlodzik 1999; Wharton 2003; Wallingford and Habas 2005; Malbon and Wang 2006). Complicating matters further, recent RNA interference screens indicate that nearly 250 genes—>1% of the fly genome—impinge upon Wnt/ β -catenin signaling (DasGupta et al. 2005).

Key Wnt signal transducers and their epistatic relationships were discovered through genetic analysis of embryonic development in *Drosophila melanogaster* (Nusslein-Volhard and Wieschaus 1980; Ingham 1988; Noordermeer et al. 1994; Siegfried et al. 1994). Following cellularization of the blastoderm embryo [embryonic stages 5–7, ~2–3 hr after egg laying (AEL)], sequentially acting "gap" and "pair-rule" transcription factors initiate "segment-polarity" gene activity with a spatial periodicity that prefigures the segmented body plan (Nusslein-Volhard and Wieschaus 1980; Ingham 1988). Segment-polarity genes largely encode transducers for Wnt and Hedgehog (Hh) signals. Pair-rule genes act in a dual capacity by conferring upon alternating cell territories a competence to produce either Hh or the Wnt protein Wingless (Wg) and by initiating *wg* and *hh* transcription in abutting single-cell-wide transverse stripes (Figure 2.1A) (Martinez Arias et al. 1988; Martinez Arias 1993; Cadigan et al. 1994). Wg has two temporally distinct activities in ectodermal patterning. First, during early to middle germband extension (stages 8–11, ~3.5–6 hr AEL), Wg maintains the transcription of the target genes *hh* and *engrailed* (*en*) at close range in the two to three rows of cells posterior to Wg-producing cells (reviewed by Dinardo et al. 1994; Hatini and Dinardo 2001). Thus the width of the *hh/en*-expressing stripe—the posterior border of which marks the segment boundary, a guidepost for axonal pathfinding and muscle attachment—is a readout of the Wg-signaling gradient (Figure 2.1A) (Larsen et al. 2003). Second, ventral cells exposed to Wg after ~6 hr AEL, upon differentiation, suppress the synthesis of cell protrusions termed denticles and appear "naked," whereas cells out of range of Wg produce denticle bands that facilitate larval locomotion (Bejsovec and Martinez Arias 1991; Dougan and Dinardo 1992). Genetic evidence suggests that early Wg/Hh and later Notch and EGF signals

influence denticle fates, the latter signal by activating the transcription factor Svb in denticle-bearing cells (Bejsovec and Wieschaus 1993; Alexandre et al. 1999; Payre et al. 1999; Hatini and Dinardo 2001; Price et al. 2006). Cuticle pattern thus is a sensitive indicator of Wg signaling: defective signaling results in a "lawn of denticles" phenotype, whereas enhanced signaling due to mutation of negative regulators such as *axin*, *apc2*, *GSK3 β* , or the aptly named *naked cuticle* (*nkd*) results in secretion of "naked" cuticles (Nusslein-Volhard and Wieschaus 1980; Siegfried et al. 1992; Hamada et al. 1999; McCartney et al. 1999; Zeng et al. 2000).

nkd is unique among known regulators of Wg signaling for its exclusively zygotic expression and genetic requirement (Jurgens et al. 1984; Zeng et al. 2000).

[Hypomorphic mutations in the fly β -catenin homolog *armadillo* (*arm*) give rise to zygotic *wg*-like phenotypes due to the lability of maternal Arm protein (Riggelman et al. 1990)]. In *nkd* mutants, the expression of *wg* and *hh/en* by stage 8 appears normal, but by stages 9–10 apparently wild-type levels of Wg broaden the territory of *hh/en* transcription to include additional posterior cells that are distant from the source of Wg (Figure 2.1A) (Martinez Arias et al. 1988; Lee et al. 1992; Tabata et al. 1992; Bejsovec and Wieschaus 1993). Increased Wg protein has been observed in posterior signal-receiving cells of stage 10 *nkd* mutants, possibly due to defective Wg trafficking (Moline et al. 1999). By stage 11, depending on the severity of the *nkd* allele, elevated Wg and Hh signaling induces a new, thin stripe of Wg that abuts the widened *hh/en* stripe (Martinez Arias et al. 1988; Bejsovec and Wieschaus 1993). Ectopic Wg transforms the fate of nearby cells from denticle producing to naked and promotes cell death, resulting in a shortened cuticle

(Bejsovec and Wieschaus 1993; Pazdera et al. 1998). Embryos homozygous for strong *nkd* alleles, such as *nkd*^{7H16} or *nkd*^{7E89}, usually produce two or fewer (but frequently no) complete denticle bands due to robust ectopic Wg production, while weaker (yet still embryonic lethal) *nkd* alleles, such as *nkd*^{6J48} or *nkd*^{42J1}, may exhibit a normal or nearly normal cuticle pattern due to rare ectopic Wg (Jurgens et al. 1984; Zeng et al. 2000; this study).

We previously showed that *Drosophila nkd* encodes a "pioneer" EF-hand protein that inhibits Wnt/ β -catenin signaling by targeting Dsh (Zeng et al. 2000; Rousset et al. 2001, 2002). Mice and humans each have two Nkd-related proteins that can bind Dsh and inhibit Wnt signaling when overproduced in cultured cells (Katoh 2001; Wharton et al. 2001; Yan et al. 2001). Nkd family proteins are distinguished from an otherwise large number of EF-hand-containing proteins by an ~60-amino-acid region of sequence homology within and immediately adjacent to the EF-hand motif that we have termed the EFX domain (Wharton et al. 2001). Surprisingly, EFX is the only region of extended sequence similarity shared between fly and mammalian Nkds, and it is sufficient to mediate cross-species binding to fly or mouse Dsh proteins (Wharton et al. 2001). Here we employ genetic, cell biological, and structure–function analyses to show that *Drosophila* Nkd uses separable, conserved motifs that target Dsh and allow nuclear entry, thereby limiting Arm/ β -catenin accumulation and Wg target gene expression.

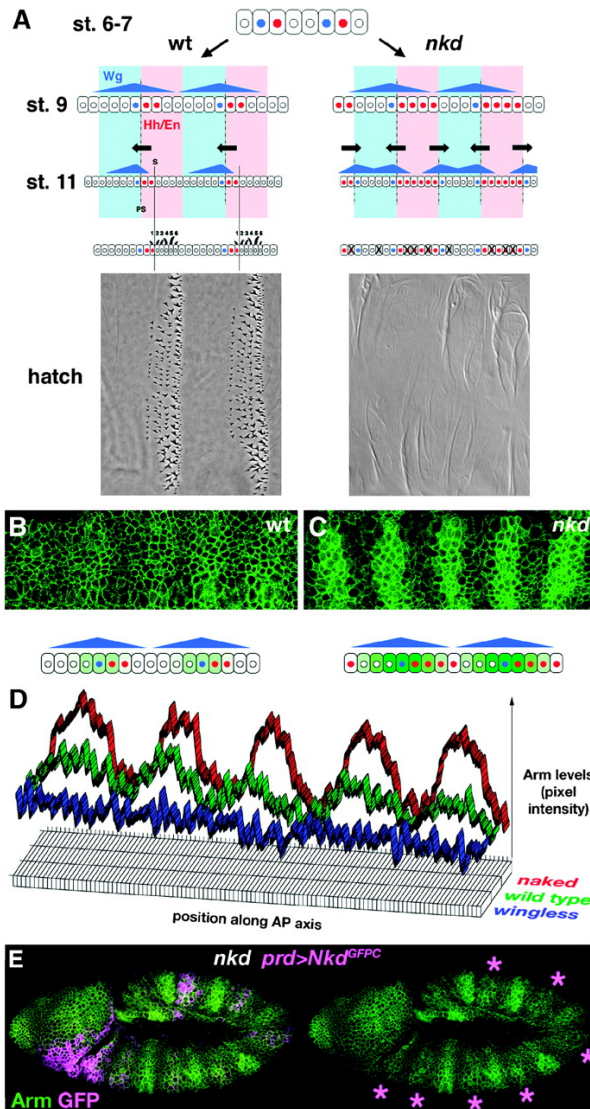


Fig. 2.1. Nkd antagonizes Arm/ β -catenin accumulation. (A) Schematic of ectodermal gene expression in wild type (wt, left) and *nkd* (right) embryos. Stages 6–7: Wg (blue) and Hh/En (red) initiate in adjacent cell rows. Stage 9: In wild type, Wg protein distributes in a gradient (blue triangle) and maintains Hh/En in approximately two cell rows while, in *nkd*, Hh/En is expressed in all competent cells (red shading). Wg expression-competent cells are in blue shading. Stage 11: In wild type, the Wg gradient is biased to the anterior while, in *nkd*, Wg is ectopically produced by some anterior Wg-competent cells, causing boundary duplications with reversed polarity (arrows). Parasegmental (PS) and segmental (S) boundaries are designated. "hatch": Denticle rows 1–6 are produced in a trapezoidal band, two belts of which are depicted. In *nkd*, ectopic Wg promotes cell death (X) and suppresses denticle synthesis. (B and C) Five segmental anlagen of stage 10 wild type (B) or *nkd*^{7H16} (C) embryos stained for Arm (green) above

schematic. (D) Mean pixel intensity across five segmental anlagen from Arm-stained stage 10 *wingless* (blue), wild-type (green), and *naked* (red) mutants. (E) Stage 10 *UAS-Nkd^{GFPC};nkd^{7H16}prd-Gal4/nkd^{7H16}* embryo stained for Arm (green) and GFP (purple). Note reduced Arm in *Nkd^{GFPC}*-expressing segments (asterisks).

2.2 Materials and methods

2.2.1 DNA constructs:

D. melanogaster Nkd (GenBank AF213376) constructs were built in Bluescript-II-KS+ (Stratagene, La Jolla, CA) with C-terminal enhanced GFP (CLONTECH, Palo Alto, CA) or *myc* tags. DNA fragments were synthesized by Pfu PCR, subcloned/sequenced, and cloned into pUAS-T (Brand and Perrimon 1993). *Nkd^{rEF/mycC}* replaced aa 179–225 with aa 87–133 of recoverin (M95858); *Nkd^{hEFX2/mycC}* replaced aa 179–248 with aa 113–178 of human Nkd2 (NM_033120). Residues deleted were the following: *Nkd^{ΔRB/mycC}* 179–292; *Nkd^{ΔEFX/GFPC}* 177–253; *Nkd^{ΔYS/GFPC}* 248–370; *Nkd^{ΔRIS/GFPC}* 179–370; *Nkd^{ΔBBg/GFPC}* 295–824; *Nkd^{ΔARBg/GFPC}* 178–824; *Nkd^{NBg/GFPC}* 827–928; *Nkd^{NGA/GFPC}* 713–928; *Nkd^{NIN4/GFPC}* 573–928; *Nkd^{NIN3/GFPC}* 448–928; *Nkd^{NBam/GFPC}* 296–928; *Nkd^{NR1/mycC}* 179–928; *Nkd^{7H/mycC}/Nkd^{7H/GFPC}* 60–928; *Nkd^{Δ30aa/GFPC}* 543–572; *Nkd^{RIS/mycC}* 1–176 and 373–928; *Nkd^{EFX/GFPC}* 1–176 and 249–928. *Nkd^{Δ30aaNLS/GFPC}* replaced aa 543–572 with the SV40 NLS (APKKKRKVGST) (Kalderon et al. 1984; Tolwinski and Wieschaus 2004). *mNkd1^{f30aa/GFPC}* replaced aa 248–274 of mNkd1 (GenBank NM_027280) with Nkd aa 543–572. *Nkd^{D201A/mycC}*, *Nkd^{NIN3/GFPC}*, *Nkd^{NBam/GFPC}*, *Nkd^{RIS/mycC}*, *Nkd^{NR1/mycC}*, and *Nkd^{EFX/GFPC}* have been previously described (Rousset et al. 2002).

2.2.2 Fly stocks and genetics:

Fly transformation/culture were performed according to standard methods. Balanced *UAS-Nkd* lines (at least three/construct) were screened for activity by examining adult progeny when crossed to *B119-Gal4* and *GMR-Gal4,UAS-Dsh* (Zeng et al. 2000; Rousset et al. 2001). Two (or more where specified) second chromosome lines with strong overexpression effects (when compared to all lines of each construct) were studied in *nkd* rescue, with the exception that a single second chromosome *UAS-Nkd^{NGA/GFP}* line was obtained. For *nkd* rescue, all crosses were performed as described (Rousset et al. 2002) at 25°. All Dsh coexpression crosses were performed with *UAS-Dsh* or *UAS-Dsh^{GFP}* (Axelrod et al. 1998; Axelrod 2001). *wg^{IL14}* (Gonzalez et al. 1991) was used at the nonpermissive temperature of 25° in the experiments in Figure 2.1D and Figure 2.12, A and B.

2.2.3 Cuticles:

Cuticle preparations were performed as previously described, with 125–600 cuticles for each cross and genotype scored as wild type, mild, moderate, or strong according to described criteria (Zeng et al. 2000; Rousset et al. 2002). For *UAS-Nkd* constructs with substantial activity, rescued *nkd* cuticles selected for photography either were identified by *nkd* head involution or spiracle elongation defects not seen in control crosses or were individually selected by the absence of balancer-linked GFP fluorescence. All crosses to assess cuticle rescue, except where indicated, were performed in a *nkd^{7H16}/nkd^{7E89}* background. Since *nkd^{7E89}* encodes a potentially truncated protein that retains Dsh-binding regions (Figure 2.9A), we confirmed that *UAS-Nkd^{ΔRIS/GFP}*, lacking the Dsh-binding

regions, rescued *nkd*^{7H16} cuticles and En stripe width to an extent comparable to *nkd*^{7H16}/*nkd*^{7E89} (not shown) to rule out the possibility that the rescuing activity of Nkd^Δ_{RIS/GFPC} was due to the presence of an intact Dsh-binding sequence encoded by the *nkd*^{7E89} chromosome. For scoring the phenotype of *nkd* alleles (Figure 2.9B), "complete" denticle bands were scored if six denticle rows could be unambiguously identified and trapezoidal morphology was evident, whereas "partial" bands had either fewer than six denticle rows (except A1, which has three rows) or discontinuous replacement of denticle rows by naked cuticle due to patchy ectopic Wg production. Although *nkd*^{47K1} and *nkd*^{7E89} have identical mutations and each has a wide En stripe during stage 11 (Figure 2.9A), their slight difference in cuticle phenotype (Figure 2.9B) could be due to the different genetic backgrounds in which each was generated (*ru cu ca* for *nkd*^{7E89} vs. *red e* for *nkd*^{47K1}).

2.2.4 Computer programs and web tools:

Figures were constructed in Adobe Photoshop and Canvas (ACD Systems). Graphs were generated in Deltagraph (Red Rock Software). Secondary structure prediction was obtained at <http://bmerc-www.bu.edu/psa>. Helical wheel output (Figure 2.10B) was obtained at <http://cti.itc.virginia.edu/~cmg/Demo/wheel/wheelApp.html>. ClustalW analysis and linked Boxshade output was obtained at <http://dot.imgen.bcm.tmc.edu:9331/multi-align/multi-align.html>.

2.2.5 Immunocytochemistry:

Embryos were collected on yeast/grape juice agar, dechorionated in 50% bleach for 2 min, fixed in 50:50 PBS + 4% formaldehyde/heptane for 20 min, devitellinized in 50:50 heptane/methanol, rehydrated in PBS + 0.1% Triton X-100 (PBT), blocked in PBT + 5%

goat serum (PBTN), and then incubated with antibodies/PBTN with rocking at 4°.

Embryo heat fixation was performed as described (Zeng et al. 2000). Primary antibodies/dilutions were the following: rat- α -Nkd (Zeng et al. 2000) 1:100; rabbit- α -Dsh (a kind gift from R. Nusse) 1:200 and α - β -gal (Molecular Probes, Eugene, OR) 1:500; biotinylated- α -GFP (Molecular Probes) 1:200; monoclonal Abs: α -En (4D9, a kind gift from N. Patel) (Patel et al. 1989) 1:200; α - β -gal (Promega, Madison, WI) 1:1000; α -myc (Sigma, St. Louis) 1:500; α -Arm [N2-7A1, Developmental Studies Hybridoma Bank (DSHB)] (Riggleman et al. 1990) 1:500; α -Wg (4D4, DSHB) (Brook and Cohen 1996) 1:50. Secondary antibodies/dilutions were the following: biotinylated- α -mouse and α -rabbit IgG, FITC- α -rat, rhodamine- α -rabbit and rhodamine- α -mouse (Jackson ImmunoResearch, West Grove, PA) 1:200. En was visualized using Vectastain ABC Elite (Vector Labs, Burlingame, CA), 3,3'-diaminobenzidine (DAB), and 30 mM NiCl enhancement. Nkd^{GFP}s were visualized by streptavidin-FITC (Jackson ImmunoResearch) at 1:1000. DNA was visualized using DRAQ5 (Alexis Biochemicals) at 1:1000 following RNase-A digestion to minimize cytoplasmic mRNA staining.

2.2.6 Microscopy:

Adult flies were photographed as described (Rousset et al. 2002). DAB-stained embryos were cleared through graded ethanols into methyl salicylate and viewed under Nomarski optics on a Zeiss Axioplan IIie. Rescued *nkd* embryos were unambiguously identified by lack of head-specific β -gal encoded by the *hb-lacZ* transgene on the TM3 balancer chromosome. At least 20 rescued stage 11 embryos were examined in each collection, and representative embryos were photographed. Fluorescent-labeled embryos were

mounted in Fluoromount G (Southern Biotechnology) and images were acquired on a Nikon C1 confocal microscope with 488-, 543-, and 633-nm lasers using 40x and 100x oil objectives and 8-pass Kalman averaging. FITC/DRAQ5 and rhodamine were sequentially scanned to prevent bleed through of FITC-emitted signals. Three or more embryos of representative stages (typically stages 9–11) were examined under multiple confocal fields for each construct/line tested. For SEM, adult flies were fixed in 100% ethanol, 2% glutaraldehyde, postfixed in 1% OsO₄ in 0.1 M cacodylate buffer, and dehydrated through graded ethanols. Specimens were mounted, critical point dried, sputter coated, and viewed on a JEOL 820A electron microscope.

2.2.7 Image analysis:

Confocal images of Arm-stained embryos were oriented along the anterior–posterior axis, analyzed in ImageJ (National Institutes of Health), and presented graphically via Deltagraph.

2.2.8 *nkd* viability assays:

Hatching frequency (Figure 2.3O) was determined by selecting, 6–12 hr AEL, GFP– (or dim, for Nkd^{GFP}-expressing constructs) embryos from the cross *UAS-Nkd;nkd^{7H16}/TM3-GFP* x *nkd^{7E89}da-Gal4/TM3-GFP* and culturing the embryos on grape juice agar at 25° until hatching. Adult viability (Figure 2.3P) was determined by individually transferring GFP– or dim crawling first instar larvae to yeast paste/grape juice agar at 21° and scoring for viability to the indicated stage until death or eclosion. All rescued adults lacked *Sb* on the TM3 balancer, confirming the rescued *nkd* genotype. *nkd^{7H16}* animals survived to a comparable degree as *nkd^{7H16}/nkd^{7E89}* animals (not shown).

2.2.9 Yeast two-hybrid:

Yeast two-hybrid and yeast extract preparation was performed as described (Rousset et al. 2001) in the yeast reporter strains Y190 (ONPG assay) and AH109 (growth assay) (CLONTECH). Figure 2.6C and Figure 2.8C show the mean \pm SD β -gal units for four independent experiments performed in triplicate for each plasmid combination.

2.2.10 Leptomycin-B treatment of embryos:

Embryos expressing constructs indicated in Figure 2.4 were dechorionated and rocked in 50:50 octane/PBS \pm 0.158 μ g/ml leptomycin-B (LMB; Sigma) for 30 min at 21°. PBS/LMB was aspirated and the embryos were fixed, stained, and imaged as described.

2.2.11 *nkd* allele sequencing:

nkd alleles were generated in an isogenized *red e* background (W. Zeng and M. P. Scott, unpublished data). Genomic DNA was prepared from adult flies carrying each *nkd* allele over a balancer chromosome. Overlapping primers for each *nkd* coding exon were designed to amplify 400- to 500-bp fragments. PCR fragments were purified on an agarose gel, eluted using the QIAquick gel extraction kit (QIAGEN, Chatsworth, CA), and sequenced from the 5'- and 3'-ends.

2.2.12 Western blots:

Dechorionated 0- to 5-hr embryos were dounce homogenized in 5 vol of cold lysis buffer [50 mM Tris-HCl, pH 7.5, 150 mM NaCl, 1% NP40, 0.5% sodium deoxycholate, 1 mM DTT, 1 mM PMSF, supplemented with complete protease inhibitor (Roche)]. The homogenate was centrifuged at 14,000 x g for 15 min to pellet debris, and 100 μ g crude

extract was resolved on 10% SDS–PAGE and transferred to PVDF membrane. For yeast Western blots, 10 µg supernatant was loaded per lane. Antibodies/dilutions were the following: rabbit α -GFP1 (Santa Cruz Biotechnology) 1:3000; mouse mAbs α -myc (Sigma) 1:6000; α -DBD-Gal4 (Santa Cruz) 1:5000; α -porin (Molecular Probes) 1:1000; α -tubulin TU27 (Covance) 1:2500 (not shown). Signals were visualized with SuperSignal West Dura extended duration substrate (Pierce Biotechnology) followed by autoradiography.

2.3 Results

Nkd antagonizes Arm/ β -catenin accumulation:

Whether or not increased levels of Arm/ β -catenin cause the expansion of Wg target gene expression in *nkd* mutants is not known; an early report, prior to the widespread use of confocal imaging, suggested that Arm levels are normal during early germ-band extension in *nkd* mutants (Riggleman et al. 1990). Confocal imaging revealed elevated Arm in *nkd* embryos by stage 10, prior to ectopic Wg synthesis (*cf.* Figure 2.1, B and C). Images of Arm-stained *nkd* embryos had peak pixel intensities increased approximately twofold over wild type (Figure 2.1D). To confirm this observation, Nkd was produced in alternate segments using *prd-Gal4* (Yoffe et al. 1995), a Gal4 driver integrated into the pair-rule locus *paired* (*prd*), so that Arm distribution in adjacent rescued and *nkd* segments could be imaged simultaneously. In stage 10 *nkd* embryos, Nkd reduced Arm to wild-type levels (Figure 2.1E). In contrast, increased Nkd did not reduce peak Arm levels in *nkd/+* or wild-type embryos (not shown).

Distributions of endogenous Nkd and Dsh:

Nkd and Dsh localizations during segmentation may provide clues about how Nkd limits Wg signaling. Endogenous Nkd was not detected by existing antibodies in formaldehyde-fixed embryos, but could be visualized by heat-fixation-induced antigen retrieval (Zeng et al. 2000). Confocal microscopy of heat-fixed embryos stained with α -Dsh and α -Nkd revealed uniform Dsh throughout each segment, whereas Nkd accumulated in a complex striped pattern similar to *nkd* mRNA (Figure 2.2, A and B) (Yanagawa et al. 1995; Zeng et al. 2000). Within cells, each protein was observed in a diffuse and punctate distribution in both cytoplasm and nucleus, with rare sites of punctate cytoplasmic and/or plasma membrane colocalization (Figure 2.2, B–B"). No segmental variation of nuclear accumulation was observed for either protein. Heat fixation compromised embryo morphology, precluding a more accurate assessment of subcellular distributions.

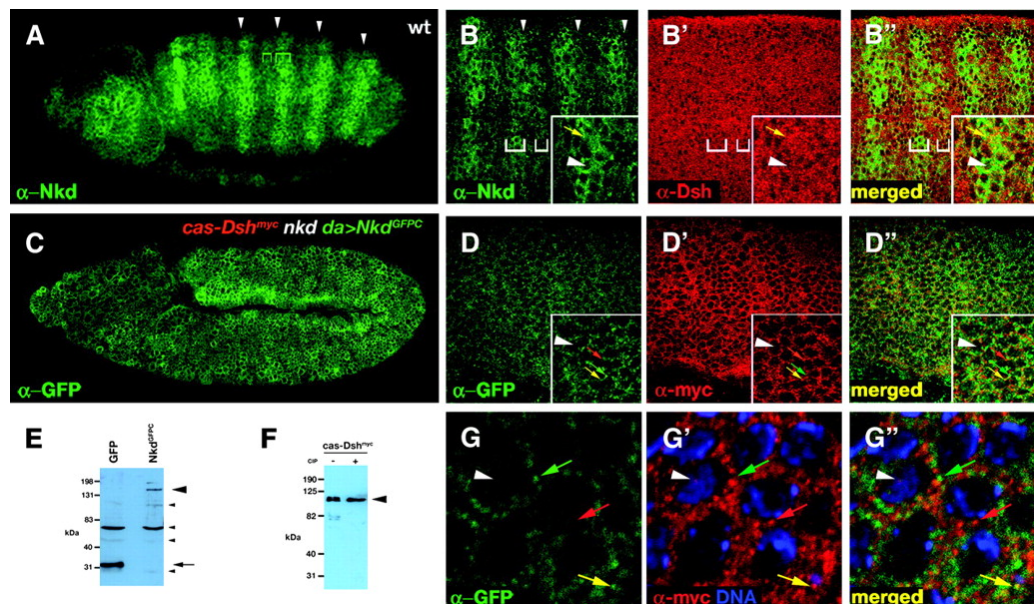


Fig. 2.2. Distributions of Nkd and Dsh in embryos. (A) Heat-fixed wild-type stage 11 embryo stained for endogenous Nkd. Arrowheads mark positions of parasegmental

boundaries. Note segmental variation in Nkd abundance (brackets, also in B). (B–B'') Heat fixed wild-type embryo stained for endogenous Nkd (green, B) and Dsh (red, B'); B'' is a merged image. Insets in B–B'': each protein is cytoplasmic and weakly nuclear (large arrowhead) with some cytoplasmic and/or plasma membrane colocalization (yellow arrows). (C) Formalin-fixed stage 11 *cas-Dsh^{myc}/UAS-Nkd^{GFPC};nkd^{7H16}da-Gal4/nkd^{7H16}* embryo stained with α -myc and α -GFP (only the latter is shown). Note uniform, predominantly cytoplasmic but low-level nuclear distribution of Nkd^{GFPC}. (D–D'') Medium power; same genotype as C. Note uniform distributions of both proteins in cytoplasm and nucleus (arrowhead in insets). Punctate areas with predominantly Nkd (green arrow), Dsh (red arrow), or both (yellow arrow) can be identified in magnified insets. (E) Western blot of extracts from 0- to 5-hr embryos expressing GFP (left) or Nkd^{GFPC} (right) and probed with α -GFP antibody highlighting specific GFP (arrow), Nkd^{GFPC} (large arrowhead), and nonspecific bands (small arrowheads). (F) Western blot of extracts from 0 to 5 hr. *cas-Dsh^{myc}* embryos probed with α -myc. Note doublet in left lane that collapses to a single band following phosphatase (CIP) treatment. (G) High power; same genotype as C, with DNA (blue) marking nuclei in G' and G''. Note punctate cytoplasmic Nkd (green arrow) and Dsh (red arrow) staining with rare cytoplasmic (yellow arrow) and nuclear (arrowhead) colocalization.

Epitope-tagged Nkd rescues *nkd* mutants to adulthood:

We sought to visualize Nkd and Dsh live or under gentle fixation, but first compared the activity of epitope-tagged Nkd to untagged Nkd in a rescue assay (Rousset et al. 2002).

Nkd fused to either a C-terminal *myc* tag (Nkd^{mycC}) or GFP (Nkd^{GFPC}), driven by the ubiquitous *da-Gal4* driver, narrowed the En stripe to two to three cells in stage 10–11 *nkd* embryos and rescued the cuticle phenotype as well as untagged Nkd (Figure 2.3, A–C, N; data not shown) (Zeng et al. 2000; Rousset et al. 2002).

Overexpressing Nkd during larval development results in adult phenotypes that mimic loss of Wg signaling; *B119-Gal4*-driven Nkd expression caused ventral eye reduction and loss and lateral displacement of sternite bristles (Figure 2.3, D–M) (Zeng et al. 2000; Wharton et al. 2001). From a panel of transgenic *UAS-Nkd* fly lines, we selected comparably "weak" and "strong" *UAS-Nkd^{mycC}* and *UAS-Nkd^{GFPC}* lines as judged by their expressivity when produced by *B119-Gal4* (Figure 2.3, D–M). Although all four tagged

UAS-Nkd lines rescued *nkd* cuticles as well as untagged Nkd (Figure 2.3N), *Nkd^{mycC}* lines rescued to later postembryonic stages than *Nkd^{GFPC}* lines (Figure 2.3, O and P). Although size and/or type of epitope tag, particularly a bulky GFP moiety, may subtly alter Nkd activity later in development, our data show that C-terminal epitope tags do not affect Nkd activity in the embryo.

Depending on the construct, transgenic line, and culture conditions, up to 60% of rescued *nkd* mutant crawling first instar larvae survived to adulthood (Figure 2.3P; data not shown). Although no *Nkd^{GFPC}*-expressing *nkd* mutant larvae survived to adulthood when cultured at 21° (Figure 2.3P), rare survivors eclosed when cultured at 18° (not shown). Dissection of pharate adults that failed to eclose revealed defects associated with altered Wg signaling, including reduced or missing wings and legs, altered sternite bristle pattern, and segmentation defects (not shown), while adults often lacked wings and/or halteres (Figure 2.3Q) (Baker 1988; Couso et al. 1993; Zeng et al. 2000). Although most of the defects in rescued mutants are associated with reduced *wg* activity (possibly due to Gal4-driven Nkd overproduction), we also observed wing-margin bristle patterns and ectopic wing bristles indicative of locally increased *wg* activity (Figure 2.3, R–T) (Couso et al. 1994).

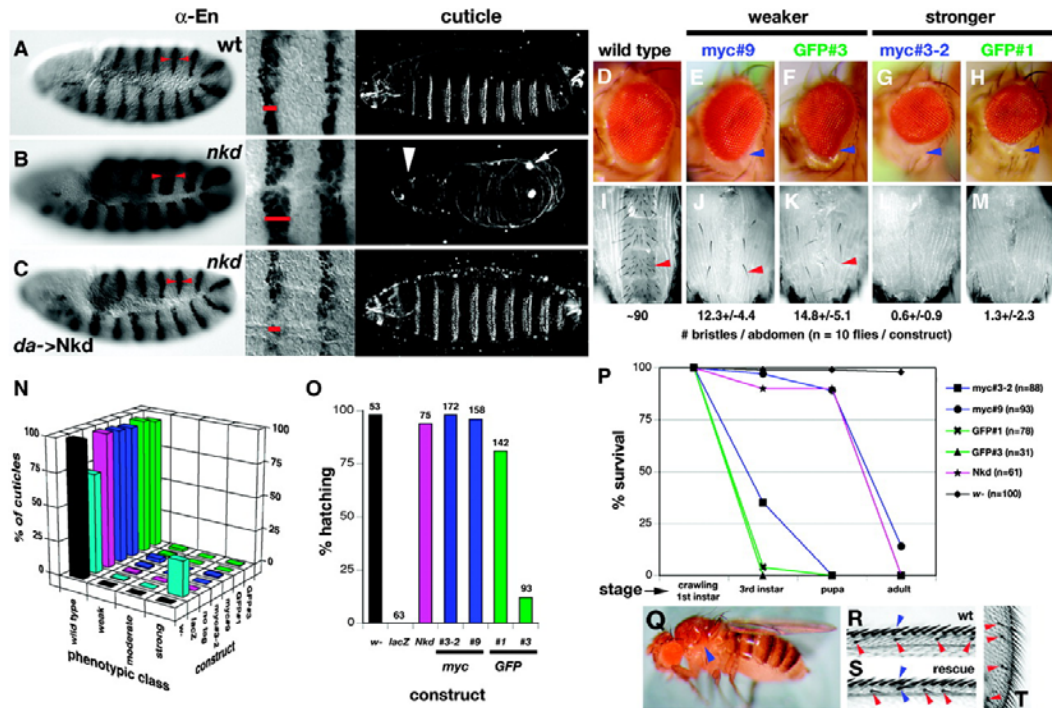


Fig. 2.3. *Nkd* rescues *nkd* mutants to adulthood. (A–C) Stage 11 embryos of indicated genotypes stained for En and viewed at low power (left) and high power showing two segments (middle). (Right) Representative cuticle. Wt (A) has a two- to three-cell En stripe (arrows and bar), while *nkd^{7H16}/nkd^{7E89}* (B) has a wide En stripe and develops a strong *nkd* phenotype with a severe head involution defect (arrowhead) and widely split posterior spiracles (arrow). (C) *UAS-Nkd^{GFP};nkd^{7E89}da-Gal4/nkd^{7H16}* has a narrow En stripe and a wild-type cuticle pattern. (D–M) Eye (D–H) or ventral abdomen (I–M) of wild type (wt) (D and I) or *B119-Gal4/UAS-Nkd* female (E–H and J–M). Weaker *UAS-Nkd* lines *Nkd^{mycC}#9* and *Nkd^{GFP}#3* produce a teardrop-shaped ventral eye (arrowheads, E and F) relative to wild type (D), whereas the stronger lines *Nkd^{mycC}#3-2* and *Nkd^{GFP}#1* cause ventral eye reduction (G and H). Wild-type female abdomen has ~90 sternite bristles (arrowhead) in the ventral aspect of segments A2–A6 (I). Weaker *UAS-Nkd* lines (J and K) caused bristle loss and lateral bristle displacement with indicated mean \pm SD bristle numbers, while stronger lines (L and M) resulted in near total bristle loss. (N) Distribution of wild-type and *nkd* cuticle phenotypes (weak, moderate, strong) in rescue cross (*UAS-X; nkd^{7H16}/TM3* x *da-Gal4,nkd^{7E89}/TM3*, where *X* is indicated construct) for each *Nkd* construct. *UAS-lacZ* (light blue) is the negative control, giving rise to an ~3:1 Mendelian ratio (75:25%) of wild-type-to-strong *nkd* mutants. *w-* is viability control, with 100% wild type. Magenta, untagged *Nkd*; blue, *Nkd^{mycC}*; green, *Nkd^{GFP}*. Note that each *UAS-Nkd* line rescues nearly all cuticles to wild type. (O) Percentage of *nkd* embryos that hatched into crawling first instar larvae as a function of *UAS-Nkd* rescue construct. *w-* and *UAS-lacZ* are controls. Above each bar is the number of embryos cultured. (P) Percentage of rescued *nkd* crawling first instar larvae that survived to indicated stage. *w-* is the control for culture conditions. Key shows the number of larvae

of each genotype that were cultured. Note that a lower percentage of Nkd^{GFPC} than Nkd^{mycC} -rescued embryos hatch and survive to later stages. (Q) $UAS-Nkd^{mycC}; nkd^{7E89} da-Gal4/nkd^{7H16}$ hatched adult with wing-to-notum transformation (arrowhead). (R) Wild-type anterior wing margin with evenly spaced stout bristles (blue arrowhead) and slender bristles (red arrowheads), each of the latter interspersed by four wing trichomes. (S and T) Wing margins from rescued nkd adult showing displaced stout bristle and decreased spacing between slender bristles (S) and ectopic sensory bristles near wing margin (T).

Distributions of tagged Nkd and Dsh:

Having established the functional equivalence of tagged and untagged Nkd in a rigorous rescue assay, we proceeded to investigate the distributions of tagged Nkd and Dsh.

Unfortunately, when expressed in embryos, we were unable to detect Nkd^{mycC} with α -myc by Western blot or immunofluorescence (not shown). Likewise, Nkd^{GFPC} was not visible with live fluorescence microscopy but was detectable with α -GFP, the specificity of which was verified by expressing Nkd^{GFPC} with striped Gal4 drivers (Figure 2.1E; data not shown). To monitor Dsh, we used a *myc*-tagged Dsh transgene driven by the endogenous *dsh* promoter (*cas-Dsh^{myc}*) that can rescue *dsh* mutants to adulthood (J. Axelrod, personal communication). Formalin-fixed *nkd* embryos ubiquitously expressing Nkd^{GFPC} carrying *cas-Dsh^{myc}* revealed α -myc- and α -GFP-staining patterns similar to endogenous Dsh and Nkd (*cf.* Figure 2.2, A and B with C and D). *da-Gal4*-driven Nkd^{GFPC} accumulated during stage 7 in a diffuse and punctate cytoplasmic pattern that persisted through stages 10–11 to include diffuse nuclear staining (Figure 2.2, C and D; data not shown). Dsh^{myc} and Nkd^{GFPC} accumulated uniformly across the segment, consistent with a lack of post-transcriptional control of steady-state Nkd or Dsh levels or distributions by physiologic levels of Wg signaling, an observation that we confirmed by

producing Nkd^{GFP} in alternate segments of *nkd* mutants using *prd-Gal4* (not shown).

Western blots of embryo extracts revealed predominant bands with slightly retarded mobilities relative to the expected M_r of each fusion protein (Nkd^{GFP} = 129 kDa; Dsh^{myc} = 79 kDa) (Figure 2.2, E and F), indicating that the distributions observed by microscopy likely correspond to that of full-length proteins as opposed to degradation products.

In contrast to the segment-polarity protein Lines, which undergoes rapid nucleocytoplasmic shuttling in response to Wg or Hh signaling, the observed embryonic distributions of Nkd^{GFP} and Dsh^{myc} were unaffected by pharmacologic inhibition of CRM1-dependent nuclear export following a 30-min exposure to leptomycin-B (Figure 2.4) (Fornerod et al. 1997; Ossareh-Nazari et al. 1997; Hatini et al. 2000).

With either fixation or staining method, Nkd and Dsh exhibited largely nonoverlapping subcellular distributions, with only rare Nkd/Dsh punctate cytoplasmic or nuclear colocalization (Figure 2.2, G–G''), observations consistent with our previous unsuccessful attempts to co-immunoprecipitate endogenous Nkd and Dsh from embryos or S2 cells (Rousset et al. 2001).

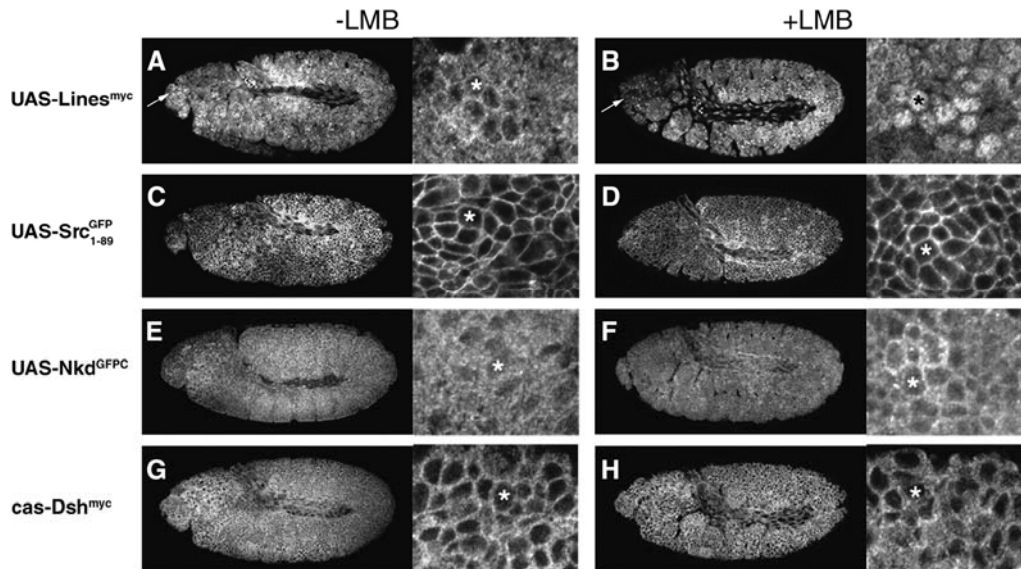


Fig. 2.4. Nkd^{GFPC} and Dsh^{myc} do not undergo rapid CRM-1-dependent nuclear export. Each panel shows low- and high-power views of representative stage 11 embryos expressing the indicated construct via *da-Gal4* (except cas-Dsh^{myc}, which expresses Dsh^{myc} at appropriate levels via the *dsh* promoter) stained with the appropriate antibody to reveal subcellular distributions ± 30 min treatment with the CRM-1-dependent nuclear export inhibitor LMB. The positive control (A and B) is Lines^{myc}, which is nuclear in Wg-receiving cells and cytoplasmic in Hh-receiving cells of the dorsal ectoderm (Hatini et al. 2000). LMB treatment drives Lines^{myc} into the nucleus of most dorsal ectoderm and head (arrow) cells. Asterisks designate positions of nuclei. The negative control (C and D) is the myristoylated, N-terminal 89 amino acids of *D. melanogaster* Src (Simon et al. 1985) fused to GFP. No change in the membrane-associated Src^{GFP} distribution is seen after LMB treatment. Nkd^{GFPC} (E) is cytoplasmic and nuclear, whereas Dsh^{myc} (G) is predominantly cytoplasmic in the absence of LMB, and these distributions remain unchanged in LMB-treated embryos (F and H).

***In vivo* requirements for Nkd/Dsh-interacting regions:**

Misexpressed Nkd can inhibit endogenous *dsh* during PCP signaling as well as Dsh-overexpression-induced gain-of-Wg signaling phenotypes (Axelrod 2001; Rousset et al. 2001). If Nkd/Dsh association is necessary for Nkd to antagonize Wnt signaling, then Nkd should not alter a gain-of-Wnt signaling phenotype induced by a Dsh protein that lacks Nkd-interacting sequences. Dsh consists of DIX, basic/PDZ, and DEP domains, of which Nkd binds to the central basic/PDZ region (Rousset et al. 2002). Misexpression of

full-length Dsh in the larval eye imaginal disc by *GMR-Gal4* resulted in adult eye phenotypes similar to those caused by a dominant *wg* allele (*wg^{Glazed}*) in which ectopic Wg causes expanded head cuticle and pigment cell fates, ommatidial apoptosis, and reduced or absent interommatidial bristles (Figure 2.5, A–C) (Cadigan and Nusse 1996; Ahmed et al. 1998; Brunner et al. 1999; Rousset et al. 2001; Cadigan et al. 2002; Tomlinson 2003; Lin et al. 2004). Nkd coexpression inhibited the Dsh-induced phenotype but had no effect on a similar phenotype induced by a mutant Dsh protein, Dsh^{ΔbPDZ}, that lacked Nkd-interacting regions (*cf.* Figure 2.5, D and E) (Axelrod et al. 1998; Rousset et al. 2001). Nkd also inhibited Dsh-induced, but not Dsh^{ΔbPDZ}-induced, ectopic wing-margin bristles (not shown).

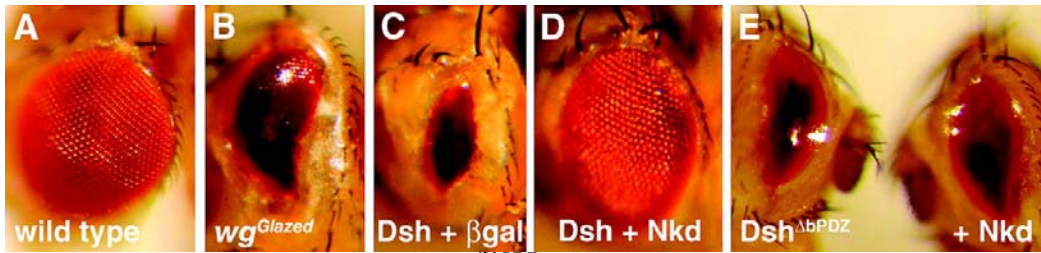


Fig. 2.5. Nkd reverses Dsh- but not Dsh^{ΔbPDZ}-induced eye phenotype. (A) Wild-type eye. (B) *wg^{Glazed}* eye. (C) *GMR-Gal4/UAS-Dsh; UAS-lacZ* eye. (D) *GMR-Gal4/UAS-Dsh; UAS-Nkd* eye showing strong suppression of Dsh-induced phenotype. (E) *GMR-Gal4/UAS-Dsh^{ΔbPDZ}; UAS-lacZ* eye (left) is identical to *GMR-Gal4/UAS-Dsh^{ΔbPDZ}; UAS-Nkd* eye (right), with no ommatidia or bristles.

Next we made Nkd proteins with mutant Dsh-binding regions. Nkd^{recEF/mycC} and Nkd^{hEFX2/mycC} replaced the Nkd EF hand with either the high-affinity Ca²⁺-binding EF hand of bovine recoverin (Flaherty et al. 1993) or the EFX of human Nkd2 (hNkd2) (Wharton et al. 2001). Nkd^{D201A/mycC} substituted an alanine for a conserved aspartate in the EF hand loop, a mutation that reduced the extent of Nkd/Dsh association by yeast two-hybrid (Y2H) (Rousset et al. 2002). All three constructs rescued the *nkd* cuticle

phenotype and adult viability, although $Nkd^{rEF/mycC}$ and $Nkd^{hEFX2/mycC}$ cuticle rescue was less efficient than wild type (Figure 2.6B; data not shown).

Surprisingly, $Nkd^{\Delta RB/mycC}$, which lacks the EFX, rescued *nkd* mutants to adulthood as well as Nkd^{mycC} (Figure 2.6B; data not shown), but the mutant protein's residual activity could be due to Dsh-association via adjacent Zn^{2+} -binding sequence in fly Nkd (Rousset et al. 2002). We made Nkd–GFP constructs lacking the EFX ($Nkd^{\Delta EFX/GFP}$) or the Zn^{2+} -binding region ($Nkd^{\Delta YS/GFP}$) or both Dsh-binding regions ($Nkd^{\Delta R1S/GFP}$). $Nkd^{\Delta EFX/GFP}$ rescued *nkd* cuticles as well as Nkd^{GFP} or $Nkd^{\Delta RB/mycC}$, but $Nkd^{\Delta YS/GFP}$ or $Nkd^{\Delta R1S/GFP}$ had a reduced but a still significant rescue activity (Figure 2.6, A and B). The Nkd proteins lacking Dsh-binding regions had reduced associations with Dsh or Dsh^{bPDZ} by quantitative Y2H (Figure 2.6C). During stages 10–11 $Nkd^{\Delta EFX/GFP}$ and $Nkd^{\Delta R1S/GFP}$, in contrast to Nkd^{GFP} , accumulated predominantly in nuclei while retaining punctate cytoplasmic distribution and rare Dsh colocalization (Figure 2.6, A and D–D"), suggesting that the EFX domain and/or Dsh association opposes nuclear localization signals in Nkd. Consequently, $Nkd^{EFX/GFP}$, consisting of only the EFX domain fused to GFP, accumulated in the cytoplasm during germ-band extension but did not inhibit Wnt signaling or rescue the *nkd* cuticle (Rousset et al. 2002; data not shown).

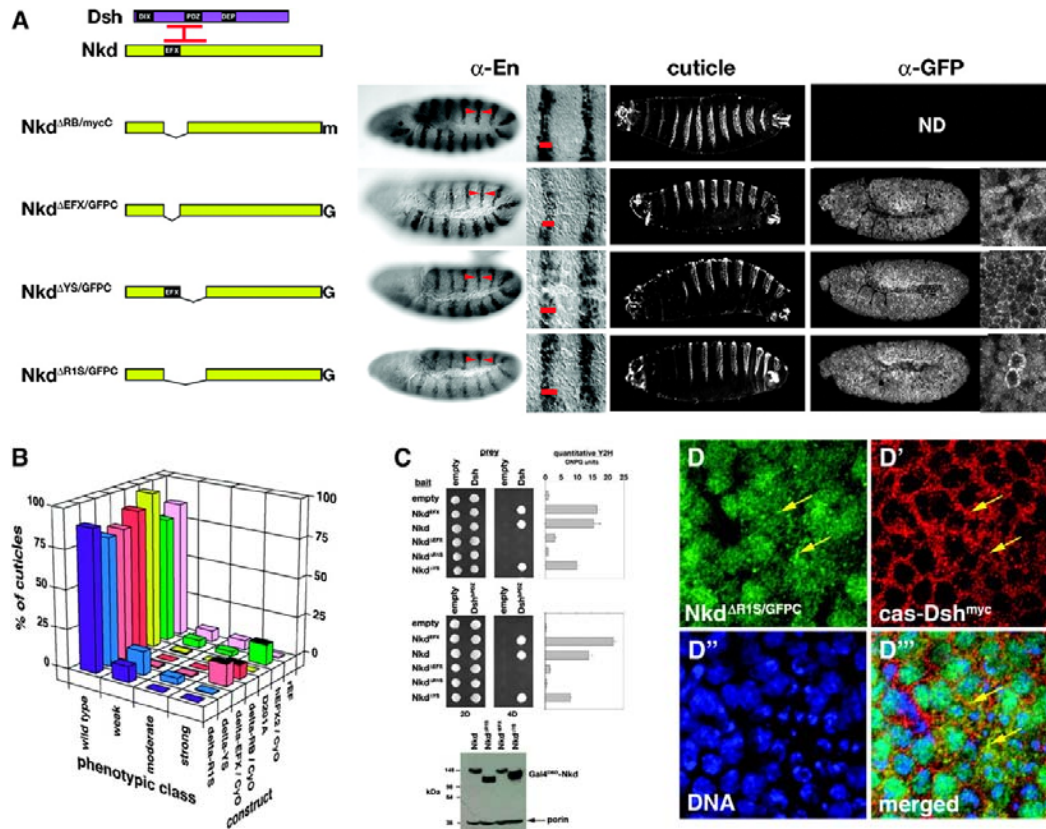


Fig. 2.6. Properties of Nkd proteins with mutant Dsh-binding regions. (A) Dsh (purple) has DIX, PDZ, and DEP domains. Nkd (yellow) has EFX domain. Red bars indicate regions that mediate Nkd/Dsh association (Rousset et al. 2002). Nkd constructs lacking Dsh-binding regions (designated by spliced-out regions) are schematized at left, with representative images from activity assay (stage 11 α -En and larval cuticle) and α -GFP localization in stage 11 embryo, depicted from left to right. The top two constructs, lacking the EFX domain, each narrowed the En stripe to two to three cells and restored cuticle pattern, while the bottom two constructs, lacking the Zn²⁺-binding domain, partially narrowed the En stripe but also restored most of the cuticle pattern. Note that EFX deletion increased the ratio of nuclear-to-cytoplasmic GFP, with the exception of the two *Nkd*^{ΔR1S/GFP}-expressing cells in the center of the field with condensed chromatin indicative of late telophase. ND, not done. (B) Distribution of wild-type and *nkd* cuticles in rescue cross for indicated Nkd construct. For crosses in which the *UAS-Nkd* insertion is lethal, the presence of the *CyO* balancer in the rescue cross results in ~12.5% of cuticles remaining unrescued and hence "strong" (indicated by the black-topped bars). Note that constructs lacking Dsh-binding regions have a reduced ability to rescue relative to wild-type Nkd, as evidenced by a reduced proportion of wild-type cuticles and increased weak and moderate cuticles. (C) Y2H of strains expressing Nkd bait constructs (left) and Dsh (top) or Dsh^{bPDZ} (middle) prey assayed for growth under double-dropout (2D) or quadruple-dropout (4D) media. Bar graphs on right show ONPG units for strains harboring indicated constructs in quantitative Y2H assay. (Bottom) Western blot of yeast

extracts expressing indicated Nkd-Gal4 DNA-binding domain (DBD) fusion proteins. Porin is loading control. (D) High power of stage 11 *UAS-Nkd^{ΔR1S/GFP}/cas-Dsh^{myc};nkd^{7H16}da-Gal4/nkd^{7H16}* epidermis stained for α-GFP (D, green), α-myc (D', red), and DNA (D'', blue); D''' is a merged image. Although the majority of Nkd^{ΔR1S/GFP} is nuclear, rare cytoplasmic Nkd/Dsh colocalization (yellow arrows) can be identified.

Dsh-binding sequences in Nkd are important to reverse the consequences of Dsh overproduction, because Nkd^{ΔR1S/GFP} restored few bristles or ommatidia to *GMR-Gal4/UAS-Dsh* eyes (cf. Figure 2.7, B and C). Conversely, Nkd^{R1S/myc}, composed of only sequences sufficient to bind Dsh, suppressed the Dsh-induced eye phenotype (Figure 2.7D). Nkd's Zn²⁺-binding sequences are important for inhibiting Dsh, because Nkd^{EFX/GFP}, lacking the Zn²⁺-binding sequences, did not alter the Dsh-induced eye phenotype (not shown). In summary, Dsh-binding regions of Nkd are necessary for full *nkd* rescue activity and are largely sufficient to inhibit Dsh.

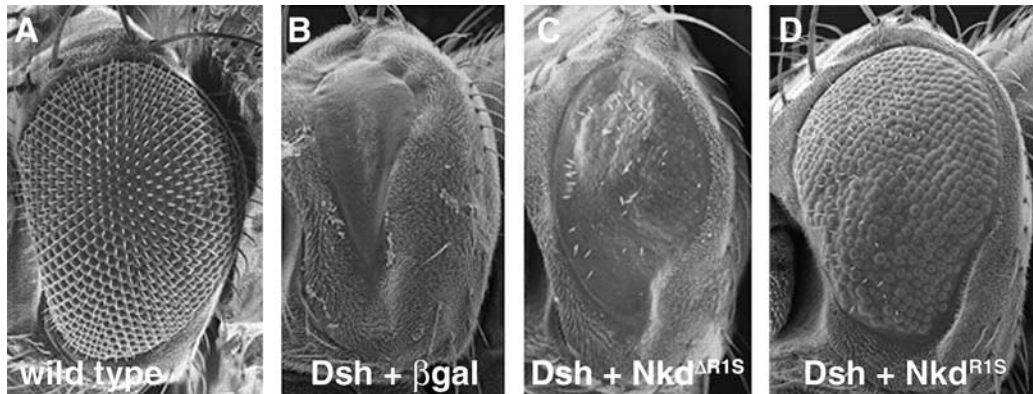


Fig. 2.7. Nkd's Dsh-binding regions are important for blocking Dsh-induced eye phenotype. (A–D) SEMs of representative wild type (A), *GMR-Gal4/UAS-Dsh;UAS-lacZ* (B), *GMR-Gal4/UAS-Dsh;UAS-Nkd^{ΔR1S/GFP}* (C), or *GMR-Gal4/UAS-Dsh;UAS-Nkd^{R1S/myc}* (D) eyes. Note that Nkd^{ΔR1S} only weakly rescues the Dsh-induced phenotype, while Nkd^{R1S}, consisting of only Dsh-binding sequences, restored ommatidia and bristles.

A 30-amino-acid motif is necessary for Nkd activity and nuclear localization:

Despite the ability of Nkd's Dsh-binding sequences to block Dsh *in vivo*, *da-Gal4*-

expressed Nkd^{R1S/mycC} had no *nkd* rescue activity (Rousset et al. 2002). To identify regions of Nkd important for function, we made additional transgenes and sequenced *nkd* alleles. Nkd^{ΔBBg/GFPC} and Nkd^{ΔRBg/GFPC}, lacking amino acids 295–824 and 178–824, respectively, did not rescue, indicating deletion of critical region(s) (Figure 2.8A). The C-terminal truncations Nkd^{NBb/GFPC} (retaining aa 1–826), Nkd^{NGA/GFPC} (1–712), and Nkd^{NIN4/GFPC} (1–572) restored cuticle pattern and narrowed the En stripe of *nkd* mutants (Figure 2.8, A and B). Nkd^{NIN3/GFPC} (1–447), which includes Dsh-association sequences, did not narrow the En stripe and only partially rescued the *nkd* cuticle (Figure 2.8A) (Rousset et al. 2002). The shorter constructs Nkd^{NBam/GFPC} (1–295), Nkd^{NR1/mycC} (1–178), or Nkd^{7H/GFPC}/Nkd^{7H/mycC} (1–59) did not affect the *nkd* phenotype (Figure 2.8A) (Rousset et al. 2002). The distributions of Nkd^{NIN4/GFPC} and longer constructs during stages 10–11 resembled Nkd^{GFPC}, whereas the shorter constructs Nkd^{NIN3/GFPC}, Nkd^{NBam/GFPC}, Nkd^{ΔRBg/GFPC}, and Nkd^{ΔBBg/GFPC} were excluded from nuclei during stages 10–11 (Figure 2.8A). Nkd^{7H/GFPC} was detectable in nucleus and cytoplasm (Figure 2.8A), suggesting that the EFX retains Nkd in the cytoplasm, consistent with deletion of the EFX domain (as in constructs Nkd^{ΔEFX/GFPC} or Nkd^{ΔR1S/GFPC}) resulting in enhanced nuclear localization relative to Nkd^{GFPC} (*cf.* Figure 2.2G with Figure 2.6, A and D). Alternatively, the small size of Nkd^{7H/GFPC} may allow free diffusion through nuclear pores. Nkd^{NIN3/GFPC}, Nkd^{NIN4/GFPC}, and longer constructs fully reversed the Dsh-induced eye phenotype, while Nkd^{NBam/GFPC}, retaining the EFX domain but lacking the Zn²⁺-binding region, restored ommatidia but few bristles (not shown). Thus Nkd aa 448–572 (the sequence in Nkd^{NIN4/GFPC} but not in Nkd^{NIN3/GFPC}) are crucial for both Nkd activity and nuclear localization but not for inhibiting overexpressed Dsh.

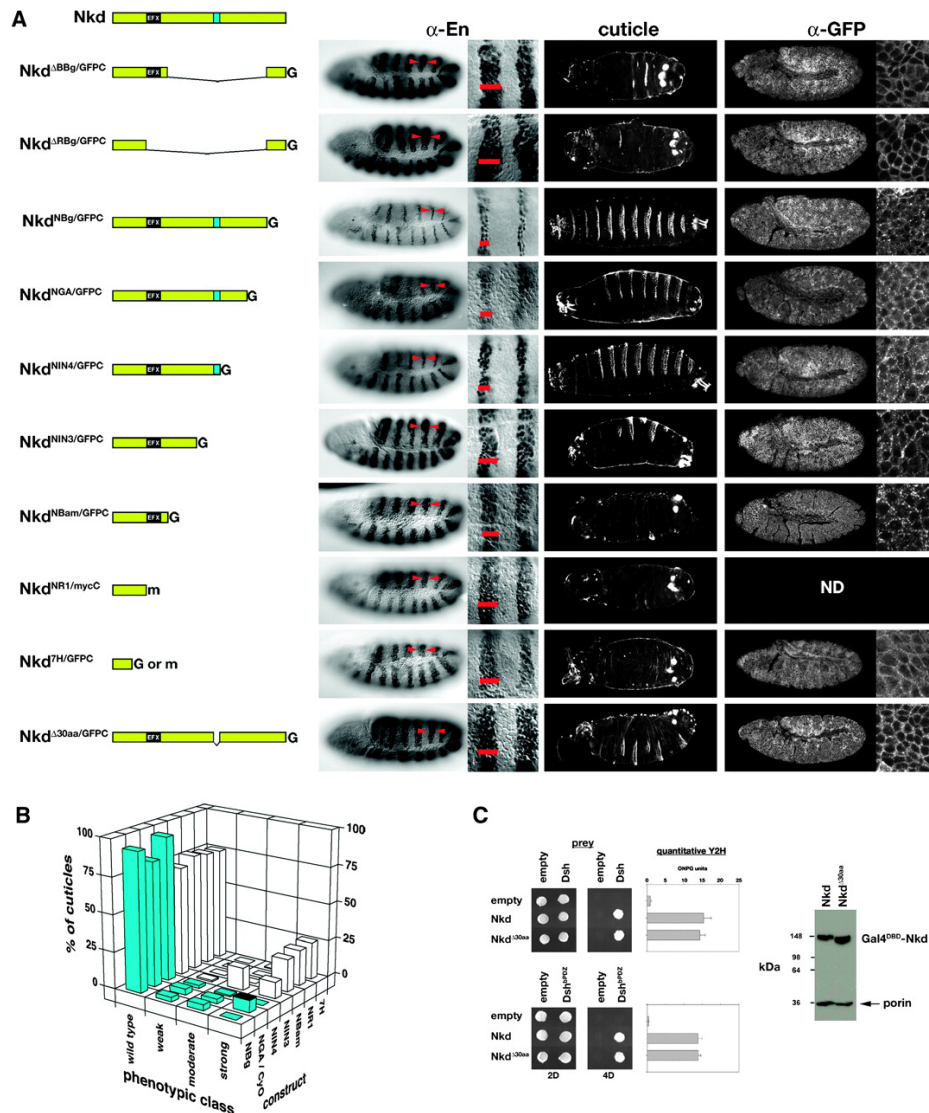


Fig. 2.8. A 30-aa motif is necessary for Nkd activity and nuclear localization. (A) Data from indicated *UAS-Nkd* constructs as described in Figure 2.6A. Note that constructs with the 30-aa motif (light blue box) narrowed the En stripe, restored cuticle pattern, and were detected in nuclei, whereas constructs lacking the 30-aa motif did not narrow the En stripe, did not restore or only partially restored cuticle pattern, and (with the exception of *Nkd*^{7H/GFPC}) were excluded from nuclei. (B) Quantitation of cuticle phenotypes. Note that constructs with a 30-aa motif (blue bars) efficiently rescued, while those lacking the 30-aa motif (white bars) partially rescued or did not rescue. (C) Y2H of Nkd or *Nkd*^{Δ30aa} binding to Dsh or Dsh^{bPDZ}. (Right) Western blot of yeast extracts expressing Nkd or *Nkd*^{Δ30aa}. Note that deletion of the 30-aa motif did not affect Dsh binding.

Sequencing DNA from flies heterozygous for a panel of lethal EMS-induced *nkd* alleles (Jurgens et al. 1984; W. Zeng and M. P. Scott, unpublished data) revealed six nonsense mutations predicted to encode truncated proteins ranging from 399 to 516 aa (Figure 2.9A and Figure 2.10A). Each mutant develops a variable *nkd* cuticle phenotype—possibly due to variation in Wg-dependent *nkd* expression, nonsense-mediated mRNA decay, or stability or activity of each truncated protein—but stage 11 embryos exhibit a wide En stripe indicative of elevated Wg signaling (Figure 2.9A). As shown in Figure 2.9B, each allele exhibits a weaker *nkd* cuticle phenotype than the first allele that we molecularly characterized, *nkd*^{7H16}, which harbors a nonsense codon at residue no. 60 (Zeng *et al.* 2000). Since Nkd^{7H/GFPC} and Nkd^{7H/mycC} lacked rescue activity (Figure 2.8, A and B), we presume that *nkd*^{7H16} represents a null allele but a definitive determination awaits examination of *nkd* deficiency chromosomes.

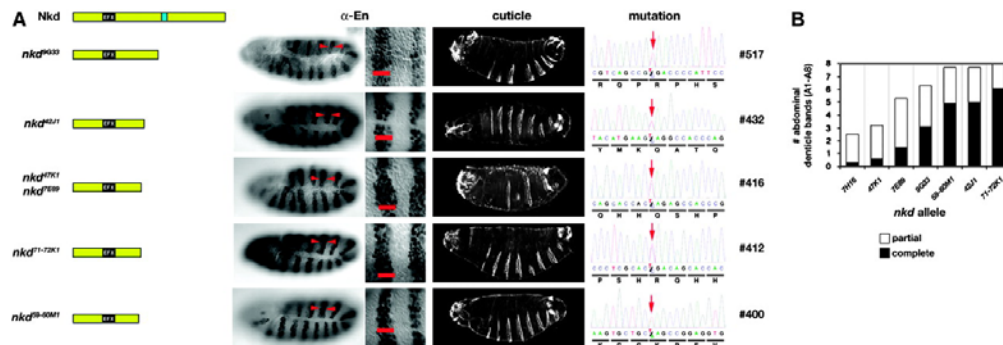


Fig. 2.9. Phenotypes and molecular lesions of *nkd* alleles. (A) Predicted truncated Nkd protein based on sequencing of indicated *nkd* allele, relative to full-length Nkd (top). Note that each predicted protein is truncated N-terminally of the 30-aa motif. Stage 11 mutant embryos have a widened En stripe and a variable *nkd* phenotype. Right column shows DNA sequence trace from a heterozygote, indicating the codon number with mutation (arrow). (B) Mean number of complete (black bars) and partial (shaded bars) abdominal denticle belts (A1–A8) in each *nkd* allele ($n = 25$ mutant cuticles scored for each allele). The molecular lesion of *nkd*^{7H16} was reported in Zeng et al. (2000).

Next we assembled a putative *nkd* cDNA sequence from the *Anopheles gambiae* genome (GenBank BK005845) (Holt et al. 2002). Mosquito Nkd is predicted to be 886 aa and $M_r = 96.7$ kDa (Figure 2.10A). Fly and mosquito Nkd share 29% aa identity, with homology clustered in four blocks interspersed by mostly dissimilar sequence (Figure 2.10A). Fly and mosquito Nkd share 22/30 identical amino acids (fly aa 543–572) that lie precisely within the interval critical for *nkd* activity defined by transgenes and alleles. Mammalian *nkd* paralogs also share four sequence blocks interspersed by variable sequence (Figure 2.10B) (Kato 2001; Wharton et al. 2001). Strikingly, the third conserved sequence block in mammalian Nkds, like those of the two insect Nkds, is exactly 30 aa, but no homology exists between insect and mammalian 30-aa motifs (Wharton et al. 2001; data not shown). However, a secondary structure prediction algorithm (see section 2.2 MATERIALS AND METHODS) indicates that insect and mammalian motifs may adopt an amphipathic α -helical secondary structure (Figure 2.10B; data not shown). Nkd ^{Δ 30aa/GFPC}, lacking the 30-aa motif, only slightly narrowed the *nkd* mutant En stripe and partially rescued the *nkd* cuticle (Figure 2.8A). Nkd ^{Δ 30aa/GFPC} and Nkd^{NIN3/GFPC} were also compromised in their ability to reduce Arm levels in stage 10 *nkd* mutants relative to Nkd^{GFPC} and Nkd^{NIN4/GFPC} (Figure 2.11, A–E). By Y2H, Nkd and Nkd ^{Δ 30aa} each interacted to a comparable extent with Dsh or Dsh^{bPDZ} (Figure 2.8C), and the fly 30-aa motif bound neither Dsh nor Dsh^{bPDZ} (not shown). Like Nkd^{NIN3/GFPC}, Nkd ^{Δ 30aa/GFPC} exhibited reduced nuclear staining in stage 11 embryos relative to Nkd^{GFPC} (Figure 2.8A; also *cf.* Figure 2.13, A and B), indicating that the 30-aa motif is necessary for Nkd function and nuclear localization during segmentation.

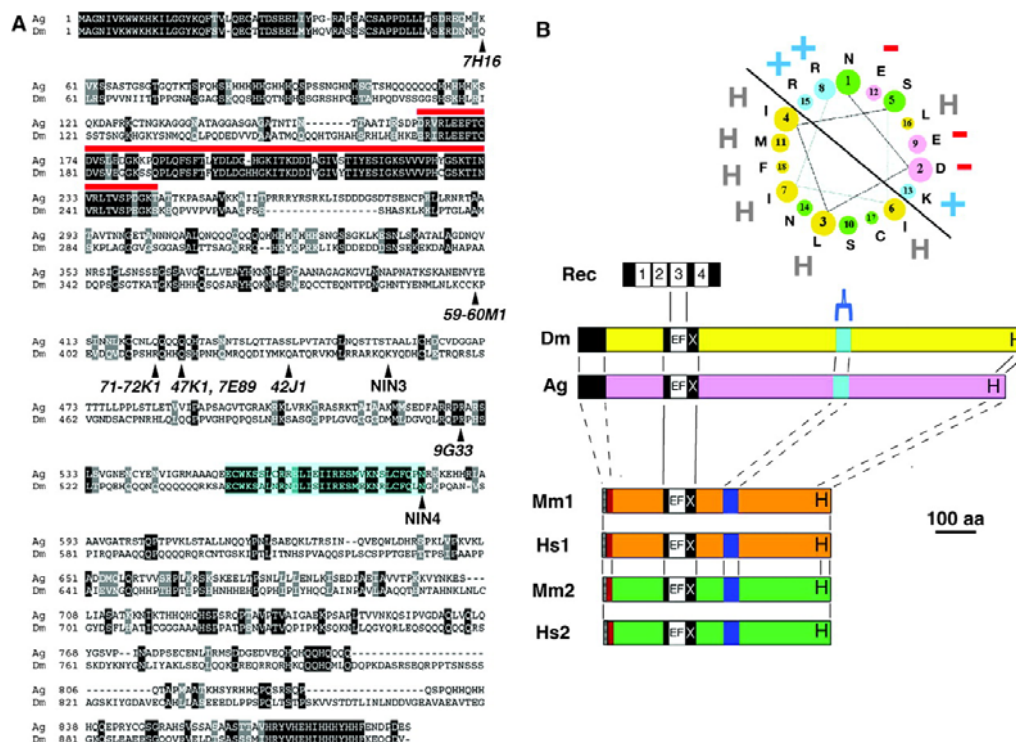


Fig. 2.10. Nkd alignment and protein family. (A) ClustalW alignment of predicted *An. gambiae* (Ag, GenBank BK005845) and *D. melanogaster* (Dm, GenBank AF213376) Nkd proteins. Identities are in a black background, and similarities are shaded. EFX is designated by a red line and the 30-aa motif by light blue shading. Arrowheads designate the position of nonsense mutations in each *nkd* allele shown in Figure 2.9A as well as the C-terminal extent of constructs Nkd^{NIN3/GFPC} and Nkd^{NIN4/GFPC} (each named for the position of *nkd* intron 3 and 4, respectively). (B) Nkd protein family showing region of EF-hand similarity between Recoverin (Rec), consisting of four EF hands, and Nkd proteins. Vertical lines indicate sequence homology, whereas dashed lines indicate preserved motif order, but not sequence conservation, between recoverin, fly and mosquito Nkd, and *Mus musculus* (Mm) and *Homo sapiens* (Hs) Nkd1 (orange) and Nkd2 (green). Thirty-amino-acid motifs (light blue in insect, dark blue in mammal) are each predicted to be an amphipathic α -helix, part of which is depicted in helical wheel format above the fly sequence (beginning with Nkd residue 552). Diagonal line separates charged (+ or -) residues on one face of the predicted helix from hydrophobic residues (H) that mostly lie on the opposite face. Residues: pink, acidic; blue, basic; orange, nonpolar; green, polar uncharged.

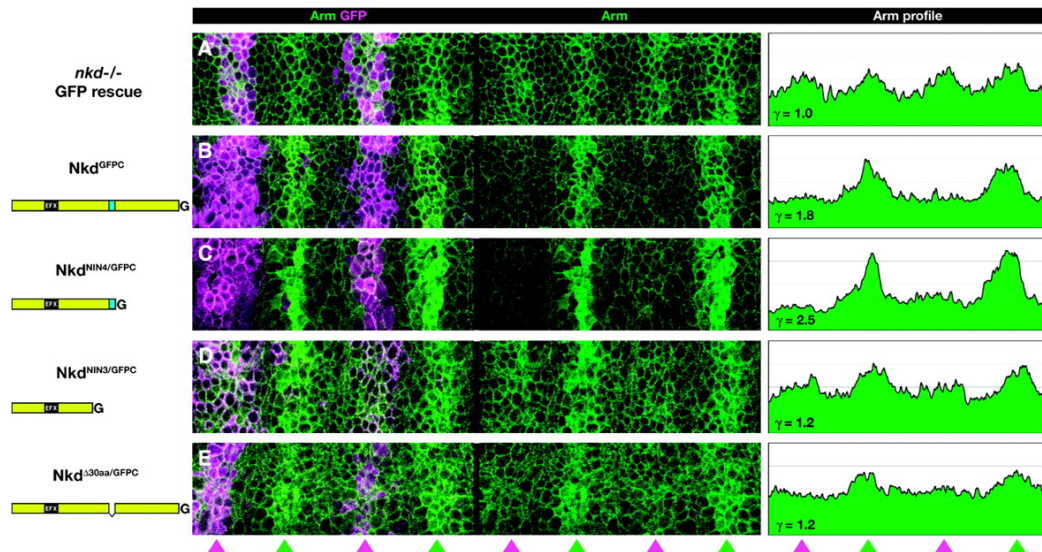


Fig. 2.11. The 30-aa motif is required for Nkd to reduce Arm/ β -catenin levels. Each panel shows four segmental anlagen of a representative stage 10 *UAS-X;nkd^{7H16}prd-Gal4/nkd^{7H16}* embryo, where *X* is each indicated Nkd construct, stained for Arm (green) and GFP (purple). Colored arrowheads indicate position of *nkd* mutant (green) and rescued (purple) segments. Right column shows mean grayscale intensity (ordinate range 0–200) of Arm staining as a function of position along the anterior–posterior axis. To quantitate the extent of Arm reduction by each Nkd construct, we defined γ as the ratio of peak grayscale intensity in *nkd* mutant segments to that in adjacent segments expressing each construct. When GFP is used in the rescue assay, $\gamma = 1.0$ (*i.e.*, no rescue), while for full-length Nkd, $\gamma > 1.8$. Both constructs that lacked the 30-aa motif had $\gamma = 1.2$, indicating a reduced ability to decrease Arm levels.

The fly 30-aa motif increases activity and confers nuclear localization to mouse

Nkd1:

The distribution and activity of the fly 30-aa motif fused to GFP did not differ from that of GFP alone (not shown). As a test of sufficiency, we replaced the mouse Nkd1 30-aa motif with the fly motif (mNkd1^{f30aa}). Previously, we reported that misexpression of mNkd1 during fly larval development induced weak *wg* loss-of-function adult phenotypes whose penetrance was sensitive to a reduced dose of *wg* (Wharton et al. 2001). When expressed by *da-Gal4*, neither mNkd1^{GFPC} nor mNkd1^{f30aa/GFPC} affected the *nkd* phenotype (not shown). However, mNkd1^{f30aa/GFPC} caused a twofold greater reduction in sternite

bristle number than did mNkd1^{GFPC} when driven by *B119-Gal4* in a *wg/+* background (Figure 12, A and B). In addition, the fly 30-aa motif conferred low-level nuclear localization to mNkd1 in stage 10 embryos but robust nuclear accumulation in third instar larval salivary glands (Figure 2.12, C–F).

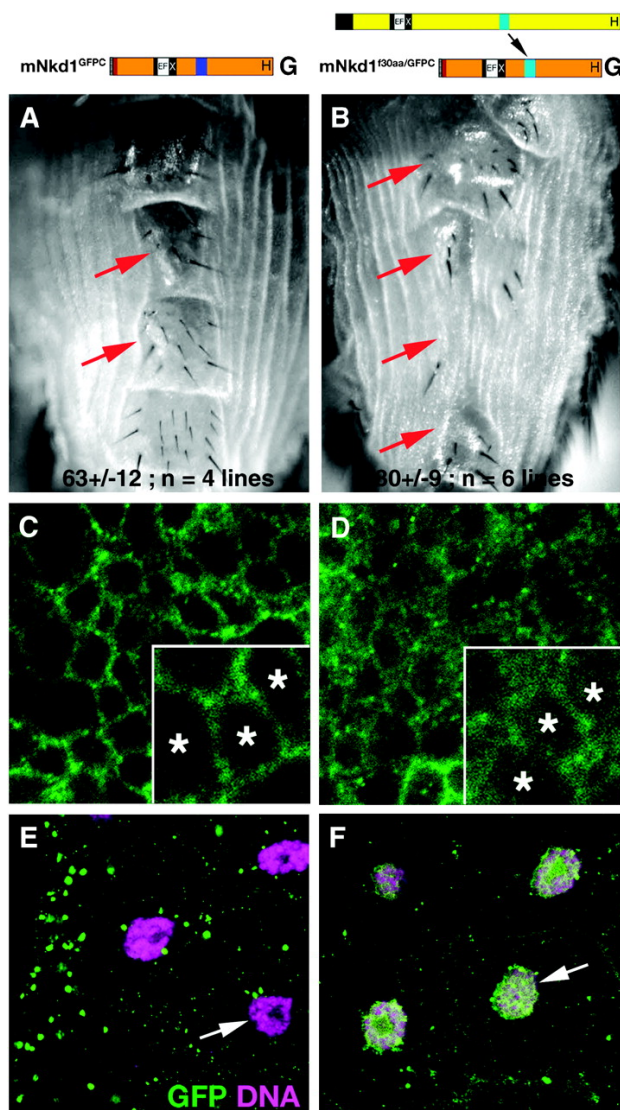


Fig. 2.12. Fly 30-aa motif increases mouse Nkd1 activity and confers nuclear localization. Schematic of mouse Nkd1^{GFPC} (left) and chimeric construct with substitution of fly 30-aa domain (light blue, right). (A and B) Representative *B119-Gal4* *wg/UAS*-

mNkd1^{GFPC} (A) or *B119-Gal4 wg/UAS-mNkd1^{f30aa/GFPC}* (B) female abdomens showing segments with reduced numbers of sternite bristles (arrows). *mNkd1^{f30aa/GFPC}* reduced sternite bristle counts approximately twofold relative to *mNkd1^{GFPC}* (the mean \pm SD of bristles for 10 flies from the indicated number of lines for each construct is shown). (C and D) Epidermal cells of stage 11 *UAS-mNkd1^{GFPC};nkd^{7H16}da-Gal4/nkd^{7H16}* (C) or *UAS-mNkd1^{f30aa/GFPC};nkd^{7H16}da-Gal4/nkd^{7H16}* embryos (D) stained with α -GFP (green). Magnified insets show low-level nuclear GFP in *mNkd1^{f30aa/GFPC}* but not *mNkd1^{GFPC}* (asterisks mark center of nuclei). C and D were stained in parallel and imaged under identical confocal settings. (E and F) Salivary gland expressing *mNkd1* constructs driven by *da-Gal4*. Note absence of nuclear GFP in *mNkd1^{GFPC}*-producing salivary gland cells (E) but abundant nuclear GFP (arrow) in *mNkd1^{f30aa/GFPC}*-producing cells (F). DNA is purple.

A heterologous nuclear localization sequence partially restores activity to Nkd ^{Δ 30aa/GFPC}

30aa/GFPC;

If Nkd acts in the nucleus to antagonize Wg signaling, then a heterologous nuclear localization sequence (NLS) may restore the ability of Nkd ^{Δ 30aa/GFPC} to enter the nucleus and rescue a *nkd* mutant. Nkd ^{Δ 30aaNLS/GFPC}, in which the SV40 NLS replaced the 30-aa motif, narrowed the En stripe and restored cuticle pattern to *nkd* mutants to an extent intermediate between Nkd ^{Δ 30aa/GFPC} and full-length Nkd (Figure 2.13, A–D). After stage 10, Nkd ^{Δ 30aaNLS/GFPC} was detectable in the nucleus and cytoplasm (Figure 2.13C), with rare punctate cytoplasmic Dsh colocalization but with no apparent effect on cas-Dsh^{myc} distribution (not shown). One of three *UAS-Nkd^{\Delta}30aaNLS/GFPC* transgenic lines (no. 7A) produced rescued crawling first instar larvae, 1.6% (of 252) of which survived to adulthood (Figure 2.13E). In contrast, no rescued crawling first instar larvae emerged from rescue crosses with two independent *UAS-Nkd^{\Delta}30aa/GFP* transgenic lines ($n > 1000$ progeny examined/line). Adults rescued by Nkd ^{Δ 30aaNLS/GFPC} exhibited more severe wing-margin bristle patterning abnormalities than those rescued by Nkd (*cf.* Figure 2.13F with 3S), indicating that enhanced nuclear localization alters Nkd activity.

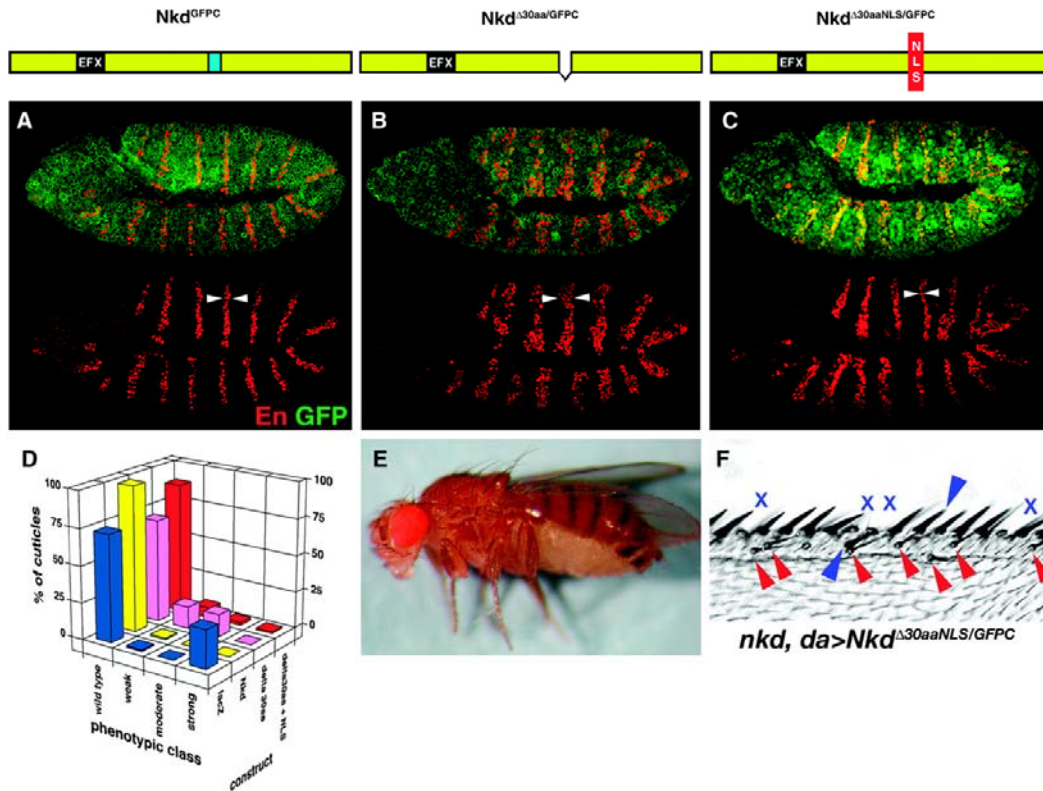


Fig. 2.13. A heterologous NLS partially restores *Nkd*^{Δ30aa} activity. (A–C) Representative stage 11 *nkd*^{7H16} mutant embryos expressing *Nkd*^{GFP} (A), *Nkd*^{Δ30aa/GFP} (B), or *Nkd*^{Δ30aaNLS/GFP} (C) stained for GFP (green) and En (red). The NLS promotes *Nkd* nuclear localization and narrows the En stripe of most segments (arrowheads). (D) Quantitation of *nkd* cuticle rescue. Note increased proportions of wild type and reduced moderate and weak *nkd* cuticles with rescue by *Nkd*^{Δ30aaNLS/GFP} (red bars) as compared to *Nkd*^{Δ30aa/GFP} (purple). (E) *UAS-Nkd*^{Δ30aaNLS/GFP}; *nkd*^{7H16} *da-Gal4/nkd*^{7H16} adult. (F) Anterior wing margin of animal in E with marked bristle disarray, including absent (x) and ectopic (blue arrowhead) stout bristles and mispatterned and ectopic slender bristles (red arrowhead).

2.4 Discussion

Here we report a structure–function analysis of *D. melanogaster* *Nkd*, a novel intracellular protein that acts in a feedback loop to limit Wnt/β-catenin signaling during embryogenesis. Our finding that *nkd* mutants have elevated Arm/β-catenin levels concomitant with broadened domains of Wg target gene expression is consistent with

prior reports of Nkd targeting Dsh, an enigmatic Wnt signal transducer that acts upstream of β -catenin degradation. Although Wnt-signal-induced Dsh accumulation has been observed in cultured cells (Yanagawa et al. 1995), transgenic mice (Millar et al. 1999), and some cancers (Uematsu et al. 2003), and recent studies indicate that Dsh, like β -catenin, can be degraded by the ubiquitin–proteasome pathway (Simons et al. 2005; Angers et al. 2006; Zhang et al. 2006), our data show that Nkd does not attenuate Wnt signaling in the embryo by significantly altering steady-state Dsh levels or distribution. If Nkd promotes Dsh degradation in the fly embryo, as has recently been proposed on the basis of overexpression of mammalian Nkd in cultured cells (Creyghton et al. 2005), it must act only on a subset of Dsh, perhaps the fraction engaged in signaling. Consistent with this idea, we observed rare, punctate Nkd/Dsh colocalization in embryonic ectodermal cells.

Several Nkd constructs with mutant or deleted Dsh-binding regions possessed a reduced but still substantial *nkd* rescue activity. Perhaps Nkd ^{Δ RI5/GFPC}, lacking both Dsh-binding regions, is able to target Dsh *in vivo* (and hence rescue a *nkd* mutant) by virtue of overexpression, through other low-affinity Nkd/Dsh-binding regions, or by as yet uncharacterized proteins that bridge Nkd to Dsh. Consistent with these possibilities, we also observed some Nkd ^{Δ RI5/GFPC}/Dsh colocalization.

Three independent lines of investigation—evolutionary sequence comparisons, sequencing of lethal *nkd* alleles, and transgenic *nkd* rescue assays—pinpointed a 30-aa motif, separable from Dsh-binding regions, that is crucial for fly Nkd activity and nuclear localization. The comparable positions, identical sequence length, and similar predicted

structure of insect and mammalian 30-aa motifs suggests that the family of Nkd proteins may inhibit Wnt signaling through a common mechanism. Given the small size and presumably simple α -helical structure of the 30-aa motif, it is unlikely to possess intrinsic catalytic activity but, in addition to its weak NLS activity, it could serve as a protein-docking motif.

In addition to several reports that have documented nucleo-cytoplasmic shuttling of β -catenin, Axin, and APC (Schneider et al. 1996; Arbesfeld et al. 2000; Cong and Varmus 2004; Rosin-Wiechens et al. 2004; Xiong and Kotake 2006), it is noteworthy that two recent reports revealed a potential role for Fz and Dsh in the nucleus (Itoh et al. 2005; Mathew et al. 2005). In response to Wg signaling at the fly neuromuscular synapse, the Fz2 C terminus was detected in puncta of postsynaptic muscle nuclei although not in ectodermal nuclei (Mathew et al. 2005), so this report's significance to Nkd's action in ectoderm is unclear. *Xenopus* Dsh has a separable NLS and nuclear export sequence (NES), with the former required for "signaling activity" in gain-of-function assays (Itoh et al. 2005). However, a vertebrate Dsh construct with a mutant NES exhibited increased nuclear accumulation but no activity increase relative to that of wild-type Dsh, arguing against nuclear Dsh concentration—at least when it is overexpressed—being rate limiting for activity (Itoh et al. 2005). Intriguingly, Dsh NES and NLS motifs seem to be conserved in *D. melanogaster* Dsh, but their significance remains to be investigated.

Our data extend our still rudimentary knowledge of Nkd action in the fly embryo. The epistatic relationship between *wg* and *nkd* suggests that, in the absence of Wg ligand, the low levels of Nkd in a *wg* mutant (because Wg normally upregulates *nkd* transcription)

inhibit spontaneous ligand-independent signaling through the Wnt receptor complex (Bejsovec and Wieschaus 1993; Zeng et al. 2000). Wg exposure promotes Arm accumulation and induction of target genes, including *en*, *hh*, and *nkd*. Nkd, synthesized in the cytoplasm, accumulates and targets an uncharacterized fraction of cytoplasmic Dsh. However, Nkd/Dsh binding alone is apparently insufficient to limit Wg signaling during stages 10–11, as Nkd uses its 30-aa motif to inhibit Arm accumulation, restrict Wg-dependent gene expression, and access the nucleus. Although it is possible that the 30-aa motif is required in the cytoplasm, and that the ability of the 30-aa motif to confer nuclear access is a consequence rather than a cause of activity, three lines of evidence support a nuclear role for Nkd: (1) a subpool of Nkd normally accumulates in the embryonic nuclei after stage 10; (2) the 30-aa motif, distinct from the Dsh-binding sequence, was necessary for both nuclear localization and activity and was sufficient to increase the activity of mouse Nkd1 when expressed in the fly; and (3) a heterologous NLS increased nuclear localization and *nkd* rescue activity of Nkd^{Δ30aa}.

While our experiments strongly suggest a role for Nkd in the nucleus, they do not reveal the nature of that role. Likewise, lacking insight into how Dsh transmits Wnt signals into the nucleus, our experiments thus far reveal neither the relevant subcellular location(s) of Nkd action nor a molecular mechanism by which Nkd inhibits Dsh activity. The punctate Nkd/Dsh colocalization that we observe in embryonic cytoplasm, and rarely, in nuclei, is consistent with Nkd either affecting Dsh nucleo-cytoplasmic transport or impinging directly on the chromatin of Wnt-responsive genes. Our inability to observe increased nuclear Nkd or Dsh after treatment with a nuclear export inhibitor suggests that nuclear

export of Nkd (and possibly Dsh) in the fly embryo (1) does not occur (*e.g.*, if each protein were degraded in the nucleus following import); (2) occurs over a longer time period relative to proteins such as Lines that can rapidly shuttle between nucleus and cytoplasm; (3) is independent of CRM-1; or (4) like the presumed Nkd/Dsh interaction, involves only a fraction of the total pool of each protein. Future experiments will be required to distinguish among these possibilities.

The four-domain structure of both insect and vertebrate Nkd's argues that there once existed an ancient "core" mechanism by which Nkd engaged Dsh to inhibit Wnt signaling. However, given the sequence divergence between insect and mammalian Nkds, their current mechanisms may share little similarity beyond Dsh binding. Recently, PR72 and PR130, two alternatively spliced B" subunits of the multi-subunit enzyme protein phosphatase 2A (PP2A), were shown to associate with mammalian Nkd and to modulate its inhibitory effect on ectopic Wnt signaling (Creyghton et al. 2005, 2006). As Dsh is phosphorylated by kinases such as CK1, CK2, and Par1 following Wnt stimulation (Yanagawa et al. 1995; Willert et al. 1997; Peters et al. 1999; Sun et al. 2001), recruitment of phosphatases to Dsh by Nkd represents an attractive hypothesis to explain the inhibitory action of Nkd on Wnt signaling via Dsh. Consistent with this possibility, Nkd, PP2A, and Dsh kinases co-immunoprecipitated with vertebrate Dsh (Angers et al. 2006). However, unlike the vertebrate Nkd/PR72 interaction, thus far we do not detect direct interactions by Y2H between the fly PR72 homolog (CG4733) and full-length fly Nkd or any of the regions in Nkd, in particular the 30-aa motif, that are crucial for activity (our unpublished observations). Thus, regulation of Nkd activity by PR72/PR130 may be

a derived, vertebrate-specific phenomenon—analogous in some ways to the effect of mammalian Nkd2 but not Nkd1 on intracellular TGF- α trafficking (Li et al. 2004)—that may be distinct from the mechanism by which Nkd regulates Wg signaling in *Drosophila*.

In *Drosophila*, *nkd* is crucial for shaping gradients of Wnt activity, but is this role conserved in vertebrates? Mouse *nkd* genes are expressed during embryogenesis in dynamic patterns reminiscent of known Wnt gradients (Wharton et al. 2001; Ishikawa et al. 2004; Nakaya et al. 2005). A recent report described *nkd1* mutant mice with a targeted deletion of exons 6 and 7 (encoding the EFX domain) but allowing in-frame splicing between exons 5 and 8, resulting in expression of a residual Nkd1 protein very much analogous to our Nkd ^{Δ RI5/GFPC} construct that lacks Dsh-binding sequences but retains three conserved motifs (Li et al. 2005). Given that *nkd1* is more broadly expressed than *nkd2* during mouse development (Wharton et al. 2001), it was surprising that *nkd1*^{−/−} mice were viable and fertile, even though mutant mouse embryo fibroblasts showed elevated Wnt reporter activity and homozygous male mice exhibited a sperm maturation defect (Li et al. 2005). Although genetic redundancy between *nkd1* and *nkd2* could account for these observations, our results suggest an alternative hypothesis, namely that the residual protein produced in the reported *nkd1* mutant mice, like our EFX-deleted Nkd ^{Δ EFX/GFPC} and Nkd ^{Δ RI5/GFPC} constructs, has significant activity *in vivo*, despite the observation that a mutant mNkd1 protein lacking the EF hand is defective at blocking Wnt signaling in cultured cells (Yan et al. 2001). Resolution of this quandary awaits an investigation of strong loss-of-function mutations in each mammalian *nkd* gene. Given the broad involvement of Wnt/ β -catenin signaling in mammalian development and cancer,

coupled with the similar loss-of-function phenotypes of fly *nkd*, *axin*, and *apc* homologs, we hope that our studies guide future investigations of vertebrate Nkd proteins as regulators of Wnt signaling and candidate tumor suppressor genes.

PREFACE TO CHAPTER THREE

CHAPTER THREE describes how Nkd inhibits Wnt signaling in cell-autonomous, myristyl-independent manner in the embryo. It is adapted from “*Chan et al., 2007 C.C. Chan, S. Zhang, T. Cagatay, and K.A. Wharton Jr., Cell-autonomous, myristyl-independent activity of the Drosophila Wnt/Wingless antagonist Naked cuticle (Nkd). Developmental Biology, 311: 538-553 (2007)*”.

For this work, I generated *UAS-Nkd^{ΔN/GFP}*, *UAS-Nkd^{m1NΔN/GFP}*, and *UAS-mNkdI^{N/β30aa/GFP}* transgenic flies. I also helped in cuticle preparations and embryo staining. Keith Wharton did all the embryo staining and confocal imaging. Tolga Cagatay and Shu Zhang performed the Kc cell culture transfections and western blots.

CHAPTER THREE

CELL-AUTONOMOUS, MYRISTYL-INDEPENDENT ACTIVITY OF THE *DROSOPHILA* WNT/WINGLESS ANTAGONIST NAKED CUTICLE

3.1 Introduction

Secreted Wnt proteins regulate development, tissue homeostasis, and stem cell renewal throughout the animal kingdom. The ability of Wnts to regulate gene expression in a concentration-dependent fashion across fields of cells and/or layers of tissue embodies their designation as “morphogens” (Hoppler and Bienz, 1995, Immergluck et al., 1990 and Zecca et al., 1996). The importance of precisely controlling Wnt signal transmission – from ligand production in signal-producing cells to signal reception and interpretation signal-receiving cells – is evidenced by the plethora of developmental defects and diseases – including cancer, osteoporosis, and diabetes – that arise as a consequence of altered signaling (Clevers, 2006). A thorough understanding of mechanisms that maintain Wnt signaling cascades within a physiological range will be a prerequisite to the effective manipulation of signaling for therapeutic purposes.

One common consequence of Wnt receptor engagement in widely diverged animals is the accumulation of β -catenin, a bifunctional adaptor protein that regulates cell adhesion and acts as a transcriptional coactivator to regulate Wnt-dependent target gene expression (Brembeck et al., 2006, Molenaar et al., 1996, Peifer et al., 1994 and Riggleman et al., 1990). Graded activity of the so-called “canonical Wnt/ β -catenin” signaling axis, elicited

by the Wnt protein Wingless (Wg), is crucial for segmentation in the embryo of the fruit fly *Drosophila melanogaster* (Baker, 1988, Bejsovec and Martinez Arias, 1991, DiNardo et al., 1994 and Noordermeer et al., 1992). Discrete phases of differential gene expression, cell–cell interactions, and cell morphogenesis are evident during segmentation: First, a hierarchy of gap, pair-rule, and segment-polarity genes specifies segmental primordia (Nüsslein-Volhard and Wieschaus, 1980). Next, Wg and Hedgehog (Hh) signals, expressed within each segmental anlage in adjacent, narrow stripes of cells, reinforce each other's expression through a $2\frac{1}{2}$ h period during germ band extension ($3\frac{1}{2}$ –6 h after egg laying, stages 9–11) (DiNardo et al., 1994). Thereafter, a dynamic and unique combination of Wg, Hh, Notch, and EGF signals influences each cell's fate (Bejsovec and Martinez Arias, 1991, Bejsovec and Wieschaus, 1993, Colosimo and Tolwinski, 2006, Hatini and DiNardo, 2001, Payre et al., 1999, Price et al., 2006, Urban et al., 2004 and Wiellette and McGinnis, 1999). Upon differentiation, ventral epidermal cells distant from Wg-producing cells secrete a belt-like array of protrusions termed denticles, while cells close to the source of Wg – except those that will make the most anterior row of denticles – suppress denticle synthesis and secrete “naked” cuticle (Bejsovec and Martinez Arias, 1991 and Dougan and DiNardo, 1992).

How Wnts and other morphogens transit through tissues to regulate target gene expression remains the subject of intense study and conjecture (Lander, 2007, Martinez Arias, 2003 and Sampedro et al., 1993), with important, early contributions made possible through the study of Wg signaling during *Drosophila* segmentation (Klingensmith and Nusse, 1994). While morphogens such as Wg may in principle freely

diffuse to distant cells (Lander et al., 2002), the facts that Wnts are glycosylated and lipid-modified (Smolich et al., 1993 and Willert et al., 2003), that there exists an extracellular jungle of proteoglycans that can bind Wnts and limit free diffusion (Baeg et al., 2004, Franch-Marro et al., 2005, Han et al., 2005 and Kirkpatrick et al., 2004), that Wg-producing and receiving cells may migrate away from the signal source prior to degrading Wg (Pfeiffer et al., 2000), and that Wg may be actively transported – “transcytosed” – through a field of cells (Greco et al., 2001 and Moline et al., 1999), indicates the existence of multiple regulatory mechanisms. In the stage 9 embryo, Wg is found in the endoplasmic reticulum and Golgi apparatus of signal-sending cells, and is symmetrically distributed in the extracellular space and in endolysosomal vesicles in a few rows of adjacent signal-receiving cells; but, by stage 11, the gradient of Wg distribution and activity is asymmetric with an anterior bias due to Hh and EGF signal-dependent Wg degradation in posterior signal-receiving cells (Dubois et al., 2001, Gonzalez et al., 1991, Sanson et al., 1999 and Van den Heuvel et al., 1989). Despite enhanced degradation of Wg in posterior cells during stages 10–12, genetic studies suggest that Wg influences the diversity of denticle morphologies synthesized by those cells (Bejsovec and Martinez Arias, 1991 and Bejsovec and Wieschaus, 1993), raising the question of how Wg reaches these cells to influence their fate.

Embryos mutant in the *naked cuticle* (*nkd*) gene have been reported to develop sequential abnormalities in Wg target gene transcription, Wg protein distribution, and *wg* mRNA expression (Bejsovec and Wieschaus, 1993, Dougan and DiNardo, 1992, Jürgens et al., 1984, Lee et al., 1992, Martinez Arias et al., 1988, Moline et al., 1999, Tabata et al.,

1992, Waldrop et al., 2006 and Zeng et al., 2000). In *nkd* mutants, *wg* and *hh* expression initiates normally, but during stage 9, the Wg target genes *hh* and *engrailed* (*en*) are transcribed in additional, posterior cells distant from Wg-producing cells, which through stage 10–11 leads to the induction of a new stripe of *wg* just posterior to the expanded *en/hh* domain (Fig. 2.1A) (Martinez Arias et al., 1988). Since later Wg signaling directs “naked” cuticle differentiation, the ectopic Wg stripe creates mirror-image pattern duplications, extra naked cuticle, and increased cell death in embryos homozygous for strong *nkd* alleles, while weaker *nkd* alleles show replacement of denticle belts by naked cuticle in proportion to the number of cells that ectopically produce Wg (Bejsovec and Martinez Arias, 1991, Dougan and DiNardo, 1992, Jürgens et al., 1984, Pazdera et al., 1998, Waldrop et al., 2006 and Zeng et al., 2000).

Although the sequence of gene expression abnormalities in *nkd* mutants is well recognized, the causal relationships between the early and later abnormalities are not understood. Intact Wg and Hh signaling is required for induction of the ectopic *wg* stripe in *nkd* mutants (Bejsovec and Wieschaus, 1993 and Dougan and DiNardo, 1992), likely due in part to a requirement for *wg* in autoregulating its own transcription (Yoffe et al., 1995), but the source of the initiating Wg signal – anterior vs. posterior to the incipient ectopic *wg* stripe – is not clear. Moreover, although Nkd can block responses to ectopic Wg in a cell-autonomous manner in eye imaginal disc (Rousset et al., 2001), whether Nkd acts cell-autonomously in the embryo has not been investigated. Previously, the observation that misexpression of *shibire*^{K44A} (*shi*^D), a dominant-negative version of the motor protein dynamin whose expression disrupts endocytosis, in *en*-expressing cells of

nkd embryos narrowed En stripes and prevented ectopic *wg* transcription was argued as evidence in support of the hypothesis that Nkd restricts the cell-to-cell transport of Wg posterior to *wg*-expressing cells (Damke et al., 1994 and Moline et al., 1999). Consistent with this possibility was an apparent increase in Wg immunoreactivity posterior to endogenous *wg* stripes in stage 10 *nkd* mutants (Moline et al., 1999). However, experiments showing that Wg signaling is not required for normal denticle synthesis in cells posterior to *en*-expressing cells (Sanson et al., 1999), coupled with the recent finding that misexpression of *shi^D* may cause toxic and/or non-specific effects on Wg signaling or cell viability (Rives et al., 2006), demand a careful reappraisal of any conclusions derived from *shi^D* misexpression.

By what mechanism does Nkd inhibit Wnt signaling? As a first step to answer this question, our laboratory has developed *in vivo* assays – including a stringent *nkd* rescue assay – to study Nkd activity in *Drosophila*, and has tested the activities of mutant and chimeric Nkd proteins in these assays (Rousset et al., 2002 and Waldrop et al., 2006). Nkd is a novel intracellular protein that inhibits Wg signaling, in part, by binding to Dishevelled (Dsh), a scaffold protein that links – in a still mysterious fashion – Wnt receptor activation to β -catenin accumulation (Rousset et al., 2001, Wallingford and Habas, 2005, Wharton, 2003 and Zeng et al., 2000). The only sequence homology shared between fly Nkd and its two mammalian homologs – Nkd1 and Nkd2 – is an EF-hand-containing domain (which we have termed “EFX,” but is a.k.a. “NH2” (Kato, 2001) or “NHR1” (Li et al., 2004)) that binds Dsh or its mammalian counterparts, the Dvl proteins (Rousset et al., 2002 and Wharton et al., 2001). Nkd also has an unconventional nuclear

localization motif, separate from Dsh-binding regions, that is essential for activity (Waldrop et al., 2006). A consensus sequence (MGXXXS) that directs the post-translational addition of a lipophilic myristoyl moiety is found at the N-terminus of mammalian Nkd1 and Nkd2, but no such sequence is found at the N-terminus of fly Nkd (Li et al., 2004, Resh, 2004, Wharton et al., 2001 and Zeng et al., 2000), raising the question of whether the fly and mammalian Nkd N-termini have homologous functions. Although possibly a coincidence, EF-hands in known Nkd proteins are most similar to EF-hand proteins of the recoverin family of “myristoyl-switch” proteins that undergo Ca^{2+} -sensitive alteration in tertiary structure to expose a buried N-terminal myristate, thereby allowing reversible, stimulus-dependent membrane association (Flaherty et al., 1993 and Zeng et al., 2000). The absence of a N-terminal myristoylation sequence in fly Nkd suggests either that Nkd does not associate with membranes, or that if it does engage membranes it might do so through protein–protein interactions as a peripheral membrane protein.

In this paper, we show that Nkd acts cell-autonomously during segmentation, independently limiting Wg signaling in cells anterior and posterior to Wg-producing cells, a result inconsistent with models that invoke posterior, cell-to-cell transport of Wg as necessary for induction of ectopic *wg* stripes in *nkd* mutants (Moline et al., 1999). Additionally, we show that the N-terminus of *Drosophila* Nkd confers unique functional and membrane-association properties that cannot be mimicked by N-terminal myristoylation. Our results suggest that Nkd acts at multiple subcellular locations in signal-receiving cells to attenuate the response to Wg signaling.

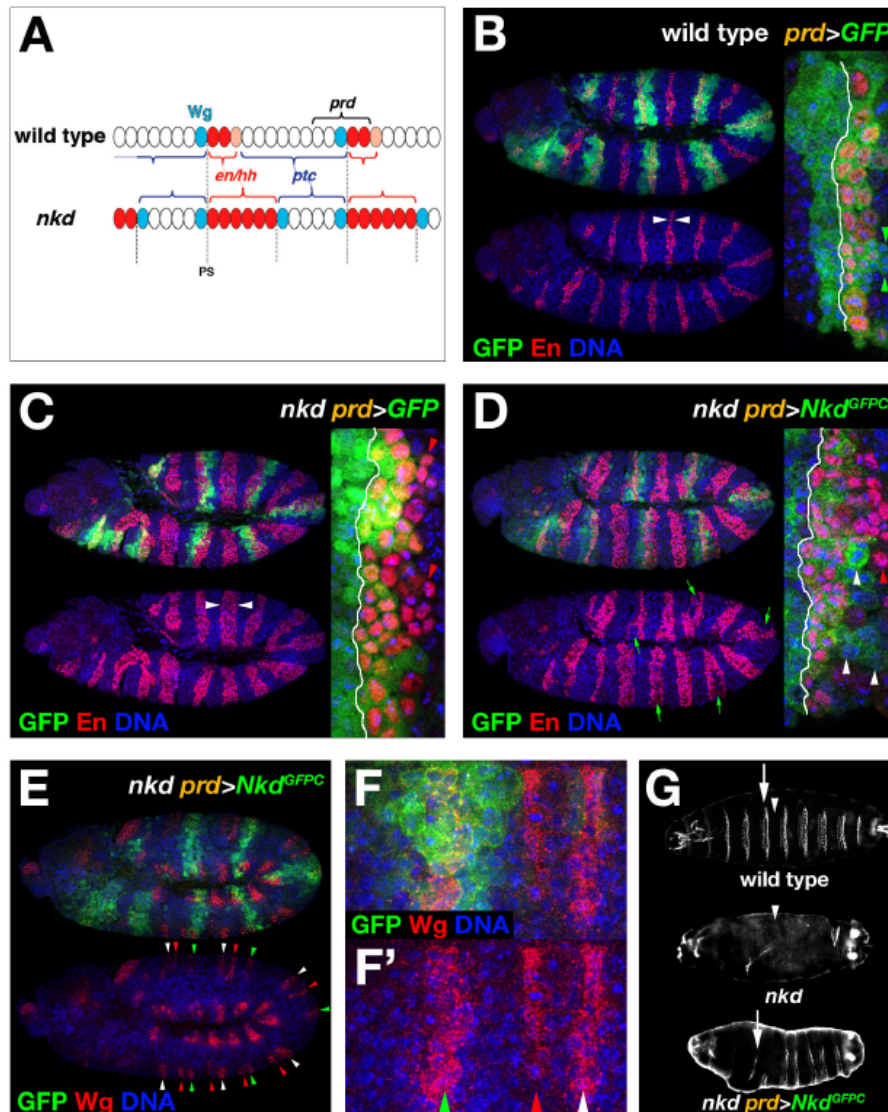


Fig. 3.1. Nkd acts cell-autonomously to inhibit Wg-dependent En production. (A) Schematic of *wg* (light blue) and *en/hh* (red) gene expression in two segmental anlage of stage 10–11 wild type (top) and *nkd*-mutant (bottom) embryo. Anterior is to the left in all panels. *prd* domain (black bracket) is ~ 5 cells wide, centered on the *wg*-expressing row of cells, and is not altered in a *nkd* mutant. *en/hh* and *ptc* domains are complementary, and each domain is shifted in *nkd* mutants as compared to wild type. Dashed lines indicate the positions of endogenous and ectopic parasegmental boundaries (PS). (B) Stage 11 *prd > GFP* embryo stained for GFP (green), En (red) and DNA (blue), with high-magnification inset of representative region around PS boundary. Note 2–3 cell wide En stripe (white arrowheads). PS boundary is marked by the white line in panels B–D. Note occasional En-negative, GFP-positive cells (green arrowheads) just posterior to

En-producing cells. (C) *nkd prd > GFP* embryo, stained as in panel B. Note uniformly widened En stripe (white arrowheads), with 2–3 rows of En-producing cells (red arrowheads) posterior to the *prd-Gal4* domain. (D–F) *nkd prd > Nkd^{GFPC}* embryo. (D) En stain. Note cells in the center of the widened En stripe with reduced to absent En immunoreactivity (green arrows) due to Nkd^{GFPC} production in those cells. In inset, note loss of En staining in Nkd^{GFPC}-producing cells (white arrowheads) at the center of the expanded En domain, with additional, En-producing cells more posterior to the *prd-Gal4* domain (red arrowhead). (E) Wg stain. Note endogenous Wg stripe with (green arrowhead) or without (white arrowhead) Nkd^{GFPC} staining, as well as variable ectopic Wg stripe (red arrowheads). (F–F') High power view showing that Wg distribution is similar in Nkd^{GFPC}-expressing (green arrowhead) and non-expressing (white arrowhead) PS. Red arrowhead shows ectopic Wg stripe. (G) Ventral surface of wild type cuticle (top) consists of alternating denticle belts (arrow) and naked cuticle (arrowhead). *nkd^{7H16}* mutant (middle) shows strong *nkd* phenotype consisting of uniform naked cuticle. *nkd prd > Nkd^{GFPC}* embryo (bottom) shows variable replacement of naked cuticle with denticle belts.

3.2 Materials and methods

3.2.1 DNA constructs

All Nkd constructs were built in Bluescript-II-KS+ (Stratagene) and cloned into the P-element vector pUAS-T for P-element transformation and misexpression using the *Gal4/UAS* system (Brand and Perrimon, 1993). Nkd^{GFPC}, Nkd^{NBg/GFPC}, Nkd^{7H/GFPC}, mNkd1^{GFPC}, mNkd1^{F30aa/GFPC}, Src^{(1–89)GFP} have been previously described (Waldrop et al., 2006). DNA fragments were synthesized by Pfu PCR and then subcloned and sequenced. Nkd^{GFPC/mycC} has linker sequence plus enhanced green fluorescent protein (EGFP) (Clontech) amino acids (aa) 1–244 inserted after Nkd aa 294 (Nkd residues underlined: ...GSIATMV...(EGFP)...GLRSGG...), with a C-terminal myc tag. Nkd^{GFPCN/mycC} has EGFP residues 1–239 fused to Nkd aa 2–928, with a C-terminal myc tag. Nkd^{SrcNBg/GFPC} has *Drosophila* Src aa 1–89 (Simon et al., 1985) fused to Nkd^{NBg/GFPC}; Nkd^{SrcG2ANBg/GFPC} is identical to Nkd^{SrcNBg/GFPC} except Gly2 was mutated to Ala. Nkd^{SrcR1Bg/GFPC} fused Src aa

1–89 to Nkd^{NB_g/GFPC} aa 177–928. Nkd^{m1NΔN/GFPC} fused mouse Nkd1 aa 1–27 to Nkd aa 79–928 to GFP. mNkd1^{fNf30aa/GFPC} fused fly Nkd aa 1–78 to mNkd1^{f30aa/GFPC} aa 28–end.

3.2.2 Fly stocks and genetics

Fly husbandry and P-element transformation were performed by standard methods. All crosses were performed at 25 °C. *nkd*^{7H16}, which harbors a nonsense mutation at codon #60 and is the strongest known *nkd* allele (Jürgens et al., 1984, Waldrop et al., 2006 and Zeng et al., 2000), was used in all rescue assays. At least three independent transgenic lines were obtained for each *UAS-Nkd* construct, and two or more independent chromosome II inserts for each line were tested in each *nkd* rescue cross: *UAS-Nkd/UAS-Nkd* or *CyO; nkd*^{7H16}/*TM3-Hb-lacZ* X *nkd*^{7H16} *da-Gal4/TM3-Hb-lacZ*. For cases where the *UAS-Nkd* line used was a lethal insertion, 12.5% of cuticles are predicted to remain unrescued *nkd* mutants due to the persistence of the *CyO* balancer in the rescue cross. Fly stocks/chromosome: *UAS-GFP* (II) (Yeh et al., 1995), *UAS-lacZ* (II) (Brand and Perrimon, 1993), *UAS-Axin*^{GFP} (II) (Cliffe et al., 2003), *UAS-dTCF*^{ΔN} (II) (van de Wetering et al., 1997), *da-Gal4* (III) (Wodarz et al., 1995), *prd-Gal4* (III) (Yoffe et al., 1995), *en-Gal4* (II) (Fietz et al., 1995), *ptc-Gal4* (II) (Hinz et al., 1994), *B119-Gal4* (II) (Zeng et al., 2000), *71B-Gal4* (III) (Brand and Perrimon, 1993).

3.2.3 Cuticle preparations

Cuticle preparations were performed, scored as wild type or weak, moderate or strong *nkd*, and selected for photography as previously described (Waldrop et al., 2006 and Zeng et al., 2000). Criteria for scoring *nkd* cuticles were based on the existing *nkd* allelic series

as well as the spectrum of *nkd* cuticle rescue observed when Nkd is expressed in a strong *nkd* mutant: “strong” class cuticles, exemplified by *nkd*^{7H16}, *nkd*^{7E89}, and *nkd*^{47K1}, are < 75% of wild-type length, have two or fewer complete denticle bands and have a fully exteriorized head skeleton and non-everted, widely spaced posterior spiracles (Jürgens et al., 1984, Waldrop et al., 2006 and Zeng et al., 2000); “moderate” class cuticles, exemplified by *nkd*^{9G33}, or *nkd*^{7H16} rescued by ubiquitous expression of a *UAS-Nkd* construct that lacks the 30 aa motif (Jürgens et al., 1984, Rousset et al., 2002 and Waldrop et al., 2006), have three or more complete denticle bands (usually in odd numbered abdominal segments), a partially internalized head skeleton, and partially to fully everted spiracles. “Weak” class cuticles, exemplified by *nkd*^{42J1}, *nkd*^{71-72K1}, and *l(3)4869* (a lethal P element inserted in the 5' end of *nkd*), have normal denticle bands in most segments but focal denticle band loss, and typically subtle or no head or tail defects (Jürgens et al., 1984, Waldrop et al., 2006 and Zeng et al., 2000). Rescue of the *nkd* head and tail defects was not as efficient with expression of the Wg antagonists dTCF^{ΔN}, Axin^{GFP}, or mNkd1^{ΔN30aa} as compared to fly Nkd, so only denticle belt criteria were used to score *nkd* phenotypic classes in Fig. 3.3 and Fig. 3.6.

3.2.4 Computer programs

Figures were prepared in Photoshop (Adobe), drawings in Canvas (ACD Systems) and Powerpoint (Microsoft), and graphs in Deltagraph (Red Rock Software). Channel spectra were maximized below saturation for selected confocal images, with the exception that anti-Arm channels were not altered. ImageJ (NIH) was used to quantitate mean greyscale pixel intensity of raw confocal images of Arm-stained embryos as previously described

(Waldrop et al., 2006). Statistical calculations were performed using Prism (GraphPad Software) and Microsoft Excel.

3.2.5 Immunocytochemistry and confocal microscopy

All embryo collection, fixation, staining procedures including antibody dilutions, and confocal microscopy were performed as previously described (Waldrop et al., 2006). Mean \pm S.D. of En stripe width was calculated by counting the number of En-positive cell diameters along the anterior–posterior axis in dorsomedian and ventral–median positions in parasegments 2–14 of five stage 11 *nkd da > Nkd* embryos for each construct (130 data points per construct).

3.2.6 Kc cell culture and transfections

pArm-GFP, or pArm-Gal4 with either pUAS-Src^{(1–89)GFP} or pUAS-Nkd^{7H/GFP} plasmids were transfected into *Drosophila* Kc cells grown at 25 °C in Schneider medium with 10% fetal bovine serum. Lysates as follows were prepared 36 h post-transfection: Whole cell lysates were obtained by scraping and dispersion of cells into *Drosophila* cell lysis buffer (50 mM Tris–HCl, pH 7.5, 150 mM NaCl, 1% NP40, 0.5% sodium deoxycholate, 1 mM PMSF and 1 \times protease inhibitor cocktail (Roche)) for 1 h on ice, then centrifuging at 12,000 \times g for 10 min. Triton–soluble fractions from cultures transfected in parallel were obtained by gently adding MES buffer, pH 6.8 (2.5 mM EDTA, 5 mM MgCl₂ and 0.5% Triton X-100) \times 3 min. and then aspirating the liquid phase into a fresh tube. The remaining, triton-insoluble lysates were obtained by adding cell lysis buffer to the remaining material, and processing above as for whole cell lysate. Samples were

concentrated with Amicon filters, and equal amounts of lysate were resolved by 10% SDS-PAGE and transferred to Hybond membrane. Western blot was probed with rabbit polyclonal anti-GFP (Santa Cruz) at 1:3,000 followed by HRP-conjugated anti-rabbit (Pierce) at 1:1000. Equal loading was confirmed by probing all blots with anti- β -tubulin (Covance) (not shown). Signals were visualized by the SuperSignal West Dura Chemiluminescent Substrate kit (Pierce). Confocal images of Kc cells pre- and post-Triton-X100 treatment were collected from transfected cells grown on coverslips and then subject to the extraction procedure described above, followed by fixation in 4% paraformaldehyde and counterstaining with DRAQ5 (Biostatus Limited).

3.3 Results

3.3.1 *Nkd* acts cell-autonomously in the embryo

The abundance of the fly β -catenin homolog Armadillo (Arm) and the width of Engrailed (En) stripes are readouts of Wg activity during segmentation of the germ band-extended *Drosophila* embryo (DiNardo et al., 1988, Martinez Arias et al., 1988, Peifer et al., 1994 and Riggelman et al., 1990). By stage 10, the markedly elevated Arm levels in *nkd* embryos are restored to wild-type levels in alternate segments when Nkd^{GFPC} (Nkd fused to a C-terminal GFP tag) is produced via *prd-Gal4*, a Gal4 driver whose expression in a ~ 5–6 cell wide domain in alternate segmental anlagen is centered on the Wg stripe (Fig. 3.1A) (Waldrop et al., 2006 and Yoffe et al., 1995). As a consequence of elevated Wg signaling in *nkd* mutants, En stripes approximately double in width along the anterior–

posterior axis (2.7 ± 0.7 cell diameters for wild type vs. 5.9 ± 1.4 cell diameters for *nkd*^{7H16} mutants) (*cf.* Figs. 3.1B, C). If *nkd* has cell-nonautonomous effects in the embryo, perhaps due to its ability to limit posterior, cell-to-cell transport of Wg (Moline et al., 1999), then we would expect to observe reduced or absent production of En in cells posterior to *prd*-expressing cells of *nkd* embryos in which Nkd^{GFPC} is driven by *prd-Gal4* (*nkd prd > Nkd*^{GFPC}) due to reduced delivery of Wg to those cells. Occasional En-negative, *prd-Gal4*-expressing cells posterior to En-producing cells allowed us to test this hypothesis (Fig. 3.1B). As shown in Fig. 3.1C, En-positive cells are readily identified posterior to GFP-positive cells of *nkd prd > GFP* embryos. As expected, in *nkd prd > Nkd*^{GFPC} embryos, reduced to absent En was observed in ventral Nkd^{GFPC}-producing cells more than 2–3 cells posterior to the source of Wg, due to the normal role of *nkd* in repressing *en* in these cells (Martinez Arias et al., 1988). However, En-producing cells were consistently observed just posterior to the Nkd^{GFPC}-producing cells (Fig. 3.1D), indicating that those cells have received Wg input. The distribution of Wg protein around endogenous *wg* stripes did not appear different between mutant and rescued segments of stage 10–11 *nkd prd > Nkd*^{GFPC} embryos (Figs. 3.1E, F–F'), suggesting that the reduced Arm in Nkd^{GFPC}-rescued cells (Waldrop et al., 2006) is due to a restored ability of those cells to appropriately respond to Wg. Cuticles secreted by *nkd prd > Nkd*^{GFPC} embryos exhibited a partial restoration of ventral denticle bands, consistent with a slight reduction in the number of ectopic Wg stripes in stage 11 *nkd prd > Nkd*^{GFPC} vs. *nkd prd > GFP* embryos (Figs. 3.1E, G, and not shown). Complete denticle bands in *nkd prd > Nkd*^{GFPC} cuticles had a wild-type assortment of denticle morphologies but subtle patterning abnormalities (*cf.* Supplementary Figs. 3.1A, B), consistent with En production in

epidermal cells fated to give rise to denticles having no effect on denticle morphology (Bejsovec and Martinez Arias, 1991). These observations, coupled with a cell-autonomous inverse relationship between Nkd^{GFPC} levels and Arm levels in *nkd prd > Nkd^{GFPC}* embryos (Waldrop et al., 2006), refute the hypothesis that *nkd* has essential cell non-autonomous roles in the embryo.

3.3.2 *Nkd* limits Arm accumulation in cells anterior to En-producing cells

Through stages 9–11, *en* transcription, whether in the presence or absence of *nkd*, requires Wg signaling (Bejsovec and Wieschaus, 1993, DiNardo et al., 1988, Dougan and DiNardo, 1992 and Martinez Arias et al., 1988), raising the question of whether Wg ligand that maintains En production in the posterior cells of *nkd prd > Nkd^{GFPC}* embryos originates from the *endogenous wg* stripe that is several cell diameters anterior to those cells, or – the more likely scenario – from an *ectopic wg* stripe just posterior to those cells. First, we confirmed that *nkd* limits Wg-dependent Arm accumulation in cells anterior to *en*-expressing cells by inhibiting Wg signaling (and Arm accumulation) within *en*-expressing cells through expression of either a GFP-tagged version of the Wnt antagonist Axin ($Axin^{GFP}$) (Cliffe et al., 2003) or a dominant-negative version of Pangolin, the transcriptional effector of Wg signaling ($dTCF^{\Delta N}$) (van de Wetering et al., 1997) via *en-Gal4* (Fietz et al., 1995); both gave similar results. (Because of the Wg-dependent nature of the expanded En domain in a *nkd* mutant, *en-Gal4* mediated expression of a Wg antagonist creates a negative feedback loop that variably reduces the width of the En stripe as well as that of *en-Gal4* itself, leading by stage 11 to patchy narrowing of the En domain.) As shown in Figs. 3.2A and B, in *nkd en > Axin^{GFP}*

embryos, cells anterior to each En domain retain high levels of Arm 4–5 cell diameters anterior to each *wg/en* boundary—evidence that *nkd* regulates Arm levels in cells anterior to En-producing cells.

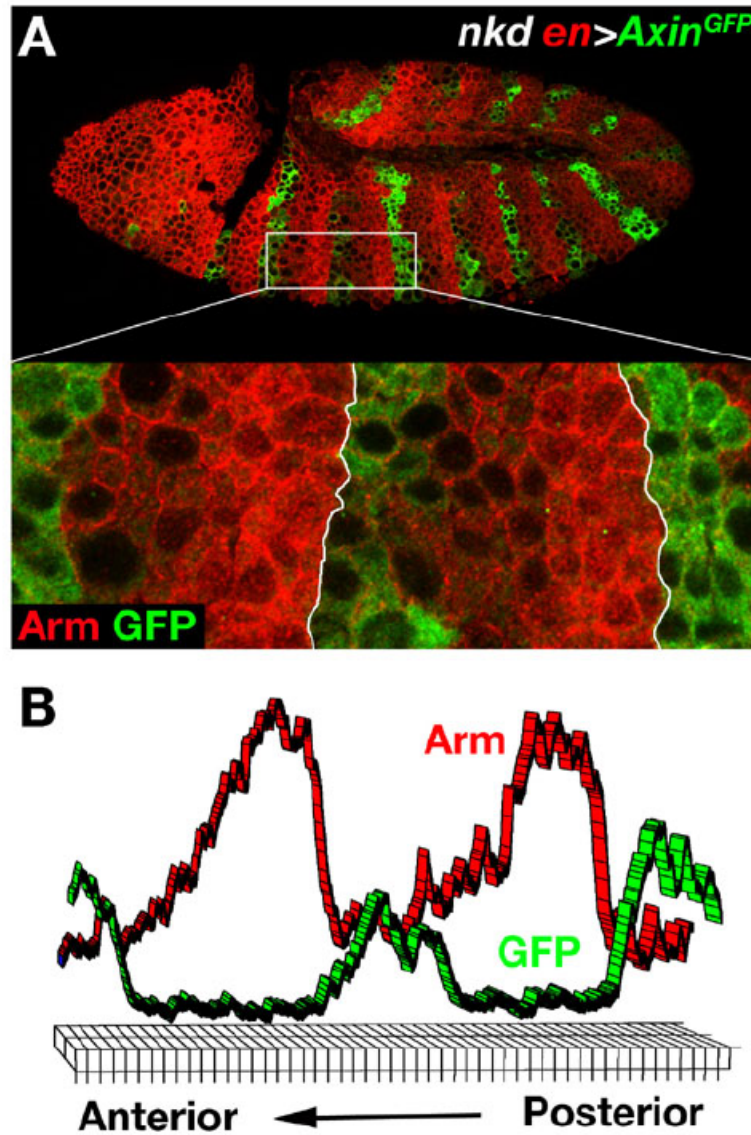


Fig. 3.2. *nkd* limits Arm accumulation in cells anterior to En-producing cells (A) *nkd en > Axin^{GFP}* embryo, stained for Arm (red) and GFP (green). In high-magnification inset below, note that Arm levels are markedly higher anterior to than posterior to the PS boundary (white line), an observation quantitated in panel B as mean greyscale pixel intensity for each channel as a function of position along the anterior–posterior axis.

3.3.3 *Nkd* is independently required in *En*-positive and *En*-negative cells

During stage 10, the segment-polarity gene *patched* (*ptc*) is expressed in epidermal cells that do not express *en*, with the normally broad domain of *ptc* expression narrowed in a *nkd* mutant due to expanded *en/hh* expression and the repressive role of *en* on *ptc* transcription (Fig. 3.1A) (Hidalgo and Ingham, 1990, Hooper and Scott, 1989 and Nakano et al., 1989). Since *en-Gal4* and *ptc-Gal4* are expressed in complementary domains (Fietz et al., 1995 and Hinz et al., 1994), we investigated which abnormalities in *nkd* embryos could be rescued by expressing *Nkd^{GFP}* using each *Gal4* driver. As with *prd-Gal4*, *En* is consistently reduced or absent in ventral epidermal cells in the middle of each expanded *en-Gal4* domain of *nkd en > Nkd^{GFP}* embryos, but not of *nkd en > GFP* embryos (Figs. 3.3A, B). However, *En* continues to be produced in the most posterior *en-Gal4*-producing cells of *nkd en > Nkd^{GFP}* embryos, again suggesting that those cells are close to a source of *Wg*, which we confirmed by staining with an antibody against *Wg* (Figs. 3.3C, D). We observed little to no difference in the number of parasegments (PS) that produce *Wg* ectopically in *nkd en > Nkd^{GFP}* embryos as compared to *nkd en > GFP* or *nkd ptc > GFP* embryos (Figs. 3.3C, D, G), indicating that providing *Nkd* to *en*-expressing cells in *nkd* mutants does not prevent the appearance of ectopic *Wg* stripes. Conversely, *nkd ptc > Nkd^{GFP}* embryos show a dramatic reduction in the number of ectopic ventral *Wg* stripes but retain wide *En* stripes (Figs. 3.3E–G). Reduced to absent

En in cells in the middle of each expanded *en* domain in *nkd en > Nkd^{GFP}* embryos is due to Nkd's activity as a Wg antagonist, because a similar but more severe reduction in the number of posterior cells that produce En can be observed in *nkd en > Axin^{GFP}* (Fig. 3.3H) or *nkd en > dTCF^{ΔN}* embryos (not shown). Accordingly, we observed a more complete restoration of ventral denticle belts and body length in *nkd* mutant cuticles when Nkd or dTCF^{ΔN} was expressed by *ptc-Gal4* than by *en-Gal4* (Figs. 3.3I, J). As with *nkd prd > Nkd^{GFP}* cuticles, ventral denticle bands in *nkd ptc > Nkd^{GFP}* and *nkd ptc > dTCF^{ΔN}* cuticles displayed mostly normal denticle morphology, but denticle bands of *nkd ptc > dTCF^{ΔN}* cuticles were markedly disarrayed (Supplementary Figs. 3.1C, D), likely due to the distinct mechanisms by which Nkd and dTCF^{ΔN} inhibit Wg signaling. As suggested by the near complete loss of ventral En in *nkd en > Axin^{GFP}* embryos (Fig. 3.3H), otherwise wild type *en > Axin^{GFP}* embryos showed complete loss of ventral En in stage 11 embryos and developed cuticles with fused denticle belts and complete loss of ventral naked cuticle (not shown), likely due to the greater strength of misexpressed Axin^{GFP} as a Wnt antagonist as compared to dTCF^{ΔN} or Nkd.

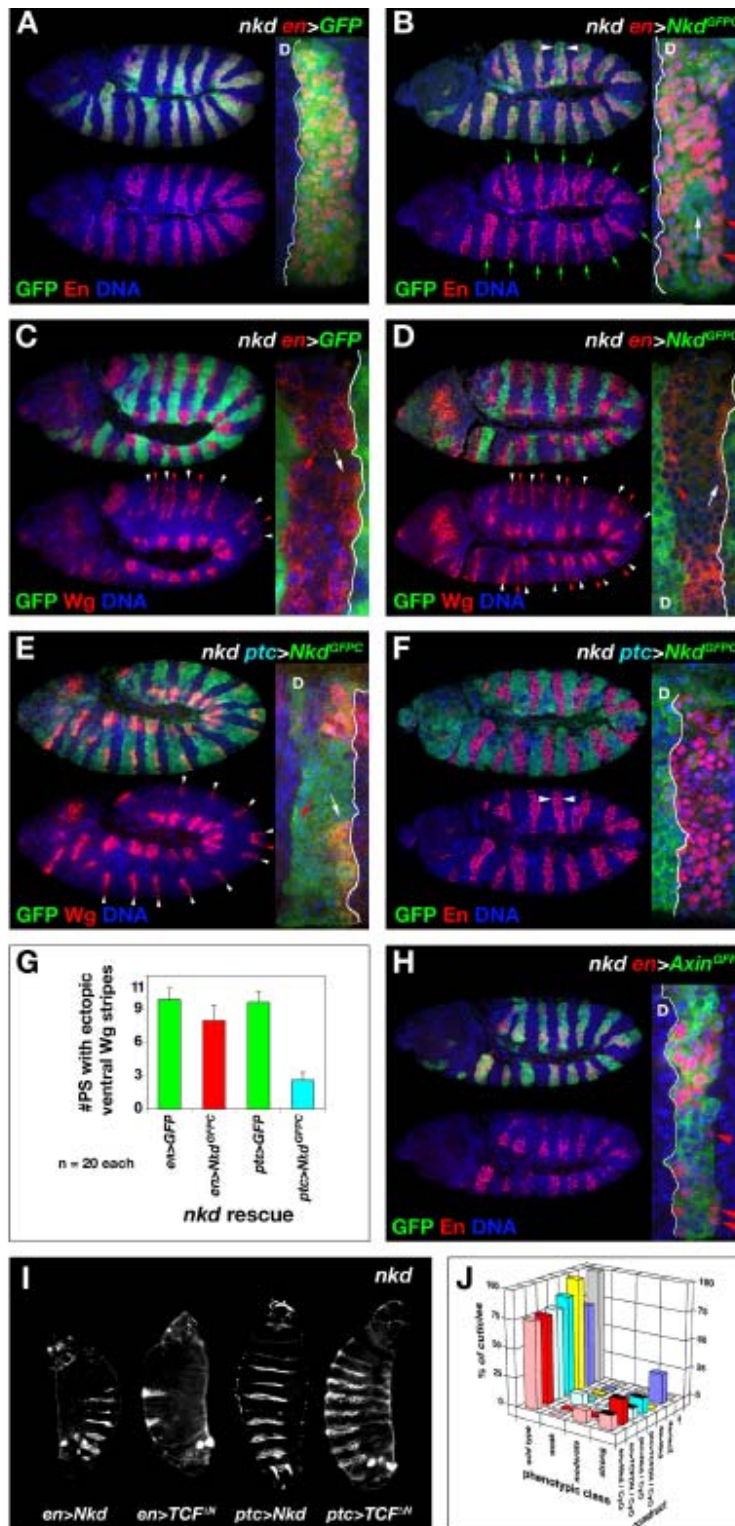


Fig. 3.3. Nkd acts independently in En-positive and En-negative cells. Panels A–F and H show lateral view of stage 11 embryos. Anterior is to the left, with the PS boundary marked with a white line and dorsal {D} ectoderm so designated in selected magnified inset panels. (A) *nkd en > GFP*, stained for GFP (green), En (red) and DNA (blue), showing concordance between expanded populations of *en > GFP* cells and En-producing cells. (B) *nkd en > Nkd^{GFP}* stained as in panel A showing loss of ventral En (green arrows) in middle of each expanded *en-Gal4* domain (white arrowheads). In inset, note En-producing cells at posterior boundary of *en-Gal4* domain despite *Nkd^{GFP}* expression in those cells. (C) *nkd en > GFP* stained as above except Wg protein is in red. Note endogenous (white arrowhead) and ectopic (red arrowhead) Wg stripes, with GFP-expressing cells abutting each Wg stripe. In inset, note endogenous (white arrow) and ectopic (red arrow) Wg stripes. (D) *nkd en > Nkd^{GFP}* stained as in panel C, showing numerous ectopic Wg stripes (red arrowheads and arrow in inset). (E) *nkd ptc > Nkd^{GFP}*, stained as in panel C, showing a single ectopic Wg stripe (red arrowhead). (F) *nkd ptc > Nkd^{GFP}*, stained as in panel B, showing expanded En stripe (arrowheads). (G) Mean \pm S.D. number of PS with ectopic ventral Wg stripes in thoracic + abdominal (11 total) segments as a function of indicated *nkd* rescue genotype ($n = 20$ mutant embryos per genotype). Note similarity between *en > GFP*, *ptc > GFP*, and *en > Nkd^{GFP}*, but dramatic reduction in *ptc > Nkd^{GFP}*. (H) *nkd en > Axin^{GFP}* embryo stained as in panel A, showing marked overall reduction in number of ventral En-producing cells, but persistence of a few En-producing cells (red arrowheads) at posterior boundary of ventral *en-Gal4* domain. (I) Representative *nkd* cuticles rescued by, from left to right, *en > Nkd*, *en > TCF^{ΔN}*, *ptc > Nkd*, *ptc > TCF^{ΔN}*. (J) Distribution of wild type and *nkd* cuticle phenotypes (weak, moderate, strong) for each *nkd* rescue cross with indicated construct. Cuticle phenotype class scoring criteria are described in Section 3.2 Materials and methods. w– (grey bars) is negative control, with 100% wild type. *da > lacZ* (violet) gives the expected Mendelian ratio of $\sim 75\%$ wild type and $\sim 25\%$ strong *nkd* mutant, while *da > Nkd* (yellow) rescues nearly all *nkd* mutants to wild type. Since *en-Gal4* and *ptc-Gal4* are each lethal inserts on chromosome II, the persistence of the CyO balancer in the rescue cross results in $\sim 12.5\%$ of cuticles remaining unrescued and hence “strong” (indicated by the black-topped bars). Note that *ptc-Gal4* (blue shade) when driving either Nkd or TCF^{ΔN} rescues *nkd* cuticles to a greater extent than *en-Gal4* (red shade).

3.3.4 Nkd N-terminus opposes nuclear localization and is required for function in vivo

Previously we showed that fusion of a myc epitope tag or GFP to the Nkd C-terminus did not alter rescue activity during embryogenesis (Waldrop et al., 2006). In contrast, fusion of GFP to the Nkd N-terminus (*Nkd^{GFPN/mycC}*), but not internally just C-terminal of the EFX (*Nkd^{GFPX/mycC}*), eliminated Nkd activity in three assays: First, when ubiquitously expressed in *nkd* mutants by *da-Gal4*, *Nkd^{GFPX/mycC}* limited En stripes to a width

comparable to those of wild type embryos (2.9 ± 0.8 cells) and rescued the *nkd* cuticle phenotype like Nkd^{GFPC} , but $\text{Nkd}^{\text{GFNP/mycC}}$ had little to no rescue activity (En stripe = 5.3 ± 1.4 cells) (Figs. 3.4A, B) (Waldrop et al., 2006). Second, when expressed by *prd-Gal4*, $\text{Nkd}^{\text{GFPC/mycC}}$ but not $\text{Nkd}^{\text{GFNP/mycC}}$ reduced Arm levels of stage 10 *nkd* mutants (Fig. 3.4C). Third, *B119-Gal4*-driven expression of $\text{Nkd}^{\text{GFPC/mycC}}$ in pupal abdomen prevented the appearance of nearly all of the sternite bristles whose induction requires Wg signaling (Shirras and Couso, 1996), but $\text{Nkd}^{\text{GFNP/mycC}}$ had no effect on sternite bristle quantity or pattern (Figs. 3.4D–G). Like endogenous Nkd and misexpressed Nkd^{GFPC} , $\text{Nkd}^{\text{GFPC/mycC}}$ localized in a punctate, predominantly cytoplasmic and diffuse nuclear pattern in embryonic epidermal cells when detected by anti-GFP immunocytochemistry (Waldrop et al., 2006), but $\text{Nkd}^{\text{GFNP/mycC}}$ was predominantly nuclear by stage 10 (Fig. 3.4A), indicating that Nkd N-terminal sequence is required to reside at the N-terminus in order for Nkd to function and to prevent Nkd from accumulating in the nucleus. Similarly, $\text{Nkd}^{\Delta\text{N/GFPC}}$, which lacks N-terminal sequence conserved in mosquito Nkd (Waldrop et al., 2006), was unable to rescue *nkd* mutant phenotypes (En stripe = 5.0 ± 1.2 cells) and showed increased nuclear localization relative to Nkd^{GFPC} when examined either in embryos or in third instar larval salivary glands (Figs. 3.4A–C; cf. Supplementary Figs. 2A, B) (Waldrop et al., 2006).

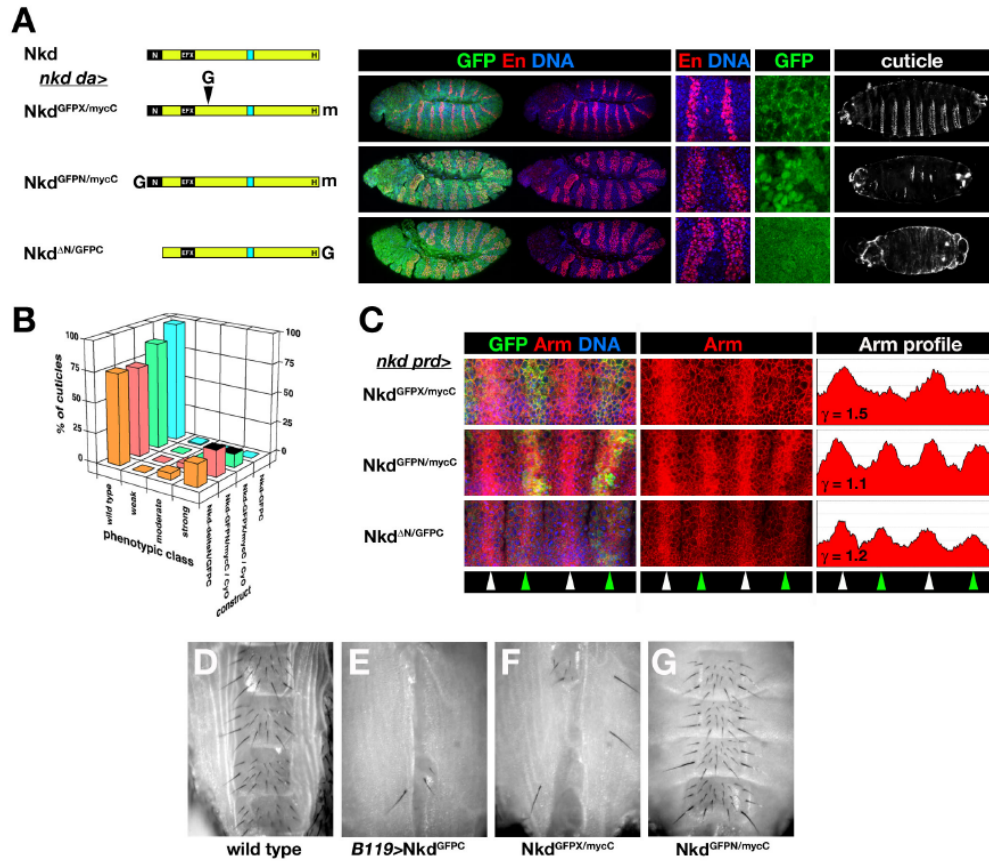


Fig. 3.4. Nkd N-terminus is required for activity. (A) Schematic of *Drosophila* Nkd protein (yellow box with indicated sequence motifs) above each *UAS-Nkd* construct in left column. From N- to C-terminal, Nkd has four regions conserved in mosquito Nkd, including an N-terminal motif (N), the Dsh-binding EFX, a 30 aa NLS motif (light blue box), and histidine-rich (H) C-terminus (Waldrop et al., 2006). Positions of GFP (G) and myc (m) epitope tags are indicated. For each construct is shown, from left to right, a representative stage 11 *nkd da> Nkd*^{GFP} embryo stained for GFP (green), En (red) and DNA (blue), with higher power images showing En in two segments as well as GFP subcellular localization as revealed by anti-GFP staining. Right column shows representative rescued *nkd* cuticle. Note that Nkd^{GFPX/mycC} narrows the En stripe and accumulates predominantly in the cytoplasm but also weakly in the nucleus like Nkd^{GFPC} (Waldrop et al., 2006), but Nkd^{GFPN/mycC} and Nkd^{ΔN/GFPC} have no rescue activity and increased nuclear GFP. (B) Distribution of cuticle phenotypes using *da-Gal4* to rescue a strong *nkd*^{7H16} mutant embryo as described in Fig. 3.3.J. The difference in the ratio of wild type/*nkd*-mutant cuticles for Nkd^{GFPX/mycC} (110/15) vs. Nkd^{GFPN/mycC} (119/42) rescue crosses, despite the presence of the *CyO* balancer in each cross, was statistically significant ($p = 0.004$; Fisher's exact test). (C) Four segmental anlagen of indicated stage 10 *nkd prd> Nkd*^{GFP} embryo stained for GFP (green), Arm (red) and DNA (blue). Middle column shows Arm channel only, and right panel is mean greyscale pixel intensity as a

function of position along anterior/posterior axis. Green arrowheads indicate segments with *prd-Gal4* expression, white arrowheads alternate segments. Previously, we defined γ as the ratio of peak Arm pixel intensity in non-rescued to rescued segments, with $\gamma = \sim 1.0$ indicating no rescue, and for Nkd^{GFPC} $\gamma = \sim 1.8$ (Waldrop et al., 2006). Note that $Nkd^{GFPX/mycC}$ reduces Arm levels to a greater extent than $Nkd^{GFPC/mycC}$ or $Nkd^{\Delta N/GFPC}$. (D–G) Ventral view of adult female abdomens showing array of sternite bristles in segments A3–A6. Wild type (D) has segmentally repeated sternite bristle clusters. *B119-Gal4* driving ectopic production of Nkd^{GFPC} (E) or $Nkd^{GFPX/mycC}$ (F) results in few bristles, while $Nkd^{GFPC/mycC}$ (G) or $Nkd^{\Delta N/GFPC}$ (not shown) have wild type bristle pattern.

3.3.5 Myristoylation reduces *Nkd* activity

Although fly *Nkd* does not have a N-terminal myristoylation consensus sequence, like the mammalian *Nkd* proteins it could act, in part, by associating with membranes. If so, then increased association of fly *Nkd* with the plasma membrane may enhance its ability to rescue a *nkd* mutant. To test this possibility, we fused the N-terminal 89 amino acids of *Drosophila* Src – which encodes a myristoylation consensus sequence and is sufficient to direct GFP to the plasma membrane – to a partially truncated but fully functional *Nkd* construct, $Nkd^{NBg/GFPC}$, to form $Nkd^{SrcNBg/GFPC}$ (Fig. 3.5A) (Simon et al., 1985 and Waldrop et al., 2006). As shown in Fig. 3.5A, *nkd da* > $Nkd^{NBg/GFPC}$ embryos have En stripes of 1.9 ± 0.8 cells wide, with rare, focal loss of En production, consistent with a slight enhancement of $Nkd^{NBg/GFPC}$ potency relative to Nkd^{GFPC} or $Nkd^{GFPX/mycC}$ (Waldrop et al., 2006). Consequently, 3.7% of cuticles in the $Nkd^{NBg/GFPC}$ rescue cross had one or more fused denticle belts due to loss of the parasegmental boundary caused by focal En repression (Martinez Arias et al., 1988). However, *nkd da* > $Nkd^{SrcNBg/GFPC}$ embryos had En stripes 3.7 ± 1.0 cells wide and gave rise to weak to moderate *nkd* cuticles, while *nkd prd* > $Nkd^{SrcNBg/GFPC}$ embryos retained higher Arm levels relative to *nkd prd* > $Nkd^{NBg/GFPC}$ (Figs. 3.5A–C). Similarly, *B119* > $Nkd^{NBg/GFPC}$ adults had no sternite bristles, but

B119 > Nkd^{SrcNBg/GFP} adults retained an intermediate number of sternite bristles (Figs. 3.5E, H). While the localization of *Nkd^{NBg/GFP}*, like *Nkd^{GFP}*, was predominantly punctate and cytoplasmic, *Nkd^{SrcNBg/GFP}* also localized in intracellular aggregates (Fig. 3.5A), indicating that *Nkd* sequences counteract *Src^{(1-89)GFP}*'s ability to localize at the plasma membrane.

Nkd^{SrcG2ANBg/GFP}, in which myristoylation was inhibited by mutation of the myristoylated glycine to an alanine (G2A) (Kamps et al., 1985), showed very weak to absent *nkd* rescue (En stripe = 4.4 ± 1.7 cells wide) and misexpression activity, but the fusion protein was undetectable by anti-GFP antibody in embryos or in transfected cells (Figs. 3.5A–C, F, H, and not shown), indicating that myristoylation also facilitates *Nkd^{SrcNBg/GFP}* protein stability. Like *Nkd^{ΔN/GFP}*, *Nkd^{SrcG2ANBg/GFP}* was localized predominantly in the nucleus when produced in larval salivary gland (Supplementary Fig. 3.2C), consistent with the N-terminal region of *Nkd* promoting protein stability and opposing nuclear localization.

We attribute the residual *nkd* rescue activity of *Nkd^{SrcNBg/GFP}* and *Nkd^{SrcG2ANBg/GFP}* to endogenous *Nkd* N-terminal sequences in the two constructs, because replacement of sequence N-terminal of the EFX motif with the *Src⁽¹⁻⁸⁹⁾* tag (*Nkd^{SrcRBg/GFP}*) further reduced *nkd* rescue activity relative to *Nkd^{SrcNBg/GFP}* (En stripe = 4.9 ± 1.2 cells) but restored predominant localization to the plasma membrane (Figs. 3.5A–C). Replacement of the fly *Nkd* N-terminus with the myristoylation consensus sequence of mouse *Nkd1* (to make *Nkd^{m1NΔN/GFP}*) also reduced *nkd* rescue activity relative to *Nkd^{GFP}* (En stripe = 4.7 ± 1.3 cells) and conferred localization to the plasma membrane (Figs. 3.5A–C). *Nkd^{SrcRBg/GFP}* may have dominant-negative properties, because *B119 > Nkd^{SrcRBg/GFP}*

adults had increased numbers of sternite bristles relative to *B119* > *GFP* adults (Figs. 3.5G, H) (Rousset et al., 2002). These experiments demonstrate that fly Nkd and mouse Nkd1 N-termini, as well as a heterologous myristoyl tag, oppose Nkd nuclear localization, but that the fly Nkd N-terminus possesses unique activity that cannot be mimicked by myristoylation.

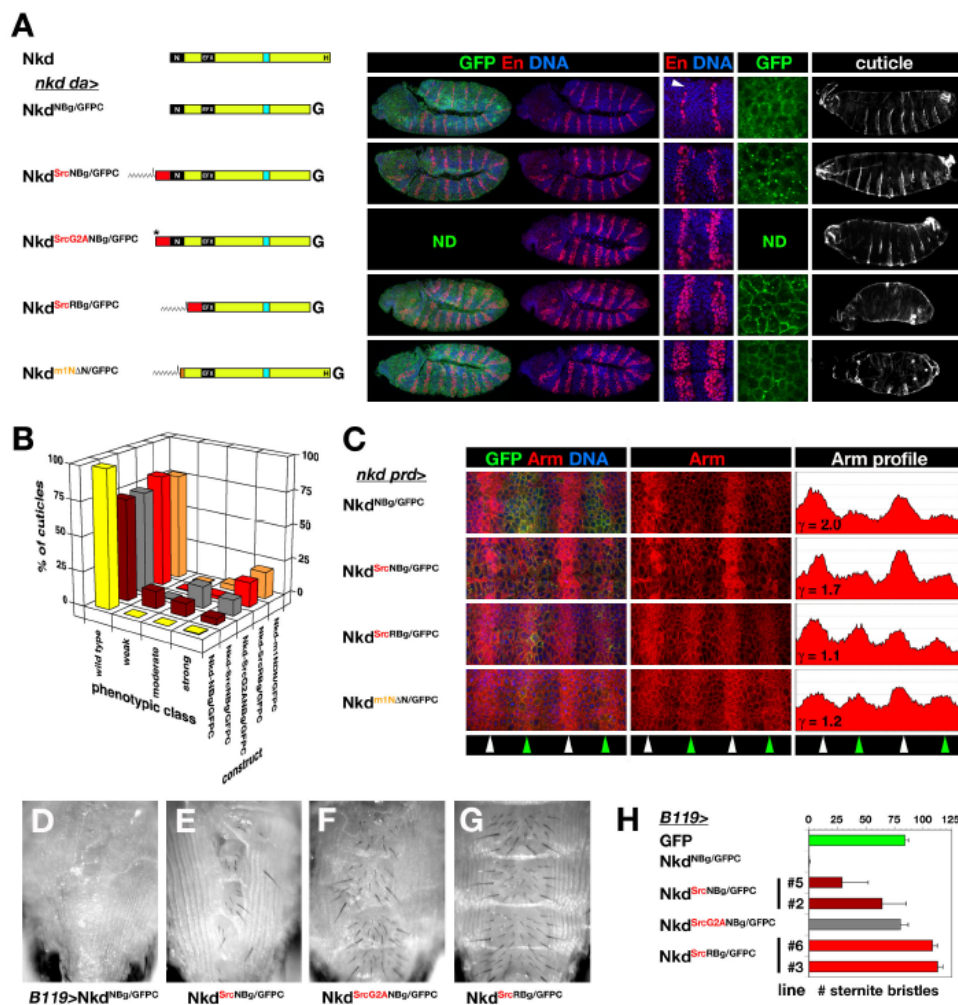


Fig. 3.5. N-terminal myristoylation inhibits Nkd activity. (A) Nkd constructs and *nkd da* > *Nkd* rescue as in Fig. 3.4A. *Nkd*^{Nkg/GFPC} results in narrow En stripes (1–2 cells) with focal loss of En stain (arrowhead), and is distributed similar to *Nkd*^{GFPC} (Waldrop et al., 2006). Fusion of the myristoylated N-terminal 89 amino acids of *Drosophila* Src (red

rectangle) to the N-terminus of $Nkd^{NBg/GFP}$ weakens rescue activity as evidenced by the 3–4 cell wide En stripe and focal naked cuticle. $Nkd^{SrcNBg/GFP}$ accumulates additionally in large cytoplasmic puncta. $Nkd^{SrcG2ANBg/GFP}$, lacking the myristoyl modification (*), has weak rescue activity but was not detected (ND) with anti-GFP. $Nkd^{SrcRBg/GFP}$ and $Nkd^{m1N\Delta N/GFP}$, myristoylated constructs that lack the fly Nkd N-terminus, have little to no rescue activity and are predominantly plasma membrane-associated. (B) Distribution of cuticle phenotypes using *da-Gal4* as in Fig. 3.3J. (C) Stage 10 *nkd prd* > Nkd^{GFP} embryos stained for Arm as in Fig. 3.4C. $Nkd^{NBg/GFP}$ reduces Arm levels as well as Nkd^{GFP} , $Nkd^{SrcNBg/GFP}$ has partial activity, while the two constructs that are membrane-anchored but lack the Nkd N-terminus have weak to absent activity. (D) *B119* > $Nkd^{NBg/GFP}$ females lack sternite bristles. (E) *B119* > $Nkd^{SrcNBg/GFP}$ have reduced numbers of sternite bristles. (F) *B119* > $Nkd^{SrcG2ANBg/GFP}$ have slight reduction in bristle numbers and abnormal bristle pattern. (G) *B119* > $Nkd^{RBg/GFP}$ have normal sternite bristle polarity and morphology but increased numbers of bristles. (H) Mean \pm S.D. of sternite bristle number ($n = 10\text{--}20$ adult females each) in *B119-Gal4* driving indicated construct and transgenic line number (#).

3.3.6 Fly Nkd N-term and 30 amino acid motifs confer embryonic Nkd activity to mouse

Nkd1

Mouse *Nkd1*, when misexpressed in otherwise wild-type flies, can induce weak loss-of-Wg signaling adult phenotypes (Wharton et al., 2001). Fly *Nkd* has a 30 amino acid (aa) motif, conserved in mosquito *Nkd*, that is crucial for function, and is sufficient, when substituted for the 30 aa motif in mouse *Nkd1* (to form $mNkd1^{f30aa/GFP}$), to confer increased Wg antagonist activity and nuclear localization (Waldrop et al., 2006 and Wharton et al., 2001). However, neither $mNkd1^{GFP}$ nor $mNkd1^{f30aa/GFP}$ had significant activity in *nkd* embryo rescue assays (En stripe = 5.1 ± 1.2 and 4.7 ± 1.2 cells, respectively) (Figs. 3.6A–C) (Waldrop et al., 2006). Importantly, replacement of mouse *Nkd1* N-terminal sequence in $mNkd1^{f30aa/GFP}$ with the fly *Nkd* N-terminus (to form $mNkd1^{fNf30aa/GFP}$) conferred partial embryonic *nkd* rescue activity when the double-chimeric protein was expressed by *da-Gal4* or *prd-Gal4* (Figs. 3.6A–C). $mNkd1^{fNf30aa/GFP}$ effectively reduced Arm levels in *nkd* mutants, but it only partially

narrowed En stripes to 3.6 ± 1.0 cells, predominantly in the ventral region of most segments (Figs. 3.6A–C), indicating that sequences in fly Nkd that are not in $mNkd1^{fN30aa/GFP}$ are required for full En repression.

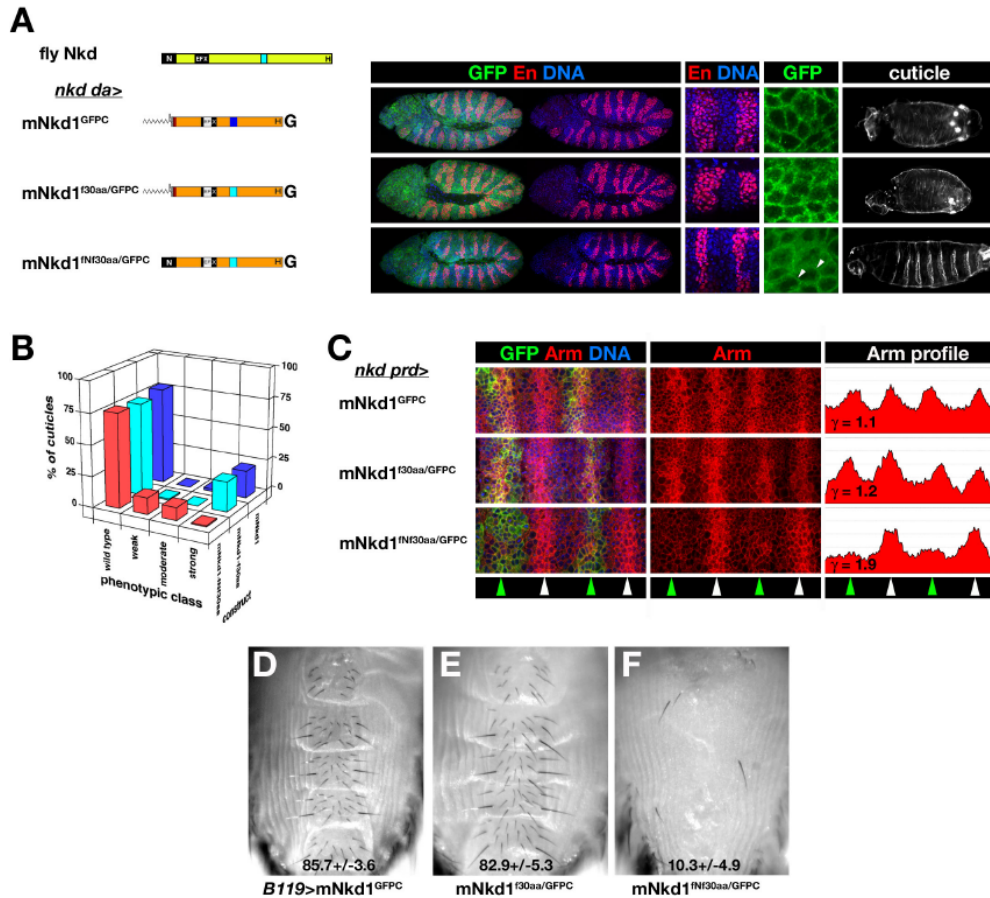


Fig. 3.6. *Drosophila* Nkd N-terminus confers activity as Wg signal antagonist. (A) Mouse Nkd1 constructs and *nkd da>* $mNkd1^{GFP}$ rescue as in Fig. 3.4A. Mouse Nkd1 shares sequence similarity with fly Nkd in the EFX and histidine-rich (H) regions, but has distinct N-termini (with myristoylation consensus) and 30 amino acid motifs (dark blue). Neither $mNkd1^{GFP}$ nor $mNkd1^{f30aa/GFP}$ (Waldrop et al., 2006) have any activity in *nkd* rescue, but the double chimera $mNkd1^{fN30aa/GFP}$ partially narrows the ventral En stripe (A) and results in weak (shown) and moderate class *nkd* cuticles. In addition, the fly N-terminus confers on $mNkd1^{f30aa/GFP}$ a more diffuse localization with plasma membrane enhancement (arrowheads). (B) Distribution of *nkd* cuticle phenotypes as a function of each $mNkd1^{GFP}$ construct when driven by *da-Gal4*. (C) Stage 10 *nkd prd>* $mNkd1^{GFP}$ embryos stained for Arm as in Fig. 3.4C. Neither $mNkd1^{GFP}$ nor $mNkd1^{f30aa/GFP}$ affect

Arm levels, but $mNkd1^{fNf30aa/GFPC}$ reduced Arm levels as well as fly Nkd. (D–F) Sternite bristle array from $B119 > mNkd1^{GFPC}$ (D), $mNkd1^{f30aa/GFPC}$ (E), or $mNkd1^{fNf30aa/GFPC}$ (F) females, showing the mean \pm S.D. number of bristles from a representative transgenic line of each construct ($n = 10$ adults each). Note severe loss of bristles induced by the double chimeric mNkd1 construct in panel F.

3.3.7 The N-terminal region of fly Nkd confers partial membrane association

Given the importance of Nkd's N-terminal region, we compared the subcellular localization and detergent solubility of the N-terminal 59 aa – a conserved block of sequence that is 75% identical and 86% similar to the mosquito Nkd N-terminus – fused to GFP ($Nkd^{7H/GFPC}$) with GFP and $Src^{(1-89)GFP}$ (Waldrop et al., 2006). When expressed in third instar salivary glands via $71B-Gal4$, GFP was diffusely cytoplasmic with some enrichment in the nucleus, while $Src^{(1-89)GFP}$ localized exclusively to the plasma membrane (Figs. 3.7A, B). In contrast to GFP, $Nkd^{7H/GFPC}$ was enriched at plasma and nuclear membranes, with the remainder diffusely distributed (Fig. 3.7C). Next, we expressed each protein in cultured *Drosophila* Kc cells and inferred their lipid solubility by determining the extent to which each protein could be extracted by brief, gentle exposure to the non-ionic detergent Triton X-100 (see Materials and methods). As shown in Fig. 3.7D, under the extraction conditions employed, all of the GFP but little to no $Src^{(1-89)GFP}$ was Triton-extractable. Consistent with the observed localizations in salivary gland cells, most $Nkd^{7H/GFPC}$ was Triton X-100-extractable and – despite the presence of protease inhibitor cocktail during extraction – degradation-sensitive, but we consistently detected some $Nkd^{7H/GFPC}$ that was insoluble and degradation-resistant (Fig. 3.7D). The subcellular distributions of each protein in Kc cells was similar to that observed in salivary glands (Figs. 3.7E–G). Examination of Kc cells post-Triton X-100 treatment

revealed residual Nkd^{7H/GFP} and Src^{(1-89)GFP} in both plasma and internal membranes, whereas nearly all GFP was extracted from GFP-expressing cells (*cf.* Fig. 3.7H vs. I, J). Thus, like the mammalian Nkd proteins, the N-terminus of fly Nkd confers membrane association.

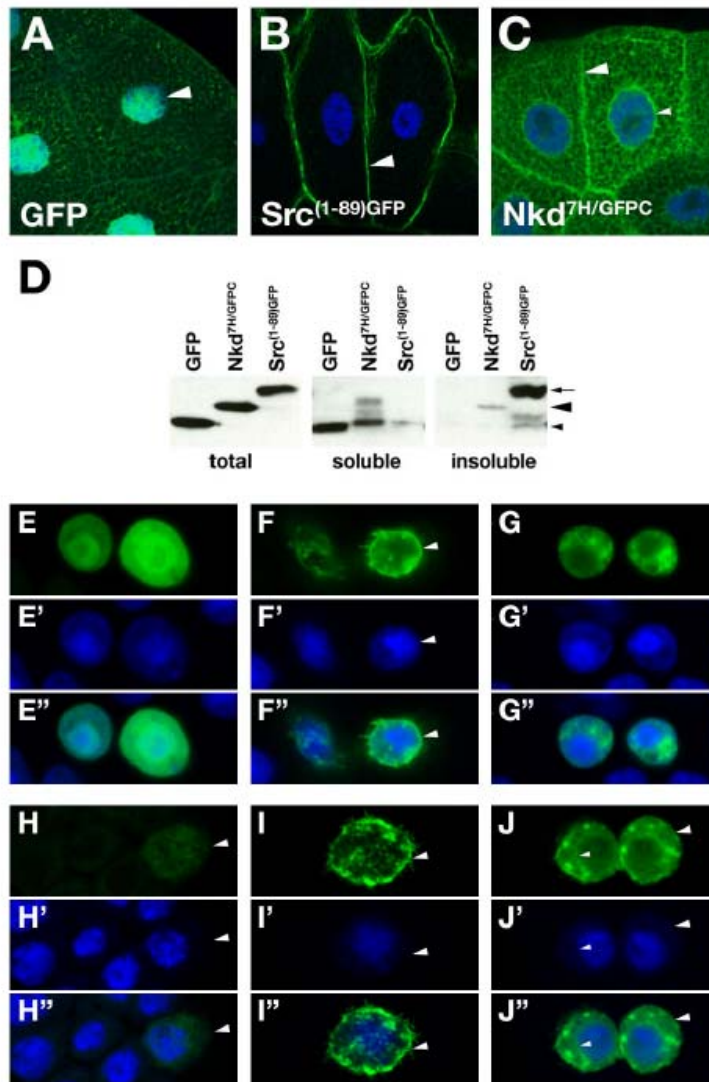


Fig. 3.7. *Drosophila* Nkd N-terminus confers membrane localization. (A–C) Confocal images of salivary gland from *71B > GFP* (A), *71B > Src^{(1-89)GFP}* (B), and

71B > *Nkd*^{7H/GFP} (C) third instar larvae visualized for GFP (green) and DNA (blue). GFP is predominantly nuclear (arrowhead) but also cytoplasmic, while *Src*^{(1-89)GFP} localizes exclusively to the plasma membrane (arrowhead). *Nkd*^{7H/GFP} adopts a distribution distinct from GFP that includes enrichment at plasma (large arrowhead) and nuclear (small arrowhead) membranes. (D) Western blots of whole-cell extracts (left) and Triton X-100-soluble (middle) and -insoluble (right) extracts from *Drosophila* Kc cells expressing indicated GFP-fusion protein. Note that all GFP (small arrowhead) and none of the *Src*^{(1-89)GFP} (arrow) is soluble; some *Nkd*^{7H/GFP} is soluble and degradation-sensitive, while the remainder is insoluble and degradation-resistant (large arrowhead). (E-J) Representative Kc cells transfected with GFP (E, H), *Src*^{(1-89)GFP} (F, I), or *Nkd*^{7H/GFP} (G, J) prior to (E-G) or 3 min. post (H-J) exposure to 0.5% Triton X-100 as described in Section 3.2 Materials and methods. Panels E-J are the GFP channel (green), panels E'-J' are DRAQ5 staining of nucleic acids (blue), and panels E_{merge}-J_{merge} are the merged images. Note that nearly all of the GFP but little to no *Src*^{(1-89)GFP} is extracted by Triton X-100 (arrowheads), and that residual *Nkd*^{7H/GFP} is present at plasma and nuclear membranes (large and small arrowheads, respectively, in panel J). DRAQ5 stains cytoplasmic RNA weakly and nuclear DNA strongly; the effect of Triton X-100 on the cells is confirmed by Triton X-100 extraction of cytoplasmic RNA in panels H'-J'.

3.4 Discussion

In this paper, we investigate the requirements for *Nkd* activity in each developing segment of the fly embryo, as well as demonstrate critical functional and membrane-anchoring roles for fly *Nkd*'s unique N-terminus. Our studies provide further support for the hypothesis that *Nkd* limits the intracellular response to Wg signaling. In contrast to a prior report (Moline et al., 1999), we observe neither consistent nor dramatic differences in the distribution of Wg protein that originates from endogenous *wg* stripes in stage 10-11 *nkd*-mutant vs. rescued segments. In this regard, it should be noted that in *nkd* embryos by stage 11 endogenous stripes of Wg protein exhibit an anterior bias just as in wild type, whereas ectopic Wg stripes adopt a mirror-image posterior bias (see Fig. 3.3C), with the diminution of Wg immunoreactivity in wide *en* domains likely due to En

and/or Hh signal-dependent enhancement of Wg degradation as observed in wild type embryos (Sanson et al., 1999).

During stages 10–11, the expression pattern of *nkd* mRNA and Nkd protein resolves into a complex, Wg-dependent striped pattern repeated across each segmental anlagen (schematized in Fig. 3.8A) (Zeng et al., 2000). There, *nkd* acts via a negative feedback mechanism to limit signaling across each segment (Fang et al., 2006; Zeng et al., 2000). Consequently, in a *wg* mutant, *nkd* mRNA decays, while in a *nkd* mutant, the defective *nkd* transcript accumulates to higher levels and more broadly across each segment (Zeng et al., 2000). That ubiquitously produced Nkd can rescue a *nkd* mutant to adulthood suggested that striped *nkd* expression is not essential for activity, although the efficiency of rescue past embryogenesis was reduced relative to wild type (Waldrop et al., 2006). In this paper we demonstrate, by driving Nkd production in defined domains of each segmental anlagen of *nkd* mutants, that the early expansion of *en* and the later induction of the ectopic *wg* stripe are separable events. Because we observe neither any cell-nonautonomous effects on Wg-dependent Arm accumulation or En production in *nkd* mutants, nor any obvious differences in Wg distribution in *nkd* mutant vs. rescued segments, we conclude that the action of Nkd can be explained by its cell-autonomous ability to attenuate responses to Wg. The observed patterns, summarized in Fig. 3.8A, are as follows.

In *nkd prd > Nkd^{GFPC}* and *nkd en > Nkd^{GFPC}* embryos, we observed En-positive cells at the posterior of each “*en*-competent” domain (defined as the population of epidermal cells that express *en* in a *nkd* mutant (Martinez Arias et al., 1988), which in the latter

genotype were in close proximity to an ectopic Wg stripe a few cells anterior to the endogenous Wg stripe. With *prd-Gal4*, Nkd was not expressed in the most posterior cells of alternate *en*-competent domains, so En production in posterior cells was likely maintained by Wg produced by an ectopic *wg* stripe just posterior to those cells. The production of Nkd in posterior cells of each *en*-competent domain in *nkd* mutants, as in *nkd en > Nkd^{GFP}* embryos, was not sufficient to reduce En levels in those posterior cells, indicating – as is observed with the endogenous 2–3 cell wide En stripe – that the relatively weak Wg-antagonist activity of Nkd is not sufficient to overcome the levels of signaling induced by the high levels of Wg ligand to which those cells are exposed. Expression of Axin, a more potent antagonist, via *en-Gal4* in *nkd* mutants led to a more extensive yet still incomplete suppression of endogenous and ectopic En, particularly in ventral epidermal cells.

In contrast, *nkd ptc > Nkd^{GFP}* embryos retained wide En stripes but developed far fewer ectopic ventral Wg stripes than *nkd* embryos. In contrast to *nkd prd > Nkd^{GFP}* and *nkd en > Nkd^{GFP}*, in *nkd ptc > Nkd^{GFP}* embryos the most posterior En-positive cells are likely receiving Wg input, at least initially, from the endogenous Wg stripe that is just to the anterior, although our experiments do not allow us to rule out the possibility that later on those cells are also sensing Wg from the further posterior source, as previously hypothesized to occur in similarly staged *nkd* mutants (Moline et al., 1999). Embryos homozygous for some weaker *nkd* alleles show a phenotype similar to *nkd ptc > Nkd* embryos: posterior expansion of En but rare to absent ectopic Wg, a further indication that *nkd*-mutant cells at the posterior of each *en*-competent domain receive Wg input

from the anterior, endogenous source of Wg. In addition to *wg* expression requiring input from Hh signaling, *wg* also autoregulates its own expression during germ band extension (Bejsovec and Martinez Arias, 1991 and Yoffe et al., 1995). Perhaps in *nkd ptc > Nkd^{GFPC}* embryos the presence of Nkd in cells anterior to each endogenous *wg* stripe – cells that are competent to express *wg* but only do so when exposed to high levels of Hh signaling – raises the threshold for activation of *wg* transcription by Wg and Hh, even though those cells are exposed to high levels of Hh. Nkd expression in the anterior *ptc*-expressing cells of *nkd* mutants was not 100% effective at preventing ectopic *wg* transcription, as 1–3 ectopic *wg* stripes per embryo were observed.

The distinct N-terminal sequences of fly and mammalian Nkd have raised the question of whether the Nkd N-termini have homologous functions *in vivo*. Previously, it was reported that mammalian Nkd2 is myristoylated and localizes to cell membranes, whereas *Drosophila* Nkd, lacking a myristoyl modification, was diffusely localized in the cytoplasm when misexpressed in cultured mammalian cells (Li et al., 2004). In this work, we show that the fly Nkd N-terminus confers membrane localization and *in vivo* activity that cannot be mimicked by heterologous membrane-targeting sequences. Taken together with our previous studies that have probed relationships between structure and function of *Drosophila* Nkd (Rousset et al., 2002 and Waldrop et al., 2006), here we show that four regions of Nkd – N-terminus, EFX, 30 aa nuclear localization sequence, and histidine-rich C-terminus, each conserved between fly and mosquito Nkd through ~250 million years – are sufficient for significant *in vivo* Nkd function. These data suggest that the four conserved regions constitute a minimal platform upon which additional

domains and/or activities may have been acquired during evolution. Consistent with this idea, Nkd2 but not Nkd1 binds to the intracellular tail of TGF- α precursor, using a motif that is between the 30 aa motif and histidine-rich regions of Nkd2 (Li et al., 2004); and, by yeast two hybrid assay the B γ protein phosphatase 2A (PP2A) subunit PR72 binds to sequences in Nkd1 between the conserved EFX and 30 aa motifs, that are not conserved in Nkd2 (C.-C.C. and K.A.W., unpublished observation) (Creyghton et al., 2005). Since the EFX – the only motif conserved in primary sequence between fly and mammalian Nkd proteins – binds Dsh or its three mammalian homologs (Wharton et al., 2001), we surmise that regulation of Dsh activity constitutes Nkd's most ancient function.

Our data suggest that the action of Nkd at the plasma membrane in flies may be very similar to the presumed mechanism by which mammalian Nkd proteins inhibit Wnt signaling, but the means by which membrane association is achieved appears distinct in flies and mammals; for mammalian Nkd, a myristoyl anchor facilitates membrane association, while in the fly it is mediated by a N-terminal \sim 60 aa motif, possibly via protein–protein interactions. That each functionally important region of fly Nkd promotes localization to different subcellular regions – the N-terminus promoting membrane association, the EFX retaining Nkd in the cytoplasm, possibly via associations with Dsh, and the 30 aa motif promoting nuclear localization (Waldrop et al., 2006) – supports the hypothesis that Nkd acts at multiple subcellular locations to attenuate Wg signaling. However, our experiments do not distinguish between models whereby separate pools of Nkd act in concert to inhibit signaling (Fig. 3.8B, Model 1), or whether Nkd action requires intracellular transport between cytoplasm, intracellular membranes, and the

nucleus (Fig. 3.8B, Model 2). Yet a third possibility, suggested by recent studies, is that Nkd impinges on the ability of Dsh to oligomerize and promote Wnt-receptor complex “signalosomes” that have been proposed to trigger intracellular signaling (Bilic et al., 2007 and Schwarz-Romond et al., 2007), but such a model does not readily account for Nkd's apparent activity in the nucleus. Future investigations that probe the subcellular dynamics of Nkd trafficking and identify additional Nkd-associated proteins will be required to generate additional clues about the mechanism by which Nkd attenuates Wnt/ β -catenin signaling.

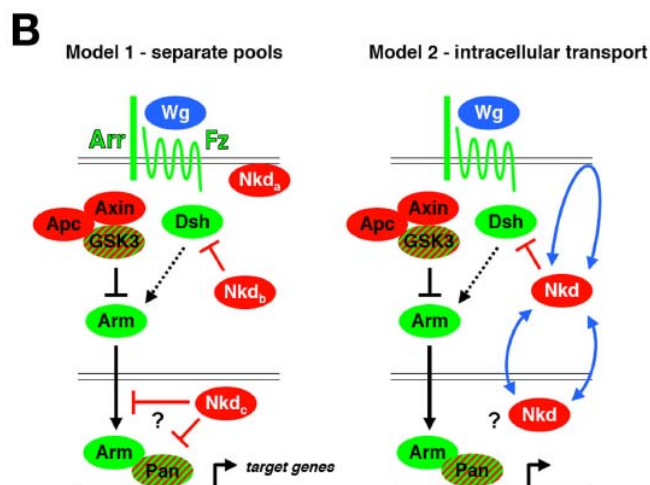
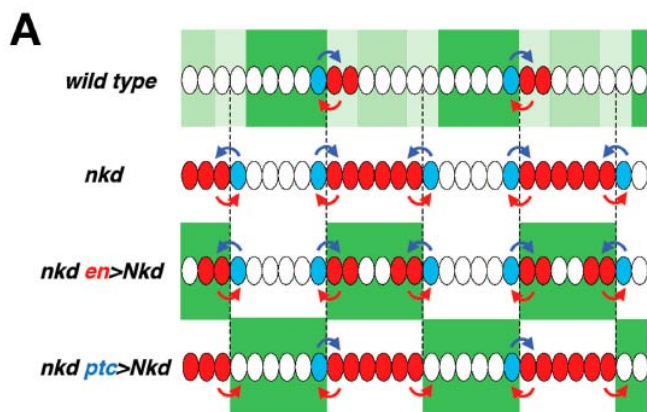


Fig. 3.8. Summary of *nkd* rescue experiments and working models of Nkd function. (A) Depicted are two schematic segments of a stage 10–11 embryo as in Fig. 3.1A. Top row: Wild type embryos have one Wg/Hh interface per segment, with mutual reinforcement of signal production by Wg (blue arrow) and Hh (red arrow). Nkd accumulates in a complex, Wg-dependent striped pattern (Zeng et al., 2000), with abundance proportional to green shade. Second row: *nkd* mutants have expanded En and Hh production (red circles) flanked by endogenous and ectopic Wg stripes (blue circles). Third row: *nkd en > Nkd^{GFP}* embryos lose En production in the middle of the expanded *en*-competent domain, but retain ectopic Wg which stimulates the production of En in posterior cells of each *en*-competent domain. Fourth row: *nkd ptc > Nkd^{GFP}* embryos retain an expanded region of En production, but fewer ectopic Wg stripes are induced due to Nkd production in cells competent to make Wg (Martinez Arias et al., 1988). (B) Models of Nkd action in *Drosophila*. A highly simplified model for activation of Wnt/ β -catenin signaling by Wg (blue) is shown in each panel (see <http://www.stanford.edu/~rnusse/pathways/cell2.html>). Components that promote signal transmission (Arr—Arrow/Lrp5–6 receptor; Fz—Frizzled and Frizzled2 receptor; Dsh scaffold; Arm— β -catenin) are green, while components that repress signal transduction (Axin, Apc, Nkd) are red. Components with positive and negative roles (Pan—Pangolin/TCF; GSK3) are depicted in red/green stripe. In Model 1 (left), separate pools of Nkd (designated a, b, c) act at the plasma membrane (a), in a cytoplasmic complex with Dsh (b), and in the nucleus (c) to inhibit signaling, but it is not known (?) whether Nkd affects nuclear transport of a critical signaling component or whether it acts on the chromatin of Wg-responsive genes. In model 2 (right), the movement of Nkd between cytoplasm and plasma membrane and/or the nucleus (blue arrows) is required for inhibition of Wg signaling.

PREFACE TO CHAPTER FOUR

CHAPTER FOUR describes the requirement of the nuclear import adaptor Importin- $\alpha 3$ for Nkd function in attenuating Wnt signaling. It is adapted from “*Chan et al., C.C. Chan, S. Zhang, R. Rousset, and K.A. Wharton Jr., Drosophila Naked cuticle engages the nuclear import adaptor Importin- $\alpha 3$ to antagonize Wnt/ β -catenin signaling, Developmental Biology, in press, 2008.*”.

For this work I contributed in several ways. I examined the interaction between Nkd and Importin- $\alpha 3$ in both Y2H and GST pulldown assays. I showed that D6 motif is sufficient and required for binding to Importin- $\alpha 3$. I generated 10 of the 14 internal deletions, domain substitutions, and point mutant UAS-Nkd constructs used in this paper. I also generated the *importin- $\alpha 3$* germ line clones. In addition, I also performed *importin- $\alpha 3$* RNAi experiments in Kc cell cultures and in salivary gland. Keith Wharton did all the confocal imaging. Raphael Rousset discovered Importin- $\alpha 3$ as a Nkd-interacting protein in Y2H screens while a postdoctoral fellow in Matthew Scott’s lab at Stanford. Shu Zhang participated in Kc cell culture experiments.

CHAPTER FOUR

***DROSOPHILA* NAKED CUTICLE ENGAGES THE NUCLEAR IMPORT ADAPTOR IMPORTIN- α 3 TO ANTAGONIZE WNT/ β -CATENIN SIGNALING**

4.1 Introduction

Wnts comprise a family of protein signals that govern morphogenesis and cell inductive events throughout the animal life cycle (Clevers, 2006). Depending on the organism, tissue, and type of cell, a Wnt signal can act locally to regulate binary cell fate decisions or over longer distances as a morphogen to orchestrate differential gene expression. Many Wnts elicit a well-conserved chain of intracellular events termed the canonical Wnt/ β -catenin pathway (see <http://www.stanford.edu/~rnusse/wntwindow.html> and references therein). In the absence of Wnt, phosphorylation of β -catenin by a “destruction complex” consisting of the Axin and Apc proteins as well as the CK1 and GSK3 kinases triggers ubiquitin-dependent proteasomal degradation of β -catenin. Association of Wnt with Lrp5-6/Arrow (Arr) and Frizzled (Fz) family co-receptors promotes Axin-Lrp5/6 interactions and inhibits β -catenin degradation via linkages with the Dishevelled (Dsh) family of scaffold proteins (Bilic et al., 2007; Wallingford and Habas, 2005). β -catenin then binds transcription factors of the TCF/Lef family to regulate Wnt target genes {reviewed in (Willert and Jones, 2006)}. Altered canonical Wnt signaling is associated with a growing list of human diseases, including cancer,

osteoporosis, and type 2 diabetes (Clevers, 2006). Therefore, understanding the mechanisms by which human cells and tissues normally control Wnt signaling has become an urgent priority of biomedical science and the biopharmaceutical industry alike.

Although much effort has been expended to understand how Wnt/ β -catenin signals are activated, much less is known about how signals are normally terminated. Naked cuticle (Nkd) is a family of intracellular proteins that antagonize Wnt signaling (Van Raay et al., 2007; Wharton et al., 2001; Zeng et al., 2000). In the fruit fly *Drosophila melanogaster*, transcription of the sole *nkd* gene is Wnt inducible, suggesting that Nkd acts in a feedback loop (Zeng et al., 2000). Known vertebrate genomes encode two dynamically expressed *nkd* paralogs, *nkd1* and *nkd2* (Kato, 2001; Van Raay et al., 2007; Wharton et al., 2001). Our current understanding of how Nkd proteins inhibit Wnt signaling derives largely from studies in *Drosophila*. Fly and mammalian Nkd proteins use an EF-hand motif ("EFX") to associate with Dsh (Rousset et al., 2002; Wharton et al., 2001), but conserved motifs that confer membrane association and - at least in *Drosophila* - mediate nuclear entry are also important for function (Chan et al., 2007; Waldrop et al., 2006). How each motif in Nkd acts in concert within a single protein to inhibit signaling *in vivo* remains unclear. A recent report suggests that vertebrate Dsh proteins act in the nucleus (Itoh et al., 2005), but what Dsh does in the nucleus, whether fly Dsh acts in the nucleus, or whether the action of Nkd in the nucleus requires Dsh association is not known.

Nkd attenuates signaling by the Wnt ligand Wingless (Wg) during early segmentation of the *Drosophila* embryo (Jürgens et al., 1984; Zeng et al., 2000). In the cellular blastoderm embryo, Wg is produced by a single transverse row of cells per segmental anlage. As the germ band extends, Wg-dependent accumulation of the β -catenin homolog Armadillo (Arm) in nearby cells activates the localized transcription of target genes including *hedgehog* (*hh*), *engrailed* (*en*), and *nkd* (Baker, 1988; DiNardo et al., 1988; Lee et al., 1992; Martinez Arias et al., 1988; Riggleman et al., 1990; Tabata et al., 1992; Zeng et al., 2000). In *nkd*-mutant embryos, the quantity and distribution of Wg is initially similar to wild type, but Arm accumulates to higher levels and genes activated by Wg are expressed in broader domains than in wild type, indicating that *nkd* mutant cells are hypersensitive to Wg (Bejsovec and Wieschaus, 1993; Dougan and DiNardo, 1992; Martinez Arias et al., 1988; Waldrop et al., 2006; Zeng et al., 2000). Later, Wg signaling instructs epidermal cell fate: cells beyond the influence of Wg secrete ventral cuticle with actin-based apical cell processes termed denticles, whereas most cells in close proximity to Wg producers suppress denticle synthesis and remain “naked” (Bejsovec and Martinez Arias, 1991; Dougan and DiNardo, 1992). In embryos homozygous for null or strongly hypomorphic *nkd* alleles, an ectopic stripe of Wg is induced in most segments, creating mirror-image pattern duplications, increased cell death, and extra naked cuticle, whereas weaker *nkd* alleles give rise to milder (yet still lethal) cuticle phenotypes due to variable ectopic Wg (Bejsovec and Wieschaus, 1993; Dougan and DiNardo, 1992; Pazdera et al., 1998; Waldrop et al., 2006).

In order for signals to impinge upon gene transcription in the nucleus, key signal transducers engage a nuclear transport machinery that is shared by a myriad of intracellular proteins. In the canonical nuclear import paradigm, the adaptor protein Importin- α links nuclear localization sequence (NLS)-containing cargo proteins to the nuclear import receptor Importin- β 1 {reviewed in (Chook and Blobel, 2001; Goldfarb et al., 2004)}. {A notable exception is β -catenin itself, which, due to its structural similarity to Importin- α is able to translocate to the nucleus in an Importin- α/β - and NLS-independent fashion (Fagotto et al., 1998).} *D. melanogaster* has three Importin- α paralogs: Importin- α 1 (Kap- α 1) (Mason et al., 2002), Importin- α 2 (Pendulin/Kap- α 2) (Kussel and Frasch, 1995; Torok et al., 1995), and Importin- α 3 (Kap- α 3) (Dockendorff et al., 1999; Mason et al., 2003; Mathe et al., 2000); and a single Importin- β 1 paralog: Fs(2)Ketel (Ket) (Lippai et al., 2000). We previously identified a 30 amino acid (aa) NLS in *Drosophila* Nkd (Waldrop et al., 2006), but how Nkd enters the nucleus is not known. Here we identify an additional NLS in Nkd and show that its interaction with Importin- α 3 is crucial for nuclear localization and function of Nkd. Our findings provide further support for the hypothesis that Nkd acts, in part, within the nucleus to inhibit Wnt signaling, and broaden our understanding of signaling pathways that engage the nuclear import machinery.

4.2 Materials and methods

4.2.1 DNA constructs

Nkd constructs were built in pBSII-KS+ (Stratagene) with C-terminal enhanced-GFP (Clontech). Nkd^{GFPC}, Nkd^{Δ30aa/GFPC}, Nkd^{Δ30aaNLS/GFPC}, and Nkd^{ΔR1S/GFPC} have been described (Waldrop et al., 2006). Mutant/junctional regions were synthesized by Pfu-PCR, subcloned/sequenced, then cloned into pUAS-T (Brand and Perrimon, 1993). Residues deleted: Nkd^{ΔD6/GFPC} 424-466; Nkd^{ΔR1SΔ30aa/GFPC} 179-370, 543-572; Nkd^{ΔR1SΔD6Δ30aa/GFPC} 179-370, 424-466, and 543-572; Nkd^{ΔD6Δ30aa/GFPC} 424-466, 543-572. Point mutations: Nkd^{R441A/GFPC} Arg441 to Ala; Nkd^{K445A/GFPC} Lys445 to Ala; Nkd^{RAKA/GFPC} Arg441 and Lys445 to Ala. Nkd^{ΔD6-HSFNLS/GFPC} substituted Nkd aa 424-466 with dHSF aa 392-435 (Genbank AAA28642); Nkd^{ΔR1SΔ30aaNLS/GFPC} deleted aa 179-370 and replaced aa 543-572 with the SV40-NLS (APKKKRKVGST) (Kalderon et al., 1984). Nkd^{D6/GFPC} consisted of aa 424-466 fused to GFP. For Y2H, Importin-α1/-α2/-α3 cDNAs (Genbank AAC26055, AAA85260, and AAD37442) were amplified by PCR from a fly embryo cDNA library, sequenced, and cloned into the pAS2-1 bait and pAct2 prey plasmids (Clontech). pAS2-Nkd and pAct-Dsh constructs have been described (Rousset et al., 2001). For GST-pulldown, the following residues of each Importin-α lacking its N-terminal auto-inhibitory Importin-β-binding (IBB) domain (Harreman et al., 2003) (ΔIBB) were cloned into pGEX-4T-1 (Amersham): Importin-α1^{ΔIBB} 118-543; Importin-α2^{ΔIBB} 93-522; Importin-α3^{ΔIBB} 65-514. Nkd or Nkd^{ΔD6} cDNAs were cloned into pBS-KS(-) (Stratagene) for in vitro transcription/translation. For *Drosophila* Kc cell transfections, the D6 motif (aa 424-466), as well as Nkd^{D6-R441A}, Nkd^{D6-K445A}, and Nkd^{D6-R441A,K445A(RAKA)} point mutant constructs fused to GFP were cloned into pAc5 (Invitrogen).

4.2.2 Yeast two-hybrid

The pAS2-Nkd bait plasmid was transformed into the yeast strain PJ69-4A (Rousset et al., 2001). A 0-24 hour *Drosophila* embryo cDNA library fused to the GAL4 transcriptional activation domain was transformed into the pAS2-Nkd-carrying yeast using a variation of the lithium acetate method (Clontech). Sequencing of one of the clones whose growth on minimal medium lacking Leu, Trp, His and Ade (4D) required the presence of pAS2-Nkd plasmid revealed the complete open reading frame of Importin- α 3. To confirm the interaction, competent yeast strain AH109 was transformed using the EZ Yeast Transformation II kit (ZymoResearch). Co-transformed yeast was grown under 2D (double dropout: -Leu-Trp) and, for stringent selection, 4D conditions. Western blot of yeast lysates showed that lack of growth of yeast strains under 4D were not due to bait or prey protein instability {data not shown and (Waldrop et al., 2006)}.

4.2.3 GST pulldown

Lysates containing each GST-fusion protein were prepared from *E. coli* strain BL21pLys as described by Amersham Biosciences, except that MTPBS buffer (Rousset et al., 2002) was used for washing. Each lysate was incubated with glutathione-Sepharose 4B beads for 1 hour at 4°C, and then washed 3X with DT80 buffer (Rousset et al., 2002). Nkd proteins were labeled with ³⁵S-Methionine using the TNT T7 coupled reticulocyte lysate system (Promega) and incubated with the beads for 2 hours at 4°C in DT80 buffer. Beads were washed 4X with DT300 buffer, and labeled proteins were eluted in SDS-PAGE sample buffer, boiled for 5 minutes, and then separated by 8% SDS-PAGE. Gels were vacuum dried, and protein bands were detected using a Typhoon phosphorimager with ImageQuant software (Molecular Dynamics).

4.2.4 Fly stocks and genetics

Fly culture and P-element transformation were performed according to standard procedures. All fly crosses were performed at 25°C. In rescue assays, the strongest known *nkd* allele, *nkd*^{7H16}, which encodes a predicted truncated 59 aa protein with no *nkd* activity (Jürgens et al., 1984; Zeng et al., 2000; Waldrop et al., 2006), was used in the following cross: *UAS-Nkd/UAS-Nkd* or *CyO;nkd*^{7H16}/*TM3-hb-lacZ* X *nkd*^{7H16}*da-Gal4/TM3-hb-lacZ*. In immunofluorescence experiments, all *nkd* mutant embryos were unambiguously identified by the absence of head-specific β-galactosidase staining from *hb-lacZ* on the balancer chromosome. Number of independent *UAS* lines of each construct that were examined in *nkd* rescue assays are as follows: GFP 1; Nkd^{GFPC} 2; Nkd^{ΔR1S/GFPC} 2; Nkd^{Δ30aa/GFPC} 3; Nkd^{Δ30aaΔR1S/GFPC} 2; Nkd^{Δ30aaNLS/GFPC} 3; Nkd^{ΔR1SΔ30aaNLS/GFPC} 3; Nkd^{ΔD6/GFPC} 3; Nkd^{ΔD6Δ30aa/GFPC} 2; Nkd^{ΔR1SΔD6/GFPC} 2; Nkd^{ΔR1SΔD6Δ30aa/GFPC} 2; Nkd^{R441A/GFPC} 2; Nkd^{K445A/GFPC} 2; Nkd^{R441A,K445A/GFPC} 2; Nkd^{ΔD6-HSFNLS/GFPC} 3. *FRT82B importin-α3*^{D93} was provided by Robert Fleming and David Goldfarb (Mason et al., 2003). *FRT82B D-axin*^P was provided by Jin Jiang (Hamada et al., 1999). *UAS-importin-α3 RNAi* flies (ID#36103 and #36104) were provided by the Vienna *Drosophila* RNAi Center (VDRC) (Dietzl et al., 2007). Fly stocks/chromosome: *UAS-lacZ* (II) (Brand and Perrimon, 1993), *da-Gal4* (III) (Wodarz et al., 1995), *prd-Gal4* (III) (Yoffe et al., 1995), *71B-Gal4* (III) (Brand and Perrimon, 1993).

4.2.5 Cuticle preparations

Cuticles were prepared and scored as described (Chan et al., 2007; Waldrop et al., 2006; Zeng et al., 2000). Briefly, each *nkd* cuticle was scored as “strong” if it had two or fewer complete denticle bands and severe head involution and tail defects, “moderate” if it had partial head involution and three or more complete denticle bands, or “weak” if it had denticle bands in every segment, complete or nearly complete head involution and tail morphogenesis, but patchy naked cuticle due to focal ectopic Wg production. 125-600 cuticles were scored for each rescue experiment.

4.2.6 Germ line clones

Females with germlines mutant for *importin- $\alpha 3^{D93}$* were generated by heat-shock of *hs-FLP; FRT82B ovo^D/FRT82B $\alpha 3^{D93}$* larvae twice a day for 1.5 hours on three consecutive days at 37°C during early larval stages (Chou et al., 1993). Female progeny were crossed to *$\alpha 3^{D93}/TM3-GFP$* males. The recovery of stage 11 embryos with uniformly elevated Arm and wide En stripes from females with germlines mutant for the Wg antagonist *D-axin* (Hamada et al., 1999), which lies on the same chromosomal arm as *importin- $\alpha 3$* , indicated that our procedure for making germline clones was successful (data not shown). *D-axin* clones were generated by heat-shock in *hs-FLP; FRT82B ovo^D/FRT82B D-axin^P* larvae. The resulting adult females were then crossed to *D-axin^P/TM6B* males.

4.2.7 Computer programs

Drawings were prepared in Canvas (ACD Systems) and Powerpoint (Microsoft), and composite figures were prepared in Photoshop (Adobe). Graphs were made in

Deltagraph (Red Rock Software). Selected confocal image channel spectra were maximized below saturation, with the exception that anti-Arm channels were not altered. ImageJ (NIH) was used to quantitate mean greyscale pixel intensity of raw confocal images of Arm-stained embryos as described (Waldrop et al., 2006). Statistical calculations were performed using Prism (GraphPad Software). ClustalW analysis and linked boxshade output were obtained at <http://dot.imgen.bcm.tmc.edu:9331/multi-align/multi-align.html>.

4.2.8 Immunocytochemistry and Microscopy

All embryo collection, salivary gland dissection, fixation, staining procedures (including antibodies and their dilutions), and confocal microscopy were performed as described (Chan et al., 2007; Waldrop et al., 2006). Mouse monoclonal anti-Importin- α 3 5E3 (Fang et al., 2001) was kindly provided by Carl Parker.

4.2.9 Cell culture, dsRNA feeding, and transfections

Drosophila Kc167 (Kc) cells were grown in Schneider's *Drosophila* medium (Invitrogen) supplemented with 10% FBS. Wild type or point mutant pAc-Nkd^{D6} or pArm-GFP were transfected with Effectene (Qiagen) into cells grown on coverslips. Forty-eight hours post-transfection, coverslips were fixed in 4% paraformaldehyde and counterstained with DRAQ5 (Biostatus Limited). GFP/DRAQ5 were imaged by confocal microscopy as previously described (Chan et al., 2007).

To deplete Importin- α 3 in Kc cells with RNAi, 37 nM double-stranded RNA (dsRNA) – synthesized according to the manufacturer's instructions using the MEGAscript in vitro transcription kit (Ambion) – was fed to Kc cells once per day (6 hour feeding in serum-free medium, followed by 18 hours with 10% FBS) for three consecutive days prior to transfection (Clemens et al., 2000). To synthesize dsRNA, the following primer pairs were used to PCR-amplify two independent *importin- α 3* DNA templates with flanking T7 polymerase promoter sequences (5'-TAATACGACTCACTATAGGG): dsRNA#1 (520 bp): 5'- (T7)TCATCACACCGACACGAACATCCT and 5'- (T7)ATCCTGGCATGAAAGGAGGTCACA; dsRNA#2 (429 bp): 5'- (T7)AGGATGAAATGCGACGTCGGAGAA and 5'- (T7)TGAGAAGTTGAAGGAAGAGCGGCA. Each *importin- α 3* dsRNA reduced Importin- α 3 protein levels and resulted in uniform distribution of Nkd^{D6/GFP} (Fig. 4. 5C and data not shown).

4.2.10 Western blots

Yeast lysates were prepared following the manufacturer's protocol (Clontech), and Kc cell lysates were prepared as described (Chan et al., 2007), with 10 μ g supernatant resolved per lane. Antibodies/dilutions were as follows: Anti-Gal4 DNA-BD sc510 (Santa Cruz Biotechnology) 1:1000; Anti-Porin (Molecular Probes) 1:1000; Anti-Importin- α 3 5E3 1:1,000; Anti- β tubulin (Covance) TU27 1:2,500. Signals were

visualized with SuperSignal West Dura Extended Duration Substrate (Pierce Biotechnology) followed by autoradiography.

4.3 Results

4.3.1 Requirement of *Nkd*'s *Dsh* binding sequences for function of a nuclear localized *Nkd*.

In the germband-extended *Drosophila* embryo, Wg signaling promotes *en* transcription in the 2-3 adjacent rows of epidermal cells posterior to Wg-producing cells (DiNardo et al., 1988; Martinez Arias et al., 1988). In *nkd* mutant embryos, Wg activates *en* during stage 9 in further posterior cells, such that by stage 10-11 approximately half of the cells in each segment express *en* (Fig. 4.1A) (Martinez Arias et al., 1988). Production of Nkd fused to a C-terminal GFP (*Nkd^{GFP}*), but not GFP alone, via the ubiquitous *da-Gal4* driver in a strong *nkd^{7H16}* mutant (*nkd da>Nkd^{GFP}*) narrowed the width of the En stripes - revealed by a monoclonal antibody against En - to 2-3 cells by stage 10-11, restored wild type cuticle pattern, and rescued some mutants to adulthood (Fig. 4.1A) (Waldrop et al., 2006; Zeng et al., 2000). Misexpression of *Nkd^{GFP}* in otherwise wild type embryos had no effect on Wg signaling or segmentation, but overexpression during larval development produced adult phenotypes characteristic of *wg* loss-of-function (Waldrop et al., 2006; Zeng et al., 2000). The subcellular localization of *Nkd^{GFP}* - as revealed by an antibody against GFP - was very similar to that of endogenous Nkd: diffuse and punctate cytoplasmic staining as well as a lower level of nuclear staining (Fig. 4.1A) (Waldrop et al., 2006; Zeng et al., 2000).

We previously showed that $Nkd^{AR1S/GFPC}$, which lacks the two adjacent Dsh-binding regions (termed “R1S”), retained a significant amount of *nkd* rescue activity but was mostly nuclear (Fig. 4.1A,B) (see Materials and methods for *nkd* cuticle scoring system) (Rousset et al., 2002; Waldrop et al., 2006). In contrast, $Nkd^{\Delta 30aa/GFPC}$, with a deleted 30aa NLS, had substantially reduced rescue activity and was predominantly cytoplasmic (Fig. 4.1A,B) (Waldrop et al., 2006). To determine whether the 30aa NLS is responsible for the nuclear localization of $Nkd^{AR1S/GFPC}$, we deleted both regions in construct $Nkd^{AR1SA\Delta 30aa/GFPC}$. *nkd da>Nkd^{AR1SA\Delta 30aa/GFPC}* embryos retained wide En stripes (Fig. 4.1A) and developed a moderate to strong *nkd* cuticle phenotype more severe than *nkd da>Nkd^{\Delta 30aa/GFPC}* embryos (Fig. 4.1B) (Waldrop et al., 2006; Zeng et al., 2000). In embryos, $Nkd^{AR1SA\Delta 30aa/GFPC}$ accessed the nucleus (Fig. 4.1A), indicating that the 30aa NLS is not necessary for nuclear localization in the absence of Nkd’s Dsh-binding sequences.

In *nkd prd>Nkd^{GFPC}* embryos, in which Nkd was expressed by the pair-rule gene driver *prd-Gal4* in alternate segments, Arm protein was reduced to wild-type levels in rescued segments by stage 10 (Waldrop et al., 2006). $Nkd^{AR1S/GFPC}$ lowered Arm levels in *nkd* mutants (Fig. 4.1C) as well as did Nkd^{GFPC} (Waldrop et al., 2006), but, like the latter construct, did not reduce Arm levels in otherwise wild-type embryos (data not shown). Despite the inability of $Nkd^{AR1SA\Delta 30aa/GFPC}$ to narrow *nkd*-mutant En stripes, *nkd prd>Nkd^{AR1SA\Delta 30aa/GFPC}* embryos had partially reduced Arm levels in alternate segments (Fig. 4.1C), indicating that $Nkd^{AR1SA\Delta 30aa/GFPC}$ retains a low but detectable level of Nkd activity.

In embryos, Dsh is predominantly cytoplasmic but can also be observed in nuclear puncta, and Nkd/Dsh colocalization can be observed in cytoplasm, and rarely, in the nucleus (Waldrop et al., 2006; Yanagawa et al., 1995). In support of the hypothesis that Nkd acts, in part, within the nucleus, Nkd^{Δ30aaNLS/GFPC} – in which the 30aa NLS was replaced by a strong SV40 NLS – rescued *nkd* embryos to a greater extent than did Nkd^{Δ30aa/GFPC} (Fig. 4.1A,B) (Waldrop et al., 2006). If Nkd/Dsh association is important for Nkd^{Δ30aaNLS/GFPC} to antagonize Wg signaling, then deletion of Dsh binding regions (to make Nkd^{ΔR1SAΔ30aaNLS/GFPC}) might eliminate Nkd activity. Conversely, if Nkd^{Δ30aaNLS/GFPC} activity is Dsh-independent, then Nkd^{ΔR1SAΔ30aaNLS/GFPC} might retain activity. As shown in Fig. 4.1A-C, Nkd^{ΔR1SAΔ30aaNLS/GFPC} was exclusively nuclear yet had no ability to reduce Arm, narrow En stripes, or rescue *nkd* cuticles (Fig. 4.1A-C), in further support of the hypothesis that Nkd/Dsh interactions contribute to Nkd's ability to inhibit Wg signaling.

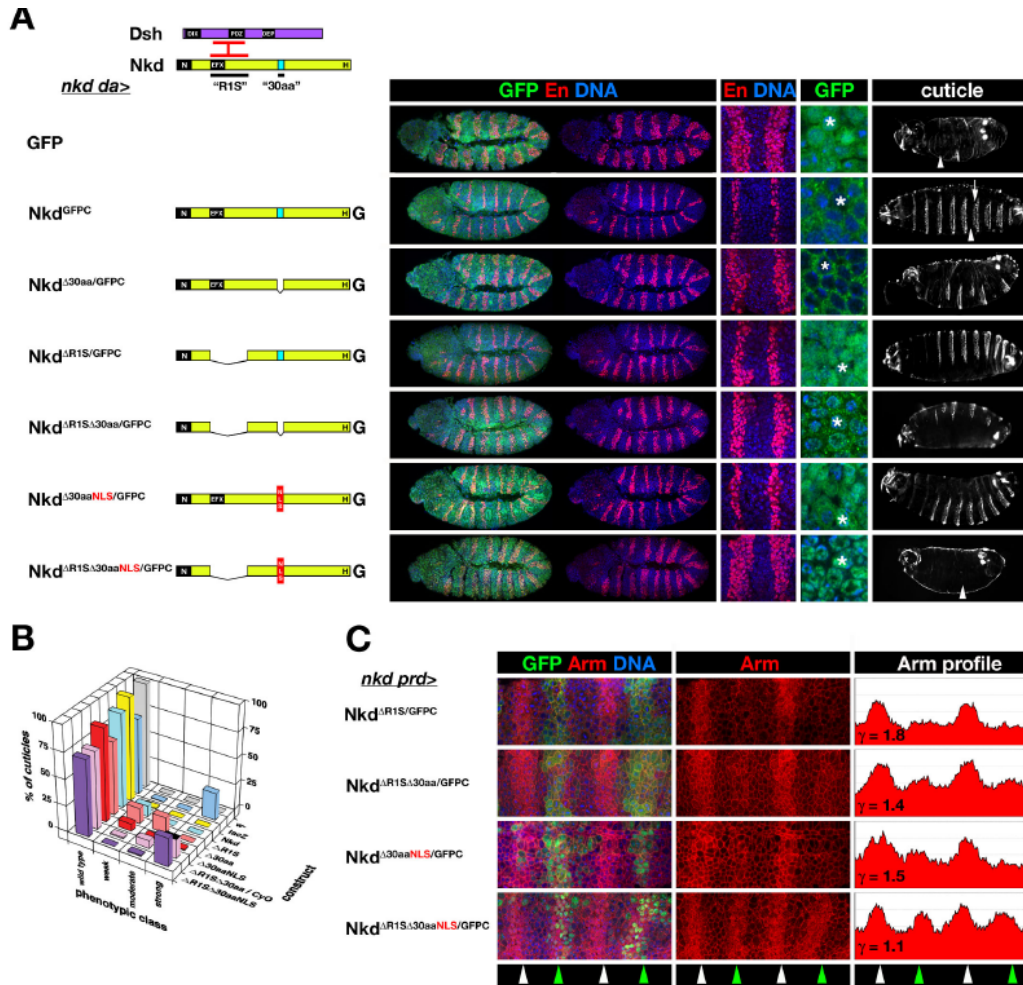


Fig. 4.1. Requirement of Nkd's Dsh-binding sequences for activity of nuclear-localized Nkd. (A) *nkd* rescue via ubiquitous expression of *UAS-Nkd* constructs via *da-Gal4* (*nkd da>*). Nkd (yellow) has N-terminal (N), EFX, 30aa NLS ("30aa" - light blue), and histidine-rich (H) motifs; Dsh (purple) has DIX, PDZ, and DEP domains. Dsh basic/PDZ region binds EFX and adjacent region of Nkd ("R1S" - interacting regions in red bars). For each rescue construct is shown, from left to right, a representative stage 11 rescued embryo stained for GFP (green), En (red) and DNA (blue), with higher power images showing En stripes in two segments and GFP subcellular localization. Rescued *nkd* cuticle is in right column, and anterior is to the left in all columns. GFP has no rescue activity, resulting in *nkd* embryos with wide En stripes that occupy half of each segmental anlage, and near uniform naked cuticle (arrowhead). Nkd^{GFPC} {Nkd with C-terminal GFP (G)} restored En stripes to 2-3 cells, localized predominantly to the cytoplasm but also in epidermal nuclei (asterisk), and restored wild type denticle bands in each abdominal segment (arrow). Nkd^{Δ30aa}/GFPC only slightly narrowed *nkd*-mutant En stripes, was predominantly cytoplasmic during stage 11, and partly rescued the *nkd*

cuticle phenotype, whereas $Nkd^{AR1S/GFPC}$ narrowed En stripes, localized predominantly to the nucleus, and restored mostly wild type cuticle pattern (Waldrop et al., 2006). $Nkd^{AR1S\Delta30aa/GFPC}$ accessed the nucleus and did not narrow En stripes but restored some denticle bands. $Nkd^{AR1S\Delta30aaNLS/GFPC}$, lacking R1S and replacing the 30aa NLS with the SV40 NLS (red box), localized to the nucleus but had no rescue activity. (B) Percent of wild type and *nkd* cuticle phenotypes {weak, moderate, strong - described in Materials and methods} for each *nkd* rescue cross with indicated *UAS-Nkd* construct. For lethal *UAS-Nkd* inserts on chromosome II, the persistence of the *CyO* balancer in the rescue cross results in ~12.5% of cuticles remaining unrescued and hence “strong” (black-topped bar in “strong” column). *w-* is negative control, with 100% wild type. *da>lacZ* rescue gives the expected Mendelian ratio of 75%/25% wild type/strong *nkd* mutant, while *da>Nkd* rescued nearly all *nkd* mutants to wild type. $Nkd^{AR1S\Delta30aaNLS/GFPC}$ had no activity, but $Nkd^{AR1S\Delta30aa/GFPC}$ produced some moderate-class cuticles indicating weak Nkd activity. (C) Rescue of elevated Arm in alternate segments of *nkd* mutants via expression of *UAS-Nkd* via *prd-Gal4* (*nkd prd>*). Four segmental anlagen of indicated stage 10 *nkd prd>Nkd* embryo stained for GFP (green), Arm (red) and DNA (blue) are shown. Since Arm/ β -catenin also links E-cadherin to the actin cytoskeleton, Arm staining is a composite of plasma membrane-associated Arm and Wg-dependent accumulation of cytoplasmic and nuclear Arm. Middle column shows Arm channel, and right panel is mean greyscale pixel intensity of Arm channel along anterior/posterior axis (ordinate axis 0-200). Green arrowheads indicate segments with *prd-Gal4* expression, white arrowheads alternate unrescued segments. Previously, we defined γ as the ratio of peak Arm intensity in non-rescued to rescued segments, with $\gamma \sim 1.0$ indicating no rescue, and for Nkd^{GFPC} $\gamma \sim 1.8$ (Waldrop et al., 2006). While the activity of $Nkd^{AR1S/GFPC}$ was comparable to Nkd^{GFPC} , the activities of $Nkd^{\Delta30aa/GFPC}$ or $Nkd^{AR1S\Delta30aa/GFPC}$ ($\gamma \sim 1.4$) were reduced relative to Nkd^{GFPC} { Nkd^{GFPC} and $Nkd^{\Delta30aa/GFPC}$ are not pictured but γ values are from (Waldrop et al., 2006)}. $Nkd^{AR1S\Delta30aaNLS/GFPC}$ had nearly absent activity ($\gamma = 1.1$) as compared to $Nkd^{\Delta30aaNLS/GFPC}$ ($\gamma = 1.5$) (Waldrop et al., 2006). Images of embryos and cuticles rescued by Nkd^{GFPC} , $Nkd^{\Delta30aa/GFPC}$, and $Nkd^{\Delta30aaNLS/GFPC}$ in panel A, as well as the *nkd* rescue data in panel B for $Nkd^{AR1S/GFPC}$, $Nkd^{\Delta30aa/GFPC}$, and $Nkd^{\Delta30aaNLS/GFPC}$ have been previously published (Waldrop et al., 2006).

4.3.2 *Nkd* associates with the nuclear import adaptor Importin- $\alpha 3$ via a motif conserved in *D. pseudoobscura*

Since $Nkd^{AR1S\Delta30aa/GFPC}$ is partly nuclear, Nkd must have NLS(s) in addition to the 30aa NLS. In a yeast-two-hybrid (Y2H) screen we recovered the nuclear import adaptor Importin- $\alpha 3$ as a Nkd-binding protein (see Materials and methods). The Nkd/Importin- $\alpha 3$ interaction is specific, because Nkd did not bind to the other two *Drosophila*

Importins, $\alpha 1$ or $\alpha 2$ (Fig. 4.2A,B). To identify the Importin- $\alpha 3$ -binding region of Nkd, we first assembled a putative *nkd* cDNA sequence from the genome of *D. pseudoobscura* (Dp) (Richards et al., 2005), a Drosophilid whose common ancestor with *D. melanogaster* (Dm) lived ~25-50 Myr ago. DpNkd is predicted to be 1009aa and $M_r = 111.8 \times 10^3$ (Fig. 4.2D). Dm/Dp Nkd alignment revealed nine regions of sequence similarity that included the four regions we previously noted to be conserved in mosquito Nkd (Fig. 4.2C,D) (Waldrop et al., 2006). Region #6 (designated “D6”) of conservation was necessary and sufficient for Importin- $\alpha 3$ interaction (Fig. 4.2E,F). The 30aa NLS - part of conserved region #7 - did not bind any of the three Importin- α s by Y2H (data not shown).

To investigate whether Importin- $\alpha 3$ is required for Nkd activity, we attempted to generate embryos that lacked Importin- $\alpha 3$. Importin- $\alpha 3$ mRNA and protein have been detected during oogenesis (Dockendorff et al., 1999; Mason et al., 2003; Mathe et al., 2000), but Importin- $\alpha 3$ protein only becomes detectable in the embryo after cell division cycle 12 (stage 4), correlating with the onset of responsiveness to heat shock-dependent transcription by dHSF (Fang et al., 2001). *importin- $\alpha 3$* mRNA is also synthesized zygotically, as mutants homozygous for the null *importin- $\alpha 3$* allele $\alpha 3^{D93}$ survive until the transition between first and second larval instars (Mason et al., 2003). Stage 11 homozygous $\alpha 3^{D93}$ embryos ($n > 50$) had En stripes indistinguishable from wild type and produced wild type cuticles ($n > 50$; data not shown), consistent with Importin- $\alpha 3$ protein translated from maternally deposited mRNA being responsible for postembryonic survival of the zygotic $\alpha 3^{D93}$ mutants (Mason et al., 2003). To eliminate the maternal

importin-α3 contribution, we used the *ovo^D* technique to generate germ-line clones of the $\alpha3^{D93}$ allele (Chou et al., 1993) (see Materials and Methods); unfortunately, $\alpha3^{D93}$ -mutant females ($n > 30$) did not lay eggs when mated with either wild type or $\alpha3^{D93}/TM3$ males, and examination of their ovarioles revealed only the *ovo^D* phenotype. Our results suggest that *importin-α3* has essential roles in oogenesis (Mathe et al., 2000), thereby precluding examination of embryos that lack maternal and zygotic *importin-α3*.

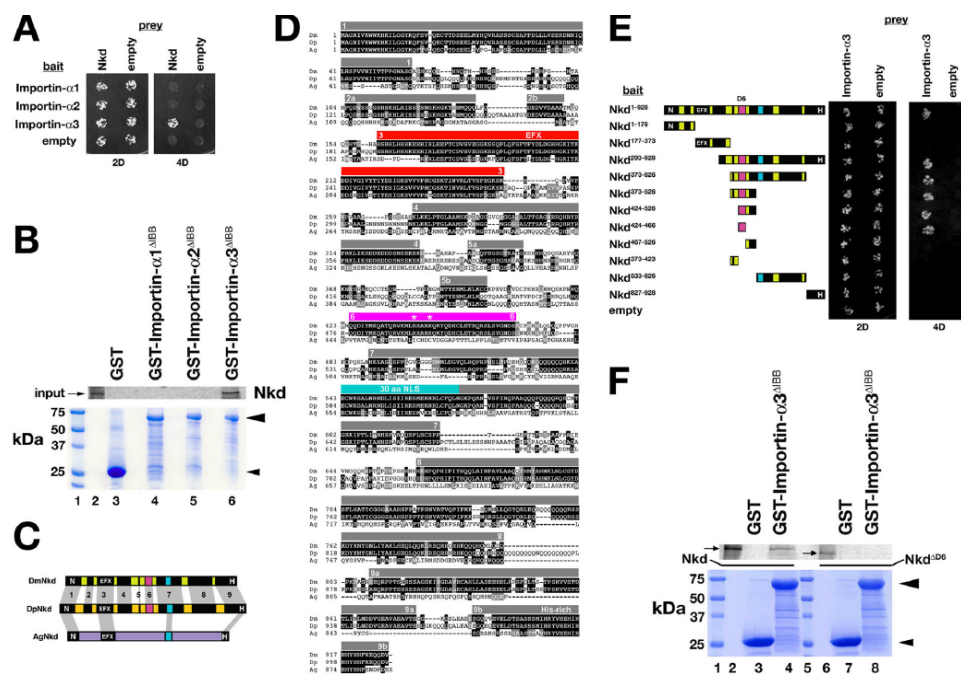


Fig. 4.2. *Drosophila* Nkd binds Importin-α3. (A) Y2H of strains expressing indicated bait (left) and prey (top) constructs under double (2D) or quadruple (4D) dropout conditions. Only strains with Nkd+Importin-α3 plasmids grew under 4D. (B) GST-pulldown assay showing that in vitro translated Nkd was retained on Glutathione agarose bound to GST-Importin-α3^{ΔIBB} (Importin-α3 residues 118-543 lacking the N-terminal Importin-β-binding (IBB) domain; see Materials and methods) in lane 6 but not to GST (lane 3), GST-Importin-α1^{ΔIBB} (lane 4) or GST-Importin-α2^{ΔIBB} (lane 5). Coomassie stained gel below confirmed that each recombinant protein (arrowheads) was bound to glutathione agarose. Size markers are in lane 1, and ³⁵S-Methionine labeled Nkd input is in lane 2. (C) Schematic of *D. melanogaster* Nkd (DmNkd), *D. pseudoobscura* Nkd (DpNkd), and *A. gambiae* Nkd (AgNkd). Grey bars show sequence similarity.

DmNkd/DpNkd have nine regions of similarity, numbered 1-9. Region #6 (D6; magenta) binds Importin- $\alpha 3$. (D) ClustalW alignment of insect Nkd proteins. Amino acid identities are dark-shaded, similarities light-shaded. Grey bars indicate regions of Dm/Dp sequence similarity (numbered). EFX-red; 30aa NLS-light blue; D6-magenta. Asterisks designate basic residues mutated in this work. (E) Nkd^{D6} (residues #424-466) binds Importin- $\alpha 3$ by Y2H. Yeast expressing indicated Nkd deletion constructs were assayed for growth as in panel A. (F) GST-pulldown assay showing that in vitro translated Nkd (lanes 2-4), but not Nkd^{AD6} (lanes 6-8), bound to glutathione agarose to which GST-Importin- $\alpha 3^{\Delta IBB}$ but not GST was bound. Coomassie-stained gel shows that equal amounts of each GST fusion protein were bound to the glutathione agarose. Size markers are in lanes 1 and 5, and Nkd or Nkd^{AD6} inputs are in lanes 2 and 6, respectively.

4.3.3 Importin- $\alpha 3$ is required for Nkd nuclear localization

Next we used RNA-interference (RNAi) to deplete Importin- $\alpha 3$. Expression of either of two *UAS-importin- $\alpha 3$ RNAi* lines (Dietzl et al., 2007) with *da-Gal4* resulted in larval lethality, but no obvious cuticle abnormalities were observed (data not shown).

Similarly, *prd-Gal4*-driven expression of *UAS-importin- $\alpha 3$ RNAi* did not affect En, Arm, or Importin- $\alpha 3$ staining in stage 10-11 embryos (data not shown), the latter perhaps due to an inability of zygotically synthesized double-stranded RNA produced by the snap-back construct to fully deplete maternal and zygotic *importin- $\alpha 3$* mRNA stores. We therefore examined the effect of Importin- $\alpha 3$ depletion on Nkd^{GFPC} distribution in post-embryonic cells. When synthesized in larval salivary gland, Nkd^{GFPC} is detected at low levels at the plasma membrane and cytoplasm and at higher levels in cytoplasmic/perinuclear puncta and in the nucleus (Fig. 4.3A). Importin- $\alpha 3$ is also enriched in salivary gland nuclei, in the presence or absence of Nkd^{GFPC} (Fig. 4.3A' and data not shown). However, co-expression of Nkd^{GFPC} and *UAS-importin- $\alpha 3$ RNAi* in salivary gland (see Materials and methods) dramatically reduced Importin- $\alpha 3$ immunoreactivity and resulted in complete exclusion of Nkd^{GFPC} from the nucleus (Fig.

4.3B-B’’). These data demonstrate that Importin- $\alpha 3$ is required for nuclear localization of Nkd.

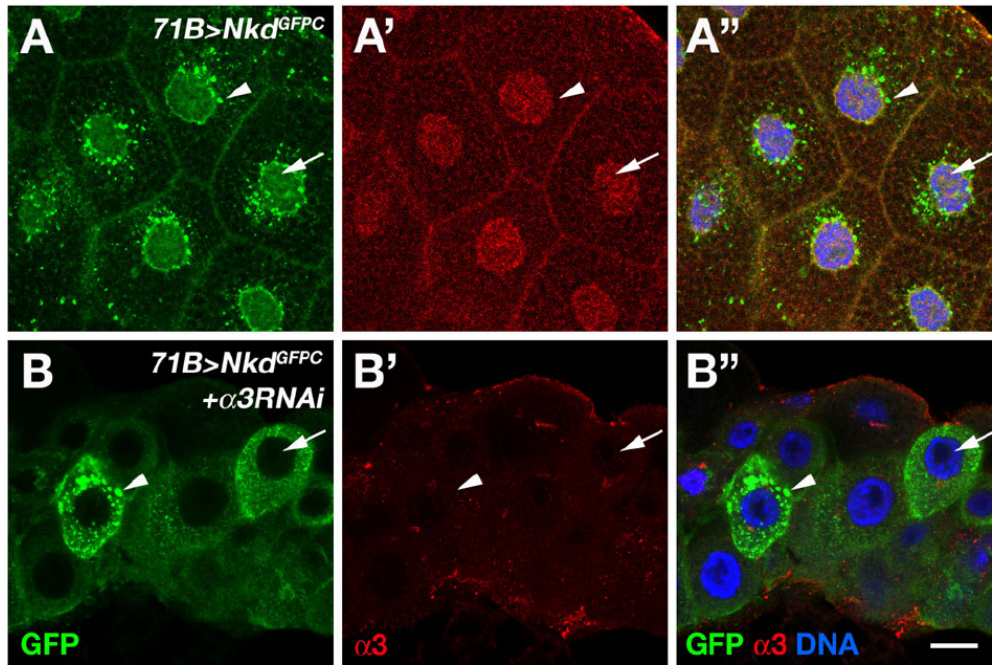


Fig. 4.3. Nkd requires *importin- $\alpha 3$* for nuclear localization. (A-A'') *71B>Nkd^{GFPC}* third instar salivary gland stained with Importin- $\alpha 3$ antibody (red channel in panel A') and imaged for GFP (green channel in panel A) and DNA (blue in merged image of panel A''). Nkd^{GFPC} localizes to the plasma membrane, in cytoplasmic/perinuclear puncta (arrowhead), and diffusely in the nucleus (arrow), whereas Importin- $\alpha 3$ is enriched in the nucleus. (B-B'') *71B>Nkd^{GFPC} + importin- $\alpha 3$ RNAi* salivary gland stained as in A. Note that Nkd^{GFPC} is completely excluded from nuclei (arrow) but cytoplasmic puncta (arrowhead) remain, and that Importin- $\alpha 3$ immunoreactivity is reduced to absent in nuclei. Scale bar in B'': 30 μ m in A-A''; 18 μ m in B-B''

4.3.4 D6 motif is required for nuclear localization and function of Nkd

Next we examined the rescue activity of Nkd^{AD6/GFPC}, a mutant construct that lacks the Importin- $\alpha 3$ -binding motif. Stage 11 *nkd da>Nkd^{AD6/GFPC}* embryos had En stripes of intermediate width (~3-5 cells) and produced weak and moderate-class *nkd* cuticles (Fig.

4.4A,B), indicating that D6 motif is required for full Nkd activity. The subcellular localization of Nkd^{ΔD6/GFP} was very similar to Nkd^{GFP}, likely due to the intact 30aa NLS in the latter construct (Fig. 4.4A). However, in contrast to Nkd^{GFP}, Nkd^{ΔD6/GFP} was predominantly cytoplasmic in larval salivary glands (*cf.* Fig. 4.3A and 4.4D). Nkd^{ΔD6/GFP} reduced Arm levels in *nkd* mutants as well as did Nkd^{GFP} (Fig. 4.4C), which is perhaps not surprising given the sufficiency of Nkd N-terminal and 30aa motifs, when substituted for the homologous regions of mouse Nkd1, for significant Nkd rescue activity (Chan et al., 2007).

Next we deleted both NLSs (Nkd^{ΔD6Δ30aa/GFP}). Although embryos rescued with either Nkd^{Δ30aa/GFP} or Nkd^{ΔD6Δ30aa/GFP} had wide En stripes and intermediate levels of Arm, cuticles rescued by the former construct were mostly weak and moderate *nkd*, while the majority of cuticles rescued by the latter construct were strong *nkd*, indicating that each NLS contributes to Nkd function (Fig. 4.4A-C) (Waldrop et al., 2006). In contrast to the marked difference in Nkd^{GFP} vs. Nkd^{Δ30aa/GFP} localizations during embryonic stage 11 {Fig. 4.1A and (Waldrop et al., 2006)}, Nkd^{Δ30aa/GFP} localized to larval salivary gland nuclei to the same extent as did Nkd^{GFP} (*cf.* Fig. 4.1A and 4.4E). In contrast, Nkd^{ΔD6Δ30aa/GFP} was excluded from embryonic and salivary gland nuclei (Fig. 4.4A,F), indicating that each NLS makes distinct contributions to nuclear localization in embryonic vs. postembryonic stages.

We previously showed that two constructs that lack the EFX motif (Nkd^{ΔEFX/GFP} and Nkd^{ΔR1S/GFP}) had substantial *nkd* rescue activity but localized predominantly to embryonic nuclei, consistent with Dsh or other EFX-binding proteins anchoring Nkd in

the cytoplasm (Waldrop et al., 2006). We assessed the requirement of the D6 motif for Nkd^{ΔR1S/GFP} activity/localization by deleting D6 to make Nkd^{ΔR1SΔD6/GFP}. As shown in Fig. 4.4A-C, Nkd^{ΔR1SΔD6/GFP} reduced Arm levels but did not narrow En stripes and gave rise to moderate and strong *nkd* cuticles. As in the embryo, Nkd^{ΔR1S/GFP} was predominantly nuclear in salivary gland (Fig. 4.4G), but Nkd^{ΔR1SΔD6/GFP} localized at the cell membrane and in the cytoplasm, with low levels in the nucleus (Fig. 4.4H), indicating that the D6 motif contributes to Nkd^{ΔR1S/GFP} nuclear localization. Nkd^{ΔR1SΔD6Δ30aa/GFP}, lacking Dsh-binding sequences and both NLSs, had no Nkd activity in any of the assays and was cytoplasmic in embryos and in salivary gland, indicating that the D6 motif is necessary for both the nuclear localization and weak activity of Nkd^{ΔR1SΔ30aa/GFP} (Fig. 4.4A-C,I).

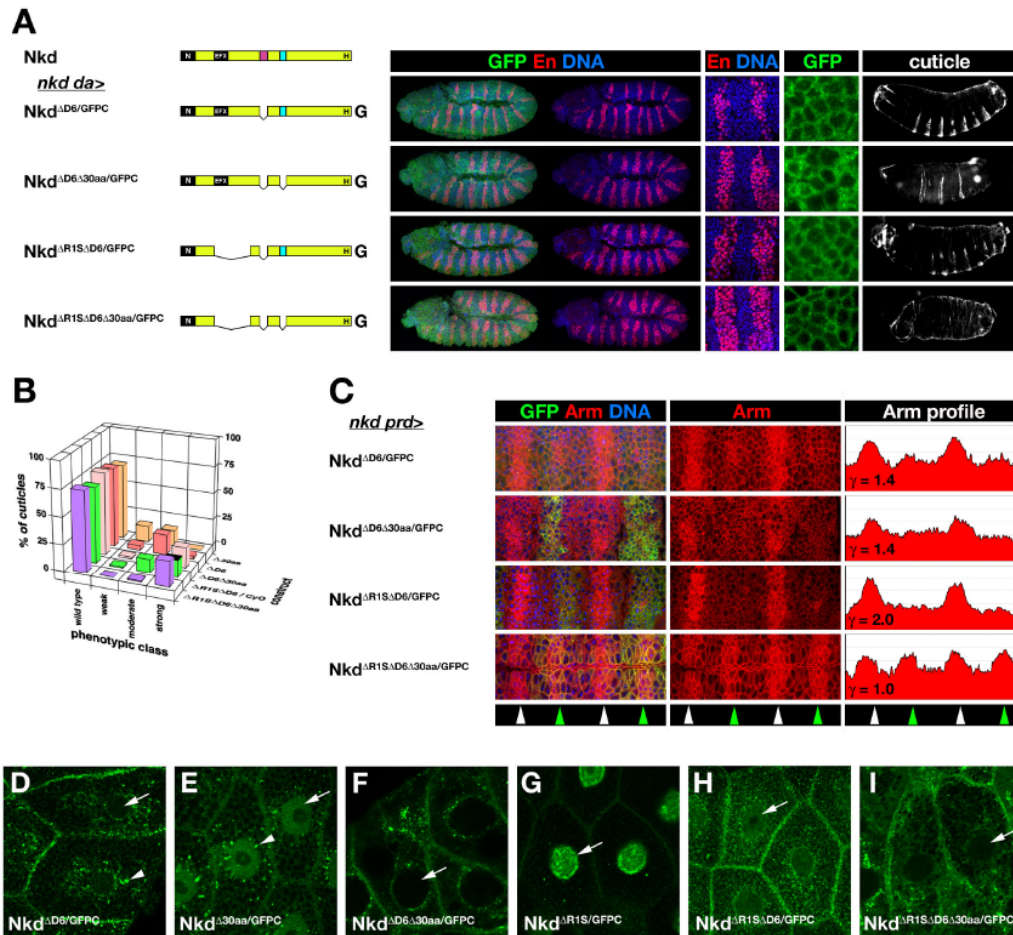


Fig. 4.4. D6 is required for Nkd function and nuclear localization. (A) *nkd da>*Nkd^{GFP} rescue and localization as in Fig. 4.1A. (B) Distribution of wild type and *nkd* cuticle phenotypes for rescue by indicated constructs as in Fig. 4.1B. (C) Rescue of elevated Arm in alternate segments of *nkd* mutants via *prd-Gal4* (*nkd prd>*) as in Fig. 4.1C (ordinate axis 0-250 pixels). (D-I) *71B>*Nkd^{GFP} third instar salivary gland imaged for GFP. Nkd^{ΔD6/GFP} (D) is in perinuclear aggregates (arrowhead) but has reduced nuclear localization (arrow) compared to Nkd^{GFP} in Fig. 4.3A. Nkd^{Δ30aa/GFP} (E) localizes to cytoplasm and nucleus in a distribution very similar to Nkd^{GFP}, but Nkd^{ΔD6:Δ30aa/GFP} (F) is excluded from nuclei. Nkd^{ΔR1S/GFP} (G) is almost exclusively nuclear, with enrichment at the nuclear membrane (arrow). Nkd^{ΔR1S:ΔD6/GFP} (H) exhibits reduced nuclear localization relative to Nkd^{ΔR1S/GFP}, while Nkd^{ΔR1S:ΔD6:Δ30aa/GFP} (I) is excluded from the nucleus.

4.3.5 The Nkd D6 NLS is similar to the dHSF Importin- α 3-binding NLS

The three *Drosophila* Importin- α s serve both unique and shared roles in development {reviewed by (Goldfarb et al., 2004)}, but sequence features that confer specificity between NLSs and each Importin- α are not known. In *Drosophila*, Importin- $\alpha 3$ has been shown to bind DNA polymerase- α 180 (DNAPol- $\alpha 180$) (Mathe et al., 2000), the transcriptional regulator Germ-cell-less (Gcl) (Dockendorff et al., 1999), and Heat-Shock Transcription Factor (dHSF) (Fang et al., 2001). We observed no obvious sequence similarity between the Nkd D6 motif and DNAPol- $\alpha 180$ or Gcl, with the exception of a few basic residues characteristic of NLSs (data not shown), but sequence alignment with dHSF-NLS revealed 33% (13/39 amino acids) similarity (Fig. 4.5A). Importantly, basic residues critical for dHSF/Importin- $\alpha 3$ binding and dHSF nuclear localization are also basic in similar positions of the Nkd-D6 motif (Fang et al., 2001; Zandi et al., 1997). Mutation of either or both of the Nkd-D6 basic residues to alanine (R441A, K445A) eliminated the D6/Importin- $\alpha 3$ interaction by Y2H (Fig. 4.5B). D6 is also sufficient to function as a NLS: when transiently produced in *Drosophila* Kc cells, the D6 motif fused to GFP (Nkd^{D6/GFP}) was exclusively nuclear, in contrast to GFP which was uniformly distributed in nucleus and cytoplasm {cf. Fig. 4.5D,E; at 27 kDa, GFP is smaller than the size – typically ~60 kDa or less - at which protein diffusion between nucleus and cytoplasm is restricted by the nuclear pore (Wang and Brattain, 2007)}. RNAi-mediated depletion of Importin- $\alpha 3$ (Fig. 4.5C; see Materials and methods) resulted in a uniform distribution of Nkd^{D6/GFP} similar to GFP or each D6 point mutant construct fused to GFP (Fig. 4.5F,G and data not shown). Thus, D6 basic residues required for Importin- $\alpha 3$ interaction are also required for the exclusive nuclear localization of Nkd^{D6/GFP}.

To test the biological significance of the basic residues required for Nkd/Importin- α 3 interaction, we introduced the point mutations into Nkd^{GFPC}. Point mutation of either or both conserved D6 basic residues eliminated the Nkd/Importin- α 3 interaction, and D6 deletion did not affect Nkd/Dsh interactions by Y2H (Fig. 4.6A). As shown in Fig. 4.6B, En stripes in embryos rescued by each point mutant construct were ~1-3 cells wider than those rescued by wild type Nkd, with focal areas of extreme widening indicative of ectopic Wg synthesized by further posterior cells (Chan et al., 2007). Consequently, the majority of *nkd* embryos rescued by each point mutant construct developed a moderate *nkd* cuticle phenotype similar to that of several lethal *nkd* alleles with nonsense mutations in the vicinity of the D6 motif (Fig. 4.6B,C) (Waldrop et al., 2006). Although the subcellular distributions of each point mutant construct appeared similar to that of Nkd^{GFPC} in stage 10-11 embryos (Fig. 4.6B; like Nkd^{AD6/GFPC} presumably due to an intact 30 aa NLS), each point mutant construct was excluded from third instar salivary gland nuclei to the same extent as Nkd^{AD6/GFPC} (data not shown). The inability of the point mutant constructs to rescue *nkd* mutants was not due to their reduced expression levels relative to Nkd^{GFPC} or to an early defect each construct's ability to lower Arm levels, because each of the three point mutant constructs lowered Arm levels during stage 10 to an extent comparable to Nkd^{GFPC} (Fig. 4.6D).

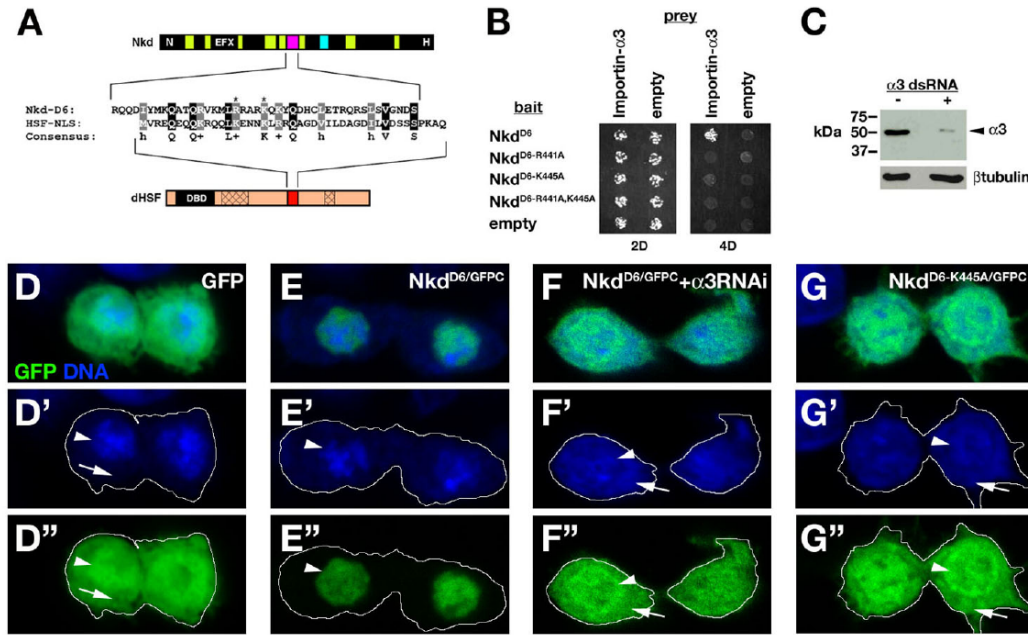


Fig. 4.5. The Nkd D6 motif is an *importin-α3*-dependent NLS. (A) Alignment of Nkd D6 motif (magenta) and HSF-NLS (red). dHSF has a DNA binding domain (DBD) and two oligomerization domains (cross-hatch). Asterisks mark Nkd basic residues R441/K445. (B) Y2H showing that D6 motif with R441A and/or K445A mutations eliminated D6/Importin-α3 binding. (C) Western blots of *Drosophila* Kc cells minus (left lane) or plus (right lane) two independent *importin-α3* dsRNAs (right lane) probed with anti-Importin-α3 antibody (top) or anti-βtubulin (bottom) (see Materials and methods). Quantitation of Importin-α3 bands, normalized to the βtubulin loading control, indicates a 92.5% reduction in Importin-α3 protein relative to the control. (D-G) Kc cells expressing GFP (D), Nkd^{D6}/GFPC (E,F) or Nkd^{D6-K445A}/GFPC (G), and imaged for GFP (green) and nucleic acids (blue). D'-G' shows DNA channel, and D''-G'' shows GFP channel, with cell outlines indicated by the white line. Peripheral nucleic acid staining corresponds to RNA in cytoplasm (arrow), while central staining (DNA) is the nucleus (arrowhead). GFP - at 27 kDa small enough to freely diffuse through nuclear pores - is uniformly distributed in nucleus and cytoplasm, while Nkd^{D6}/GFP (32 kDa - also below the nuclear pore diffusion limit of ~60 kDa) is exclusively nuclear (E-E''). Feeding either or both independent *importin-α3* dsRNAs resulted in uniform localization of Nkd^{D6}/GFPC (e.g. F-F''), similar to the uniform localization of Nkd^{D6-K445A}/GFPC (G-G''). Nkd^{D6-R441A}/GFPC and Nkd^{D6-R441A,K445A}/GFPC were also uniformly localized (data not shown).

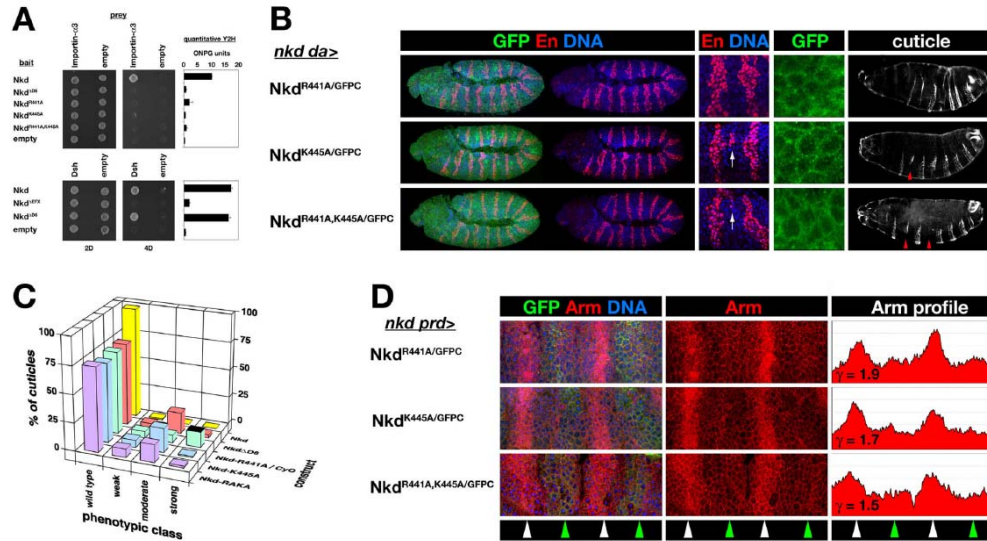


Fig. 4. 6. D6 NLS basic residues are required for Nkd function. (A) Y2H showing that Nkd R441A and/or K445A mutations disrupted Nkd/Importin- α 3 interactions, but unlike EFX deletion, D6 deletion did not affect the Nkd/Dsh interaction. Quantitative Y2H assay is depicted in bar graphs on the right. (B) *nkd da>* *Nkd*^{GFP} rescue and localization as in Fig. 4.5A. Note that rescue by each point mutant construct results in En stripes widened by 1-3 cells relative to embryos rescued by *Nkd*^{GFP} (cf. Fig. 4.1A), with focally ectopic En indicative of ectopic Wg production in cells just posterior to the En⁺ cells (arrow) (Chan et al., 2007), and moderate-class rescued *nkd* cuticle with deleted denticle bands (arrowheads). Each point mutant protein localized in a pattern – cytoplasmic and weakly nuclear – similar to wild type *Nkd*^{GFP} (cf. Fig. 4.1A). (C) Distribution of wild type and *nkd* cuticle phenotypes for rescue by indicated *Nkd*^{GFP} point mutant constructs as in Fig. 4.1B. (D) Representative stage 10 *nkd prd>* *Nkd*^{GFP} (point mutant) embryos stained for Arm as in Fig. 4.1C (ordinate axis=0–250 pixels). Note that each construct lowered Arm to an extent comparable to *Nkd*^{GFP} ($\gamma \sim 1.8$) (Waldrop et al., 2006).

4.3.6 dHSF NLS restores Importin- α 3 binding and nuclear localization but not function to *Nkd*

If Importin- α 3-dependent nuclear import is necessary for Nkd function, then replacing the D6-NLS with the dHSF-NLS (to make the construct *Nkd*^{AD6-HSFNLS/GFP}) might restore nuclear localization and function to *Nkd*^{AD6/GFP}. The dHSF-NLS, either by itself or when placed in *Nkd*^{AD6}, bound to Importin- α 3, and replacement of the Nkd D6 motif with the

(arrowheads). (C) *nkd da>Nkd^{AD6-HSFNLS/GFP}* cuticle, with 3 complete denticle belts indicative of moderate-class *nkd* cuticle. (D) Distribution of *nkd* cuticle phenotypes for *Nkd^{AD6-HSFNLS/GFP}* rescue cross (n=number of cuticles scored). (E) Stage 10 *nkd prd>Nkd^{AD6-HSFNLS/GFP}* embryo stained for GFP (green), Arm (red), and DNA (blue) in top panel, with Arm-only channel and Arm greyscale intensity profile (ordinate axis 0-200 pixels) in middle and lower panels, similar to Fig. 4.1C. (F) Model for fly Nkd function. Wg signaling at the plasma membrane (PM) leads to Arm/Pan-dependent transcription of target genes, including *nkd* (see Introduction for details). Nkd targets Dsh in the cytoplasm and/or plasma membrane, and binds Importin- α 3 to traverse the nuclear membrane (NM). In the nucleus, whether Nkd inhibits nucleocytoplasmic transport of Arm or another molecule, or whether Nkd directly regulates target gene transcription, remains unknown.

4.4 Discussion

A growing body of evidence indicates that the traditionally “cytoplasmic” Wnt signal transducers Axin, Apc, and Dsh also act in the nucleus {reviewed by (Willert and Jones, 2006)}. In the cytoplasm, Apc promotes β -catenin degradation and regulates the cytoskeleton, but nuclear Apc can recruit transcriptional corepressors to Wnt target genes and, like Axin, escort β -catenin from the nucleus {(Cong and Varmus, 2004; Sierra et al., 2006; Wiechens et al., 2004); reviewed in (Aoki and Taketo, 2007)}. In light of recent evidence that Axin/Dsh oligomers crosslink Wnt-bound receptors at the plasma membrane during signal activation (Bilic et al., 2007), it remains unclear whether any nuclear roles for Axin or Dsh are similar to their cytoplasmic functions or whether they, like Apc, have novel nuclear functions.

Nkd is also a conserved Wnt signal regulator whose subcellular localization initially suggested a cytoplasmic site of action (Zeng et al., 2000). Our studies have shown that fly Nkd is composed of discrete motifs that confer membrane localization and

binding to Dsh, as well as two NLSs {(Chan et al., 2007) and this work}. In addition to Nkd targeting an uncharacterized fraction of Dsh in the cytoplasm and/or at the plasma membrane, our data strongly support a nuclear role for Nkd, but whether Nkd inhibits Wnt signaling by altering nucleo-cytoplasmic transport of critical signaling components, such as Dsh or Arm, or by acting on the chromatin of Wnt target genes remains to be elucidated (Fig. 4.7F).

Epistasis can be a powerful means to infer the regulatory logic of signal transduction cascades. Because Nkd is a “side-regulator” whose loss-of-function phenotype is dependent on intact Wg signaling, double-mutants between *nkd* and *dsh* or *arm* did not help us to discern at which level Nkd inhibits the linear Wg signaling pathway (Rousset et al., 2001). However, Nkd overexpression suppressed the gain-of-Wg signaling phenotype caused by overexpression of Dsh but not that caused by overexpression of an N-terminally deleted and hence degradation-resistant Arm/ β -catenin (Pai et al., 1997; Rousset et al., 2001; Waldrop et al., 2006); taken together with the observation that Nkd binds Dsh, our previous epistasis experiments allowed us to conclude that Nkd acted at the level of Dsh and not “downstream” of Arm/ β -catenin in Wg signaling (Rousset et al., 2001). However, in view of the present data, Nkd might also act in the nucleus at or above the level of Arm/ β -catenin. Unfortunately, overproduction of wild type Arm is without phenotypic consequence (Pai et al., 1997), presumably because of an excess capacity of the β -catenin “destruction complex” to degrade ectopic Arm, thus preventing us from making further conclusions at present

about the epistatic relationship between Nkd and endogenous, degradation-sensitive Arm/ β -catenin.

Despite the deletion of Dsh-binding sequences in otherwise wild type Nkd having only a minor effect on cuticle rescue activity (Waldrop et al., 2006), the present experiments further support the hypothesis that the Nkd/Dsh interaction is important for Nkd to inhibit Wg signaling. However, our experiments thus far do not clarify how the interaction is regulated *in vivo* or whether it occurs in the cytoplasm, nucleus, or both locations. Nevertheless, several lines of evidence indicate that a Nkd/Dsh interaction in the cytoplasm and/or near the plasma membrane is important for Nkd function: First, both proteins are predominantly cytoplasmic and/or membrane-associated (Axelrod, 2001; Chan et al., 2007; Waldrop et al., 2006; Yanagawa et al., 1995). Second, punctate cytoplasmic Nkd/Dsh colocalization can be observed in embryos and in salivary gland (Rousset et al., 2001; Waldrop et al., 2006). Third, the Dsh-binding EFX motif fused to GFP was predominantly cytoplasmic (Waldrop et al., 2006). Fourth, deletion of Dsh-binding sequences in Nkd promoted nuclear localization, consistent with Dsh anchoring Nkd in the cytoplasm (Waldrop et al., 2006). Fifth, deletion of both Nkd NLSs eliminated nuclear localization whether or not Dsh-binding sequences were present, but Dsh-binding sequences were required for Nkd activity.

How Nkd acts on Dsh in the cytoplasm to inhibit Wg signaling is not known. One possibility is that Nkd sequesters Dsh away from Fz and/or Axin during signal activation, freeing Axin to regenerate β -catenin destruction complexes. Alternatively, Nkd might target “activated” Dsh, possibly the pool of Dsh bound to the Wnt receptor

complex, for degradation; consistent with Nkd targeting only a fraction of Dsh is the minimal colocalization of the two proteins in embryos as well as the lack of any obvious changes in Dsh levels in *nkd* mutants (Waldrop et al., 2006). Since Nkd can block the gain-of-Wg signaling phenotypes caused by overexpression of the Dsh kinase CK1 (Zhang et al., 2006), a third possibility is that Nkd blocks CK1-dependent phosphorylation of Dsh via a steric mechanism, although the relationship between Dsh phosphorylation status and activity remains unclear. Future experiments should clarify this issue, because each of these hypotheses makes distinct predictions about the phosphorylation status and associated proteins in a Nkd/Dsh complex.

Our studies also provide several lines of evidence that Nkd/Dsh is not sufficient for Nkd to inhibit Wg signaling (Rousset et al., 2001; Waldrop et al., 2006), and that a Nkd/Dsh binding event in the nucleus might also be required to fully antagonize Wg signaling. First, the Dsh-binding regions of Nkd when overexpressed blocked phenotypes induced by Dsh overexpression but had no *nkd* rescue activity (Waldrop et al., 2006). Second, (fly) Nkd and (vertebrate) Dsh have NLSs, although it is not yet known whether fly Dsh acts in the nucleus. Third, rare punctate Nkd/Dsh nuclear colocalization can be observed by confocal microscopy in fly embryos (Waldrop et al., 2006). Fourth, the SV40-NLS increased Nkd^{Δ30aa/GFP^C} activity when Dsh-binding sequences were intact but reduced activity when Dsh-binding sequences were deleted {(Waldrop et al., 2006) and this study}. We cannot rule out the possibility that the activity of Nkd^{Δ30aaNLS/GFP^C}, some of which remains outside the nucleus despite the strong heterologous NLS, is due to cytoplasmic Nkd/Dsh interactions. Similarly,

Nkd^{ΔR1SA30aaNLS/GFPC}, which was exclusively nuclear in embryos, might lack activity because of its inability to bind and be retained by Dsh in the cytoplasm. While one must be cautious when inferring site(s) of protein action from subcellular localizations, our studies collectively suggest that fly Nkd is required at multiple locations in Wg-receiving cells.

The Nkd-D6 motif has been subject to intense selection pressure, as it is identical in Nkd from *D. pseudoobscura*, a fly species that diverged from *D. melanogaster* approximately one billion generations ago. Similarly, the 30aa NLS is part of a 58 aa motif, and the EFX is part of a 91 aa motif, which are also identical in the two *Drosophila* species. Using Y2H, we have identified Nkd-EFX residues that are either dispensable or critical for Nkd^{EFX}/Dsh^{bPDZ} interactions (K.W. and C.-C. C., unpublished data), suggesting that interactions between the EFX motif and proteins other than Dsh might enforce strict motif conservation. Although each NLS contributes to Nkd activity and nuclear localization, heterologous NLSs did not fully replace the function of each Nkd NLS in rescue assays, and in both cases in this work a heterologous NLS was deleterious to protein function. Absolute conservation of each of these motifs implies that both the tertiary structure and every square angstrom of each motif's surface are necessary for species survival. Taken together with our previous work (Chan et al., 2007; Waldrop et al., 2006), our experiments also suggest that each Nkd motif is required for distinct thresholds and/or duration of Wg signal inhibition: the N-terminal and 30 aa motifs were required for reduction of Arm levels by stage 10, whereas the Dsh-binding EFX and Importin-α3-binding D6 motifs were dispensable for Arm reduction but were

required, either directly or indirectly, to fully repress *en* and/or *wg* transcription by stage 11. Since the deletion of two highly conserved motifs (EFX and D6) preserved the mutant Nkd protein's ability to reduce Arm levels during stage 10, it seems unlikely that these motifs will be shown to possess an intrinsic catalytic activity. We therefore favor the hypothesis that Nkd acts as an inducible protein scaffold, with each of the conserved motifs able to bind additional protein(s). Perhaps there exist distinct Nkd-complexes depending on the subcellular compartment, state of signal activation, or time following signal initiation.

Alignment of the Importin- α 3-binding NLSs in Nkd and dHSF revealed several conserved residues. Interestingly, the dHSF-NLS has been shown to be bifunctional, suppressing dHSF trimerization in the absence of heat shock, and in response to heat or other stresses conferring Importin- α 3-dependent dHSF nuclear translocation and transcriptional induction of heat-responsive genes such as *hsp70* (Voellmy, 2004; Wu, 1995; Zandi et al., 1997). Our data suggest that the Nkd D6-NLS is also bifunctional, conferring Importin- α 3-dependent nuclear localization as well as possibly binding nuclear protein(s) that repress Wg target gene transcription in some cells through stages 10-11. While non-import – presumably scaffolding - functions for Importin- α s have been inferred from phenotypes observed with *importin- α* deficiency in flies and worms {reviewed in (Goldfarb et al., 2004)}, all of our experiments support the hypothesis that the Nkd/Importin- α 3 interaction promotes nuclear localization. The central region of Importin- α consists of ten alpha-helical “Arm” repeats - so named because they were first identified in the *Drosophila* Arm protein (Peifer et al., 1994) - stacked to form a

banana-shaped molecule, the concave side of which harbors a groove that binds basic residues within NLSs {reviewed in (Lange et al., 2007)}. At present, it is not possible based on primary sequence to predict which Importin- α a given NLS will bind, although both the NLS and its three dimensional context (i.e. adjacent sequence) have been demonstrated to contribute to NLS/Importin- α specificity (Friedrich et al., 2006). Future experiments will determine whether the residues conserved between Nkd and dHSF represent a consensus Importin- α 3-specific binding motif.

Vertebrate Nkds have a conserved 30aa motif between the EFX and C-terminal histidine-rich regions (Waldrop et al., 2006), but whether the vertebrate proteins act in the nucleus like fly Nkd is not known. In this regard, we observed no obvious difference between the subcellular localizations of mouse Nkd1 fused to C-terminal GFP (mNkd1^{GFPC}) vs. a similar construct that lacks the 30aa motif (mNkd1 ^{Δ 30aa/GFPC}) when either protein was produced in cultured mammalian cells (T. Cagatay and K. W., unpublished data) (Waldrop et al., 2006). However, we also observed no obvious difference between fly Nkd vs. Nkd ^{Δ 30aa} localizations in *Drosophila* S2 cells (T. Cagatay and K. W., unpublished data), but the differences in localization and function of these two constructs when produced in *nkd* mutant embryos were dramatic. Our findings illustrate the importance of investigating the subcellular localizations of mutant proteins in a native environment that lacks the endogenous wild-type protein. It might therefore be interesting to examine the subcellular localization of vertebrate Nkds in *nkd*-mutant mice or zebrafish just as we have done in *Drosophila*. More importantly, future

experiments must address the critical question of how Nkd antagonizes Wnt/ β -catenin signaling in each of the compartments to which it localizes.

CHAPTER FIVE

EXPERIMENTS IN PROGRESS TO INVESTIGATE NKD FUNCTION

5.1. *nkd* loss-of-function by RNAi causes post-embryonic phenotypes

5.1.1 *nkd* knockdown mimics *Wg* gain-of-function phenotype

Wg signaling is required for several developmental processes including embryo development, head development, and imaginal disc development {reviewed in (Klingensmith and Nusse, 1994)}. However, *nkd* is only known to antagonize *Wg* signaling during early embryogenesis (Zeng et al., 2000). It is not clear whether Nkd plays a role in post-embryonic stages. *nkd* mRNA can be induced by *Wg* in the imaginal disc (Zeng et al., 2000), although whether or how Nkd functions in wing disc development remains to be elucidated. *nkd* was found to genetically interact with misexpressed *arm* in wing imaginal discs, suggesting that *nkd* might regulate *Wg* signaling in the developing wing (Greaves et al., 1999). *nkd* was also found to genetically interact with the cadherin *dachsous* to regulate *Wg* signaling during leg development (Rodriguez 2004). *Wg* signaling suppresses the bristle formation in the eye margin, and *nkd*^{7E89} clones exhibited similar phenotypes of bristle inhibition as does activated *arm* (Cadigan et al., 2002; Rousset et al., 2001). However, previous clonal analysis of two *nkd* hypomorphic alleles, *nkd*^{9G33} and *nkd*^{7E89}, did not produce significant phenotypes in the *Drosophila* legs and wing margin (Zeng et al., 2000). The explanation for the lack of clonal phenotype is that both alleles encode for truncated Nkd proteins that

retain functional domains (e.g. the RIS region) that contributes to Nkd's ability to antagonize Wg signaling, such that the clonal phenotype is too subtle to be observed. One strong allele, *nkd*^{7H16}, which encodes the N-terminal 59aa, gives rise to clones that have loss of wing margin bristles and rough eyes (Zeng et al., 2000; Keith Wharton, unpublished data). However the chromosome on which *nkd*^{7H16} resides also has a mutation (*h*¹) in the pair rule gene *hairy* (*h*) - a pair-rule gene that genetically interacts with *nkd* (Zeng et al., 2000), raising the possibility that the *nkd*^{7H16} clonal phenotype might be caused by *hairy*¹-*nkd* interactions. *UAS-Nkd*^{7H16}, which encodes for the 59aa protein predicted to accumulate in the homozygous *nkd*^{7H16} mutant, showed no rescue activity in *nkd* rescue assay, suggesting that *nkd*^{7H16} is a null allele. However, the phenotype of *nkd*^{7H16} cuticles is not as “naked” as *zw3* mutant cuticles, indicating that the encoded 59aa protein might have remaining activity. Alternatively, the null mutant *zw3* phenotype might simply be more severe than the null *nkd* phenotype. Therefore, the complete loss-of-function phenotype of *nkd* in post-embryonic stages remains an interesting question.

It has been shown that *nkd* can be knocked down effectively by dsRNA injection in the embryo (Rousset et al., 2001). Recently, I utilized two transgenic flies bearing different *UAS-RNAi* constructs (NR1 and NR2) targeting different regions of *nkd* to knockdown Nkd with various *Gal4* drivers in a tissue-specific manner (Kalidas et al., 2002) (Fig 5.1). Wg is required for the specification of wing margin (Blair 1994). By using *C96-Gal4* driver (Axelrod et al., 1996) to express *nkd* RNAi in the wing margin, ectopic bristles near the wing margin were observed (Keith Wharton, unpublished data); supporting the

role of *nkd* in repressing Wg signaling in the developing wing. By using *71B-Gal4* driver to express both *nkd* RNAi constructs in the dorsal part of the leg imaginal disc, a gain-of-sternopleural bristles phenotype was observed that mimics a *wg* gain-of-function phenotype similar to the previously reported *wg^{Sp}* allele (Fig 5.2) (Neumann et al., 1996). The fact that both *nkd-RNAi* constructs give rise to similar results to *wg^{Sp}* allele suggests that the phenotype may be either *nkd*-specific or RNAi-specific.

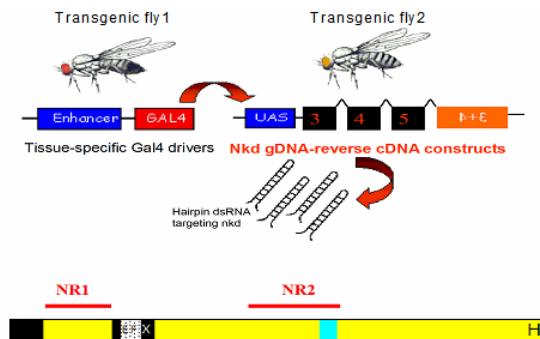


Fig 5.1. Generation of an inducible Nkd “knock-down” using RNA interference. *nkd* snapback sequence is constructed into UAS-vector for subsequent expression driven by tissue specific Gal4 drivers. 2 constructs (NR1) and (NR2) are generated targeting different regions of *nkd*.

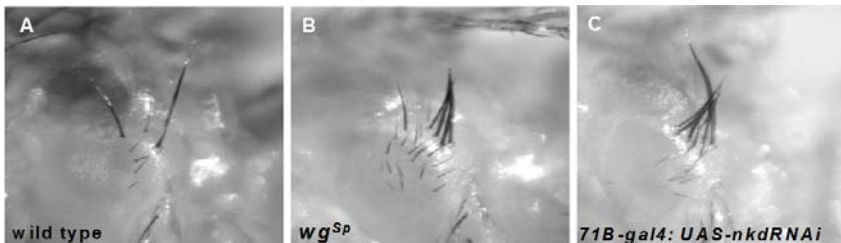


Fig 5.2 Nkd knockdown mimics Wg gain-of-function phenotype. (A) wild type *Drosophila* adult sternopleural bristles. (B) *wg^{Sp}* allele causes gain of sternopleural bristle. (C) Knockdown of *nkd* by RNAi resembles *wg^{Sp}* phenotype (Neumann et al., 1996).

5.1.2 Experiments to verify specificity of *nkd* knockdown effect

To determine whether *nkd* RNAi construct knocks down Nkd specifically, I will perform in situ hybridization experiments using *en-gal4* to express *nkd* RNAi in the posterior compartment of the wing imaginal disc, wherein Wg functions and *nkd* mRNA is Wg-inducible. The predicted result would be that *nkd* mRNA is decreased where *nkd*-RNAi construct is expressed in the posterior compartment. However, since *nkd* itself is the target of Wg signaling, knocking down Nkd by RNAi may result in increased Wg signaling activity that may eventually increase *nkd* mRNA. In chapter 3, mNkd1^{fNf30aa/GFPC} - consisting of the fly N-terminus and fly 30-aa in the mouse Nkd1 backbone - antagonized Wnt signaling effectively in the embryo (Chan et al., 2007). mNkd1^{fNf30aa/GFPC} is predicted to be targeted by NR2, which targets the 30-aa motif and adjacent regions (Fig 5.1). The GFP intensity of mNkd1^{fNf30aa/GFPC} should only be decreased when NR2 is cooverexpressed, but not with the co-overexpression of NR1, which only targets fly Nkd regions between the N-terminus and 30-aa. Also, the ability of mNkd1^{fNf30aa/GFPC} to inhibit Wg signaling should only be affected by RNA interference induced by NR2, but not by NR1. Therefore the downstream readouts such as restricted Arm levels caused by mNkd1^{fNf30aa/GFPC} should only be affected by construct NR2, but not by NR1.

5.1.3 Experiments to discover the function of *nkd* in post-embryonic stages

To answer the question “Does Nkd inhibit Wg signaling in post-embryonic stages?”, *nkd* loss-of-function phenotypes will need to be more carefully examined in the wing and eye imaginal discs, where we know Wg signaling functions. Several *Gal4* drivers will be utilized to induce RNAi to knockdown Nkd in a tissue-specific manner. For example, *en-*

gal4 will drive the expression of *nkd* RNAi in the posterior compartment, where one can examine whether loss-of-*nkd* affects Wg distribution, or Arm levels, or the expression of downstream target genes. By examination of loss-of-*nkd* phenotypes, we shall be able to address whether *nkd* functions in the wing. More specifically, by inducing *nkd* RNAi clones in the wing disc, we shall be able to examine whether *nkd* affects Wg transport in the developing wing; hence validating whether the cell-autonomous function of Nkd in the embryo is specific to the embryo and the eye, or is true in all tissues (Chan et al., 2007). Furthermore, as clones of different *nkd* mutant alleles give distinct clonal phenotypes in the eye, to generate *nkd* RNAi clones in the eye disc should help us verify whether Nkd inhibit Wg signaling in the developing eye. The predicted phenotype of eye clones of *nkd* RNAi is the suppression of interommatidial bristles in the eye margin, which mimics the *nkd*^{7E89} clonal phenotype.

As an ultimate test of *nkd* function, clonal analysis of *nkd* null alleles needs be performed to validate the findings from *nkd* RNAi experiments. As a first step, the *h*^l mutation will be removed from the chromosome where *nkd*^{7H16} resides by recombination. *nkd*^{7H16} clones will be generated in the developing wing discs. Readouts such as Arm levels or expression of downstream targets will be compared to test whether results from *nkd* RNAi or *nkd*^{7H} clones give similar results. Nonetheless, the assumption that *nkd*^{7H16} is a null allele may not be true, and so to generate a *nkd* null allele by homologous recombination and to analyze the clonal phenotype of the null allele will complement the findings of *nkd* RNAi clones.

5.2 α -Actinin negatively regulates Nkd activity

5.2.1 Introduction to α -Actinin

α -Actinin is an actin-crosslinking protein that is associated with a variety of actin-based structures including lamellopodia or filopodia. α -Actinin is an ancient protein conserved from fission yeast to humans (Virel and Backman, 2004). The protein structure of α -Actinin consists of an N-terminal actin-binding domain, a middle region of four spectrin repeats, and a C-terminal calmodulin-like domain with two EF-hand motifs (Djinovic-Carugo et al., 1999). The native form is an antiparallel dimer (Fig 5.3) (Winkler et al., 1997). α -Actinin belongs to the spectrin protein superfamily, which is characterized by the presence of spectrin repeats, actin binding domains, and EF hands {reviewed in (Roper et al., 2002)}. A recent report suggest that another membrane of the spectrin super family MACF1 - microtubule actin cross-linking factor 1- functions as positive regulator in Wnt signaling (Chen et al., 2006). Decreased level of MACF1 resulted in a decrease in nuclear β -catenin, and resulted in an inhibition of Wnt-induced β -catenin-dependent transcriptional activation (Chen et al., 2006). MACF1 binds to Axin, and appeared to translocate Axin from cytoplasm to the plasma membrane when Wnt ligand was present (Chen et al., 2006). This report associates Wnt signaling with the spectrin superfamily, which mainly functions to link cytoskeleton to membrane-associated junctions (Roper and Brown, 2003).

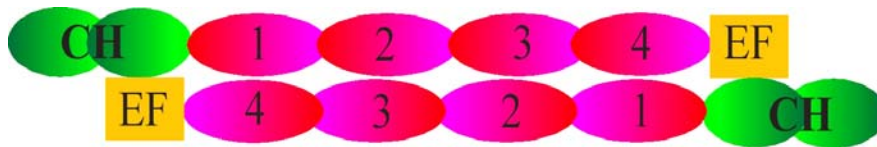


Fig 5.3 Schematic drawing of an α -Actinin dimer. Each molecule consists of an N-terminal actin-binding domain composed of two calponin-homology domains (CH), a central region with four α -spectrin repeats (1-4) and a C-terminal Calmodulin domain with two EF-hand motifs (EF). The molecules in a dimer are aligned in antiparallel fashion.

α -Actinin is expressed in both muscle and non-muscle cells (Clark and Hirst, 2002; Lazarides and Burridge, 1975). In muscle, α -Actinin is localized in the Z-disc to crosslink actin filaments from adjacent sarcomeres. Besides Actin-cross linking, α -Actinin also plays a role in the regulation of cell migration (Honda et al., 1998; Knudsen et al., 1995) and vesicle trafficking (Kato et al., 1996; Yan et al., 2005). Mammals have four *α -Actinin* genes, which give rise to at least 6 isoforms by alternative splicing (MacArthur and North, 2004). The most intensively investigated α -Actinins are *ACTN3* and *ACTN4* (MacArthur et al., 2008; Henderson et al., 2008). A common nonsense polymorphism (R577X) in the *ACTN3* gene encodes a truncated α -Actinin3 protein which is unstable (MacArthur et al., 2008). *ACTN3* knockout mice showed enhanced recovery from fatigue and improved athletic endurance (MacArthur et al., 2008). On the other hand, an inherited, late-onset form of kidney failure is caused by point mutations in the actin-binding domain of α -Actinin4 (Weins et al., 2007). Mutations in *ACTN4* which result in increased actin-binding are associated with proteinuric renal disease such as segmental glomerulosclerosis (Henderson et al., 2008; Weins et al., 2007).

In non-muscle cells, α -Actinin is found in multiple subcellular compartments such as cell-cell and cell-matrix contact sites and cellular protrusions (Otey and Carpen, 2004).

Recent studies found that besides binding to Actin, α -Actinin can also associate with ~29 different proteins (Otey and Carpen, 2004). The interaction between α -Actinin and various proteins are cell-type-dependent. The α -Actinin-interacting proteins range from adhesion molecules, such as the β subunit of integrin and intracellular adhesion molecule-1 (ICAM-1) (Otey et al., 1990; Carpen et al., 1992), to signal transduction molecules, such as PI3-kinase (Shibasaki et al., 1994) and MEKK1- a MAP kinase kinase that regulates cell migration (Christerson et al., 1999). Therefore α -Actinin might link the cytoskeleton to many different proteins in multiple subcellular regions where α -Actinin exists. α -Actinin may also serve as a platform for the many signaling proteins that have been found associated with it, or it may link the cytoskeleton to signal transduction pathways.

While humans have four α -Actinin homologs, *Drosophila* has only a single gene. *Drosophila* α -Actinin (Actn) is ~ 70% identical in amino acid levels to vertebrate α -Actinins (Beggs et al., 1992). *Drosophila* has three isoforms of α -Actinins - non-muscle, larval muscle-specific, and adult muscle-specific - that are created by alternative splicing of a single gene (Fyrberg et al., 1990; Roulier et al., 1992). The non-muscle isoform is the only isoform detected in the embryos (Wahlstrom et al., 2004). Null mutations in the *Drosophila Actn* are lethal at larval stages, with only muscle defects being reported (Fyrberg et al., 1990). One reason that *Actn* mutant flies do not show significant defects during embryogenesis is that the maternally loaded *Actn* mRNA might be sufficient for *Drosophila* to survive embryonic development. Germline clone analysis of one *Actn* inversion allele *EA82^{HC207}* (inverted between chromosomal bands 2C3-7B1) showed that

in 5% of the embryos, each segment appears to be duplicated in a mirror-image pattern, suggesting that Actn may be required for segmentation (Perrimon et al., 1985). Since the inversion is close to the *arm* loci (2B15-17), the authors hypothesized that the embryo patterning defect was due to position-effect dependent alteration in the function of the *arm* gene (Perrimon et al., 1985). Nonetheless, one cannot rule out the possibility that it is *Actn* that causes the *arm*-like phenotype, which would be consistent with *Actn*'s role as a inhibitor of the Wg signaling inhibitor (*nkd*).

5.2.2 Nkd uses a conserved 30aa motif, previously reported to be critical for function, to interact with α -Actinin

Actn was identified as a Nkd-binding protein from Y2H screens by Raphael Rousset (University of Nice, France). I have mapped the Actn-interacting domain on Nkd to the 30aa motif by Y2H assay. This motif is necessary and sufficient to bind Actn (Fig 5.3). More binding assays, such as GST pulldown or co-IP, are required to validate the interaction. However, since we know this 30 aa motif is critical for Nkd function, identifying Actn as a Nkd-binding protein should help elucidate how Nkd function is regulated.

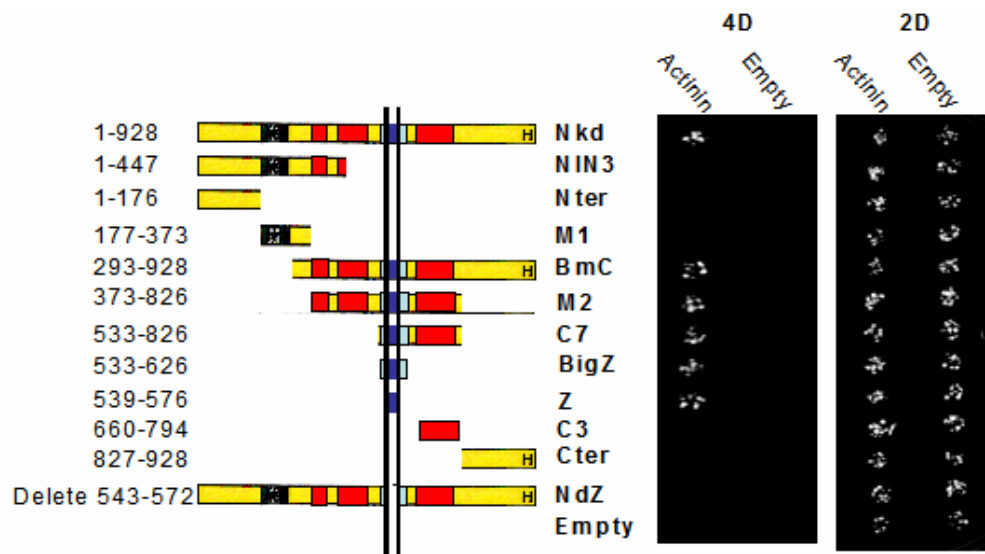


Fig 5.4. Nkd uses its 30-aa motif to interact with α -Actinin in Y2H assay. Deep blue box is the 30-aa motif. While 30-aa motif by itself binds to α -Actinin, Nkd lacking 30-aa motif fail to bind α -Actinin.

5.2.3 The mechanism by which α -Actinin regulates Nkd activity

Does Actn modify Nkd activity? To examine the genetic interaction between Nkd and Actn, I generated *UAS-Actn* non muscle isoform transgenic flies. *UAS-Actn-RNAi* flies were also requested from the Vienna RNAi collection (Dietzl et al., 2007) as a means to knockdown Actn. Overexpression or RNAi knockdown of Actn using *GMR-Gal4* did not cause morphological change of the eye (Fig 5.4 A', B', C'). Then, Actn was either overexpressed or knocked down in the eye under the genetic background of overexpressed Nkd and Dsh. While Actn overexpression decreased the eye size, knockdown of Actn gave rise to increased eye size (Fig 5.4 A, B, C). One explanation for Actn's ability to modify the eye phenotype is that Actn negatively regulates Nkd

activity. However the reverse can be true in that Actn positively regulates Dsh activity.

Further studies will be required to dissect the function of α -Actinin on Nkd.

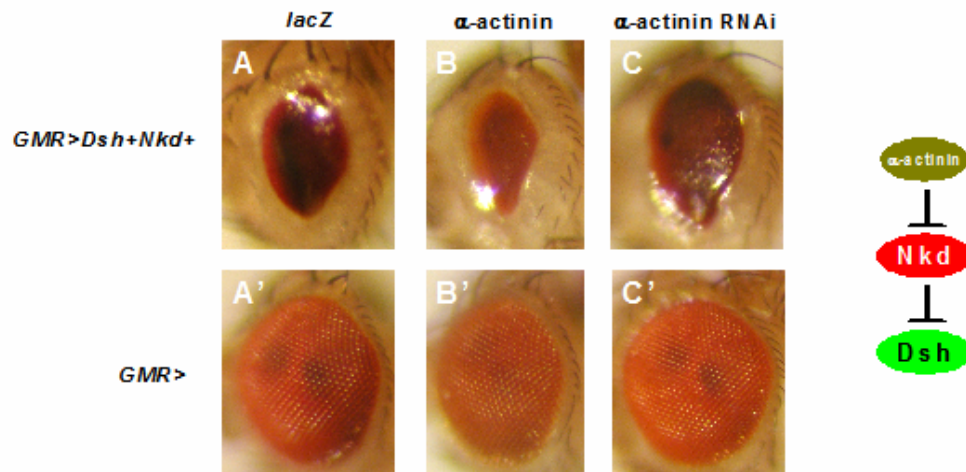


Fig 5.5. α -Actinin inhibits Nkd activity. (cf. A, A') cooverexpression of Nkd and Dsh in the eye causes glazed eye phenotype. (cf. A, B) cooverexpression of α -Actinin, Nkd, and Dsh causes even smaller eye. (cf. A, C) knockdown of α -Actinin increase the ommatidial number.

What is the biological significance of interactions between a signal antagonist (Nkd) and a cytoskeletal protein (α -Actinin)? The interaction between Nkd and α -Actinin raises several interesting questions:

The first question is “Does Nkd-Actn interaction happen *in vivo*?” To assess the Nkd/Actn interaction, the subcellular distribution of Actn in the rescued *nkd* embryos will be examined. The distribution of Actn in either Nkd- or Nkd ^{Δ 30aa}-rescued embryos will be compared. Since Nkd functions in the membrane, cytoplasm, and nucleus, Nkd and Actn will also be co-stained to examine where inside the cell they colocalize. Since Actn is associated with adherens junctions, the markers for adherens junctions will also be co-

stained. Furthermore, to test whether Nkd-Actn interaction is Wg-dependent, the intracellular localization of both proteins will be examined in each row of cells in a segment. If Nkd-Actn interaction is regulated by Wg signaling, then the intracellular localization of both proteins should be different in cells far away from Wg source vs. in Wg-synthesizing cells.

Does Actn regulate Wnt signaling? If so, by what mechanism? The data (Fig 5.4) suggest that Actn negatively regulates Nkd activity in the eye. If this is also true in the embryo, loss of function of *Actn*, such as in *Actn* mutant, may cause Nkd over-activation; hence decreased Wg activity. However, since Nkd's expression is Wg-dependent, one may not be able to observe abnormal Wg signaling in *Actn* mutant. Nonetheless, careful examination of Wg-signaling readouts such as Arm levels or *en* stripes in *Actn* mutant embryos should reveal whether Actn regulates Wnt signaling.

Moreover, since Actn and Nkd physically interact, one model would be Actn sequesters Nkd from its site of function. If Actn sequesters Nkd in the cytoskeleton, then one may be able to observe Actn-Nkd colocalization, possibly in the cytoskeleton. Moreover, when Actn is overexpressed, more Nkd should be sequestered, assuming excess Actn is incorporated into the cytoskeleton. Therefore in *nkd* rescue experiment, cooverexpression of Nkd and Actn may impair Nkd's ability to rescue *nkd* mutants; hence one may see increased Arm levels and widened En stripes in the rescued mutant embryos.

The novel Wnt component MACF1 has a single *Drosophila* homolog *short stop* (*shot*) (Lee and Kolodziej, 2002, Roper et al., 2002). Like Actn, Shot has an N-terminal actin-binding domain and a C-terminal calmodulin-like domain with two EF-hand motifs, but the middle region consists of more than 30 spectrin repeats (Roper et al., 2002). To examine if Nkd/Actn interaction can be generally applied to the spectrin superfamily, the first step would be to map the Nkd-binding domain on Actn. For example, if Nkd binds to the C-terminus of Actn, then we can examine whether Nkd also bind to the C-termini of other members of the superfamily. Given that MACF1 is a positive regulator of Wnt signaling, it will be interesting to examine the interaction between Nkd and MACF1's *Drosophila* homolog- Shot.

CHAPTER SIX

DISCUSSION AND CONCLUSIONS

6.1 The domain functions of Nkd protein

By what mechanism does Nkd inhibit Wnt signaling? As a first step to assess Nkd function, our lab began with an *in vivo* structure-function study. The Nkd family of proteins is conserved through evolution, with 9 regions of sequence similarity between *D. melanogaster* and *D. pseudoobscura*; 4 of the 9 regions are shared between *Drosophila* and mosquito. Based on the results from chapters 2 to 4, the characterized functions of each domain and its known binding partners are summarized below.

6.1.1 N-terminus confers membrane association and is required for function

Mammalian Nkd1 and Nkd2 have sequence in their N-termini for post-translational lipid modification and membrane anchoring (Li et al., 2004; Wharton et al., 2001). *Drosophila* Nkd's N-terminus, unlike its mammalian counterparts, does not possess a myristoylation consensus sequence. Nonetheless an N-terminal block of sequence is conserved between *Drosophila* and mosquito Nkds. The N-terminal homology region of fly Nkd was sufficient for partial membrane association in a cell culture system and in larval salivary gland (Chan et al., 2008). N-terminal deletion or GFP addition (possibly masking the N-terminus) resulted in defective *nkd* rescue activity, indicating a requirement of the N-terminus for function (Chan et al., 2007). Replacing the fly N-terminus with mouse Nkd1 N-terminus restored membrane localization of Nkd, but not

rescue activity (Chan et al., 2007). This suggests that although the N-terminus of both *Drosophila* and mammals perform a similar biochemical function - membrane association - the underlying molecular mechanisms for fly vs. vertebrate N-terminus to associate with the membrane may be different. Unlike mammalian Nkds, *Drosophila* Nkd associates with plasma membrane via its N-terminus possibly through other modes of lipid modification, such as palmitoylation (Bijlmakers and Marsh, 2003) or octanoylation (Yang et al, 2008), or through protein-protein interaction. To elucidate the molecular mechanism by which *Drosophila* Nkd associates with the membrane, it is required to discover additional protein(s) that interact with the N-terminus.

6.1.2 The Dsh-interacting domain ("R1S" region) is required for cytoplasmic localization of Nkd, and is required for the full activity of Nkd

Nkd uses a region we have termed "R1S", which includes EFX domain and adjacent regions, to interact with Dsh (Rousset et al., 2002). EFX is the only region conserved between *Drosophila* and mammals; cross species interactions between Nkd^{EFX}/Dsh^{bPDZ} suggest that Nkd/Dsh interaction is ancient (Wharton et al., 2001). Several lines of evidence suggest that Nkd/Dsh interaction is critical for Nkd to antagonize Wnt signaling in *Drosophila* (see chapter 2 and Rousset et al., 2002), and protein binding data suggest that R1S is sufficient and necessary for Nkd/Dsh interaction (Rousset et al., 2002; Waldrop et al., 2006). However, the ultimate test - the *nkd* rescue assay - clearly demonstrated that this region contributes little to Nkd function, although this assay assumes that Nkd^{AR1S} wouldn't interact with Dsh when overexpressed *in vivo* (Waldrop et al., 2006). Another explanation for the rescue potent activity of Nkd^{AR1S} is that there

might be an intermediate protein that bridges Nkd and Dsh. Nonetheless, Nkd lacking R1S region is mostly nuclear, indicating that the R1S region may be required for cytoplasmic localization of Nkd. Therefore, in this region there might be nuclear export signals or binding sites for cytoplasmic proteins. Dsh could be the responsible protein for the cytoplasmic retention of Nkd. However, in the embryo the subcellular distributions of Dsh and Nkd are largely non-overlapping. Nkd may use its R1S region to bind to cytoplasmic proteins other than Dsh (Waldrop et al., 2006). The EFX motif is part of a 91 aa motif conserved between *D. melanogaster* and *D. pseudoobscura*. By examining the interaction between Nkd^{EFX} and Dsh^{bPDZ} in Y2H, several highly conserved residues in EFX are dispensable for the interaction (Rousset et al., 2002; C. -C. Chan and K. A. Wharton, unpublished data), suggesting that other as yet unidentified proteins enforce motif conservation. Therefore, identification of more Nkd-interacting proteins that specifically binds to Nkd R1S region will help to address this question.

6.1.3 The 30 aa motif, most critical for function, is a NLS

The *Drosophila* and mammalian Nkd proteins each have a 30aa motif that is unrelated by sequence alignment. The *Drosophila* Nkd 30aa motif is conserved within insects, and is predicted to form an amphipathic α -helix. Therefore, the 30aa motif is not likely to possess enzymatic activity based on its small size and the predicted simple structure (Waldrop et al., 2006). Perhaps this domain functions as a protein-protein interaction site. All of the known *nkd* alleles that display defective rescue activity encode proteins truncated N-terminal of this motif (Waldrop et al., 2006). Internal deletion of this motif resulted in severely disrupted rescue activity, indicating that it is critical for Nkd function

(Waldrop et al., 2006). Deletion of this region also caused increased cytoplasmic localization of Nkd, and replacement of this motif with a heterologous NLS restored nuclear localization and increased *nkd* rescue activity, indicating this motif may function as a nuclear localization sequence (Waldrop et al., 2006). Substitution of 30aa of the mouse Nkd1 with *Drosophila* 30aa enhanced the nuclear localization of mNkd1 when overexpressed in the salivary gland, suggesting that this motif is a NLS. However, this motif did not interact with any of the Importin- α s by Y2H, indicating the mechanism of nuclear entry mediated by this motif is different than the D6 motif (Chan et al., 2008). My preliminary data suggests that 30aa motif is sufficient and required for interaction with α -Actinin, a cytoskeletal protein that negatively regulates Nkd activity (See Section 5.1). This finding supports the role of the 30aa motif as a possible docking site for protein-protein interactions. It is possible that additional proteins that positively regulate Nkd function also bind to the 30aa motif, and it is possible that discovering more 30aa-binding proteins may reveal the function of this motif. Furthermore, more experiments will be required to discern the relationship between nuclear targeting and α -Actinin binding.

6.1.4 The D6 region, interacting with importin-alpha3, is a second NLS

The D6 region is conserved between *D. melanogaster* and *D. pseudoobscura* (Chan et al., 2008). Neither mosquito nor mammalian Nkds possess sequence similar to the D6 motif. The D6 motif is sufficient and required for Nkd to interact with Importin- α 3. The D6 motif is thought to be a NLS for Nkd because: 1) basic residues characteristic of a NLS

are conserved between Nkd and dHSF (previously described in chapter 4) in similar positions, and were required for Nkd function and nuclear localization (Fang et al., 2001; Chan et al., 2008); 2) D6-GFP was nuclear when transfected into Kc cells, but became ubiquitous when Importin- $\alpha 3$ was depleted by dsRNA treatment targeting *importin-- $\alpha 3$* . Point mutants of the basic residues in D6 also resulted in D6-GFP observed in the cytoplasm and nucleus, possibly through free diffusion through nuclear pore because of the small size (Chan et al., 2008); 3) Full length Nkd-GFP failed to enter the nucleus in salivary gland when *Importin- $\alpha 3$* was knocked down, indicating the necessity of *Importin- $\alpha 3$* for Nkd nuclear entry (Chan et al., 2008). Heterologous substitution of D6 with dHSF-NLS restored the Nkd/Importin- $\alpha 3$ interaction and Nkd nuclear localization, but did not restore Nkd function. It is possible that dHSF-NLS mislocalized Nkd from its normal site of action. The region of Nkd from EFX motif to the 30aa motif, was found to associate with itself in a Y2H assay (C.-C. Chan and K. A. Wharton, unpublished data), although the biological significance of the dimerization is not known. Since dHSF-NLS can also prevent oligomer formation (Zandi et al., 1997), it is also possible that, by replacing D6 with dHSF-NLS and thus potentially prevent the oligomerization, Nkd^{AD6-dHSFNLS} impaired Nkd function. Furthermore, the kinetics of dHSF-NLS-mediated and D6 motif-mediated nuclear import may be completely different such that Nkd^{AD6-dHSFNLS} might not enter the nucleus at the same time as wild type Nkd time even though in confocal imaging showed a high level of Nkd^{AD6-dHSFNLS} in the nucleus. Most notably, the intra-nuclear localization of Nkd-GFP and Nkd^{AD6-dHSFNLS}-GFP in salivary are different (data not shown), suggesting that dHSF-NLS directs Nkd to the incorrect subnuclear-compartments. More detailed biochemical characterization, such as time-lapse

comparison of the localizations between Nkd-GFP and Nkd^{AD6-dHSFNLS}-GFP, might provide further clues about the molecular function of D6 motif.

6.2 Working models of Nkd function

Chapters 2 to 4 demonstrate that Nkd is found in several intracellular compartments, including the membrane (Chan et al., 2007), cytoplasm (Zeng et al., 2000; Waldrop et al., 2006), and the nucleus (Waldrop et al., 2006; Chan et al., 2008), and that the presence of Nkd in each compartment is critical for Nkd function. This observation raises an interesting question: do different pools of Nkd function in different compartments, or does Nkd cycle intracellularly in order to function? Two models for Nkd function have proposed (see Fig 3.8B), and experimental strategies to distinguish the two models are suggested below.

6.2.1 Model1: Separate pools of Nkd proteins antagonize Wingless signaling in different compartments: membrane, cytoplasm, and nucleus.

In this model, separate pools of Nkd function at different sites, with each pool of Nkd functioning independently. Chapter 2 and other papers (Rousset et al., 2002; Wharton et al., 2001) demonstrate that both *Drosophila* and mammalian Nkds targets Dsh in the cytoplasm. Chapter 3 and other papers (Li et al., 2004; Wharton et al., 2001) indicate that the membrane association mediated by N-terminus is a property of Nkd both in *Drosophila* and in mammals. Based on results from chapter 4, the nuclear import complex including Importin- α 3 is involved in the nuclear entry of Nkd. However it is not clear by which mechanism Nkd functions in the nucleus. Several questions arise: Does

Nkd regulate the nucleo-cytoplasmic shuttling of Wg signaling components? Does Nkd target Wnt components that functions in the nucleus? Does Nkd associate with chromatin in Wnt-responsive genes? More investigations of Nkd in the nucleus will be required to answer this question. Nonetheless, model 1 assumes that Nkd need not to circulate in subcellular regions, thus if different forms of Nkd that are exclusively localized to distinct subcellular locations are coexpressed, then one should see a rescued *nkd* embryo. However, if co-expression of these mutant proteins do not rescue, then it supports the hypothesis that cycling between the sites must occur for Nkd to function.

6.2.2 Model 2: Nkd circulates intracellularly among membrane, cytoplasm and nucleus.

The cycling is required for Nkd to inhibit Wingless signaling

In this model, the movement of Nkd between cytoplasm, plasma membrane, and nucleus is required for attenuating Wnt signaling. Model 2 suggests that Nkd functions in a sequential fashion; however the sequence whether it starts from nucleus to the membrane or membrane to the nucleus is not examined in this model. Therefore, when Nkd is completely localized in certain compartments, Nkd fails to function. Due to the labile nature of Nkd proteins it has been difficult to monitor the dynamic intracellular movement of Nkd during embryogenesis. Recent studies have shown that Dsh mediates oligomerization of the Wnt receptor complex in the membrane (Schwarz-Romond et al., 2007; Bilic et al., 2007). *Xenopus* Dsh also possesses NLS required for its activity in a gain-of-function assay (Itoh et al., 2005), although it is not clear whether *Drosophila* Dsh possesses a nuclear function. Dsh itself may be cycling among the membrane, cytoplasm, and nucleus for function, or different pools of Dsh might function

independently to transmit the Wnt signal. If the sole function of Nkd is to target Dsh, one would imagine that Nkd and Dsh colocalization should be observed in several subcellular compartments. However Nkd/Dsh association was only observed in a punctuate fashion in the cytoplasm and rarely in the nucleus, suggesting that only a subset of Nkd targets Dsh. Overexpressed Nkd was capable of relocating Dsh in the salivary gland cytoplasm but not the nucleus (Keith Wharton, unpublished data), however no bulk Dsh movement was observed in the *nkd* mutant embryos when several *nkd* transgenes were overexpressed that encode for Nkd proteins of different intracellular distribution (Waldrop et al, 2006).

6.2.3 Experimental strategies to discern the above two models

To distinguish the above 2 models, one approach would be to analyze the separated and combined activities of multiple *nkd* transgenes that confer different intracellular localization. As shown in chapter 2 and 3, while both Nkd^{ΔN} and Nkd^{Δ30aa} were defective in rescuing *nkd* mutants, mNkd1^{fNf30aa} partially narrowed the En stripe and resulted in weak and moderate class *nkd* cuticles (Chan et al., 2007). The chimeric protein mNkd1^{fNf30aa} contains the *Drosophila* N-terminus and 30aa, and the evolutionarily conserved EFX domain and histidine-rich C-terminus from mouse Nkd1 backbone, indicating that these 4 domains are sufficient for significant *in vivo* Nkd function. In addition, whereas the intracellular distribution of Nkd^{ΔN} is exclusively nuclear, Nkd^{Δ30aa} is mostly cytoplasmic. If Nkd functions in separate pools, then the combination of the two transgenes might significantly increase the rescue ability. On the other hand, if Nkd needs to circulate among different compartments in order to function, then the combined

transgenes should result in nearly no rescue activity, as does the 2 individual transgenes. Nonetheless, if dimerization happens between $\text{Nkd}^{\Delta\text{N}}$ and $\text{Nkd}^{\Delta 30\text{aa}}$, such that a heterodimer of $\text{Nkd}^{\Delta\text{N}}$ and $\text{Nkd}^{\Delta 30\text{aa}}$ may present at separate pools, then one will not be able to distinguish between model 1 and model 2. To rule out the dimerization effect, one will have to characterize the dimerization domain of Nkd, and then make internal deletion constructs of $\text{Nkd}^{\Delta\text{N}}$ and $\text{Nkd}^{\Delta 30\text{aa}}$. Coexpression of $\text{Nkd}^{\Delta\text{N}}$ and $\text{Nkd}^{\Delta 30\text{aa}}$, each without the dimerization motif (if possible), might allow one to distinguish the above 2 models.

6.3 Future directions in unveiling the molecular mechanisms of Nkd function

6.3.1 Focus on the nucleus: by what mechanism does Nkd antagonize Wingless signaling in the nucleus?

Several cytoplasmic negative regulators of Wnt signaling, such as Axin and Apc, have been found to possess NLSs and nuclear export sequences (NESs). The NESs of Apc have been found both in human and *Drosophila* (Henderson, 2000; Neufeld et al., 2000; Rosin-Arbesfeld et al., 2001); the Apc NLS has been found in human, but not in *Drosophila* Apc (Zhang et al., 2000). Despite Apc's cytoplasmic role in participating in the destruction complex to phosphorylate β -catenin for degradation, Apc's NES is responsible for the nuclear export of β -catenin to reduce β -catenin-dependent transcription of Wnt-targets (Henderson, 2000; Neufeld et al., 2000; Rosin-Arbesfeld et al., 2001; Bienz, 2002). Apc also bind to the nuclear transcriptional corepressor, CtBP, to counteract β -catenin-mediated transcription activation of target genes (Sierra et al.,

2006). Similarly, Axin has also been found in the nucleus and promotes the cytoplasmic accumulation of β -catenin (Cong and Varmus, 2004; Wiechens et al., 2004). What functions these negative regulators perform in the nucleus to antagonize Wnt signaling is not known. Whether these proteins associate with β -catenin at the DNA, or function in nuclear trafficking, or by regulating transcription, remain to be answered. *Xenopus* Dsh, the Wnt signal transducer, also possesses a NLS and a NES, both of which are important for gain-of-function activities (Itoh et al., 2005). However, the nuclear function of Dsh remains to be elucidated.

Endogenous Nkd protein is mostly cytoplasmic, although a low level of nuclear staining was observed in the embryo (Waldrop et al., 2006). However, in chapter 2 and 4, evidence indicates that Nkd possesses 2 NLSs, both of which are required for function (Waldrop et al., 2006; Chan et al., 2008). Based on sequence alignment, the vertebrate Dsh NLS is conserved in *Drosophila* (T. Cagatay and K. A. Wharton, unpublished data), an implication that Nkd may target Dsh in the nucleus. Whether Nkd's nuclear function requires Dsh remains to be elucidated. Identifying additional Nkd-binding proteins may help to reveal how Nkd functions. In a candidate approach, Nkd may interact with nuclear components of Wnt signaling, such as Arm or Pan, or regulate the nuclear import process of Wnt players, such as Apc and Arm. It has been shown that Nkd does not associate with Armadillo in Y2H assay (Rousset et al., 2001). However, with more papers revealing more proteins that regulate Wnt signaling in the nucleus, it will be interesting to examine if Nkd associate with these proteins, including Pygo (Kramps et al., 2002; Parker et al., 2002), Legless (Kramps et al., 2002), and Chibby (Takemaru et

al., 2003). Therefore, a systemic examination of physical interactions between Nkd and known Wnt components might provide information about what Nkd does besides targeting Dsh, to antagonize Wnt signaling. I would also suggest a biochemical purification approach to discover the nuclear fraction of Nkd-containing complexes (more discussion in section 6.3.2).

6.3.2 To identify additional Nkd-interacting proteins

Although Y2H screens revealed several Nkd-binding proteins, Y2H may not reveal the critical Nkd-binding proteins because of the nature of this technique. For example, Y2H assumes that any post-translational modification of Nkd, which if exists might be required for partner binding, is conserved between *Drosophila* and yeast. Also, Y2H assumes binary interactions, which might not be true if Nkd needs an intermediate protein to form a complex with a critical protein. Moreover, because of the high percentage of false-positive results, we may never identify the critical Nkd-binding partner if the protein abundance of that partner is too low. Even if the mRNA of the critical protein is abundant in the prey library, we can still miss the protein if the protein is not stable in yeast. Therefore, to discover the nuclear function of Nkd, A biochemical purification of a *bona fide* Nkd-containing complex followed by mass spectrometry seems to be a feasible alternative approach which complements the Y2H screens. Since the focus is to figure out how Nkd may function in the nucleus, one has to consider modifying the purification steps to reveal the nuclear Nkd-containing complex. Some consideration are as follows: 1) The Nkd protein is very labile, possibly due to degradation signals throughout the protein; 2) endogenous Nkd protein is at greater abundance in the

cytoplasm than in the nucleus; and 3) Nkd only functions in the embryo. To circumvent the aforementioned difficulties and to effectively discover Nkd-interacting nuclear proteins some purification steps might need to be employed as follows: 1) increasing the protein stability by deleting the C-terminus; 2) enriching the nuclear fraction; and 3) purifying the Nkd-containing complex from fly embryos instead of cell culture or larval tissues. Based on the above criteria, NIN4-GFP, a truncated Nkd protein that deletes sequence C-terminal of the 30aa motif, seems to be a good candidate for the purification of NIN4-containing complex because it potently rescues *nkd* mutants and accumulates to levels higher than wild type Nkd-GFP in the embryo. Since 30aa is the most critical region, a differential purification to compare NIN4- and NIN4^{Δ30aa}-interacting protein should reveal critical binding partners for Nkd. If needed, a nuclear fractionation can be performed to exclude non-nuclear binding-partners.

6.3.3 Does Nkd associate with chromatin in Wg-signal-dependent target genes?

Shortly after Wnt ligand binds to its receptor complex, the signal is relayed from the cytoplasm to the nucleus. β -catenin accumulates in the cytoplasm and translocates into the nucleus, then binds to TCF, converting TCF from transcriptional repressor to an activator (van Es et al., 2003; Parker et al., 2008). Activation of the Wnt pathway results in histone acetylation - a sign of gene activation (Robyr et al., 2002; Grewal and Moazed, 2003) - at Wnt response elements (WREs) in several target genes (Kioussi et al., 2002; Feng et al., 2003; Sierra et al., 2006). *nkd* and another Wg signal antagonist *notum* (Gerlitz and Basler, 2002; Giraldez et al., 2002) are direct targets of Wg-signaling in *Drosophila*; and their WRE sites have been defined (Fang et al., 2006; Hoffmans et al.,

2005; Li et al., 2007). The *en* genes also have molecularly defined WREs, which resides in the first intron (~300bp), and in a *nkd* mutant the *en-WRE-lacZ* reporter gene showed expanded stripes (Kassis, 1990).

Without further information about how Nkd functions in the nucleus, one possibility is that Nkd regulates Wnt-responsive genes by associating with chromatin. Chromatin immunoprecipitation (ChIP) assays allow one to determine whether Nkd binds to a particular region on the endogenous chromatin of living cells. However, ChIP assay assumes that one knows the specific DNA fragments where Nkd binds, and in general requires a highly specific antibody to recognize the protein in question. In a candidate approach, the *en*, *nkd*, and *notum* WRE sites would be good candidate target sites for Nkd. In chapter 2, Nkd-GFP extracted from embryos can be detected by anti-GFP antibody; hence provides us a good tool to detect Nkd-GFP in ChIP assays. It will be interesting to examine whether Nkd-GFP can be immunoprecipitated in association with chromatin of Wg target genes from *Drosophila* embryos during stage 9-11, when *nkd* is known to function. Moreover, without knowing which DNA regions Nkd may associate with, an unbiased identification of Nkd-regulating WREs will require a DNA microarray following the ChIP assay (ChIP-on-chip) (Sandmann et al., 2006).

Bibliography

- Ahmed, Y., Hayashi, S., Levine, A., and Wieschaus, E. (1998). Regulation of armadillo by a *Drosophila* APC inhibits neuronal apoptosis during retinal development. *Cell* 93, 1171–1182.
- Ahmed, Y., Nouri, A., and Wieschaus, E. (2002). *Drosophila* Apc1 and Apc2 regulate Wingless transduction throughout development. *Development* 129, 1751–1762.
- Alexandre, C., Lecourtois, M., and Vincent, J. (1999). Wingless and Hedgehog pattern *Drosophila* denticle belts by regulating the production of short-range signals. *Development* 126, 5689–5698.
- Akong, K., Grevengoed, E., E., Price, M., H., McCartney, B., M., Hayden, M., A., DeNofrio, J., C., and Peifer, M. (2002). *Drosophila* APC2 and APC1 play overlapping roles in wingless signaling in the embryo and imaginal discs. *Dev Biol.* 250, 91–100.
- Angers, S., Thorpe, C. J., Biechele, T. L., Goldenberg, S. J., Zheng, N. et al., (2006) The KLHL12-Cullin-3 ubiquitin ligase negatively regulates the Wnt- β -catenin pathway by targeting Dishevelled for degradation. *Nat. Cell Biol.* 8, 348–357.
- Aoki, K., and Taketo, M. M. (2007). Adenomatous polyposis coli (APC): a multi-functional tumor suppressor gene. *J Cell Sci* 120, 3327–35.
- Aulehla, A., and Johnson, R., L. (1999). Dynamic expression of lunatic fringe suggests a link between notch signaling and an autonomous cellular oscillator driving somite segmentation. *Dev Bio.* 207, 49–61.
- Aulehla, A., Wehrle, C., Brand-Saberi, B., Kemler, R., Gossler, A., Kanzler, B., Herrmann, B., G. (2003). Wnt3a plays a major role in the segmentation clock controlling somitogenesis. *Dev Cell* 4, 395–406.
- Axelrod, J. D. (2001). Unipolar membrane association of Dishevelled mediates Frizzled planar cell polarity signaling. *Genes Dev* 15, 1182–1187.
- Axelrod, J., D., Matsuno, K., Artavanis-Tsakonas, S., and Perrimon, N. (1996). Interaction between Wingless and Notch signaling pathways mediated by dishevelled. *Science* 271, 1826–1832.
- Axelrod, J. D., Miller, J. R., Shulman, J. M., Moon, R. T. and Perrimon, N. (1998). Differential recruitment of Dishevelled provides signaling specificity in the planar cell polarity and Wingless signaling pathways. *Genes Dev.* 12, 2610–2622.
- Baeg, G.H., Selva, E.M., Goodman, R.M., Dasgupta R., and Perrimon, N. (2004). The Wingless morphogen gradient is established by the cooperative action of frizzled and heparan sulfate proteoglycan receptors. *Dev. Biol.* 276, pp. 89–100.
- Baker, N. E. (1988). Localization of transcripts from the wingless gene in whole *Drosophila* embryos. *Development* 103, 289–98.
- Bartscherer, K., Pelte, N., Ingelfinger, D., and Boutros, M. (2006). Secretion of Wnt ligands requires Evi, a conserved transmembrane protein. *Cell* 125, 523–533.
- Beggs, A., H., Byers, T., J., Knoll, J., H., Boyce, F., M., Bruns, G., A., and Kunkel, L., M. (1992). Cloning and characterization of two human skeletal muscle alpha-actinin genes located on chromosomes 1 and 11. *J Biol Chem.* 267, 9281–9288.
- Behrens, J., Jerchow, B., A., Würtele, M., Grimm, J., Asbrand, C., Wirtz, R., Köhl, M., Wedlich, D., Birchmeier, W. (1998). Functional interaction of an axin homolog, conductin, with beta-catenin, APC, and GSK3beta. *Science* 280, 596–599.
- Bejsovec, A., and Martinez Arias, A. (1991). Roles of wingless in patterning the larval epidermis of *Drosophila*. *Development* 113, 471–85.
- Bejsovec, A., and Wieschaus, E. (1993). Segment polarity gene interactions modulate epidermal patterning in *Drosophila* embryos. *Development* 119, 501–17.
- Bejsovec, A., and Wieschaus, E. (1995). Signaling activities of the *Drosophila* wingless gene are separately mutable and appear to be transduced at the cell surface. *Genetics* 139, 309–320.
- Belenkaya, T., Y., Wu, Y., Tang, X., Zhou, B., Cheng, L., Sharma, Y., V., Yan, D., Selva, E., M., and Lin, X. (2008). The retromer complex influences Wnt secretion by recycling wntless from endosomes to the trans-Golgi network. *Dev Cell* 14, 120–131.
- Ben-Zur, T., Feige, E., Motro, B., and Wides, R. (2000). The mammalian Odz gene family: homologs of a *Drosophila* pair-rule gene with expression implying distinct yet overlapping developmental roles. *Dev Biol.* 217, 107–120.
- Bessho, Y., Sakata, R., Komatsu, S., Shiota, K., Yamada, S., and Kageyama, R. (2001). Dynamic expression and essential functions of Hes7 in somite segmentation. *Genes Dev.* 15, 2642–2647.

- Bienz, M. (2002). The subcellular destinations of APC proteins. *Nat Rev Mol Cell Biol.* 3, 328-338.
- Bienz, M. (2005). β -Catenin: a pivot between cell adhesion and Wnt signalling. *Curr. Biol.* 15, R64-R67.
- Bienz, M., and Clevers, H. (2000). Linking colorectal cancer to Wnt signaling. *Cell* 103, 311-320.
- Bienz, M., and Clevers, H. (2003). Armadillo/beta-catenin signals in the nucleus--proof beyond a reasonable doubt? *Nat Cell Biol.* 5, 179-182.
- Bilic, J., Huang, Y. L., Davidson, G., Zimmermann, T., Cruciat, C. M., Bienz, M., and Niehrs, C. (2007). Wnt induces LRP6 signalosomes and promotes dishevelled-dependent LRP6 phosphorylation. *Science* 316, 1619-22.
- Boutpos, M., and Mlodzik, M. (1999). Dishevelled: at the crossroads of divergent intracellular signaling pathways. *Mech. Dev.* 83, 27-37.
- Brand, A. H., and Perrimon, N. (1993). Targeted gene expression as a means of altering cell fates and generating dominant phenotypes. *Development* 118, 401-15.
- Brembeck, F. H., Rosario M., and Birchmeier, W. (2006). Balancing cell adhesion and Wnt signaling, the key role of β -catenin. *Curr. Opin. Genet. Dev.* 16, pp. 51-59.
- Brook, W. J., and Cohen, S. M. (1996). Antagonistic interactions between wingless and decapentaplegic responsible for dorsal-ventral pattern in the *Drosophila* leg. *Science* 273, 1373-1377.
- Brunner, E., Brunner, D., Fu, W., Hafen E., and Basler, K. (1999). The dominant mutation Glazed is a gain-of-function allele of wingless that, similar to loss of APC, interferes with normal eye development. *Dev. Biol.* 206, 178-188.
- Cadigan, K. M., and Liu, Y. I. (2006). Wnt signaling: complexity at the surface. *J. Cell Sci.* 119, 395-402.
- Cadigan, K. M., and Nusse, R. (1996). wingless signaling in the *Drosophila* eye and embryonic epidermis. *Development* 122, 2801-2812.
- Cadigan, K. M., and Nusse, R. (1997). Wnt signaling: a common theme in animal development. *Genes Dev.* 11, 3286-3305.
- Cadigan, K. M., GROSSNIKLAUS, U., and Gehring, W. J. (1994). Localized expression of sloppy paired protein maintains the polarity of *Drosophila* parasegments. *Genes Dev.* 8, 899-913.
- Cadigan, K. M., Jou, A. D. and Nusse, R. (2002). Wingless blocks bristle formation and morphogenetic furrow progression in the eye through repression of Daughterless. *Development* 129, 3393-3402.
- Campos-Ortega, J. A., and Hartenstein, V. (1985) The embryonic development of *Drosophila melanogaster*. Berlin/Heidelberg/New-York/Tokyo.: Springer-Verlag.
- Capelluto, D. G., Kutateladze, T. G., Habas, R., Finkielstein, C. V., He, X. et al., (2002). The DIX domain targets dishevelled to actin stress fibres and vesicular membranes. *Nature* 419, 726-729.
- Carpén, O., Pallai, P., Staunton, D., E., and Springer, T., A. (1992). Association of intercellular adhesion molecule-1 (ICAM-1) with actin-containing cytoskeleton and alpha-actinin. *J Cell Biol.* 118, 1223-1234.
- Cavallo, R., A., Cox, R., T., Moline, M., M., Roose, J., Polevoy, G., A., Clevers, H., Peifer, M., and Bejsovec, A. (1998). *Drosophila* Tcf and Groucho interact to repress Wingless signalling activity. *Nature* 395, 604-608.
- Chan, C.-C., Zhang, S., Cagatay, T., and Wharton Jr., K. A. (2007). Cell-autonomous, myristyl-independent activity of the *Drosophila* Wnt/Wingless antagonist Naked cuticle (Nkd). *Dev Biol* 311, 538-53.
- Chen, H., J., Lin, C., M., Lin, C., S., Perez-Olle, R., Leung, C., L., and Liem, R., K. (2006). The role of microtubule actin cross-linking factor 1 (MACF1) in the Wnt signaling pathway. *Genes Dev.* 20, 1933-1945.
- Chook, Y. M., and Blobel, G. (2001). Karyopherins and nuclear import. *Curr Opin Struct Biol* 11, 703-15.
- Chou, T. B., Noll, E., and Perrimon, N. (1993). Autosomal P[ovo^{DL}] dominant female-sterile insertions in *Drosophila* and their use in generating germ-line chimeras. *Development* 119, 1359-69.
- Christerson, L., B., Vanderbilt, C., A., and Cobb, M., H. (1999). MEKK1 interacts with alpha-actinin and localizes to stress fibers and focal adhesions. *Cell Motil Cytoskeleton.* 43, 186-198.
- Clark, M., A., and Hirst, B., H. (2002). Expression of junction-associated proteins differentiates mouse intestinal M cells from enterocytes. *Histochem Cell Biol.* 118, 137-147.
- Clemens, J. C., Worby, C. A., Simonson-Leff, N., Muda, M., Maehama, T., Hemmings, B. A., and Dixon, J. E. (2000). Use of double-stranded RNA interference in *Drosophila* cell lines to dissect signal transduction pathways. *Proc Natl Acad Sci U S A* 97, 6499-503.
- Clevers, H. (2006). Wnt/ β -Catenin Signaling in Development and Disease. *Cell* 127, 469-80.

- Cliffe, A., Hamada, F., and Bienz, M. (2003) A role of Dishevelled in relocating Axin to the plasma membrane during wingless signaling. *Curr. Biol.* 13, pp. 960–966.
- Colosimo, P.F., and Tolwinski, N.S. (2006) Wnt, hedgehog and junctional armadillo/ β -catenin establish planar polarity in the *Drosophila* embryo. *PLoS ONE* 1, p. e9.
- Cong, F., Schweizer, L., Chamorro, M., and Varmus, H. (2003). Requirement for a nuclear function of β -catenin in Wnt signaling. *Mol Cell Biol.* 23, 8462–8470.
- Cong, F., and Varmus, H. (2004). Nuclear-cytoplasmic shuttling of Axin regulates subcellular localization of β -catenin. *Proc Natl Acad Sci U S A* 101, 2882–7.
- Cooke, J., and Zeeman, E., C. (1976). A clock and wavefront model for control of the number of repeated structures during animal morphogenesis. *J Theor Biol.* 58, 455–476.
- Coudreuse, D., Y., Roël, G., Betist, M., C., Destree, O., and Korswagen, H., C. (2006). Wnt gradient formation requires retromer function in Wnt-producing cells. *Science* 312, 921–924.
- Couso, J. P., Bate, M., and Martinez-Arias, A. (1993). A wingless-dependent polar coordinate system in *Drosophila* imaginal discs. *Science* 259, 484–489.
- Couso, J. P., Bishop, S. A. and Martinez-Arias, A. (1994). The wingless signalling pathway and the patterning of the wing margin in *Drosophila*. *Development* 120: 621–636.
- Creyghton, M.P., Roel, G., Eichhorn, P.J., Hijmans, E.M., Maurer, I. Destree, O., and Bernards, R. (2005). PR72, a novel regulator of Wnt signaling required for Naked cuticle function. *Genes Dev.* 19, pp. 376–386.
- Creyghton, M. P., Roel, G., Eichhorn, P. J., Vredevel, L. C., Destree, O., et al., (2006). PR130 is a modulator of the Wnt-signaling cascade that counters repression of the antagonist Naked cuticle. *Proc. Natl. Acad. Sci. USA* 103: 5397–5402
- Damen, W. G. (2002). Parasegmental organization of the spider embryo implies that the parasegment is an evolutionary conserved entity in arthropod embryogenesis. *Development* 129, 1239–1250.
- Damen, W. G. (2007). The origin and evolution of segmentation. *Dev Dyn.* 236, 1379–1391.
- Damke, H., Baba, T., Warnock, D.E., and Schmid, S.L. (1994). Induction of mutant dynamin specifically blocks endocytic coated vesicle formation. *J. Cell Biol.* 127, pp. 915–934.
- Dasgupta, R., Kaykas, A., Moon R. T., and Perrimon, N. (2005). Functional genomic analysis of the Wnt-wingless signaling pathway. *Science* 308, 826–833.
- Davidson, G., Wu, W., Shen, J., Bilic, J., Fenger U., et al., (2005). Casein kinase 1 γ couples Wnt receptor activation to cytoplasmic signal transduction. *Nature* 438, 867–872.
- Davis, G. K., and Patel, N. H. (1999). The origin and evolution of segmentation. *Trends Cell Biol.* 9, M68–72.
- Dearden, P., K., and Akam, M. (2001). Early embryo patterning in the grasshopper, *Schistocerca gregaria*: wingless, decapentaplegic and caudal expression. *Development* 128, 3435–3444.
- Dgany, O., and Wides, R., (2002). The *Drosophila* *odz/ten-m* gene encodes a type I, multiply cleaved heterodimeric transmembrane protein. *Biochem J.* 363, 633–643.
- Dierick, H., A., and Bejsovec, A. (1998). Functional analysis of Wingless reveals a link between intercellular ligand transport and dorsal-cell-specific signaling. *Development* 125, 4729–4738.
- Dietzl, G., Chen, D., Schnorrer, F., Su, K. C., Barinova, Y., Fellner, M., Gasser, B., Kinsey, K., Oppel, S., Scheiblaue, S., Couto, A., Marra, V., Keleman, K., and Dickson, B. J. (2007). A genome-wide transgenic RNAi library for conditional gene inactivation in *Drosophila*. *Nature* 448, 151–6.
- DiNardo, S., Kumer, J., M., Theis, J., and O'Farrell, P., H. (1985). Development of embryonic pattern in *D. melanogaster* as revealed by accumulation of the nuclear engrailed protein. *Cell* 43, 59–69.
- DiNardo, S., Sher, E., Heemskerk-Jongens, J., Kassis, J. A., and O'Farrell, P. H. (1988). Two-tiered regulation of spatially patterned engrailed gene expression during *Drosophila* embryogenesis. *Nature* 332, 604–9.
- DiNardo, S., Heemskerk, J., Dougan S., and O'Farrell, P.H. (1994). The making of a maggot: patterning the *Drosophila* embryonic epidermis. *Curr. Opin. Genet. Dev.* 4, pp. 529–534.
- Djinović-Carugo, K., Young, P., Gautel, M., and Saraste, M. (1999). Structure of the α -actinin rod: molecular basis for cross-linking of actin filaments. *Cell* 98, 537–546.
- Dockendorff, T. C., Tang, Z., and Jongens, T. A. (1999). Cloning of karyopherin- $\alpha 3$ from *Drosophila* through its interaction with the nuclear localization sequence of germ cell-less protein. *Biol Chem* 380, 1263–72.

- Dougan, S., and DiNardo, S. (1992). *Drosophila* wingless generates cell type diversity among engrailed expressing cells. *Nature* 360, 347-50.
- Dubois, L., Lecourtis, M., Alexandre, C., Hirst E., and Vincent, J.P. (2001). Regulated endocytic routing modulates wingless signaling in *Drosophila* embryos. *Cell* 105, pp. 613-624.
- Dubrulle, J., McGrew, M., J., and Pourquié, O. (2001). FGF signaling controls somite boundary position and regulates segmentation clock control of spatiotemporal Hox gene activation. *Cell* 106, 219-232.
- Eaton, S. (2008). Retromer retrieves wntless. *Dev Cell* 14, 4-6.
- Fagotto, F., Gluck, U., and Gumbiner, B. M. (1998). Nuclear localization signal-independent and importin/karyopherin-independent nuclear import of β -catenin. *Curr Biol* 8, 181-90.
- Fang, M., Li, J., Blauwkamp, T., Bhamhani, C., Campbell N., and Cadigan, K.M. (2006). C-terminal-binding protein directly activates and represses Wnt transcriptional targets in *Drosophila*. *EMBO J.* 25, pp. 2735-2745.
- Fang, X., Chen, T., Tran, K., and Parker, C. S. (2001). Developmental regulation of the heat shock response by nuclear transport factor karyopherin- α 3. *Development* 128, 3349-58.
- Feng, Y., Lee, N., and Fearon, E., R. (2003). TIP49 regulates beta-catenin-mediated neoplastic transformation and T-cell factor target gene induction via effects on chromatin remodeling. *Cancer Res.* 63, 8726-8734.
- Fietz, M.J., Jacinto, A., Taylor, A.M., Alexandre C., and Ingham, P.W. (1995). Secretion of the amino-terminal fragment of the hedgehog protein is necessary and sufficient for hedgehog signalling in *Drosophila*. *Curr. Biol.* 5, pp. 643-650.
- Flaherty, K.M., Zozulya, S., Stryer, L., and McKay, D.B. (1993). Three-dimensional structure of recoverin, a calcium sensor in vision. *Cell* 75, pp. 709-716.
- Fleming, R., J., Scottgale, T., N., Diederich, R., J., Artavanis-Tsakonas, S. (1990). The gene Serrate encodes a putative EGF-like transmembrane protein essential for proper ectodermal development in *Drosophila melanogaster*. *Genes Dev.* 4, 2188-2201.
- Fornerod, M., Ohno, M., Yoshida, M., and MATTAJ, I. W. (1997). CRM1 is an export receptor for leucine-rich nuclear export signals. *Cell* 90, 1051-1060.
- Forsberg, H., Crozet, F., and Brown, N., A. (1998). Waves of mouse Lunatic fringe expression, in four-hour cycles at two-hour intervals, precede somite boundary formation. *Curr Biol.* 8, 1027-1030.
- Franch-Marro, X., Marchand, O., Piddini, E., Ricardo, S., Alexandre C., and Vincent, J.P. (2005). Glypicans shunt the Wingless signal between local signalling and further transport. *Development* 132, pp. 659-666.
- Franch-Marro, X., Wendler, F., Guidato, S., Griffith, J., Baena-Lopez, A., Itasaki, N., Maurice, M., M., and Vincent, J., P. (2008). Wingless secretion requires endosome-to-Golgi retrieval of Wntless/Evi/Sprinter by the retromer complex. *Nat Cell Biol.* 10, 170-177.
- Freeman, M., (2000). Feedback control of intercellular signalling in development. *Nature* 408, 313-319.
- Friedrich, B., Quensel, C., Sommer, T., Hartmann, E., and Kohler, M. (2006). Nuclear localization signal and protein context both mediate importin α specificity of nuclear import substrates. *Mol Cell Biol* 26, 8697-709.
- Fyrberg, E., Kelly, M., Ball, E., Fyrberg, C., and Reedy, M., C. (1990). Molecular genetics of *Drosophila* alpha-actinin: mutant alleles disrupt Z disc integrity and muscle insertions. *J Cell Biol.* 110, 1999-2011.
- Gat, U., Dasgupta, R., Degenstein, L., and Fuchs, E. (1998). De novo hair follicle morphogenesis and hair tumors in mice expressing a truncated β -catenin in skin. *Cell* 95, 605-614.
- Gerlitz, O., and Basler, K. (2002). Wingful, an extracellular feedback inhibitor of Wingless. *Genes Dev.* 16, 1055-1059.
- Giráldez, A., J., Copley, R., R., and Cohen, S., M. (2002). HSPG modification by the secreted enzyme Notum shapes the Wingless morphogen gradient. *Dev Cell* 2, 667-676.
- Goldfarb, D. S., Corbett, A. H., Mason, D. A., Harreman, M. T., and Adam, S. A. (2004). Importin α : a multipurpose nuclear-transport receptor. *Trends Cell Biol* 14, 505-14.
- Gong, Y., Slee, R., B., Fukai, N., Rawadi, G., Roman-Roman, S. et al. (2001). LDL receptor-related protein 5 (LRP5) affects bone accrual and eye development. *Cell* 107, 513-523.
- Gonzalez, F., Swales, L., Bejsovec, A., Skaer H., and Martinez Arias, A. (1991). Secretion and movement of wingless protein in the epidermis of the *Drosophila* embryo. *Mech. Dev.* 35, pp. 43-54.

- Grant, S., F., Thorleifsson, G., Reynisdottir, I., Benediktsson, R., Manolescu, A., Sainz, J. et al. (2006). Variant of transcription factor 7-like 2 (TCF7L2) gene confers risk of type 2 diabetes. *Nat Genet.* 38, 320-323.
- Grau, Y., and Simpson, P. (1987). The segment polarity gene costal-2 in *Drosophila*. II. The origin of imaginal pattern duplications. *Dev Biol.* 122, 186-200.
- Greaves, S., Sanson, B., White, P., and Vincent, J., P. (1999). A screen for identifying genes interacting with armadillo, the *Drosophila* homolog of beta-catenin. *Genetics* 153, 1753-1766.
- Greco, V., Hannus, M., and Eaton, S. (2001). Argosomes: a potential vehicle for the spread of morphogens through epithelia. *Cell* 106, pp. 633-645.
- Grewal, S., I., and Moazed, D. (2003). Heterochromatin and epigenetic control of gene expression. *Science* 301, 798-802.
- Gritzan, U., Hatini, V., and DiNardo, S. (1999). Mutual antagonism between signals secreted by adjacent wingless and engrailed cells leads to specification of complementary regions of the *Drosophila* parasegment. *Development* 126, 4107-4115.
- Hahn, H., Wojnowski, L., Miller, G., and Zimmer, A. (1999). The patched signaling pathway in tumorigenesis and development: lessons from animal models. *J Mol Med.* 77, 459-468.
- Hamada, F., Tomoyasu, Y., Takatsu, Y., Nakamura, M., Nagai, S., Suzuki, A., Fujita, F., Shibuya, H., Toyoshima, K., Ueno, N., and Akiyama, T. (1999). Negative regulation of Wingless signaling by D-axin, a *Drosophila* homolog of axin. *Science* 283, 1739-42.
- Han, C., Yan, D., Belenkaya, T.Y., and Lin, X. (2005). *Drosophila* glypicans Dally and Dally-like shape the extracellular Wingless morphogen gradient in the wing disc. *Development* 132 pp. 667-679.
- Harreman, M. T., Hodel, M. R., Fanara, P., Hodel, A. E., and Corbett, A. H. (2003). The auto-inhibitory function of importin α is essential in vivo. *J Biol Chem* 278, 5854-63.
- Harris, T. J., and Peifer, M. (2005). Decisions, decisions: β -catenin chooses between adhesion and transcription. *Trends Cell Biol.* 15, 234-237.
- Hatini, V., and DiNardo, S. (2001). Divide and conquer: pattern formation in *Drosophila* embryonic epidermis. *Trends Genet.* 17, pp. 574-579.
- Hatini, V., Bokor, P., Goto-Mandeville R., and Dinardo, S. (2000). Tissue- and stage-specific modulation of Wingless signaling by the segment polarity gene lines. *Genes Dev.* 14, 1364-1376.
- Hays, R., Gibori, G. B., and Bejsovec, A. (1997). Wingless signaling generates pattern through two distinct mechanisms. *Development* 124, 3727-3736.
- He, X., Semenov, M., Tamai, K., and Zeng, X. (2004). LDL receptor-related proteins 5 and 6 in Wnt/beta-catenin signaling: arrows point the way. *Development* 131, 1663-1677.
- Henderson, B., R. (2000). Nuclear-cytoplasmic shuttling of APC regulates beta-catenin subcellular localization and turnover. *Nat Cell Biol.* 2, 653-660.
- Henderson, J., M., Al-Waheeb, S., Weins, A., Dandapani, S., V., and Pollak, M., R. (2008). Mice with altered alpha-actinin-4 expression have distinct morphologic patterns of glomerular disease. *Kidney Int.* 73, 741-750.
- Hidalgo, A., and Ingham, P. (1990). Cell patterning in the *Drosophila* segment: spatial regulation of the segment polarity gene patched. *Development* 110, pp. 291-301.
- Hinz, U., Giebel, B., and Campos-Ortega, J.A. (1994). The basic-helix-loop-helix domain of *Drosophila* lethal of scute protein is sufficient for proneural function and activates neurogenic genes. *Cell* 76, pp. 77-87.
- Hoch, M., and Jackle, H. (1993). Transcriptional regulation and spatial patterning in *Drosophila*. *Curr Opin Genet Dev.* 3, 566-573.
- Hoffmans, R., Städeli, R., and Basler, K. (2005). Pygopus and legless provide essential transcriptional coactivator functions to armadillo/beta-catenin. *Curr Biol.* 15, 1207-1211.
- Holt, R. A., Subramanian, G. M., Halpern, A., Sutton, G. G., Charlab, R., et al., (2002). The genome sequence of the malaria mosquito *Anopheles gambiae*. *Science* 298, 129-149.
- Honda, K., Yamada, T., Endo, R., Ino, Y., Gotoh, M., Tsuda, H., Yamada, Y., Chiba, H., and Hirohashi, S. (1998). Actinin-4, a novel actin-bundling protein associated with cell motility and cancer invasion. *J Cell Biol.* 140, 1383-1393.
- Hooper, J.E., and Scott, M.P. (1989). The *Drosophila* patched gene encodes a putative membrane protein required for segmental patterning. *Cell* 59, pp. 751-765.

- Hooper, J.E., and Scott, M.P. (1992). The molecular genetic basis of positional information in insect segments. *Results Probl Cell Differ.* 18, 1-48.
- Hoppler, S., and Bienz, M. (1995). Two different thresholds of wingless signalling with distinct developmental consequences in the *Drosophila* midgut. *EMBO J.* 14, pp. 5016–5026.
- Hsiung, F., Ramirez-Weber, F., A., Iwaki, D., D., and Kornberg, T., B. (2005). Dependence of *Drosophila* wing imaginal disc cytonemes on Decapentaplegic. *Nature* 437, 560-563.
- Huelsken, J., Vogel, R., Erdmann, B., Cotsarelis, G. and Birchmeier, W. (2001). β -Catenin controls hair follicle morphogenesis and stem cell differentiation in the skin. *Cell* 105, 533–545.
- Hughes, C., L., and Kaufman, T., C. (2002). Hox genes and the evolution of the arthropod body plan. *Evolution and Development* 4, 459-499.
- Hülskamp, M., and Tautz, D. (1991). Gap genes and gradients--the logic behind the gaps. *Bioessays* 13, 261-268.
- Ikeda, S., Kishida, S., Yamamoto, H., Murai, H., Koyama, S., and Kikuchi, A. (1998). Axin, a negative regulator of the Wnt signaling pathway, forms a complex with GSK-3 β and β -catenin and promotes GSK-3 β -dependent phosphorylation of β -catenin. *EMBO J.* 17, 1371-1384.
- Immergluck, K., Lawrence, P.A., and Bienz, M. (1990). Induction across germ layers in *Drosophila* mediated by a genetic cascade. *Cell* 62, pp. 261–268.
- Ingham, P. W., (1988). The molecular genetics of embryonic pattern formation in *Drosophila*. *Nature* 335, 25–34.
- Ingham, P., W., and McMahon, A., P. (2001). Hedgehog signaling in animal development: paradigms and principles. *Genes Dev.* 15, 3059-3087.
- Ingham, P., W., and Nakano, Y. (1989). Cell Patterning and Segment Polarity Genes in *Drosophila*. *Development, Growth & Differentiation* 32, 563-574.
- Ishikawa, A., Kitajima, S., Takahashi, Y., Kokubo, H., Kanno, J., et al., (2004). Mouse Nkd1, a Wnt antagonist, exhibits oscillatory gene expression in the PSM under the control of Notch signaling. *Mech. Dev.* 121, 1443–1453.
- Itoh, K., Brott, B. K., Bae, G. U., Ratcliffe, M. J., and Sokol, S. Y. (2005). Nuclear localization is required for Dishevelled function in Wnt/ β -catenin signaling. *J Biol* 4, 3.
- Itoh, K., Krupnik, V., E., and Sokol, S., Y. (1998). Axis determination in *Xenopus* involves biochemical interactions of axin, glycogen synthase kinase 3 and β -catenin. *Curr Biol.* 8, 591-594.
- Jiang, J., and Struhl, G. (1998). Regulation of the Hedgehog and Wingless signalling pathways by the F-box/WD40-repeat protein Slimb. *Nature* 391, 493-496.
- Jouve, C., Palmeirim, I., Henrique, D., Beckers, J., Gossler, A., Ish-Horowicz, D., and Pourquié, O. (2000). Notch signalling is required for cyclic expression of the hairy-like gene HES1 in the presomitic mesoderm. *Development* 127, 1421-1429.
- Jürgens, G., Wieschaus, E., Nüsslein-Volhard, C., and Kluding, H. (1984). Mutations affecting the pattern of the larval cuticle in *Drosophila melanogaster*. II. Zygotic loci on the third chromosome. *Wilhelm Roux Arch. Dev. Biol.* 193, 283-295.
- Kalderon, D., Roberts, B. L., Richardson, W. D., and Smith, A. E. (1984). A short amino acid sequence able to specify nuclear location. *Cell* 39, 499-509.
- Kamps, M.P., Buss J.E., and Sefton, B.M. (1985). Mutation of NH₂-terminal glycine of p60src prevents both myristoylation and morphological transformation. *Proc. Natl. Acad. Sci. U. S. A.* 82, pp. 4625–4628.
- Kassis, J., A. (1990). Spatial and temporal control elements of the *Drosophila* engrailed gene. *Genes Dev.* 4, 433-443.
- Kato, M., Sasaki, T., Ohya, T., Nakanishi, H., Nishioka, H., Imamura, M., and Takai, Y. (1996). Physical and functional interaction of rabphilin-3A with α -actinin. *J Biol Chem.* 271, 31775-31778.
- Katoh, M. (2001). Molecular cloning, gene structure, and expression analyses of NKD1 and NKD2. *Int J Oncol* 19, 963-9.
- Kim, J., W., Kim, M., J., Kim, K., J., Yun, H., J., Chae, J., S., Hwang, S., G., Chang, T., S., Park, H., S., Lee, K., W., Han, P., L., Cho, S., G., Kim, T., W., Choi, E., J. (2005). Notch interferes with the scaffold function of JNK-interacting protein 1 to inhibit the JNK signaling pathway. *Proc Natl Acad Sci U S A.* 102, 14308-14313.
- Kimelman, D., and Xu, W. (2006). β -catenin destruction complex: insights and questions from a structural perspective. *Oncogene* 25, 7482-7491.

- Kioussi, C., Briata, P., Baek, S., H., Rose, D., W., Hamblet, N., S., Herman, T., et al. (2002). Identification of a Wnt/Dvl/beta-Catenin --> Pitx2 pathway mediating cell-type-specific proliferation during development. *Cell* 111, 673-685.
- Kirkpatrick, C.A., Dimitroff, B.D., Rawson, J.M., and Selleck, S.B. (2004). Spatial regulation of Wingless morphogen distribution and signaling by Dally-like protein. *Dev. Cell* 7, pp. 513-523.
- Kléber, M., and Sommer, L. (2004). Wnt signaling and the regulation of stem cell function. *Curr Opin Cell Biol.* 16, 681-687.
- Klingensmith, J., and Nusse, R. (1994). Signaling by wingless in *Drosophila*. *Dev. Biol.* 166, pp. 396-414.
- Knudsen, K., A., Soler, A., P., Johnson, K., R., and Wheelock, M., J. (1995). Interaction of alpha-actinin with the cadherin/catenin cell-cell adhesion complex via alpha-catenin. *J Cell Biol.* 130, 67-77.
- Kornberg, T. (1981). Compartments in the abdomen of *Drosophila* and the role of the engrailed locus. *Dev Biol.* 86, 363-372.
- Kornberg, T., B., and Tabata, T. (1993). Segmentation of the *Drosophila* embryo. *Curr Opin Genet Dev.* 3, 585-594.
- Kramps, T., Peter, O., Brunner, E., Nellen, D., Froesch, B., Chatterjee, S., Murone, M., Züllig, S., Basler, K. (2002). Wnt/wingless signaling requires BCL9/legless-mediated recruitment of pygopus to the nuclear beta-catenin-TCF complex. *Cell* 109, 47-60.
- Kreuger, J., Perez, L., Giraldez, A., J., and Cohen, S., M. (2004). Opposing activities of Dally-like glypican at high and low levels of Wingless morphogen activity. *Dev Cell* 7, 503-512.
- Krishnan, V., Bryant, H., U., and Macdougald, O., A. (2006). Regulation of bone mass by Wnt signaling. *J. Clin Invest.* 116, 1202-1209.
- Kussel, P., and Frasch, M. (1995). Pendulin, a *Drosophila* protein with cell cycle-dependent nuclear localization, is required for normal cell proliferation. *J Cell Biol* 129, 1491-507.
- Lander, A.D. (2007). Morpheus unbound: reimagining the morphogen gradient. *Cell* 128, pp. 245-256.
- Lander, A.D., Nie, Q., and Wan, F.Y. (2002). Do morphogen gradients arise by diffusion?. *Dev. Cell* 2, pp. 785-796.
- Lange, A., Mills, R. E., Lange, C. J., Stewart, M., Devine, S. E., and Corbett, A. H. (2007). Classical nuclear localization signals: definition, function, and interaction with importin α . *J Biol Chem* 282, 5101-5.
- Larsen, C. W., Hirst, E., Alexandre, C., and Vincent, J. P. (2003). Segment boundary formation in *Drosophila* embryos. *Development* 130, 5625-5635.
- Lazarides, E., and Burridge, K. (1975). Alpha-actinin: immunofluorescent localization of a muscle structural protein in nonmuscle cells. *Cell* 6, 289-298.
- Lee, J. J., von Kessler, D. P., Parks, S., and Beachy, P. A. (1992). Secretion and localized transcription suggest a role in positional signaling for products of the segmentation gene hedgehog. *Cell* 71, 33-50.
- Lee, S., and Kolodziej, P., A. (2002). The plakin Short Stop and the RhoA GTPase are required for E-cadherin-dependent apical surface remodeling during tracheal tube fusion. *Development* 129, 1509-1520.
- Li, C., Franklin, J.L., Graves-Deal, R., Jerome, W.G., Cao, Z., and Coffey, R.J. (2004). Myristoylated Naked2 escorts transforming growth factor alpha to the basolateral plasma membrane of polarized epithelial cells. *Proc. Natl. Acad. Sci. U. S. A.* 101, pp. 5571-5576.
- Li, J., Sutter, C., Parker, D., S., Blauwkamp, T., Fang, M., and Cadigan, K., M. (2007). CBP/p300 are bimodal regulators of Wnt signaling. *EMBO J.* 26, 2284-2294.
- Li, Q., Ishikawa, T. O., Miyoshi, H., Oshima M., and Taketo, M. M. (2005). A targeted mutation of Nkd1 impairs mouse spermatogenesis. *J. Biol. Chem.* 280, 2831-2839.
- Lin, H. V., Rogulja, A., and Cadigan, K. M. (2004). Wingless eliminates ommatidia from the edge of the developing eye through activation of apoptosis. *Development* 131, 2409-2418.
- Lin, X., and Perrimon, N. (1999). Dally cooperates with *Drosophila* Frizzled 2 to transduce Wingless signalling. *Nature* 400, 281-284.
- Lippai, M., Tirian, L., Boros, I., Mihaly, J., Erdelyi, M., Beleczi, I., Mathe, E., Posfai, J., Nagy, A., Udvardy, A., Paraskeva, E., Gorlich, D., and Szabad, J. (2000). The Ketel gene encodes a *Drosophila* homologue of importin- β . *Genetics* 156, 1889-900.
- Liu, H., Fergusson, M., M., Castilho, R., M., Liu, J., Cao, L., Chen, J., Malide, D., Rovira, I., I., Schimel, D., Kuo, C., J., Gutkind, J., S., Hwang, P., M., Finkel, T. (2007). Augmented Wnt signaling in a mammalian model of accelerated aging. *Science* 317, 803-806.

- Liu, F., Virshup, D., M., Nairn, A., C., and Greengard, P. (2002). Mechanism of regulation of casein kinase I activity by group I metabotropic glutamate receptors. *J Biol Chem.* 277, 45393-45399.
- Logan, C. Y., and Nusse, R. (2004). The Wnt signaling pathway in development and disease. *Annu. Rev. Cell Dev. Biol.* 20, 781-810.
- MacArthur, D., G., and North, K., N. (2004). A gene for speed? The evolution and function of alpha-actinin-3. *Bioessays* 26, 786-795.
- MacArthur, D., G., Seto, J., T., Chan, S., Quinlan, K., G., Raftery, J., M., Turner, N., Nicholson, M., D., Kee, A., J., Hardeman, E., C., Gunning, P., W., Cooney, G., J., Head, S., I., Yang, N., North, K., N. (2008). An Actn3 knockout mouse provides mechanistic insights into the association between {alpha}-actinin-3 deficiency and human athletic performance. *Hum Mol Genet.* [Epub ahead of print]
- Maderspacher, F., Bucher, G., and Klingler, M. (1998). Pair-rule and gap gene mutants in the flour beetle *Tribolium castaneum*. *Dev Genes Evol.* 208, 558-568.
- Malbon, C. C., and Wang, H. Y. (2006). Dishevelled: a mobile scaffold catalyzing development. *Curr. Top. Dev. Biol.* 72, 153-166.
- Mann, R., K., and Beachy, P., A. (2004). Novel lipid modifications of secreted protein signals. *Annu Rev Biochem.* 73, 891-923.
- Mao, J., Wang, J., Liu, B., Pan, W., Farr, G., H., Flynn, C., Yuan, H., Takada, S., Kimelman, D., Li, L., and Wu, D. (2001). Low-density lipoprotein receptor-related protein-5 binds to Axin and regulates the canonical Wnt signaling pathway. *Mol Cell* 7, 801-809.
- Martinez Arias, A., (1993). Development and patterning of the larval epidermis of *Drosophila*, pp. 517-608 in *The Development of Drosophila melanogaster*, edited by A. MARTINEZ ARIAS and M. BATE. Cold Spring Harbor Laboratory Press, Plainview, NY.
- Martinez Arias, A. (2003). Wnts as morphogens? The view from the wing of *Drosophila*. *Nat. Rev., Mol. Cell Biol.* 4, pp. 321-325.
- Martinez Arias, A., Baker, N. E., and Ingham, P. W. (1988). Role of segment polarity genes in the definition and maintenance of cell states in the *Drosophila* embryo. *Development* 103, 157-70.
- Martinez-Arias, A., and Lawrence, P., A. (1985). Parasegments and compartments in the *Drosophila* embryo. *Nature* 313, 639-642.
- Mason, D. A., Fleming, R. J., and Goldfarb, D. S. (2002). *Drosophila melanogaster* importin $\alpha 1$ and $\alpha 3$ can replace importin $\alpha 2$ during spermatogenesis but not oogenesis. *Genetics* 161, 157-70.
- Mason, D. A., Mathe, E., Fleming, R. J., and Goldfarb, D. S. (2003). The *Drosophila melanogaster* importin $\alpha 3$ locus encodes an essential gene required for the development of both larval and adult tissues. *Genetics* 165, 1943-58.
- Mathe, E., Bates, H., Huikeshoven, H., Deak, P., Glover, D. M., and Cotterill, S. (2000). Importin- $\alpha 3$ is required at multiple stages of *Drosophila* development and has a role in the completion of oogenesis. *Dev Biol* 223, 307-22.
- Mathew, D., Ataman, B., Chen, J., Zhang, Y., Cumberledge, S., et al., (2005). Wingless signaling at synapses is through cleavage and nuclear import of receptor DFrizzled2. *Science* 310, 1344-1347.
- McCartney, B. M., Dierick, H. A., Kirkpatrick, C., Moline, M. M., Baas, A., et al., (1999). *Drosophila* APC2 is a cytoskeletally-associated protein that regulates wingless signaling in the embryonic epidermis. *J. Cell Biol.* 146, 1303-1318.
- Millar, S. E., Willert, K., Salinas, P. C., Roelink, H., Nusse, R., et al., (1999). WNT signaling in the control of hair growth and structure. *Dev. Biol.* 207, 133-149.
- Miura, G., I., and Treisman, J., E. (2006). Lipid modification of secreted signaling proteins. *Cell Cycle* 5, 1184-1188.
- Mohler, J. (1988). Requirements for hedgehog, a segmental polarity gene, in patterning larval and adult cuticle of *Drosophila*. *Genetics* 120, 1061-1072.
- Molenaar, M., van de Wetering, M., Oosterwegel, M., Peterson-Maduro, J., Godsave, S., Korinek, V., Roose, J., Destree, O., and Clevers, H. (1996). XTcf-3 transcription factor mediates β -catenin-induced axis formation in *Xenopus* embryos. *Cell* 86, pp. 391-399.
- Moline, M.M., Southern, C., and Bejsovec, A. (1999). Directionality of wingless protein transport influences epidermal patterning in the *Drosophila* embryo. *Development* 126, pp. 4375-4384.
- Moon, R., T., Bowerman, B., Boutros, M., and Perrimon, N. (2002). The promise and perils of Wnt signaling through beta-catenin. *Science* 296, 1644-1646.

- Moon, R. T., Kohn, A. D., De Ferrari, G. V., and Kaykas, A. (2004). WNT and β -catenin signalling: diseases and therapies. *Nat. Rev. Genet.* 5, 691–701.
- Nakano, Y., Guerrero, I., Hidalgo, A., Taylor, A., Whittle, J.R., and Ingham, P.W. (1989). A protein with several possible membrane-spanning domains encoded by the *Drosophila* segment polarity gene *patched*. *Nature* 341, pp. 508–513.
- Nakaya, M. A., Biris, K., Tsukiyama, T., Jaime, S., Rawls J. A. et al., (2005). Wnt3a links left-right determination with segmentation and anteroposterior axis elongation. *Development* 132, 5425–5436.
- Neufeld, K., L., Nix, D., A., Bogerd, H., Kang, Y., Beckerle, M., C., Cullen, B., R., White, R., L. (2000). Adenomatous polyposis coli protein contains two nuclear export signals and shuttles between the nucleus and cytoplasm. *Proc Natl Acad Sci U S A.* 97, 12085–12090.
- Neumann, C., J., and Cohen, S., M. (1996). *Sternopleural* is a regulatory mutation of *wingless* with both dominant and recessive effects on larval development of *Drosophila melanogaster*. *Genetics* 142, 1147–1155.
- Noordermeer, J., Johnston, P., Rijsewijk, F., Nusse, R., and Lawrence, P.A. (1992). The consequences of ubiquitous expression of the *wingless* gene in the *Drosophila* embryo. *Development* 116, pp. 711–719.
- Noordermeer, J., Klingensmith, J., Perrimon, N., and Nusse, R. (1994). *dishevelled* and *armadillo* act in the *wingless* signalling pathway in *Drosophila*. *Nature* 367, 80–83.
- Nusse, R., Samos, C., H., Brink, M., Willert, K., Cadigan, K., M., Wodarz, A., Fish, M., and Rulifson, E. (1997). Cell culture and whole animal approaches to understanding signaling by Wnt proteins in *Drosophila*. *Cold Spring Harb Symp Quant Biol.* 62, 185–190.
- Nusse, R., and Varmus, H. E. (1982). Many tumors induced by the mouse mammary tumor virus contain a provirus integrated in the same region of the host genome. *Cell* 31, 99–109.
- Nüsslein-Volhard, C., and Wieschaus, E. (1980). Mutations affecting segment number and polarity in *Drosophila*. *Nature* 287, pp. 795–801.
- O'Keefe, L., Dougan, S., T., Gabay, L., Raz, E., Shilo, B., Z., and DiNardo, S. (1997). *Spitz* and *Wingless*, emanating from distinct borders, cooperate to establish cell fate across the *Engrailed* domain in the *Drosophila* epidermis. *Development* 124, 4837–4845.
- Oppenheimer, D., I., MacNicol, A., M., and Patel, N., H. (1999). Functional conservation of the *wingless-engrailed* interaction as shown by a widely applicable baculovirus misexpression system. *Curr Biol.* 9, 1288–1296.
- Orenic, T., Chidsey, J., and Holmgren, R. (1987). *Cell* and *cubitus interruptus* dominant: two segment polarity genes on the fourth chromosome in *Drosophila*. *Dev Biol.* 124, 50–56.
- Ossareh-Nazari, B., Bachelierie, F., and dargemont, C. (1997). Evidence for a role of CRM1 in signal-mediated nuclear protein export. *Science* 278, 141–144.
- Otey, C., A., and Carpen, O. (2004). α -actinin revisited: a fresh look at an old player. *Cell Motil Cytoskeleton.* 58, 104–111.
- Otey, C., A., Pavalko, F., M., and Burrridge, K. (1990). An interaction between α -actinin and the β 1 integrin subunit in vitro. *J Cell Biol.* 111, 721–729.
- Pai, L. M., Orsulic, S., Bejsovec, A., and Peifer, M. (1997). Negative regulation of *Armado*, a *Wingless* effector in *Drosophila*. *Development* 124, 2255–66.
- Panáková, D., Sprong, H., Marois, E., Thiele, C., and Eaton, S. (2005). Lipoprotein particles are required for *Hedgehog* and *Wingless* signalling. *Nature* 435, 58–65.
- Pankratz, M.J., and Jaekle, H. (1993). Blastoderm segmentation. *Bate, Martinez Arias, 1993* : 467--516.
- Parker, D., S., Jemison, J., and Cadigan, K., M. (2002). *Pygopus*, a nuclear PHD-finger protein required for *Wingless* signaling in *Drosophila*. *Development* 129, 2565–2576.
- Parker, D., S., Ni, Y., Y., Chang, J., L., Li, J., and Cadigan, K., M. (2008). *Wingless* signaling induces widespread chromatin remodeling of target Loci. *Mol Cell Biol.* 28, 1815–1828.
- Patel, N. H., Martin-Blanco, E., Coleman, K. G., Poole, S. J., Ellis, M. C., et al., (1989). Expression of *engrailed* proteins in arthropods, annelids, and chordates. *Cell* 58, 955–968.
- Payre, F., Vincent, A., and Carreno, S. (1999). *ovo/svb* integrates *Wingless* and *DER* pathways to control epidermis differentiation. *Nature* 400, pp. 271–275.
- Pazdera, T. M., Janardhan, P., and Minden, J. S. (1998). Patterned epidermal cell death in wild-type and segment polarity mutant *Drosophila* embryos. *Development* 125, 3427–36.

- Peel, A. D., Chipman, A. D., Akam, M., (2005). Arthropod segmentation: beyond the *Drosophila* paradigm. *Nat Rev Genet.* 6, 905-916.
- Peifer, M., Berg, S., and Reynolds, A. B. (1994). A repeating amino acid motif shared by proteins with diverse cellular roles. *Cell* 76, 789-91.
- Peifer, M., and Polakis, P. (2000). Wnt signaling in oncogenesis and embryogenesis--a look outside the nucleus. *Science* 287, 1606-1609.
- Perrimon, N., Engstrom, L., and Mahowald, A., P. (1985). Developmental genetics of the 2C-D region of the *Drosophila* X chromosome. *Genetics*. 111, 23-41.
- Perrimon, N., Engstrom, L., and Mahowald, A., P. (1989). Zygotic lethals with specific maternal effect phenotypes in *Drosophila melanogaster*. I. Loci on the X chromosome. *Genetics* 121, 333-352.
- Perrimon, N., Mahowald, A., P. (1987). Multiple functions of segment polarity genes in *Drosophila*. *Dev Biol.*, 119, 587-600.
- Perrimon, N., and Smouse, D. (1989). Multiple functions of a *Drosophila* homeotic gene, *zeste-white 3*, during segmentation and neurogenesis. *Dev Biol.* 135, 287-305.
- Peters, J. M., McKay, R. M., McKay J. P., and Graff, J. M. (1999). Casein kinase I transduces Wnt signals. *Nature* 401, 345-350.
- Pfeiffer, S., Alexandre, C., Calleja, M., and Vincent, J.P. (2000). The progeny of wingless-expressing cells deliver the signal at a distance in *Drosophila* embryos. *Curr. Biol.* 10, pp. 321-324.
- Pinson, K., I., Brennan, J., Monkley, S., Avery, B., J., and Skarnes, W., C. (2000). An LDL-receptor-related protein mediates Wnt signalling in mice. *Nature* 407, 535-538.
- Polakis P. (2000). Wnt signaling and cancer. *Genes Dev.* 14, 1837-1851.
- Polakis, P. (2007). The many ways of Wnt in cancer. *Curr Opin Genet Dev.* 17, 45-51.
- Port, F., Kuster, M., Herr, P., Furger, E., Bänziger, C., Hausmann, G., Basler, K. (2008). Wingless secretion promotes and requires retromer-dependent cycling of Wntless. *Nat Cell Biol.* 10, 178-185.
- Pourquié, O. (1999). Notch around the clock. *Curr Opin Genet Dev.* 9, 559-565.
- Pourquié, O. (2001). Vertebrate somitogenesis. *Annu Rev Cell Dev Biol.* 17, 311-350.
- Price, M.H., Roberts, D.M., McCartney, B.M., Jezuit, E., and Peifer, M. (2006). Cytoskeletal dynamics and cell signaling during planar polarity establishment in the *Drosophila* embryonic denticle. *J. Cell Sci.* 119, pp. 403-415.
- Ramain, P., Khechumian, K., Seugnet, L., Arbogast, N., Ackermann, C., Heitzler, P. (2001). Novel Notch alleles reveal a Deltex-dependent pathway repressing neural fate. *Curr Biol.* 11, 1729-1738.
- Ramírez-Weber, F., A., and Kornberg, T., B. (1999). Cytonemes: cellular processes that project to the principal signaling center in *Drosophila* imaginal discs. *Cell* 97, 599-607.
- Resh, M.D. (2004). Membrane targeting of lipid modified signal transduction proteins. *Subcell. Biochem.* 37, pp. 217-232.
- Reya, T., and Clevers, H. (2005). Wnt signalling in stem cells and cancer. *Nature* 434, 843-850.
- Richards, S., Liu, Y., Bettencourt, B. R., Hradecky, P., Letovsky, S., Nielsen, R., et al. (2005). Comparative genome sequencing of *Drosophila pseudoobscura*: chromosomal, gene, and cis-element evolution. *Genome Res* 15, 1-18.
- Riggleman, B., Schedl, P., and Wieschaus, E. (1990). Spatial expression of the *Drosophila* segment polarity gene *armadillo* is posttranscriptionally regulated by wingless. *Cell* 63, 549-60.
- Rives, A.F., Rochlin, K.M., Wehrli, M., Schwartz, S.L., and DiNardo, S. (2006). Endocytic trafficking of Wingless and its receptors, Arrow and DFrizzled-2, in the *Drosophila* wing. *Dev. Biol.* 293 pp. 268-283.
- Robyr, D., Suka, Y., Xenarios, I., Kurdistani, S., K., Wang, A., Suka, N., and Grunstein, M. (2002). Microarray deacetylation maps determine genome-wide functions for yeast histone deacetylases. *Cell* 109, 437-446.
- Rodríguez, I. (2004). The dachsous gene, a member of the cadherin family, is required for Wg-dependent pattern formation in the *Drosophila* wing disc. *Development* 131, 3195-3206.
- Röper, K., and Brown, N., H. (2003). Maintaining epithelial integrity: a function for gigantic spectraplakins isoforms in adherens junctions. *J Cell Biol.* 162, 1305-1315.
- Röper, K., Gregory, S., L., and Brown, N., H. (2002). The 'spectraplakins': cytoskeletal giants with characteristics of both spectrin and plakin families. *J Cell Sci.* 115, 4215-4225.
- Rosin-Arbesfeld, R., Ihrke, G., and Bienz, M. (2001). Actin-dependent membrane association of the APC tumour suppressor in polarized mammalian epithelial cells. *EMBO J.* 20, 5929-5939.

- Rosin-Arbesfeld, R., Townsley, F. and Bienz, M. (2000). The APC tumour suppressor has a nuclear export function. *Nature* 406, 1009–1012.
- Roullet, E., M., Fyrberg, C., and Fyrberg, E. (1992). Perturbations of *Drosophila* alpha-actinin cause muscle paralysis, weakness, and atrophy but do not confer obvious nonmuscle phenotypes. *J Cell Biol.* 116, 911–922.
- Rousset, R., Mack, J. A., Wharton, K. A., Jr., Axelrod, J. D., Cadigan, K. M., Fish, M. P., Nusse, R., and Scott, M. P. (2001). naked cuticle targets dishevelled to antagonize Wnt signal transduction. *Genes Dev* 15, 658–71.
- Rousset, R., Wharton, K. A., Jr., Zimmermann, G., and Scott, M. P. (2002). Zinc-dependent interaction between dishevelled and the *Drosophila* Wnt antagonist Naked cuticle. *J Biol Chem* 277, 49019–26.
- Saga, Y., and Takeda, H. (2001). The making of the somite: molecular events in vertebrate segmentation. *Nat Rev Genet.* 2, 835–845.
- Sampedro, J., Johnston, P., and Lawrence, P.A. (1993). A role for wingless in the segmental gradient of *Drosophila*?. *Development* 117, pp. 677–687.
- Sandmann, T., Jakobsen, J., S., Furlong, E., E. (2006). ChIP-on-chip protocol for genome-wide analysis of transcription factor binding in *Drosophila melanogaster* embryos. *Nat Protoc.* 1, 2839–2855.
- Sanson, B. (2001). Generating patterns from fields of cells. Examples from *Drosophila* segmentation. *EMBO Rep.* 2, 1083–1088.
- Sanson, B., Alexandre, C., Fascetti, N., and Vincent, J.P. (1999). Engrailed and hedgehog make the range of Wingless asymmetric in *Drosophila* embryos. *Cell* 98, pp. 207–216.
- Sawada, A., Shinya, M., Jiang, Y., J., Kawakami, A., Kuroiwa, A., and Takeda, H. (2001). Fgf/MAPK signalling is a crucial positional cue in somite boundary formation. *Development* 128, 4873–4880.
- Schneider, S., Steinbeisser, H., Wagra, R. M., and Hausen, P. (1996). β -Catenin translocation into nuclei demarcates the dorsalizing centers in frog and fish embryos. *Mech. Dev.* 57, 191–198.
- Schoopmeier, M., and Damen, W. G. M. (2005). Suppressor of Hairless and Presenilin phenotypes imply involvement of canonical Notch-signaling in segmentation of the spider *Cupiennius salei*. *Dev. Biol.* 280, 211–224.
- Schwarz-Romond, T., Merrifield, C., Nichols, B. J., and Bienz, M. (2005). The Wnt signalling effector Dishevelled forms dynamic protein assemblies rather than stable associations with cytoplasmic vesicles. *J. Cell Sci.* 118, 5269–5277.
- Schwarz-Romond, T., Fiedler, M., Shibata, N., Butler, P.J., Kikuchi, A., Higuchi, Y., and Bienz, M. (2007). The DIX domain of Dishevelled confers Wnt signaling by dynamic polymerization. *Nat. Struct. Mol. Biol.* 14, pp. 484–492.
- Shibasaki, F., Fukami, K., Fukui, Y., and Takenawa, T. (1994). Phosphatidylinositol 3-kinase binds to alpha-actinin through the p85 subunit. *Biochem J.* 302, 551–557.
- Shirras, A.D., and Couso, J.P. (1996). Cell fates in the adult abdomen of *Drosophila* are determined by wingless during pupal development. *Dev. Biol.* 175, pp. 24–36.
- Sierra, J., Yoshida, T., Joazeiro, C. A., and Jones, K. A. (2006). The APC tumor suppressor counteracts β -catenin activation and H3K4 methylation at Wnt target genes. *Genes Dev* 20, 586–600.
- Siegfried, E., Chou, T. B., and Perrimon, N. (1992). wingless signaling acts through zeste-white 3, the *Drosophila* homolog of glycogen synthase kinase-3, to regulate engrailed and establish cell fate. *Cell* 71, 1167–1179.
- Siegfried, E., Wilder, E. L., and Perrimon, N. (1994). Components of wingless signalling in *Drosophila*. *Nature* 367, 76–80.
- Simons, M., Gloy, J., Ganner, A., Bullerkotte, A., Bashkurov M. et al., (2005). Inversin, the gene product mutated in nephronophthisis type II, functions as a molecular switch between Wnt signaling pathways. *Nat. Genet.* 37, 537–543.
- Simon, M.A., Drees, B., Kornberg, T., and Bishop, J.M. (1985). The nucleotide sequence and the tissue-specific expression of *Drosophila* c-src. *Cell* 42, pp. 831–840.
- Smalley, M. J., Signoret, N., Robertson, D., Tilley, A., Hann, A. et al., (2005). Dishevelled (Dvl-2) activates canonical Wnt signalling in the absence of cytoplasmic puncta. *J. Cell Sci.* 118, 5279–5289.
- Smith, U. (2007). TCF7L2 and type 2 diabetes--we WNT to know. *Diabetologia.* 50, 5–7.
- Smolich, B.D., McMahon, J.A., McMahon A.P., and Papkoff, J. (1993). Wnt family proteins are secreted and associated with the cell surface. *Mol. Biol. Cell* 4, pp. 1267–1275.

- Stolletwerk, A., Schoppmeoer, M., and Damen, W. G. M. (2003) Involvement of Notch and Delta genes in spider segmentation. *Nature* 423, 863-865.
- Strigini, M., and Cohen, S., M. (2000). Wingless gradient formation in the *Drosophila* wing. *Curr Biol.* 10, 293-300.
- Sun, T. Q., Lu, B., Feng, J. J., Reinhard, C., Jan, Y. N. et al., 2001 PAR-1 is a Dishevelled-associated kinase and a positive regulator of Wnt signalling. *Nat. Cell Biol.* 3, 628-636.
- Szűts, D., Freeman, M., and Bienz, M. (1997). Antagonism between EGFR and Wingless signalling in the larval cuticle of *Drosophila*. *Development* 124, 3209-3219.
- Tabata, T., Eaton, S., and Kornberg, T. B. (1992). The *Drosophila* hedgehog gene is expressed specifically in posterior compartment cells and is a target of engrailed regulation. *Genes Dev* 6, 2635-45.
- Takemaru, K., Yamaguchi, S., Lee, Y., S., Zhang, Y., Carthew, R., W., and Moon, R., T. (2003). Chibby, a nuclear beta-catenin-associated antagonist of the Wnt/Wingless pathway. *Nature* 422, 905-909.
- Tamai, K., Semenov, M., Kato, Y., Spokony, R., Liu, C., Katsuyama, Y., Hess, F., Saint-Jeannet, J., P., and He, X. (2000). LDL-receptor-related proteins in Wnt signal transduction. *Nature* 407, 530-535.
- Tanaka, K., Kitagawa, Y., and Kadowaki, T. (2002). *Drosophila* segment polarity gene product porcupine stimulates the posttranslational N-glycosylation of wingless in the endoplasmic reticulum. *J Biol Chem.* 277, 12816-12823.
- Tolwinski, N. S., and Wieschaus, E. (2004). A nuclear function for armadillo/ β -catenin. *PLoS Biol.* 2, E95.
- Tolwinski, N. S., Wehrli M., Rives A., Erdeniz N., Dinardo S. et al., (2003). Wg/Wnt signal can be transmitted through arrow/LRP5,6 and Axin independently of Zw3/Gsk3 β activity. *Dev. Cell* 4, 407-418.
- Tomlinson, A. (2003). Patterning the peripheral retina of the fly: decoding a gradient. *Dev. Cell* 5, 799-809.
- Torok, I., Strand, D., Schmitt, R., Tick, G., Torok, T., Kiss, I., and Mechler, B. M. (1995). The overgrown hematopoietic organs-31 tumor suppressor gene of *Drosophila* encodes an Importin-like protein accumulating in the nucleus at the onset of mitosis. *J Cell Biol* 129, 1473-89.
- Torres, M. A., and Nelson, W. J. (2000). Colocalization and redistribution of dishevelled and actin during Wnt-induced mesenchymal morphogenesis. *J. Cell Biol.* 149, 1433-1442.
- Tsuda, M., Kamimura, K., Nakato, H., Archer, M., Staatz, W., Fox, B., Humphrey, M., Olson, S., Futch, T., Kaluza, V., Siegfried, E., Stam, L., and Selleck, S., B. (1999). The cell-surface proteoglycan Dally regulates Wingless signalling in *Drosophila*. *Nature* 400, 276-280.
- Tuma, P., L., and Hubbard, A., L. (2003). Transcytotic efflux from early endosomes is dependent on cholesterol and glycosphingolipids in polarized hepatic cells. *Mol Biol Cell.* 14, 2689-2705.
- Uematsu, K., Kanazawa S., You, L., He, B., Xu, Z., et al., (2003). Wnt pathway activation in mesothelioma: evidence of Dishevelled overexpression and transcriptional activity of β -catenin. *Cancer Res.* 63, 4547-4551.
- Urban, S., Brown, G., and Freeman, M. (2004). EGF receptor signalling protects smooth-cuticle cells from apoptosis during *Drosophila* ventral epidermis development. *Development* 131, pp. 1835-1845.
- Van de Wetering, M., Cavallo, R., Dooijes, D., van Beest, M., van Es, J., Loureiro, J., Ypma, A., Hursh, D., Jones, T., Bejsovec, A., Peifer, M., Mortin, M., and Clevers, H. (1997). Armadillo coactivates transcription driven by the product of the *Drosophila* segment polarity gene dTCF. *Cell* 88, pp. 789-799.
- Van den Heuvel, M., Nusse, R., Johnston, P., and Lawrence, P.A. (1989). Distribution of the wingless gene product in *Drosophila* embryos: a protein involved in cell-cell communication. *Cell* 59, pp. 739-749.
- van Es, J., H., Barker, N., and Clevers, H. (2003). You Wnt some, you lose some: oncogenes in the Wnt signaling pathway. *Curr Opin Genet Dev.* 13, 28-33.
- Van Raay, T. J., Coffey, R. J., and Solnica-Krezel, L. (2007). Zebrafish Naked1 and Naked2 antagonize both canonical and non-canonical Wnt signaling. *Dev Biol* 309, 151-68.
- Veeman, M. T., Axelrod, J. D., and Moon, R. T. (2003). A second canon. Functions and mechanisms of β -catenin-independent Wnt signaling. *Dev. Cell* 5, 367-377.
- Vincent, J., P., and Dubois, L. (2002). Morphogen transport along epithelia, an integrated trafficking problem. *Dev Cell* 3, 615-623.
- Virel, A., and Backman, L. (2004). Molecular evolution and structure of alpha-actinin. *Mol Biol Evol.* 21, 1024-1031.

- Voellmy, R. (2004). On mechanisms that control heat shock transcription factor activity in metazoan cells. *Cell Stress Chaperones* 9, 122-33.
- Waldrop, S., Chan, C.-C., Cagatay, T., Zhang, S., Rousset, R., Mack, J., Zeng, W., Fish, M., Zhang, M., Amanai, M., and Wharton, K. A., Jr. (2006). An unconventional nuclear localization motif is crucial for function of the *Drosophila* Wnt/wingless antagonist Naked cuticle. *Genetics* 174, 331-48.
- Wallingford, J. B., and Habas, R. (2005). The developmental biology of Dishevelled: an enigmatic protein governing cell fate and cell polarity. *Development* 132, 4421-36.
- Wang, R., and Brattain, M. G. (2007). The maximal size of protein to diffuse through the nuclear pore is larger than 60kDa. *FEBS Lett* 581, 3164-70.
- Wehrli, M., Dougan, S., T., Caldwell, K., O'Keefe, L., Schwartz, S., Vaizel-Ohayon, D., Schejter, E., Tomlinson, A., and DiNardo, S. (2000). arrow encodes an LDL-receptor-related protein essential for Wingless signalling. *Nature* 407, 527-530.
- Weins, A., Schlondorff, J., S., Nakamura, F., Denker, B., M., Hartwig, J., H., Stossel, T., P., Pollak, M., R. (2007). Disease-associated mutant alpha-actinin-4 reveals a mechanism for regulating its F-actin-binding affinity. *Proc Natl Acad Sci U S A*. 104, 16080-16085.
- Weir, M., P., and Kornberg, T. (1985). Patterns of engrailed and fushi tarazu transcripts reveal novel intermediate stages in *Drosophila* segmentation. *Nature* 318, 433-439.
- Wharton Jr., K.A. (2003). Runnin' with the Dvl: proteins that associate with Dsh/Dvl and their significance to Wnt signal transduction. *Dev. Biol.* 253, pp. 1-17.
- Wharton, K. A., Jr., Zimmermann, G., Rousset, R., and Scott, M. P. (2001). Vertebrate proteins related to *Drosophila* Naked Cuticle bind Dishevelled and antagonize Wnt signaling. *Dev Biol* 234, 93-106.
- Wiechens, N., Heinle, K., Englmeier, L., Schohl, A., and Fagotto, F. (2004). Nucleo-cytoplasmic shuttling of Axin, a negative regulator of the Wnt- β -catenin Pathway. *J Biol Chem* 279, 5263-7.
- Wiellette, E.L., and McGinnis, W. (1999). Hox genes differentially regulate Serrate to generate segment-specific structures. *Development* 126, pp. 1985-1995.
- Wieschaus, E., Nusslein-Volhard, C., and Kluding, H. (1984) Krüppel, a gene whose activity is required early in the zygotic genome for normal embryonic segmentation. *Dev Biol.* 104, 172-186.
- Willert, K., Brown, J.D., Danenberg, E., Duncan, A.W., Weissman, I.L., Reya, T., Yates, J.R., and Nusse, R. (2003). Wnt proteins are lipid-modified and can act as stem cell growth factors. *Nature* 423, pp. 448-452.
- Willert, K., Brink, M., Wodarz, A., Varmus, H. and Nusse, R. (1997) Casein kinase 2 associates with and phosphorylates dishevelled. *EMBO J.* 16, 3089-3096.
- Willert, K., and Jones, K. A. (2006). Wnt signaling: is the party in the nucleus? *Genes Dev* 20, 1394-404.
- Willert, K., Logan, C., Y., Arora, A., Fish, M., and Nusse, R. (1999). A *Drosophila* Axin homolog, Daxin, inhibits Wnt signaling. *Development* 126, 4165-4173.
- Winkler, J., Lünsdorf, H., and Jockusch, B., M. (1997). Flexibility and fine structure of smooth-muscle alpha-actinin. *Eur J Biochem.* 248, 193-199.
- Wodarz, A., Hinz, U., Engelbert, M., and Knust, E. (1995). Expression of crumbs confers apical character on plasma membrane domains of ectodermal epithelia of *Drosophila*. *Cell* 82, 67-76.
- Wodarz, A., and Nusse, R. (1998). Mechanisms of Wnt signaling in development. *Annu Rev Cell Dev Biol.* 14, 59-88.
- Wong, H., C., Bourdelas, A., Krauss, A., Lee, H., J., Shao, Y., Wu, D., Mlodzik, M., Shi, D., L., and Zheng, J. (2003). Direct binding of the PDZ domain of Dishevelled to a conserved internal sequence in the C-terminal region of Frizzled. *Mol Cell* 12, 1251-1260.
- Wu, C. (1995). Heat shock transcription factors: structure and regulation. *Annu Rev Cell Dev Biol* 11, 441-69.
- Xiong, Y., and Kotake Y., (2006). No exit strategy? No problem: APC inhibits β -catenin inside the nucleus. *Genes Dev.* 20, 637-642.
- Yan, D., Wallingford, J. B., Sun, T. Q., Nelson, A. M., Sakanaka, C., et al., (2001). Cell autonomous regulation of multiple Dishevelled-dependent pathways by mammalian Nkd. *Proc. Natl. Acad. Sci. USA* 98, 3802-3807.
- Yan, Q., Sun, W., Kujala, P., Lotfi, Y., Vida, T., A., and Bean, A., J. (2005). CART: an Hrs/actinin-4/BERP/myosin V protein complex required for efficient receptor recycling. *Mol Biol Cell* 16, 2470-2482.

- Yanagawa, S., van Leeuwen, F., Wodarz, A., Klingensmith, J., and Nusse, R. (1995). The dishevelled protein is modified by wingless signaling in *Drosophila*. *Genes Dev* 9, 1087-97.
- Yang, J., Brown, M. S., Liang, G., Grishin, N. V., and Goldstein, J. L. (2008). Identification of the Acyltransferase that octanoylates Ghrelin, an appetite-stimulating peptide hormone. *Cell* 132, 387-396.
- Yang, P., T., Lorenowicz, M., J., Silhankova, M., Coudreuse, D., Y., Betist, M., C., Korswagen, H., C. (2008). Wnt signaling requires retromer-dependent recycling of MIG-14/Wntless in Wnt-producing cells. *Dev Cell* 14, 140-147.
- Yeh, E., Gustafson, K., and Boulianne, G.L. (1995). Green fluorescent protein as a vital marker and reporter of gene expression in *Drosophila*. *Proc. Natl. Acad. Sci. U. S. A.* 92, pp. 7036-7040.
- Yoffe, K. B., Manoukian, A. S., Wilder, E. L., Brand, A. H., and Perrimon, N. (1995). Evidence for engrailed-independent wingless autoregulation in *Drosophila*. *Dev Biol* 170, 636-50.
- Zandi, E., Tran, T. N., Chamberlain, W., and Parker, C. S. (1997). Nuclear entry, oligomerization, and DNA binding of the *Drosophila* heat shock transcription factor are regulated by a unique nuclear localization sequence. *Genes Dev* 11, 1299-314.
- Zecca, M., Basler, K., and Struhl, G. (1996). Direct and long-range action of a wingless morphogen gradient. *Cell* 87, pp. 833-844.
- Zechner, D., Fujita, Y., Hulsken, J., Muller, T., Walther, I., et al., (2003). β -Catenin signals regulate cell growth and the balance between progenitor cell expansion and differentiation in the nervous system. *Dev. Biol.* 258, 406-418.
- Zeng, W., Wharton, K. A., Jr., Mack, J. A., Wang, K., Gadbaw, M., Suyama, K., Klein, P. S., and Scott, M. P. (2000). naked cuticle encodes an inducible antagonist of Wnt signalling. *Nature* 403, 789-95.
- Zeng, X., Tamai, K., Doble B., Li S., Huang, H., et al., (2005). A dual-kinase mechanism for Wnt co-receptor phosphorylation and activation. *Nature* 438, 873-877.
- Zhai, L., Chaturvedi, D., and Cumberledge, S. (2004). *Drosophila* wnt-1 undergoes a hydrophobic modification and is targeted to lipid rafts, a process that requires porcupine. *J Biol Chem.* 279, 33220-33227.
- Zhang, F., White, R., L., and Neufeld, K., L. (2000). Phosphorylation near nuclear localization signal regulates nuclear import of adenomatous polyposis coli protein. *Proc Natl Acad Sci U S A.* 97, 12577-12582.
- Zhang, L., Jia, J., Wang, B., Amanai, K., Wharton, K.A, Jr., Jiang., J. (2006) Regulation of wingless signaling by the CK1 family in *Drosophila* limb development. *Dev Biol* 299, 221-237.

VITAE

Chih-Chiang Chan was born in Changhua, Taiwan, on November 7, 1974, the eldest son of Pi-Feng Chou and Ming-Ho Chan. He spent his childhood and adolescence in a small house in the countryside of Changhua, where he enjoyed exploring and working with farm animals. After completing his work at Taichung First Senior High School, Taiwan in 1993, he entered National Taiwan University (NTU), where he also met his future wife, Shuyi. While in college he worked as a fast food preparer, a private tutor, and a summer intern in a physiology lab. He received the degree of Bachelor of Science with a major in Zoology from NTU in June, 1997. Dreaming of a career in biological research, in 1997 he entered the Graduate Institute of Physiology, NTU, where he worked on transmembrane ion transport in cardiomyocytes. For his academic endeavors he garnered the Outstanding Research award for Graduate Students from the College of Medicine, NTU. After graduating with a Master's degree in 1999, he spent almost 2 years in the mandatory military service, working as a medical officer in charge of a first aid station. After he retired from the Army, he was employed as a teaching assistant by his old institute. There he was in charge of a student physiology lab. Fascinated with molecular biology, as well as being a diehard Dallas Mavericks' fan, he entered University of Texas Southwestern Graduate School at Dallas, TX in 2002. His graduate experience was frustrating, painful, infuriating, inspiring, and deeply satisfying. Through the process, as difficult as it had to be, he learned how to do research the right way and enjoy science. Now he is looking forward to his postdoctoral training. In his spare time, late at night, he loves to build LEGO.

Permanent Address: 378, Sec1, Yuanlu Rd.
Pusin Township, Changhua County, Taiwan